การนำเข้ากลูตาเมตและลักษณะสมบัติของตัวขนส่งกลูตาเมตในไซยาโนแบคทีเรียทนเค็ม *Aphanothece halophytica*

นางสาวบงกช บุญบูรพงศ์

วิทยานิพนธ์นี้เป็นส่วนหนึ่งของการศึกษาตามหลักสูตรปริญญาวิทยาศาสตรดุษฎีบัณฑิต
สาขาวิชาชีวเคมี ภาควิชาชีวเคมี
คณะวิทยาศาสตร์ จุฬาลงกรณ์มหาวิทยาลัย
ปีการศึกษา 2556
ลิขสิทธิ์ของจุฬาลงกรณ์มหาวิทยาลัย

GLUTAMATE UPTAKE AND CHARACTERIZATION OF GLUTAMATE TRANSPORTER IN HALOTOLERANT CYANOBACTERIUM *Aphanothece halophytica*

Miss Bongkoj Boonburapong

A Dissertation Submitted in Partial Fulfillment of the Requirements
for the Degree of Doctor of Philosophy Program in Biochemistry
Department of Biochemistry
Faculty of Science
Chulalongkorn University
Academic Year 2013

Thesis Title	GLUTAMATE UPTAKE AND CHARACTERIZATION OF GLUTAMATE TRANSPORTER IN HALOTOLERANT CYANOBACTERIUM *Aphanothece halophytica*
By	Miss Bongkoj Boonburapong
Field of Study	Biochemistry
Thesis Advisor	ProfessorAran Incharoensakdi, Ph.D.
Thesis Co-Advisor	ProfessorTeruhiro Takabe, Ph.D.

Accepted by the Faculty of Science, Chulalongkorn University in Partial Fulfillment of the Requirements for the Doctoral Degree

.....Dean of the Faculty of Science

(ProfessorSupot Hannongbua, Dr.rer.nat.)

THESIS COMMITTEE

.....Chairman

(ProfessorAnchalee Tassankajon, Ph.D.)

.....Thesis Advisor

(ProfessorAran Incharoensakdi, Ph.D.)

.....Thesis Co-Advisor

(ProfessorTeruhiro Takabe, Ph.D.)

.....Examiner

(Assistant ProfessorSaowarath Jantaro, Ph.D.)

.....Examiner

(Associate ProfessorTeerapong Buaboocha, Ph.D.)

.....External Examiner

(Associate ProfessorWipa Chungjatupornchai, Ph.D.)

.....External Examiner

(Surasak Laloknam, Ph.D.)

บงกช บุญบูรพงศ์ : การนำเข้ากลูตาเมตและลักษณะสมบัติของตัวขนส่งกลูตาเมตในไซยาโนแบคทีเรียทนเค็ม *Aphanothece halophytica*. (GLUTAMATE UPTAKE AND CHARACTERIZATION OF GLUTAMATE TRANSPORTER IN HALOTOLERANT CYANOBACTERIUM *Aphanothece halophytica*) อ.ที่ปรึกษาวิทยานิพนธ์หลัก: ศ. ดร.อรัญ อินเจริญศักดิ์, อ.ที่ปรึกษาวิทยานิพนธ์ร่วม: Prof.Teruhiro Takabe Ph.D., 313 หน้า.

ไซยาโนแบคทีเรียชนิดทนเค็ม *Aphanothece halophytica* สามารถเจริญภายใต้ภาวะที่มีความเครียดจากเกลือโซเดียมคลอไรด์ตั้งแต่ 0.2 – 3.0 โมลาร์ โดยเกลือโซเดียมคลอไรด์ 0.5 โมลาร์เป็นความเข้มข้นที่เหมาะสมต่อการเจริญ (ภาวะปกติ) สำหรับภาวะเครียดจากเกลือที่ทำให้อัตราการเจริญลดลงเป็นครึ่งหนึ่งของสภาวะปกติ คือที่ความเข้มข้น 2.0 โมลาร์ อัตราการเจริญที่ลดลงที่เป็นผลจากภาวะเครียดจากเกลือหมดไปเมื่อมีการเติมกลูตาเมต 50 มิลลิโมลาร์ลงในอาหารเลี้ยงเชื้อ โดยผลการทดลองดังกล่าวชี้ชัดว่ากลูตาเมตที่อยู่ภายนอกเซลล์ถูกขนส่งเข้าสู่เซลล์และทำให้การเจริญเติบโตของ *A. halophytica* สูงขึ้น การนำเข้ากลูตาเมตของ *A. halophytica* ในภาวะที่มีเกลือโซเดียมคลอไรด์ 0.5 และ 2.0 โมลาร์แสดงอิ่มตัวด้วยค่าคงที่มิเคลลิส เมนเทนเท่ากับ 11.76 และ 9.91 ไมโครโมลาร์ และมีค่าความเร็วสูงสุดเท่ากับ 6.67 และ 5.20 นาโนโมลต่อนาทีต่อมิลลิกรัมโปรตีน ตามลำดับ การนำเข้ากรดอะมิโนกลูตาเมตลดลงอย่างมากเมื่อมีการใช้ตัวยับยั้งที่ทำลายเกรเดียนต์ของไอออน และยังถูกยับยั้งการนำเข้าด้วยตัวยับยั้งกระบวนการเมตาบอลิซึม และโปรโตโนฟอร์อีกด้วย จากผลการทดลองข้างต้นทำให้ทราบว่าตัวขนส่งกลูตาเมตใน *A. halophytica* มีอย่างน้อย 2 ระบบ คือ ตัวขนส่งกลูตาเมตแบบที่ต้องใช้พลังงาน และตัวขนส่งกลูตาเมตแบบที่ต้องใช้โซเดียมอิออนในการนำเข้ากลูตาเมต และจากข้อมูลจากการทำ shot gun sequencing พบว่าใน *A. halophytica* มีตัวขนส่งกลูตาเมตแบบที่ต้องใช้โซเดียมอิออน (ApGltS) ซึ่งประกอบด้วยกรดอะมิโน 476 เรซิดิว มีมวลโมเลกุลจากการคำนวณเท่ากับ 51 กิโลดาลตัน ประกอบด้วย 11 ทรานส์เมมเบรน โดยลำดับกรดอะมิโนของ ApGltS มีความคล้ายคลึงต่ำเมื่อเปรียบเทียบกับ GltS ของ *Synechocystis* sp. strain PCC 6803 และ *Escherichia coli* แต่มีความคล้ายคลึงสูงในบริเวณอนุรักษ์ที่อยู่ภายในส่วน pore-loop regions โดยยีน *ApgltS* ถูกนำมาโคลนและศึกษาลักษณะสมบัติใน *E. coli* ME9107 ที่ไม่มีตัวขนส่งกลูตาเมต โดยพบว่า ME9107 ที่มีการแสดงออกของ ApGltS สามารถนำเข้ากลูตาเมต และอัตราการนำเข้ากลูตาเมตเพิ่มขึ้น เมื่อความเข้มขันของเกลือโซเดียมคลอไรด์เพิ่มขึ้น ผลการศึกษาจลนพลศาสตร์พบว่า ApGltS เป็นตัวขนส่งกลูตาเมตที่มีความสามารถในการจับสูงด้วยค่าคงที่มิเคลลิส เมนเทนประมาณ 5 ไมโครโมลาร์ และค่าความเร็วสูงสุด เพิ่มขึ้นประมาณ 3 เท่าเมื่อใน assay medium มีเกลือโซเดียมคลอไรด์ 0.5 โมลาร์ การนำเข้ากรดอะมิโนกลูตาเมตถูกยับยั้งด้วยกรดอะมิโนกลูตาเมต กลูตามีน แอสพาเตท และแอสพาราจีน นอกจากนี้ยีน *ApgltS* ถูกนำมาใส่เข้าไปใน *Synechococcus* sp. PCC 7942 และแสดงออกภายใต้โปรโมเตอร์ของยีน *ApgltS* โดยผลการศึกษาจลนพลศาสตร์มีความคล้ายคลึงกับใน ME9107 คือ ค่าความเร็วสูงสุดของ *Synechococcus* sp. PCC 7942 ที่มีการแสดงออกของ ApGltS เพิ่มขึ้นเมื่อความเข้มขันของเกลือโซเดียมคลอไรด์เพิ่มขึ้น นอกจากนี้ *Synechococcus* sp. PCC 7942 ที่มีการกลายพันธุ์ที่ยีน *natD* ที่มีการแสดงออกของ ApGltS มีแอคติวิตี้ในการขนส่งกลูตาเมตเพิ่มขึ้นอย่างชัดเจนเมื่อเปรียบเทียบกับทรานส์ฟอร์มแมนต์ที่มี control vector ผลการทดลองเหล่านี้บ่งชี้ว่า *A. halophytica* มีตัวขนส่งกลูตาเมตแบบต้องใช้โซเดียมอิออน และพบว่ากลูตาเมตเป็นกรดอะมิโนภายในเซลล์หลักใน *A. halophytica* โดยปริมาณกลูตาเมตภายในเซลล์ของ *A. halophytica* ที่เจริญภายใต้ภาวะเครียดจากเกลือในช่วง mid-log จะเพิ่มขึ้น 2 เท่า โดยกลูตาเมตสามารถถูกใช้เป็นแหล่งพลังงานและสารตั้งต้นสำหรับสารอื่นๆ เช่น กาบา ไกลซีน อาร์จีนีน วาลีน ลิวซีน และไกลซีน บีเทน โดยพบว่าปริมาณไกลซีน บีเทน และกาบาภายในเซลล์ของ *A. halophytica* ที่เจริญภายใต้ภาวะเครียดจากเกลือในช่วง mid-log จะเพิ่มขึ้น 2.8 และ 2 เท่า ตามลำดับเมื่อเทียบกับภาวะปกติ โดยปริมาณไกลซีน บีเทน และกาบาภายในเซลล์จะเพิ่มสูงสุด 4.8 และ 2.2 เท่า ตามลำดับ เมื่อใช้เซลล์ในช่วง mid-log ที่เลี้ยงในภาวะปกติ มาย้ายลงอาหารใหม่ที่มีเกลือโซเดียมคลอไรด์ 2.0 โมลาร์และมีการเติมกลูตาเมต 5 มิลลิโมลาร์ เป็นเวลา 4 ชั่วโมง เมื่อเทียบกับภาวะควบคุม ภายใต้ภาวะเจริญปกติ *A. halophytica* มีความสามารถในการสะสมกาบาสูงกว่าไซยาโนแบคทีเรียสายพันธุ์อื่นๆที่ทำการทดสอบประมาณ 2 – 4 เท่า ยกเว้น *Arthrospira platensis*

ภาควิชา ชีวเคมี	ลายมือชื่อนิสิต .....
สาขาวิชา ชีวเคมี	ลายมือชื่อ อ.ที่ปรึกษาวิทยานิพนธ์หลัก .....
ปีการศึกษา 2556	ลายมือชื่อ อ.ที่ปรึกษาวิทยานิพนธ์ร่วม .....

5173828923 : MAJOR BIOCHEMISTRY
KEYWORDS: APHANOTHECE HALOPHYTICA / HALOTOLERANT CYANOBACTERIA / SALT STRESS / GLUTAMATE TRANSPORTER / GAMMA-AMINOBUTYRIC ACID / GLUTAMATE DECARBOXYLASE

BONGKOJ BOONBURAPONG: GLUTAMATE UPTAKE AND CHARACTERIZATION OF GLUTAMATE TRANSPORTER IN HALOTOLERANT CYANOBACTERIUM *Aphanothece halophytica*. ADVISOR: PROF.ARAN INCHAROENSAKDI, Ph.D., CO-ADVISOR: PROF.TERUHIRO TAKABE, Ph.D., 313 pp.

Halotolerant cyanobacterium *Aphanothece halophytica* grown under various NaCl concentrations from 0.2 – 3.0 M showed the optimum NaCl concentration for growth at 0.5 M NaCl. The salt stress condition that decreased growth to half of maximum growth rate was 2.0 M NaCl. The growth inhibitory effect from salt stress condition was eliminated when 50 mM glutamate was present in the medium. These results indicated that exogenous glutamate was taken up by *A. halophytica* cells and enhanced growth of *A. halophytica*. Glutamate uptake of *A. halophytica* in the assay medium containing 0.5 M NaCl and 2.0 M NaCl exhibited the typical of Michaelis-Menten saturation kinetics with an apparent Michaelis constant value of 11.76 and 9.91 μM, respectively, and maximum velocity of 6.67 and 5.20 $nmol.min^{-1}.mg^{-1}$ protein, respectively. Glutamate uptake was strongly inhibited by inhibitors of dissipating ion gradients and slightly inhibited by various metabolic inhibitors and protonophores. Results of uptake experiment suggested that there are at least 2 glutamate transport system in *A. halophytica*, energy-dependent and sodium ion-stimulated. Based on the shot gun sequencing, *A. halophytica* contained a sodium dependent glutamate transporter (ApGltS) consisted of 476 deduced amino acid residues with a 51 kDa calculated molecular weight of 11 transmembrane segments. The deduced amino acid sequence of ApGltS exhibits low homology to GltS from *Synechocystis* sp. PCC 6803 and Escherichia coli but highly conserved especially in the putative pore-loop regions. The *ApgltS* gene was isolated and expressed in glutamate transporter deficient *E. coli* ME9107. ApGltS expressing ME9107 took up glutamate and its rates increased with the increasing NaCl concentrations. Kinetics studies revealed that ApGltS is a high affinity glutamate transporter with a Michaelis constant value of about 5 μM. The presence of 0.5 M NaCl in the assay medium increased the maximum velocity by 3-fold. Competition experiments indicated that glutamate, glutamine, aspartate and asparagine inhibited glutamate uptake. ApGltS was expressed under its own promoter in *Synechococcus* sp. PCC 7942. Similar kinetic properties of ApGltS expressing ME9107, the maximum velocity values of *Synechococcus* sp. PCC 7942 expressing ApGltS slightly increased upon the increase of NaCl concentrations. Moreover, the glutamate uptake activity in *natD*-deficient *Synechococcus* sp. PCC 7942 expressing ApGltS was significantly increased comparing with control vector transformants. These results indicated that *A. halophytica* has sodium dependent glutamate symporter. We found that glutamate is major intracellular amino acid in *A. halophytica*. Content of intracellular glutamate in *A. halophytica* was increased 2-fold in mid-log phase cells grown under salt stress condition. The results showed that in *A. halophytica*, glutamate can be used as metabolic fuel and as precursor of other compounds such as gamma-aminobutyric acid (GABA), glycine, arginine, valine, leucine and also glycine betaine. Glycine betaine and GABA accumulation in mid-log phase cells grown under salt stress condition were increased about 2.8 and 2 folds, respectively comparing with normal growth condition. The glycine betaine and GABA content were increased maximally about 4.8 and 2.2 folds when mid-log phase cells were grown under salt stress condition and adapted in the medium contained 2.0 M NaCl supplemented with 5 mM glutamate for 4 hours. Under normal growth condition, *A. halophytica* accumulated about 2-4 fold higher GABA content than other tested cyanobacterial strains excepted for *Arthrospira platensis*.

Department:	Biochemistry	Student's Signature	.....
Field of Study:	Biochemistry	Advisor's Signature	.....
Academic Year:	2013	Co-Advisor's Signature	.....

ACKNOWLEDGEMENTS

It would not have been possible to finish my dissertation without the help and support of the kind people around me, to only some of whom I would like to give particular mention here.

Foremost, I would like to express my sincere gratitude to my advisor, Professor Dr. Aran Incharoensakdi for the continuous support of my Ph.D study and research, for his patience, motivation, enthusiasm, and immense knowledge. His guidance helped me in all the time of research and writing of this thesis. I could not have imagined having a better advisor and mentor for my Ph.D study.

Very special thanks go out to my co-advisor Professor Dr. Teruhiro Takabe and all members in Research Institute of Meijo University, Meijo University, Nagoya, Japan for technical support, valuable comments and for all the instances in which their assistance helped me along the way.

Besides my advisor and co-advisor, I would like to express my appreciation to the thesis committee members: Professor Anchalee Tassanakajon, Associate Professor Dr. Teerapong Buaboocha, Assistant Professor Dr. Saowarath Jantaro, Associate Professor Dr. Wipa Chungjatupornchai and Dr. Surasak Laloknam for their encouragement, insightful comments, and helpful suggestions.

My thankfulness is also expressed to Dr. Santhana Nakapong, Dr. Wiraya Srisimarat, Dr. Surachet Burut-archanai, Dr. Wanthanee Khetkorn, Dr. Kanteera Soontharapirakkul, and Dr. Worrawat Promden for technical assistance, valuable comments and interesting discussions.

I would also like to thank all CYB members, department staffs and friends at Department of Biochemistry, Chulalongkorn University for their assistances and friendships. My research would not have been possible without their helps.

Last, but by no means least, I would like to thank my family for their unlimited love, understanding and supporting me spiritually throughout my life.

Finally, I recognize that this research would not have been possible without the financial support from the Office of the Higher Education Commission, Thailand through a grant in the program “Strategic Scholarships for Frontier Research Network for the Ph.D. Program, Thai Doctoral degree” Grant No. 178/2551 and the 90th Anniversary of Chulalongkorn University Fund (Ratchadaphiseksomphot Endowment Fund). I would like to express my gratitude to those agencies.

CONTENTS

Page

Page

Page

Page

Page

Page

Page

Page

Page

Page

LIST OF TABLES

Page

LIST OF FIGURES

Page

LIST OF ABBREVIATIONS

A	Absorbance
Amp	Ampicillin
bp	Base pair
BSA	Bovine serum albumin
CCCP	Carbonyl cyanide *m*-chlorophenylhydrazone
Cm	Chloramphenicol
Ci	Curie
cpm	Count per minute
DCCD	*N, N'*- dicyclohexylcarbodiimide
DMSO	Dimethyl sulfoxide
°C	Degree Celsius
DNA	Deoxyribonucleic acid
EDTA	Ethylenediaminetetraacetic acid
et al.	Et. Alii (latin), and others
g	Gram
hr	Hour
kb	Kilobase
kDa	KiloDalton
l	Liter
M	Molar

µE	Microeinstein
µg	Microgram
µl	Microliter
µM	Micromolar
mA	Milliampere
mg	Milligram
min	Minute
ml	Milliliter
mM	Millimolar
MW	Molecular weight
NBT	*p*-Nitro blue tetrazolium chloride
NEM	*N*-ethylmaleimide
ng	Nanogram
nm	Nanometer
nmol	Nanomol
OD	Optical density
ONPG	*O*-nitrophenyl-beta-galactopyranoside
OPA	*O*-phthalaldehyde
ORF	Open reading frame
PAGE	Polyacrylamide gel electrophoresis
PCR	Polymerase chain reaction
PMF	Proton motive force

rpm	Revolution per minute
SDS	Sodium dodecyl sulphate
Strep	Streptomycin
TBE	Tris-borate-EDTA
TEMED	N,N,N',N'-tetramethylene ethylene diamine
V	Volt
X-gal	5-bromo-4-chloro-3-indolyl-b-D-galactopyranoside

CHAPTER I

INTRODUCTION

1.1 Statement of the problem

The salinity in soils and in aqueous environment is an important physical factor that affects growth and survival of living organisms. Salt stress, contributed largely by NaCl, has dramatic impact on plant growth, agricultural productivity and known to restrict use of land. High salt concentration cause ion imbalance resulting in ion toxicity and hyperosmotic stress [126]. Drastic changes in water and ion homeostasis cause physical damage to cellular components (such as cell wall, membrane and protein) and lead to growth inhibition [126]. The main toxic ion is *s*odium ion (Na^+) because Na^+ influx elevates the cytoplasmic Na^+ concentration to the excessive level. High Na^+ concentration inhibits the uptake of potassium ion (K^+) which is one of essential monovalent cations for growth and development [47]. Moreover, high concentration of Na^+ also inhibits the activities of many cytosolic K^+-binding enzymes. In addition, salt stress accelerates the formation of reactive oxygen species (ROS) and inhibits several metabolic processes such as respiration, photosynthesis, nitrogen fixation and protein synthesis [1, 32, 50].

Attempts to understand the mechanisms of osmoregulation and the ability to adapt to fluctuations in the external osmolarity have been studied earlier. Various strategies have been adopted by the cells in order to survive and proliferate in the presence of reduced water activity. However, the mechanisms of adaptation processes under high salinity condition remain largely unknown. Our research group has been studying on the mechanism of salt tolerance in *Aphanothece halophytica*.

The basic mechanisms of salt tolerance in *A. halophytica* involve the accumulation of main compatible solutes glycine betaine for osmotic stabilization and the active extrusion of Na^+ through the enhancement of Na^+/H^+ exchanger and ATPase activity. For glycine betaine accumulation, we observed that *A. halophytica* accumulated large amounts of glycine betaine under salt stress and this cyanobacterium can synthesizes glycine betaine from glycine by three-step methylation [46, 118]. In addition, the co-expression of *A. halophytica N*-methyltransferases ApGSMT and ApDMT in *Synechococcus* drastically improves the salt tolerance of these cells [114]. Moreover, *A. halophytica* contains betaine transporter *which* plays a role of salt stress tolerance at alkaline pH [59, 116].

For Na^+-homeostasis, our previous results demonstrated that Na^+/H^+ exchangers of *A. halophytica* play the important role for the regulation of intracellular levels of both Na^+ and H^+ [117]. In addition, overexpression of *A. halophytica* Na^+/H^+ exchanger genes in *E. coli* as well as a freshwater cyanobacterium *Synechococcus* sp. PCC 7942 could tolerate high salinity [115]. Recently, we reported that *A. halophytica* has P-type Na^+-stimulated ATPase and Na^+-dependent F1F0-ATPase in plasma membranes which contributes to the salt stress tolerance [104, 120].

With regard to the acquisition of nitrogen, most cyanobacteria assimilate nitrate and ammonium, and many strains are also able to assimilate urea or dinitrogen. Some cyanobacteria have been shown to be able to take up some amino acids mostly asparagine, arginine, glutamine and glutamate and can be used as the nitrogen sources [72, 74, 113]. In a preliminary study, the effect of several amino acids on the growth of *A. halophytica* was examined. The results suggested that glutamate enhanced growth of *A. halophytica* under salt stress condition. However,

the understanding of cyanobacterial amino acid transporter is scarce and only a few studies have been reported in other cyanobacteria. Until now, Glutamate transporter has not been reported for *A. halophytica*. In the present study, we propose to investigate the effect of salinity and glutamate supplementation on growth of *A. halophytica* and examine the glutamate uptake activity in *A. halophytica*. To gain deeper insight into the *Aphanothece* glutamate transporter, the molecular cloning of glutamate transporter gene will be carried out together with the bioinformatics analysis of glutamate transporter in cyanobacteria as well as examined expression of *A. halophytica* glutamate transporter in *E. coli* mutant.

1.2 Objectives

1.2.1 To study the effect of salinity and glutamate on growth of *A. halophytica*

1.2.2 To study glutamate uptake of *A. halophytica*

1.2.3 To isolate *A. halophytica* glutamate transporter gene and express *A. halophytica* glutamate transporter in *E. coli* mutant

1.2.4 To characterize *A. halophytica* glutamate transporter in *E. coli* mutant

1.3 Hypothesis

Glutamate supplementation in the growth medium enhanced growth of *A. halophytica*. It means that exogenous glutamate was taken up by *A. halophytica* cells via glutamate transporter and can be used as carbon and nitrogen source and as also substrate for osmoprotectant synthesis.

1.4 Statement of the response

These studies will provide information on glutamate transporter in *A. halophytica* in order to obtain additional basic knowledge with respect to the mechanism of glutamate transport and the importance of glutamate as the protective mechanisms for cells thriving in changing salinity environment. It was the first biochemical characterization of glutamate uptake in halotolerant cyanobacteria.

CHAPTER II

THEORETICAL BACKGROUND AND LITERATURE REVIEWS

2.1 Cyanobacteria

Cyanobacteria, known as blue-green algae, are ancient gram negative oxygenic photosynthetic prokaryote. They can be found in almost every terrestrial, aquatic habitat and also in extreme environments. The name "cyanobacteria" comes from the cell colour (Greek word: kyanós which means blue) which is a result of the combination of the unique bluish pigment (phycocyanin) and the green pigment (chlorophyll a). In addition, they contain various pigments such as the yellowish pigment (carotenoids) and the red pigment. They were classified in the phylum Cyanobacteria within domain Bacteria. They can use the solar energy to synthesize biomass-stored chemical energy using only simple inorganic compounds [34]. In recent years, cyanobacteria have drawn much attention as a rich source of bioactive compounds and considered as one of the most promising groups of organisms to produce them [16, 33]. They are also reported as a source of renewable fuel, functional food and secondary metabolites with potential biotechnological applications especially in marine cyanobacteria [76].

On the basis of their salt tolerance, cyanobacteria can be subdivided into three groups: salt sensitive freshwater cyanobacteria, moderately halotolerant cyanobacteria and extremely halotolerant cyanobacteria [87]. Example genus for each groups include *Anabaena*, *Synechocystis* and *Aphanothece*, respectively. Under the high salinity condition, cyanobacteria maintain their osmotic balance through the activation of adaptation processes: 1) the active extrusion of Na^+, 2) the

accumulation of organic compatible solutes by the *de novo* synthesis and/or uptake, 3) the membrane lipid composition modifications and 4) increase the energetic capacity through respiration, electron transport system and also photosystem I.

The accumulation of compatible solutes is one of the salt tolerance mechanisms in cyanobacteria. Compatible solutes are low-molecular-weight organic osmolytes including carbohydrates, polyols, amino acid and their derivatives. Sucrose, trehalose, glucosyiglycerol, glutamate, and glycine betaine are the common compatible solutes present in cyanobacteria. The compatible solute accumulation occur either by transport from environment or from *de novo* synthesis. They are compatible with cellular metabolisms even at high amounts. The functions of these organic compounds are: 1) maintaining osmotic equilibrium, 2) stabilizing the photosystem II complex, 3) protecting the structure of enzymes, proteins and nucleic acid, 4) maintaining membrane fluidity, and 5) scavenging reactive oxygen species (ROS) [6, 65, 66, 75, 77, 89, 91, 97, 101].

2.2 *Aphanothece halophytica*

The unicellular alkaliphilic halotolerant cyanobacterium *Aphanothece halophytica* was classified in order *Chroococcales* with in subclass *Oscillatoriophycideae*. This cyanobacterium can be found abundantly in hypersaline environments like salt lakes and saltern ponds [14, 18]. It is an important model organism to study the adaptation mechanisms of phototrophic life at high salt concentration condition. *Aphanothece* cells reproduce asexually by binary fission. Cell feature of *Aphanothece* cells is the ovoid or short cylindrical shape covered with mucous membrane and varies in cell size between 2-10 μm [124]. Na^+ is

required for growth of *A. halophytica* and could not be replaced with other inorganic monovalent cation [53]. *A. halophytica* can grow at high NaCl concentrations up to 3.0 M NaCl and at alkaline condition up to pH 11 [108]. The optimum NaCl concentration for growth of *Aphanothece* was in range of 0.5–1.0 M [108]. Under salt stress condition, *A. halophytica* accumulate the quaternary ammonium compound glycine betaine as primary compatible solute, and also accumulate glucosylglycerol and proline as minor osmolytes [40].

2.3 Glutamate

Amino acids are organic compounds composed of an acidic carboxyl group (-COOH), a basic amino group (-NH_2) and an organic R group (side chain). Amino acids are the building blocks of proteins and act as intermediate in many metabolic processes. Glutamate is one of the most abundant free amino acid in prokaryote and eukaryote, which plays a central role in multiple metabolic processes. Molecular structure of glutamic acid HOOC-(CH2)2-CH(NH_3)-COOH as shown in Figure 2.1. Glutamate, a negatively charged amino acid, is a molecule broken down to serve as an energetic source such as glycolysis, gluconeogenesis and the tricarboxylic acid cycle (TCA) [105]. It is non-essential amino acid necessitated in amino acid metabolism, protein synthesis and protein degradation. In addition, glutamate is a key molecule in nitrogen assimilation via GDH and GS-GOGAT pathways [61, 106].

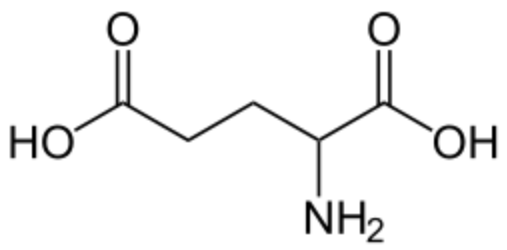

Figure 2.1 Chemical structure of glutamate.

In general, glutamate can be synthesized through the activity of glutamate dehydrogenase (GDH), glutamine synthase (GS), and aminotransferase. When the ammonia concentration is high (› 1 mM), glutamate is synthesized from the reductive amination of α-ketoglutarate, an intermediate in the TCA cycle, with concomitant oxidation of NADPH catalyzed by glutamate dehydrogenase. The coupled reactions of glutamine synthetase (GS) and glutamate synthase (glutamine: 2-oxoglutarate aminotransferase; GOGAT) is responsible for glutamate formation in the presence of low ammonia concentration. Moreover, glutamate can be synthesized from (*S*)-1-pyrroline-5-carboxylate, NAD^+, and H_2O via 1-Pyrroline-5-carboxylate dehydrogenase [5] and from putrescine and α-ketoglutarate via putrescine aminotransferase [83, 90].

Glutamate is the central intermediate for carbon and nitrogen metabolism. It functions as the primary amino group doner in most amino acid biosynthesis [88]. Glutamate also provides the carbon skeleton for the biosynthesis of glutamine, proline, arginine and orinithine [88]. Glutamate also acts as an amino donor to glyoylate in higher plant[119], green algae [4, 60], *A. cylindrical* [23] and *Synechocystis* sp. PCC 6803 [56]. Moreover, glutamate is a precursor of many physiological substances such as gamma-aminobutyric acid (GABA) [56] and glutathione etc [15].

The role of glutamate is becoming better understood. Glutamate is the major mediator of excitatory neurotransmitters in the vertebrate central nervous system [67] and also acts as signaling molecule in plants and bacteria [21, 37, 38]. Glutamate and its isomers are known to be a major compatible solute of many species [38, 41, 48, 54]. Because glutamate is zwitterionic molecules to play majority an anionic solute, it is usually accompanied by a monovalent cation to maintain charge balance such as K^+. To counterbalance the K^+, glutamate was accumulated either through biosynthesis or through uptake from the environment. Potassium glutamate acts as the intracellular signaling molecule of osmotic stress and stimulates transcription of osmoprotectant-related genes [9, 19, 62, 84]. In addition, glutamate acts as the precursor for chlorophyll synthesis in developing leaves [122].

2.4 Amino acid transporter in cyanobacterial

The array of cyanobacterial amino acid transport systems has been characterized only for *Synechocystis* sp. PCC 6803 [35, 58, 85] and *Anabaena* sp. PCC 7120 [44, 71, 72]. *Synechocystis* sp. PCC 6803 contains three amino acid transport systems, one specific for basic amino acids and glutamine, one specific for neutral amino acids (excluding glutamine), and the other one specific for glutamine and glutamate, have been described [58]. Whereas, *Anabaena* sp. PCC 7120 contains three amino acid transport systems: neutral amino acids transporters (system I and system II) and basic amino acids transporter [44, 71, 72].

2.5 Glutamate transport family

Glutamate transporter family has been identified in three groups based on substrate specificity: glutamate/aspartate transporters (found in bacteria and eukaryotes), neutral-amino-acid transporters (found in bacteria and eukaryotes) and C_4-dicarboxylate transporters (found in bacteria) as shown in Table 2.1 [100]. Glutamate transporters are secondary active transporter using the free energy stored in Na^+ gradient over the membrane to drive transport [52]. A typical secondary transporter consists of a single polypeptide component that forms a bundle of membrane-spanning α-helices connected by loops. The glutamate transporter family includes mammalian neutral-amino-acid transporters [3, 63, 94], retinal glutamate transporters from vertebrates [2, 30] and bacterial nutrient uptake proteins [31, 79, 110-112, 123].

Table 2.1 Substrate specificity of the members of the glutamate transport family [100].

Subfamily	Substrate[a]	Mode of energy coopling
glutamate/aspartate transporters	Glutamate, aspartate, glutamate analogues	H^+ symport; H^+/Na^+ symport; H^+/Na^+ symport-K^+ antiport
neutral-amino-acid transporters	Alanine, serine, cysteine, threonine (asparagine, glutamine)	Exchange; Na^+ symport
C_4-dicarboxylate transporters	Succinate, fumarate, malate (orotate, aspartate)	Unknown

[a]High-affinity substrates are shown.

The earliest investigations for bacterial glutamate transport were performed in-depth with *Escherichia coli* cells. It was established that three glutamate transport systems have been classified: 1) a binding protein-dependent, Na^+-independent, glutamate/aspartate transport system, 2) a binding protein-independent, Na^+-independent glutamate/aspartate system, and 3) a binding protein-independent, Na^+-dependent glutamate specific system (GltS) [17, 42, 43, 70, 92]. The main transport system for glutamate in *E. coli* is mediated by a glutamate carrier, the *gltS* gene product. Frank and Hopkins (1969) have found that glutamate transport in *E. coli* B is stimulated by Na^+ and that this stimulation is due to an increase in affinity for the substrate [39]. It was demonstrated that glutamate transport occurred via a Na^+ symport mechanism. Na^+ is the predominant cotransported cation for solute transport in marine and halophilic bacteria and obligate alkalophiles [27]. The GltS is an extremely hydrophobic integral membrane protein located in the cytoplasmic membrane [70]. Besides the glutamate transporters in *E. coli*, only three more bacterial glutamate transport systems have been characterized in *Bacillus subtilis, Bacillus caldotenax* and *Bacillus stearothermophilus* [112].

2.6 Membrane topology of Na^+-glutamate transporter GltS of *E. coli*

The Na^+-glutamate transporter GltS of *E. coli,* EcGltS, is the only characterized member of the ESS family of secondary transporters. GltS of *E. coli* contain 10 transmembrane segments (TMS). Both the N- and C-termini are located in the periplasm. Two times five segments (TMSs I-V and TMSs VI-X) form two homologous domains that are connected by a large hydrophilic loop. In between the fourth and fifth TMS of each domain, the connecting loop folds back between the TMSs. The

poreloop in the N-terminal domain (loop Vb) enters the membrane embedded part from the periplasmic side, the one in the C-terminal domain (loop Xa) from the cytoplasmic side of the membrane. The two loops are believed to contact each other in the three-dimensional structure, where they would form the translocation path as shown in Figure 2.2 [28].

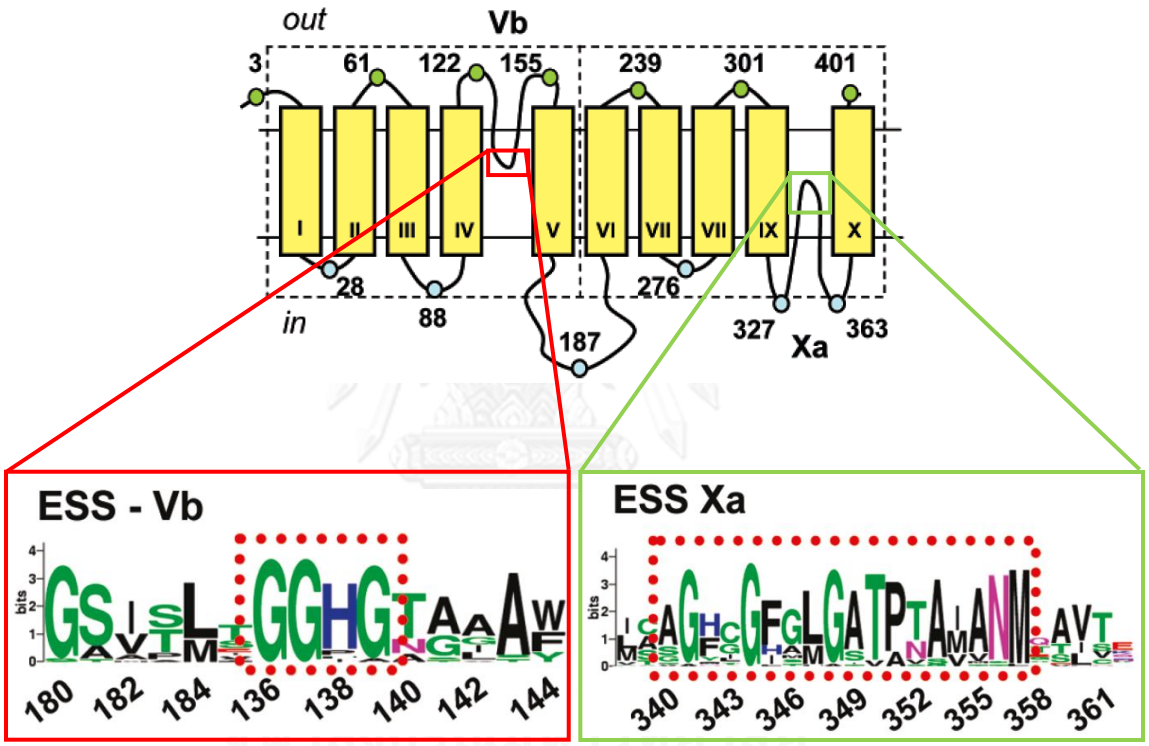

Figure 2.2 **Membrane topology model of the EcGltS by Dobrowolski et al. (2007) [28].**

Dash boxes indicate two homologous domains with inverted orientation in the membrane. Vb and Xa correspond to pore-loop structures. Sequence logos of regions Vb and Xa showing the GGXG sequence motif in the ESS families. Position numbers correspond to the residue numbers in the GltS (ESS) sequences.

2.7 Glutamate transporter in cyanobacteria

Recently, Quintero and colleague (2001) have found that the glutamate transport activity of *Synechocystis* sp. PCC 6803 is mainly from Na^+-dependent. In addition, this cyanobacterium contains two permeases involved in this activity: GltS, a monocomponent secondary permease, and GtrABC, a TRAP type transporter [85]. The cyanobacterial glutamate transport activity was also characterized only in *Synechocystis* sp. PCC 6803. Under the presence of 12.5 mM Na^+ ions, it shows a glutamate uptake activity with apparent *Ks* of 49 μM and the V_{max} values of 529 $nmol.min^{-1}.mg^{-1}$ Chl [72]. However, maximal activity was decreased when Tricine-KOH substituted for Tricine-NaOH as the incubation buffer. Other Na^+-dependent glutamate transport system(s) must be present in *Synechocystis* sp. PCC 6803 because GltS and GtrABC would together account for no more than about 60% of the wild-type activity [85].

The complete sequence of the chromosome of *Synechocystis* sp. PCC 6803 has been determined [51]. It has been reported that ORF *slr1145* of *Synechocystis* sp. PCC 6803 would encode a protein with 42% identity to the GltS Na^+/glutamate permease of *Escherichia coli.* GltS of *Synechocystis* sp. PCC 6803 is composed of 12 hydrophobic membrane-spanning segments containing 5 conserved amino acid residues (Gly42--Ala82-X-X-X-X-Leu87-X-X-X-Gly91-Arg92), which commonly exists in four Na^+ symport carrier proteins [26]. However, little is known about Na^+/glutamate transport by other cyanobacteria.

2.8 gamma-aminobutyric acid

The γ-aminobutyric acid (GABA), a non-protein four-carbon amino acid (Figure 2.3), is a valuable component of the free amino acid pool that is widely distributed in nature among prokaryotes and eukaryotes [10]. In animals, GABA is well known as a major inhibitory neurotransmitter of the nervous system and it has several physiological functions such as hypotensive and diuretic effect [49]. GABA in plants probably plays a dual role as both a signaling molecule and a metabolite. Recently, GABA is reported to have a potential for bioactive ingredient in many products. Because of its properties, GABA is useful for relaxation and as a sleep aid and has been claimed to boost levels of growth hormone and act as a sedative and vasodilator.

Figure 2.3 Chemical structure of gamma-aminobutyric acid

Currently, GABA has been discovered in a wide variety of organisms including plant and bacterial species. In plants and animals, GABA is mainly metabolized through GABA shunt pathway which bypasses two steps of the tricarboxylic acid cycle. The first step of this shunt is the irreversible α-decarboxylation of glutamate using a pyridoxal 5'-phosphate-dependent glutamate decarboxylase (GAD, EC 4.1.1.15). The second enzyme is GABA transaminase (GABA-T; EC 2.6.1.19) which catalyzes the reversible conversion of GABA to succinic semialdehyde. The last step is irreversible oxidation of succinic semialdehyde to succinate, catalyzed by succinic

semialdehyde dehydrogenase (SSADH; EC 1.2.1.16) [10, 56, 95, 96, 105]. The GABA shunt had been reported to be associated with various physiological responses including the regulation of cytosolic pH, nitrogen metabolism, carbon fluxes into the tricarboxylic acid cycle, deterrence of insects, protection against oxidative stress, osmoregulation and signaling [10].

GABA is highly soluble in water and its physiological role in salt tolerance has been suggested to be involved in osmotic regulation and de-toxication of reactive oxygen radicals [10, 22, 95]. It is zwitterionic at physiological pH. GABA levels in plant tissues are low but increase several fold in response to stresses. In some higher plants, it is likely that high level of GABA under salt stress may be used as a compatible solute to stabilize and mitigate the toxic effects of salt [13]. In addition, it has been proposed that stress-induced GABA synthesis can contribute to pH regulation because the activity of GABA synthesizing enzyme, glutamate decarboxylase (GAD), consumes H^+ [11],. Moreover, GABA is a temporary nitrogen store [73, 93].

Many reports suggested that cyanobacteria have an in complete TCA cycle and lack the genes encoding for 2-oxoglutarate dehydrogenase (OGDH) complex [24, 57, 68, 78]. Many cyanobacteria, including *Synechocystis* sp. PCC 6803, have genes encoding for two enzymes that replace the lacking OGDH complex: A 2-oxoglutarate decarboxylase (sll1981, EC 4.1.1.71) and a succinate semialdehyde dehydrogenase (slr0370, EC 1.2.1.16). GABA shunt was used as bypass of TCA cycle from 2-oxoglutarate, via glutamate, γ-aminobutyric acid (GABA) and succinate semialdehyde, to succinate as shown in Figure 2.4 [57]. In 2010, Knoop and colleague reported that flux through the GABA shunt was used during respiratory metabolism

[57]. Until now, metabolism and function of GABA in cyanobacteria is still obscure and not much investigated.

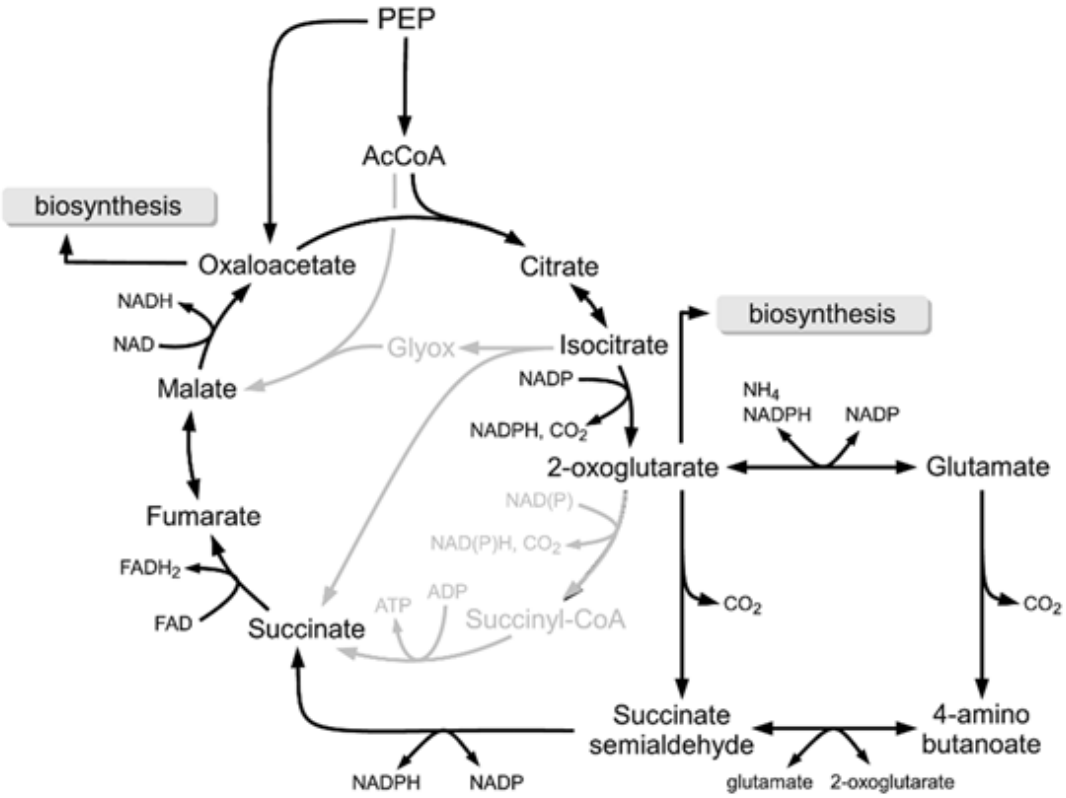

Figure 2.4 Schematic summary of the in complete TCA cycle in cyanobacteria [57].

CHAPTER III

MATERIALS AND METHODS

3.1 Materials

3.1.1 Equipments

Autoclave: Model HA-30, Hirayama Manufacturing Cooperation, Japan

Autoclave: Model MLS-3020, Sanyo Electric Co. Ltd., Japan

Auto pipette: Pipetman, Gilson, France

Balance: Model AB204-S, Mettler Toledo, Switzerland

Balance: Model PB303-S METTLER TOLEDO, USA

Balance: Model LC 620S, Sartorius, USA

Betascanner BS -4125: Shimadzu, Japan

Centrifugal concentrator: Model VC-12S, TaiTec, Japan

Centrifuge, refrigerated centrifuge: Model J-21C, Beckman Instrument Inc, USA

Centrivap concentrator: Model 7970001, Labconco Corporation, USA

DNA electrophoresis chamber: Gelmate 2000, Toyobo, Japan

Digital Lux meter FT710: Taiwan

Electrophoresis unit: Model Mini-protein II cell: Biorad, USA

Flight mass spectroscopy: KOMPACT MALDI IV tDE, Shimadzu, Japan

French pressure cell: SIM-Aminco Spectronic Instrument, USA

GeneAmp5700: Perkin Elmer, Japan

Gel documentation system: ImageMaster VDS, Pharmacia Biotech, USA

GeneAmpPCR system: Model 2400, Perkin Elmer, USA

Genetic analyzer: ABI PRISM 3100-Avant, Hitachi, Japan

High performance liquid chromatography: Model Hewlette Packard series 1050, Japan

High performance liquid chromatography: Prominence Ultra-Fast Liquid Chromatography System, Shimadzu Scientific Instruments Inc., Japan

Hot air oven: Isotemp oven, Fisher Scientific, USA

Hot plate/stirrer: PMC, PMC Industries, Singapore

Illuminated/Refrigerated orbital: Sanyo, England

Incubator: Haraeus, Germany

Incubator shaker: Model 1H-100, Gallenkamp, UK

Ion analyzer: Model PIA-1000, Shimadzu, Japan

Larminar flow: Model BVT-124, International Scientific Supply Co. Ltd., Thailand

Luminometer: Model GloMax™ 20/20, Promega, USA

Microcentrifuge: Kubota, Japan

Microcentrifuge, refrigerated centrifuge: Model 5417C, Eppendorf, Germany

Microcentrifuge, refrigerated centrifuge: Hettich Zentrifugen Mikro 22 R, Hettich Laborapparate, Germany

Microscope: Olympus, USA

Microwave: Model edition I, Daewoo Electronics America, USA

Peristaltic pump: Pharmacia LKB, Sweden

Personal ion analyzer: Applied Biosystems, Foster city, CA, USA

pH meter: PHM 83 Autocal pH meter, Radiometer, Denmark

pH meter: SevenEasy, Mettler Toledo, Switzerland

Power supply: Model EC135-90, E-C Apparatus Corporation, USA

Power supply: Pharmacia, England

Scintillation counter: Pharmacia LKB Wallac, Reckbet 1218, England

Spectrophotometer UV-240: Shimadzu, Japan and

Spectrophotometer Du series 650: Beckman, USA

Ultracentrifuge: OPTIMA™ L-100 XP, Beckman Coulter, USA

Ultrasonic laboratory homogenizer: SONOPULS HD 2070, BANDELIN electronic, Germany

Trans-Blot Transfer Cell: Bio-Craft, Japan

Vacuum dry: Taitech, Japan

Vortex: Touch mixer model 232, Fisher Scientific, USA

Water bath: Model G-76, New Brunswick Scientific Co. Inc., USA

Water bath: Model WB29, Memmert, Germany

3.1.2 Chemicals

Acetic acid: BDH, England

Acetone: Merck, Germany

Acetonitrile: Honeywell Burdick & Jackson

Acrylamide: Merck, Germany

Agar: Scharlau Microbiology, Spain

Agarose: Seakem, USA

Amiloride: Sigma, USA

Amino acid and derivatives: Sigma, USA

Ammonium chloride: Katayama Chem, Japan

Ammonium persulfate: Katayama Chem, Japan

Ampicillin: Katayama, Japan

Antimycin A: Sigma, USA

Bacto peptone: Merck, Germany

Bacto tryptone: Difco, USA

D11-betaine: Sigma, USA

1,4-bis(5-phenyl-2-oxazolyl) benzene (POPOP): BDH, England

Bovine serum albumin (BSA): Sigma, USA

5-bromo-4-chloro-3-indolyl-b-D-galactopyranoside (X-gal): Fermentas, USA

5-Bromo-4-chloro-3-indolyl phosphate (BCIP): Sigma, USA

Bromophenol blue: Sigma, USA

Buffer-saturated phenol: Invitrogen, New Zealand

Beta-mercaptoethanol: Katayama Chem, Japan

Calcium chloride: Merck Ag Darmstadt, Germany

Carbonyl-cyanide trifluoromethoxyphenylhydrazone (CCCP): Sigma, USA

Chloramphenicol: Sigma, USA

Chloroform: Katayama Chem, Japan

Citric acid: Scharlau Chemie S.A., Spain

Coomasie brilliant blue G-250: Sigma, USA

Coomasie brilliant blue R-251: Sigma, USA

Cysteine: Sigma, USA

Dialysis tube: Sigma, USA

N, N'-diclyclohexylcarbodiimide (DCCD): Sigma, USA

Dimethyl sulfoxide: Katayama Chem, Japan

3-(3,4-dichlorophenyl)-1, 1-dimethyl urea (DCMU): Sigma, USA

2, 4-dinitrophenol (DNP): Sigma, USA

Dithiothreitol (DTT): Sigma, USA

Ethylenediaminetetraacetic acid (EDTA): Sigma, USA

Ethanol: Katayama Chem, Japan

Ethidium bromide: Sigma, USA

Ethylenediaminetetraacetic acid (EDTA): Fluka, Switzerland

N-Ethylmaleimide (NEM): Sigma, USA

Ferric sulfate: BDH, England

Folin-Ciocalteu's reagent: Carlo Erba Reagenti, France

Fructose: Sigma, USA

Glucose: Fluka, Switzerland

Glycerol: Scharlau Chemie S.A., Spain

Gramicidine D: Sigma, USA

Glycerol: Merck Ag Darmstadt, Germany

[U-^{14}C] glutamate: American Radiolabeled Chemicals, Inc., St. Louis, USA

[U-^{14}C] glycine: American Radiolabeled Chemicals, Inc., St. Louis, USA

N-2-hydroxyethylpiperazine-*N*'-2-ethanesulfonic acid (HEPES): Sigma, USA

Kanamycin: Sigma, USA

Isopropyl β-D-1-thiogalactopyranoside (IPTG): Sigma, USA

Isoamylalcohol: Katayama Chem, Japan

Isopropanol: Sigma, USA

Lactate: Sigma, USA

Lamda DNA: Toyobo, Japan

Lithium chloride: Katayama Chem, Japan

Manganese chloride: Ajax Finechem, Australia

Manitol: BDH, England

Magnesium sulfate: Scharlau Chemie S.A., Spain

Magnesium chloride: Ajax finechem, Australia

Mercaptoethanol: Sigma, USA

Methanol: Scharlau Chemie S.A., Spain

N, N'-methylene-bis-acrylamide: Sigma, USA

Metylene blue: Sigma, USA

Monensin: Sigma, USA

Nigericin: Sigma, USA

p-nitro blue tetrazolium chloride (NBT): Wako, Japan

O-nitrophenyl-beta-galactopyranoside (ONPG): Wako, Japan

Phenol: BDH, England

O-phthalaldehyde (OPA) reagent: Agilent Technologies, Inc., CA

Potassium arsenate: Sigma, USA

Potassium chloride: Merck Ag Darmatadt, Germany

Potassium cyanide: Sigma, USA

Potassium phosphate, monobasic: Scharlau Chemie S.A., Spain

Potassium dihydrogen phosphate: Scharlau Chemie S.A., Spain

Potassium fluoride: Sigma, USA

Potassium nitrate: BDH, England

Potassium thiocyanate: Sigma, USA

[U-^{14}C] proline: American Radiolabeled Chemicals, Inc., St. Louis, USA

Pyridoxal 5'-phosphate (PLP): Sigma, USA

Rotenone: Sigma, USA

[U-^{14}C] serine: American Radiolabeled Chemicals, Inc., St. Louis, USA

Sodium acetate: Katayama Chem, Japan

Sodium arsenate: Sigma, USA

Sodium azide: Sigma, USA

Sodium bicarbonate: Ajax finechem, Australia

Sodium carbonate: Ajax finechem, Australia

Sodium chloride: Ajax finechem, Australia

Sodium hypochlorite: KAO Industrial (Thailand) Co., Ltd., Thailand

Sodium phosphate, monobasic: Scharlau Chemie S.A., Spain

Sodium dihydrogen phosphate: Scharlau Chemie S.A., Spain

Sodium dodecyl sulfate: Sigma, USA

Sodium fluoride: Sigma, USA

Sodium nitrate: Sigma, USA

Sodium sulfate: Ajax finechem, Australia

Sorbitol: BDH, England

Streptomycin: Sigma, USA

Sucrose: Katayama Chem, Japan

Sulfuric acid: BDH, England

N,N,N',N'-tetramethylene ethylene diamine (TEMED): BDH, England

Trifluorocarbonylcyanide phenylhydrazone (FCCP): Sigma, USA

Tris-hydrochloride: Katayama Chem, Japan

Triton X-100: Packard, USA

Valinomycin: Sigma, USA

Vanadate: Sigma, USA

Xylene cyanol FF : Sigma, USA

Yeast extract: Scharlau Microbiology, Spain

3.1.3 Supplies

Blot absorbent filter paper: Biorad, USA

Cellulose acetate membrane: Whatman International, England

0.45 µm HAWP cellulose acetate filter paper: Millipore Corporation, USA

Micropure-EZ: Millipore Corporation, USA

Midisart 2000 vent filter: Sartorius, Germany

Polyvinylidine Fluoride membrane (PVDF): Whatman International, England

Whatman No.1 filter paper: Whatman International, England

Whatman 3MM paper: Whatman International, England

4.6 x 150 mm, 5.0 µm Agilent Zorbax Eclipse AAA analytical column: Agilent Technologies Inc., USA

4.6 x 12.5 mm, 5.0 µm guard column: Agilent Technologies Inc., USA

3.1.4 Kits

Anti-6X-histidine purified mouse monoclonal IgG_1: R&D Systems, Japan

Anti-mouse IgG (H&L) (AP-linked antibody): Cell Signaling Technology, USA

BigDye terminator v3.1 cycle sequencing kit: Applied Biosystems, USA

Blunting kination ligation kit: Takara, Japan

DNA ligation kit: TaKaRa, Japan

DNA marker: 1 kb GeneRuler™ (#SM 0311), Fermentas, USA

DNA marker: 100 bp GeneRuler™ (#SM 0241), Fermentas, USA

GeneAmp dNTP mix: Roache, USA.

LMW calibration kit for SDS electrophoresis: Amersham Biosciences, England

Precision plus protein dual color standards: Bio-Rad, USA

TA cloning kit: Invitrogen, USA

Ligation kit version 1: Takara, Japan

Suprec^{Tm}-O1 (cartridge for recovery DNA): Takara, Japan

Suprec^{Tm}-O2 (cartridge for DNA concentration and Primers elimination): Takara, Japan

3.1.5 Enzymes

Alkaline phosphatase (calf intestine): Takara, Japan

AmpliTaq Gold: Roache, USA

Lysozyme: Sigma, USA

LA Taq: TaKaRa, Japan

ProteinaseK: Katayama Chem, Japan

Restriction enzymes: TaKaRa, Japan

RNase A: US Biological, USA

3.1.6 Microorganisms

3.1.6.1 Cyanobacteria

Aphanothece halophytica was originally isolated from the Dead Sea in Israel. The organism was kindly provided by Professor. Dr. Teruhiro Takabe of the research institute of Meijo university, Japan.

Synechococcus sp. PCC 7942 is a freshwater cyanobacterium. The organism was kindly provided from Professor Dr. Teruhiro Takabe.

Synechocystis sp. PCC 6803 is a freshwater cyanobacterium.

Arthrospira platensis is a filamentous non-N2-fixing cyanobacterium.

Anabaena sp. PCC 7120 is a filamentous, nitrogen-fixing, heterocyst-forming cyanobacterium.

Anabaena siamensis TISTR 8012 is a filamentous, nitrogen-fixing, heterocyst-forming cyanobacterium.

3.1.6.2 Bacteria

Escherichia coli strains DH5α, genotype (F^-, φ80d*lacZ*ΔM15, Δ(*lacZYA-argF*)U169, *deoR*, *recA*1, *endA*1, *hsdR*17(rk^-, mk^+), *phoA*, *supE*44, λ^-, *thi*-1, *gyrA*96, *relA*1), was used as a host for plasmid propagation. The organism was obtained from Professor Dr. Teruhiro Takabe.

Escherichia coli strains ME9107, genotype (F, HfrKL16(po61), *recB*21, *sbcA*8, *thr*-300, *ilv*-318, *spc*300) was used a host for biochemical studies of *ApgltS* expression. The organism was obtained from Professor Dr. Teruhiro Takabe.

3.1.7 Plasmids

pBluescript® SK (+) (Toyobo, Japan): cloning vector; β-galactosidase α-fragment coding sequence (lacZ') is present in this phagemid but the coding sequence is interrupted by the large polylinker. Phagemid having no inserts in the polylinker will produce blue colonies in *E. coli* while phagemid that have inserts will produce white colonies using the same strain, because the inserts disrupt the

coding region of the *lac*Z gene fragment. The organism was kindly provided from Professor Dr. Teruhiro Takabe. Circle maps are shown in APPENDIX 1.

pTrcHis2C (Invitrogen, USA): expression vector of recombinant proteins containing C-terminal 6xHis tags in *E. coli*. Moreover, this vector contains ampicillin resistance gene which allows selection of the plasmid in *E. coli*. The organism was kindly obtained from Professor Dr. Teruhiro Takabe. Circle maps are shown in APPENDIX 2.

pCR 2.1 (Invitrogen, USA): cloning vector provides 3'-T overhangs for direct ligation of *Taq*-amplified PCR products containing T7 promoter for *in vitro* RNA. This vector contains ampicillin resistance gene and kanamycin resistance gene which allows selection of the plasmid in *E. coli*. The organism was kindly provided from Dr. Worrawat Promden. Circle maps are shown in APPENDIX 3.

pQF50: broad-host range *lacZ* promoter-probe vector (Farinha and Kropinski, 1990). This vector contains ampicillin resistance gene which allows selection of the plasmid in *E. coli*. The organism was kindly obtained from Dr. Worrawat Promden. Circle maps are shown in APPENDIX 4.

pUC303: *E. coli/Synechococcus* shuttle vector for expression of recombinant proteins; this vector contains chloroamphenicol resistance gene which allows selection of the plasmid in *Synechococcus*. The organism was kindly provided from Professor Dr. Teruhiro Takabe. Circle maps are shown in APPENDIX 5.

3.2 Methods

3.2.1 Strains and growth conditions

The halotolerant cyanobacterium, *Aphanothece halophytica* was grown photoautotrophically in BG_{11} medium plus 18 mM $NaNO_3$ and Turk Island salt solution (APPENDIX 6) containing 0.5 M NaCl. Other cyanobacterial strains, *Synechocystis* sp. PCC 6803, *Synechococcus* sp. PCC 7942, *Arthrospira platensis, Anabaena siamensis* TISTR 8012 and *Anabaena* sp. PCC 7120 were grown in normal BG_{11} liquid medium (APPENDIX 6). These media were buffered with 10 mM HEPES-KOH (pH 7.6). The cultures were grown aerobically under continuous illumination of 40 µE $m^{-2}s^{-1}$ with cool white fluorescent lamps from two sides on a rotatory shaker at 160 rpm and 30 °C. These will be referred to as standard growth condition.

E. coli DH5α cells were grown in Luria-Bertani (LB) medium as described in APPENDIX 7. *E. coli* strain ME9107 which is analogous to JS5412 [110] and deficient for uptake of glutamate was obtained from National Institute of Genetics (Mishima, Shizuoka, Japan). *E. coli* ME9107 were grown in minimal medium A, pH 7.5 (MMA, APPENDIX 8) containing 0.2% glucose and 50 $\mu g.ml^{-1}$ ampicillin (APPENDIX 9). The cell growth at 37 °C was monitored by measuring turbidity of the culture using a spectrophotometer set at a wavelength of 620 nm.

3.2.2 Effect of NaCl concentration on growth rate of *A. halophytica*

Mid-log phase *A. halophytica* cells grown in BG_{11} medium plus 18 mM $NaNO_3$ and Turk Island salt solution containing 0.5 M NaCl were used as the starting culture. The starting culture was inoculated into BG_{11} medium plus 18 mM $NaNO_3$ and Turk Island salt solution containing various concentrations of NaCl from 0.0 -3.0 M and continued culture at 30 °C with shaking 160 rpm under continuous illumination of 40 $\mu Em^{-2}s^{-1}$ with cool white fluorescent lamps. The initial cell concentration was adjusted to an OD_{750} of 0.1. The growth was monitored by measuring an optical density at 750 nm (OD_{750}).

3.2.3 Effect of amino acid supplementation on growth rate of *A. halophytica* under normal and salt stress conditions

Mid-log phase *A. halophytica* cells grown in BG_{11} medium plus 18 mM $NaNO_3$ and Turk Island salt solution containing 0.5 M NaCl were used as the starting culture. The starting culture was inoculated into BG_{11} medium plus 18 mM $NaNO_3$ and Turk Island salt solution containing 0.5 M NaCl (normal growth condition) and 2.0 M NaCl (salt stress condition) supplemented with 1 mM each of 20 amino acids and continued culture at 30 °C with shaking 160 rpm under continuous illumination of 40 $\mu Em^{-2}s^{-1}$ with cool white fluorescent lamps. The initial cell concentration was adjusted to an OD_{750} of 0.1. The growth was monitored by measuring an optical density at 750 nm (OD_{750}).

3.2.4 Effect of glutamate supplementation on growth rate of *A. halophytica* under normal and salt stress conditions

Mid-log phase *A. halophytica* cells grown in BG_{11} medium plus 18 mM $NaNO_3$ and Turk Island salt solution containing 0.5 M NaCl were used as the starting culture. The starting culture was inoculated into BG_{11} medium plus 18 mM $NaNO_3$ and Turk Island salt solution containing 0.5 M NaCl (normal growth condition) and 2.0 M NaCl (salt stress condition) supplemented with various concentrations of glutamate from 0-50 mM and continued culture at 30 °C with shaking 160 rpm under continuous illumination of 40 $\mu Em^{-2}s^{-1}$ with cool white fluorescent lamps. The initial cell concentration was adjusted to an OD_{750} of 0.1. The growth was monitored by measuring an optical density at 750 nm (OD_{750}).

3.2.5 Characterization of glutamate transport in *A. haolphytica*

3.2.5.1 Glutamate uptake assay

Mid log phase cells at were harvested by centrifugation (3,500 *xg*, 10 min, $4^{o}C$), washed twice with 50 mM *N*-2-hydroxyethylpiperazine-*N'*-2-ethanesulfonic acid (HEPES)-KOH buffer pH 7.6, and suspended to a concentration of 0.1 mg of cell protein ml^{-1} in the assay buffer containing same NaCl concentration with the growth medium. The uptake experiment was initiated by adding [U-^{14}C]-glutamate with a specific activity of 218 μCi μmol^{-1} at a final concentration of 0.1 μM. For K_m and V_{max} determinations, the concentrations of glutamate were varied from 0 to 100 μM.

Various co-factors, cations and anions were added to the indicated concentrations. Competitions for glutamate uptake were performed in the presence of 100-fold molar excess competitors. The cells suspension was withdrawn rapidly filtered through HAWP cellulose acetate filters (0.45 μm pore size; Millipore). The filters were washed twice with 3 ml of buffer (the same salinity as assay buffer) and the radioactivity trapped in the cells was measured with scintillation fluid (APPENDIX 10) and determined with a liquid scintillation counter. Protein content will be determined by method of Bradford (1976) [12] using bovine serum albumin as a standard as shown in APPENDIX 11.

3.2.5.2 Effect of NaCl concentration on glutamate uptake in *A. halophytica*

The glutamate uptake was done as described in 3.2.5.1 by varying the NaCl concentration from 0.0 to 3.0 M in the assay medium.

3.2.5.3 Effect of pH on glutamate uptake in *A. halophytica*

The glutamate uptake was done as described in 3.2.5.1 by varying the pH from 5.5 to 10.5., 100 mM potassium phosphate buffer pH 5.5-6.5, 100 mM Tris-HCl, pH 7.0-9.0 and 100 mM Borate buffer pH 9.5-10.5.

3.2.5.4 Substrate specificity of glutamate uptake in *A. halophytica*

The specificity of glutamate uptake was determined by measuring the initial rate of [U-^{14}C] glutamate uptake as described in 3.2.5.1 in the presence of 100 folds excess of unlabeled competitive substrate in the assay medium.

3.2.5.5 Effect of different energy sources on glutamate uptake in *A. halophytica*

Mid-log phase cells were starved by suspending cells in the assay buffer in the dark for 2 h. The starved cells were assayed for glutamate uptake as described in 3.2.5.1 in the presence of different energy sources

3.2.5.6 Effect of metabolic inhibitors, ionophores and ATPase inhibitors on glutamate uptake in *A. halophytica*

Mid-log phase cells were pre-incubated with the tested compound(s) in the dark for 30 min. The starved cells were assayed for glutamate uptake as described in 3.2.5.1 in the presence of different metabolic inhibitors.

3.2.6 Isolation of *A. halophytica* glutamate transporter gene (*ApgltS*)

3.2.6.1 Database searches

Based on the shot gun sequencing of *A. halophytica,* we found that *A. halophytica* contained Na^+-dependent glutamate transporter (*ApgltS*) gene consisted of 1431 bp long. The nucleotide sequence of *ApgltS* gene was used as query for conversion to protein sequence by translation tool (http://web.expasy.org/translate/). The theoretical pI (isoelectric point) and Mw (molecular weight) of ApGltS were computed by Compute pI/Mw tool (http://web.expasy.org/compute_pi/). The deduced amino acid sequence of ApGltS was used as a query for domain search using InterProScan (http://www.ebi.ac.uk/InterProScan) and transmembrane prediction using Hydropathy analysis (http://www.tcdb.org/progs/hydro.php) and TMHTMM Server v. 2.0 (http://www.cbs.dtu.dk/services/TMHMM/). To identify members of cyanobacteria Na^+-dependent glutamate transporter, the Basic Local Alignment Search Tool (BLAST) algorithms (BlastP and BlastN) of the Cyanobase and NCBI database using the sequence of *A. halophytica* Na^+-dependent glutamate transporter as query was conducted. Nucleotide and amino acid sequences as well as information regarding each gene of interest were obtained.

3.2.6.2 Alignments and tree construction

Deduced sequences of proteins identified by InterProScan as containing a Na^+/glutamate symporter domain, IPR004445 were aligned with one another comparing with ApGltS by Align (http://www.ebi.uk.ac) and the percentage of amino acid identity was calculated by dividing the number of identical amino acids by the total number of amino acid residues of the aligned sequences. Deduced amino acid sequences of ApGltS and cyanobacterial IPR004445-containing proteins were subjected to phylogenetic analysis. Multiple alignments of amino acid sequences were performed by ClustalX program [109] using default settings. Alignments were carried out and protein trees were constructed using the neighbor-joining algorithm by Clustal X program (default settings) [109]. Bootstrap analysis with 1000 replicates was used to evaluate the significance of the nodes. Na^+/glutamate transporter of *Escherichia coli* (EcGltS; GenBank: AP_004139) are used as outgroup.

Comparison of 7 cyanobacterial IPR004445-containing proteins with ApGltS by multiple sequence alignment was performed by Clustal X program [109]. For generating the phylogenetics tree of marine cyanobacterial GltS and bacterial glutamate transporter, we used Clustal X program (default settings) [109] and neighbor-joining method with Bootstrap analysis with 1000 replicates.

3.2.6.3 Oligonucleotides

Oligonucleotide primers were designed from the nucleotide sequence of *A. halophytica* Na^+-dependent glutamate transporter (*ApgltS*) gene obtained from the shot gun sequencing of *A. halophytica.* PCR amplification was carried out using forward and reverse oligonucleotide primers shown in Table 3.1.

Table 3.1 Oligonucleotide primers of *A. halophytica* Na^+/glutamate transporter.

Primer name	Primer sequences (5′ to 3′)	Product length (bp)	Purpose
*ApgltS*proBamHI-F	CTT**GGTCCA**GTAACTTAATCTAGAT	273	*ApgltS* upstream PCR amplification
*ApgltS*proNcoI-R	GT**CCATGG**GACTATAATCCTTCCTCTTC		
*ApgltS*NcoI-F	TC**CCATGG**ACACCACTAACTTAGGATTA	1,439	Coding region of *ApgltS* PCR amplification
*ApgltS*SalI-R	CT**GTCGAC**CATCAAAGTTTTCGGTTTAAC		

3.2.6.4 *A. halophytica* genomic DNA extraction

Mid-log phase cells were harvested by centrifugation (3,500 *xg*, 10 min, 4 °C) and washed twice with SET buffer (20% sucrose, 50 mM EDTA and 50 mM Tris-HCl, pH 7.6). Pellet was frozen at -20 °C for 2 hrs, then thawed at 65 °C for 10 min and re-suspended in SET buffer. Cells were lyzed

by using lysozyme (final concentration 0.5 $mg.ml^{-1}$), incubated at 37 °C for 30 min under gentle shaking. Subsequently, 0.5% SDS and 0.25 $mg.ml^{-1}$ RNase were added. After an incubation at 37 °C for 3 hrs, 0.25 $mg.ml^{-1}$ proteinase K was added and further incubated for 30 min. The mixture was extracted once with equal volume of phenol/chloroform/isoamylalcohol (25:24:1), mixed gently and centrifuged at 8,000 *xg* for 5 min at 25 °C. The aqueous layer was collected and re-extracted at least 3 times with equal volume of phenol/chloroform/isoamylalcohol. High molecular weight DNA was precipitated by adding 2 volume of absolute ethanol and chilled at -20 °C for 1-2 hrs. Chromosomal DNA was collected by centrifugation at 8,000 *xg* for 5 min at 4 °C and washed once with 70% ethanol. Chromosomal DNA was allowed to dry under vacuum and suspended with TE buffer, pH 8.0 (10 mM Tris-HCl, pH 8.0 and 1 mM EDTA). This DNA solution was then stored at -20 °C until use. To determine concentration and purity of chromosomal DNA, sampled was diluted with TE buffer and checked by measuring the ratio of OD_{260}/OD_{280}.

3.2.6.5 Isolation of *ApgltS* gene

The coding region of *ApgltS* was amplified by PCR using *A. halophytica* genomic DNA as template and the primer set, *ApgltS*NcoI-F and *ApgltS*SalI-R (Table 3.1) containing *NcoI* site and *Sal*I site, respectively. The 50 µl of reaction mixture contained 5 U of *Taq* DNA polymerase, 200 µM

dNTPs, 1x PCR buffer, 2.5 mM $MgCl_2$, 50-100 pmole of *A. halophytica* genomic DNA, and 10 pmole of each primer. PCR amplification was performed as follows: pre-denaturation at 94 °C for 5 mins, 35 cycles of denaturation at 94°C for 2 mins, annealing at 50°C for 1.5 mins, and extension at 72°C for 2 mins for coding region *of ApgltS* gene. The final extension step was performed at 72 °C for 10 mins. PCR products were separated by agarose gel electrophoresis (APPENDIX 12) and visualized by ethidium bromide staining and UV transilluminator and photographed.

3.2.6.6 Cloning of *ApgltS* gene into cloning vector pBluescript® II SK (+)

The resulting PCR products were purified by Suprec™-O2 followed by ligation into cloning vector pBluescript® II SK (+) digested at *EcoR*V site (APPENDIX 13). The resulting plasmid, $pBSK^+$-*ApgltS*, was transformed into *E. coli* DH5α cells by heat shock method (Appendix 17). The positive clones were selected on LB agar containing 100 $\mu g.ml^{-1}$ ampicillin and 32 $\mu g.ml^{-1}$ X-gal, allowed to grow at 37 °C for 16 hrs and the plasmids were extracted by alkaline lysis method (Appendix 18). Insert fragment of an expected size 1,439 kb was sequenced with primer set, M13-F and M13-R (Table 3.2).

Table 3.2 Sequencing primers of *A. halophytica* Na^+/glutamate transporter.

Primer name	Primer sequences (5′ to 3′)	Purpose
M13-F	GTAAAACGACGGCCAGT	Sequencing primer
M13-R	CCTTTGTCGATACTGGTACT	Sequencing primer
TrcgltS1481-F	GCTGCAAATGGTCGATCCAGCTA	Sequencing primer
TrcgltS624-R	CGCGAGGATCGATTCTGGTA	Sequencing primer
terTrcgltS-R	GCGTCACCGACAAACAACAGAT	Sequencing primer
6XHisStopBamHI-R	GTGGATCCTCAATGATGATGATGATG	Sequencing primer and reverse primer for PCR amplification

3.2.6.7 Construction of pTrcHis2_C recombinant plasmid containing *ApgltS* gene

The recombinant plasmid, pBSK$^+$-*ApgltS*, was double digested with *Nco*I and *Sal*I (APPENDIX 13). The cohesive end fragment was ligated into *Nco*I and *Sal*I site of the digested pTrcHis2_C expression vector. The resulting plasmid, p*ApgltS* harboring *ApgltS*, encoding glutamate transporter gene fused in frame to six histidines at the C terminus, was transformed first into *E. coli* DH5α cells by heat shock method. The positive clones was selected on LB agar containing ampicillin, allowed to grow at 37 °C for 16 hrs and the plasmids were extracted by alkaline lysis method (Appendix 18). The

recombinant plasmid, p*ApgltS*, was digested with restriction enzyme (APPENDIX 13) and confirmed from the mobility of agarose electrophoresis of DNA fragments (APPENDIX 12). To confirm the insertion of purified *ApgltS* fragment into pTrcHis2_C, DNA sequencing was performed with primers as shown in Table 3.2.

3.2.6.8 Expression of ApGltS in *E. coli* ME9107 under trc promoter using anti-His-tag antibodies

The recombinant plasmid, p*ApgltS*, was extracted and then transformed to *E. coli* strain ME9107 cell, which is analogous to JS5412 and deficient for uptake of glutamate was obtained from National Institute of Genetics (Mishima, Shizuoka, Japan). The *ApgltS* expressing *E. coli* ME9107 and *E. coli* ME9107 transformed with pTrcHis2_C were grown at 37 °C in MMA, pH 7.5 containing 0.2% glucose and 50 $\mu g.ml^{-1}$ ampicillin and were inoculated into the same fresh medium with an OD_{620} of 0.05. The *ApgltS* expressing *E. coli* ME9107 were grown at 37 °C until optical density at 620 nm reached 0.3. Then, 1 mM isopropyl β-D-1-thiogalactopyranoside (IPTG) was added. After 5 h of incubation, cells were harvested, washed twice and with 20 mM Tris-HCl, pH 7.6 containing 1.0 M sucrose. The collected cells were re-suspended in periplasting buffer (20% sucrose, 1 mM EDTA). The sample was incubated on ice for 5 min and gently mixed by slow pipetting. The sample was again incubated on ice for another 5 min. The sample was

centrifuged at 8,000 *xg* for 2 min to recover the supernatant as the periplasmic fraction and the pellet contained spheroplast. Spheroplasts are lysed using a lysis buffer (10 mM Tris-HCl pH 7.5, 50 mM KCl, 1 mM EDTA, and 0.1% Deoxycholate). The sample was allowed to sit at room temperature for 5 min to cause spheroplast swelling and lysis. The sample was then sonicated with a micro-tip at approximately 30-40% full power in 2 second bursts. Spheroplasmic fraction in the supernatant obtained by centrifugation at 12,000 *xg* for 15 mins. The spheroplasmic fraction was further fractionated by ultra-centrifugation to separate the membranes from the cytoplasmic fraction. The spheroplasmic fraction was centrifuged at 138,000 *xg* for 1 hr. The supernatant was reserved as the cytoplasmic fraction and the pellet was reserved as membrane fraction.

Fifty microgram of membrane fraction were separated by 12.0% sodium dodecyl polyacrylamide gel electrophoresis (SDS-PAGE) (APPENDIX 19) and transferred to PVDF membrane by blotting transfer buffer (APPENDIX 20). Blotting was done at 150 $mA.in^{-2}$ for 1 hr followed by blocking in blocking solution (APPENDIX 20) for 2 hrs. The PVDF membrane was incubated with anti-6xHis as primary antibody (an antibody raised against 6-histidine, 6xHis tag) for 1 hr and washed with 100 ml of PBS plus 5% skim milk solution for 15 mins, 3 times. After washing with PBS buffer plus 0.5% skim milk, the membrane was immediately incubated with anti-mouse immunoglobulin G as secondary antibody (an antibody raised against mouse) for 1 hr and washed

with 100 ml of PBS plus 5% skim milk buffer for 15 mins, 3 times. The PVDF membrane was visualized after incubation with the detection reagent (APPENDIX 21) for 30 min.

3.2.6.8.1 Effect of IPTG concentration on the expression of ApGltS in *E. coli* ME9107

The western blot was done as described in 3.2.6.8 by varying the concentrations of IPTG 0.0 to 3.0 mM in induction step.

3.2.6.8.2 Effect of NaCl in the growth medium on the expression of ApGltS in *E. coli* ME9107

The western blot was done as described in 3.2.6.8 by varying the concentrations of NaCl 0.0 to 0.5 mM in MMA, pH 7.5.

3.2.7 Characterization of ApGltS in *E. coli* ME9107

3.2.7.1 Complementation tests of *ApgltS* expressing *E. coli* ME9107

For the complementation test on liquid medium, *E. coli* ME9107 transformed with pTrcHis2_C and transformed with p*ApgltS* which were grown overnight at 37 °C in MMA, pH 7.5 containing 0.2% glucose and 50 $\mu g.ml^{-1}$ ampicillin were inoculated into MMA, pH 7.5 containing 0.2% glucose, 50 $\mu g.ml^{-1}$ ampicillin, 1 mM IPTG, and indicated concentrations of NaCl (0, 0.25 and 0.5 M) supplemented with 0, 1 and 5 mM glutamate with an OD_{620}

of 0.05 and incubated at 37°C for the indicated times. The growth was monitored by measuring optical density of culture at 620 nm.

3.2.7.2 Transport assays

The *E. coli* ME9107 transformed with pTrcHis2_C and transformed with p*ApgltS* which were grown overnight at 37 °C in MMA, pH 7.5 containing 0.2% glucose and 50 μg.ml^{-1} ampicillin were inoculated into the same fresh medium with an OD_{620} of 0.05. 1 mM IPTG was added into medium. After 3 h of incubation, cells were harvested, washed twice, and suspended to an OD_{620} of 1.0 in 100 mM sodium phosphate buffer pH 7.5 containing 5 mM glucose. Subsequently, the cell suspension was shaken for 5 min at 37 °C, and the uptake was initiated by the addition of 0.1 mM [U-^{14}C] glutamate as described in 3.2.5.1. For K_m and V_{max} determinations, the concentrations of glutamate were varied from 0.5 to 100 μM. Various co-factors, cations and anions were added to the indicated concentrations. Competitions for glutamate uptake were performed in the presence of 100-fold molar excess competitors. The cells suspension was withdrawn rapidly filtered through HAWP cellulose acetate filters (0.45 μm pore size; Millipore). The filters were washed twice with 3 ml of buffer (the same salinity as assay buffer) and the radioactivity trapped in the cells was measured with scintillation fluid and determined with a liquid scintillation counter. Protein content will be

determined by method of Bradford (1976) [12] using bovine serum albumin as a standard.

3.2.8 Construction of expression plasmid pUC303-pGH-Amp

3.2.8.1 Promoter region of *ApgltS* gene

3.2.8.1.1 Promoter analysis

From the shot gun sequencing of *A. halophytica*, we found the 262-bp of non-coding region within 5' upstream region of the *ApgltS* gene. The putative promoter sequence of *ApgltS* gene was used as a query for promoter analysis. First, transcription start site and promoter prediction was performed using The Berkeley Drosophila Genome Project (BDGP: http://www.fruitfly.org/seq_tools/promoter.html). The consensus sequence at -10 and -35 regions were predicted by GENETYX7. The putative lactococcal-like sigmaA binding domain was identified using Prokaryotic Promoter Prediction (PPP: http://bioinformatics.biol.rug.nl/websoftware/ppp/ppp_start.php).

3.2.8.1.2 Amplification of promoter region of *ApgltS* gene

The promoter region of *ApgltS* was amplified by PCR using *A. halophytica* genomic DNA as template and the primer set, *ApgltS*proBamH-F and *ApgltS*proNco-R (Table 3.1) containing *BamH*I site and *NcoI* site, respectively. The 50 µl of reaction mixture contained 5 U of *Taq* DNA polymerase, 200 µM dNTPs, 1x PCR buffer, 2.5 mM $MgCl_2$,

50-100 pmole of *A. halophytica* genomic DNA, and 10 pmole of each primer. PCR amplification was performed as follows: pre-denaturation at 94 °C for 5 mins, 35 cycles of denaturation at 94°C for 2 mins, annealing at 50°C for 0.5 min, and extension at 72°C for 2 mins for promoter region *of ApgltS* gene. The final extension step was performed at 72 °C for 10 mins. PCR products were separated by agarose gel electrophoresis and visualized by ethidium bromide staining and UV transilluminator and photographed.

3.2.8.1.3 Construction of *ApgltS* promoter-probe vector

The resulting PCR products were purified by Suprec™-O2 followed by ligation into cloning vector pCR®2.1 (APPENDIX 3). The resulting plasmid, pCR®2.1-progltS, was transformed into *E. coli* DH5α cells by heat shock method. The positive clones were selected on LB agar containing 100 μg.ml^{-1} ampicillin, allowed to grow at 37 °C for 16 hrs and the plasmids were extracted by alkaline lysis method. To verify the insertion of PCR products, pCR®2.1-progltS was double restriction digested with *Nco*I and *Sph*I, then analyzed by 1% agarose gel electrophoresis.

The 318-bp promoter region of *ApgltS* gene was purified by Suprec™-O1 and ligated into the *NcoI/Sph*I sites of promoter-probe vector, pQF50. The recombinant plasmid, pQF50-promotergltS, was transformed into the *E. coli* DH5α by heat shock method. The

transformants were selected by blue-white colony screening on ampicillin agar plates containing 32 μg.ml^{-1} X-gal. Blue colonies were randomly selected and cultured in 1 ml LB broth containing 100 μg.ml^{-1} ampicillin and 32 μg.ml^{-1} X-gal at 37 °C overnight and the cultures were subjected to plasmid extraction.

To verify the insertion of DNA fragments into pQF50, the recombinant plasmid, pQF50-promotergltS, was used as template for PCR amplification using primer set, *ApgltS*proBamH-F and *ApgltS*proNco-R (Table 3.1) and analyzed by 1% agarose gel electrophoresis.

3.2.8.1.4 Promoter activity characterization of pQF50-promotergltS

The *E. coli* DH5α transformed with pQF50-promotergltS were grown overnight at 37 °C on rotary shaker at 250 rpm in LB medium containing 100 μg.ml^{-1} ampicillin. One ml of culture was collected and washed with equal volume of basal medium. Cell suspension was dilute fivefold on basal medium containing 100 μg.ml^{-1} ampicillin and inducer (0, 0.25 and 0.50 mM NaCl and/or 0, 1 and 5 mM glutamate). After shaking the culture for 6 hrs at 37°C, cultures were incubated on ice to stop growth. Measure A_{620} of the culture medium and reread the absorbance. The β-galactosidase activity induced was determined according to the procedure of Miller [69].

For most activities, 0.1 ml cells and 0.9 ml Z buffer (APPENDIX 26) will produce a desirable amount of yellow color in 7-60 mins. The diluted cells were permeabilized by adding 100 µl chloroform and 50 µl 0.1% SDS and mixed. The mixture was then incubated at 30°C for 10 mins. The reaction was started by adding 0.2 ml *O*-nitrophenyl-beta-D-galactoside (4 $mg.ml^{-1}$ ONPG) then incubated at 37°C and stopped the reaction after sufficient yellow color (A_{420} should be in the range of 0.6 to 0.9) has developed by adding 0.5 ml of 1.0 M Na_2CO_3 then vortex and recorded the reaction time precisely. Transferred 1 ml to a microtube, centrifuged at 12,000 rpm for 5 mins to remove debris and chloroform. Recorded the absorbance at 420 nm and at 550 nm for each tube and calculated the unit of activity using the equation shown below.

$$\text{Miller Unit} = 1000 \times [(A_{420} - 1.75 \times A_{550})] / (T \times V \times A_{620})$$

A_{420} and A_{550} are read from the reaction mixture

A_{620} reflects cell density in the cultured cell

T represents time of the reaction in minutes

V represents volume of culture used in the assay in ml

3.2.8.2 Construction of pBluescript® II SK$^+$ recombinant plasmid containing promoter region of *ApgltS* gene

The purified PCR products of *ApgltS* promoter region were ligation into cloning vector pBluescript® II SK (+) digested at *EcoR*V site. The resulting plasmid, pBSK$^+$-promoter*ApgltS*, was transformed into *E. coli* DH5α cells by heat shock method. The positive clones were selected on LB agar containing 100 μg.ml^{-1} ampicillin and 32 μg.ml^{-1} X-gal, allowed to grow at 37 °C for 16 hrs and the plasmids were extracted by alkaline lysis method. The recombinant plasmid, pBSK$^+$-promoter*ApgltS*, was digested with restriction enzyme and confirmed from the mobility of agarose electrophoresis of DNA fragments. To confirm the insertion of purified promoter region of *ApgltS* gene into pBSK$^+$, DNA sequencing was performed with primer set, M13-F and M13-R as shown in Table 3.2.

3.2.8.3 Amplification of the coding region of *ApgltS* gene containing 6xHis-tag

The coding region of *ApgltS* gene containing 6xHis-tag was amplified by PCR using p*ApgltS* as template and the primer set, *ApgltS*NcoI-F (Table 3.1) and 6XHisStopBamHI-R (Table 3.2) containing *BamH*I site and *NcoI* site, respectively. The 50 μl of reaction mixture contained 5 U of *Taq* DNA polymerase, 200 μM dNTPs, 1x PCR buffer, 2.5 mM $MgCl_2$, 50-100 pmole of p*ApgltS*, and 10 pmole of each primer. PCR amplification was performed as

follows: pre-denaturation at 94 °C for 5 mins, 35 cycles of denaturation at 94°C for 2 mins, annealing at 55°C for 0.5 min, and extension at 72°C for 2 mins for promoter region *of ApgltS* gene. The final extension step was performed at 72 °C for 10 mins. PCR products were separated by agarose gel electrophoresis and visualized by ethidium bromide staining and UV transilluminator and photographed.

3.2.8.4 Construction of pBluescript® II SK$^+$ recombinant plasmid containing the coding region of *ApgltS* gene containing 6xHis-tag

The resulting PCR products were purified by Suprec^{Tm}-O2 followed by ligation into cloning vector pBluescript® II SK (+) digested at *EcoR*V site. The resulting plasmid, pBSK$^+$-promoter*ApgltS*, was transformed into *E. coli* DH5α by heat shock method. The positive clones were selected on LB agar containing 100 μg.ml^{-1} ampicillin and 32 μg.ml^{-1} X-gal, allowed to grow at 37 °C for 16 hrs and the plasmids were extracted by alkaline lysis method. To verify the insertion of PCR products into pBSK$^+$, the recombinant plasmid, pBSK$^+$-promoter*ApgltS*, was digested with restriction enzyme and confirmed from the mobility of agarose electrophoresis of DNA fragments.

3.2.8.5 Construction of pBluescript® II SK$^+$ recombinant plasmid containing the promoter region and coding region of *ApgltS* gene containing 6xHis-tag

pBSK$^+$-*gltSHis-F* was double digested with *Nco*I and *Sac*I. The coding region of *ApgltS* gene containing 6xHis-tag fragments was analyzed by agarose gel electrophoresis and purified by Suprec^{Tm}-O1. The purified fragments were ligated into the *Nco*I/*Sac*I sites of pBSK$^+$-promoter*ApgltS.* The recombinant plasmid, pBSK$^+$-promoterGltSHis, was transformed into the *E. coli* DH5α cells by heat shock method. The positive clones were selected on LB agar containing 100 μg.ml^{-1} ampicillin and 32 μg.ml^{-1} X-gal, allowed to grow at 37 °C for 16 hrs and the plasmids were extracted by alkaline lysis method. To verify the insertion of DNA fragments into pBSK$^+$, the recombinant plasmid, pBSK$^+$-promoterGltSHis, was amplified using primer set, *ApgltS*proBamHI-F and 6XHisStopBamHI-R and analyzed by agarose gel electrophoresis.

The 50 μl of reaction mixture contained 5 U of *Taq* DNA polymerase, 200 μM dNTPs, 1x PCR buffer, 2.5 mM $MgCl_2$, 50-100 pmole of DNA template, and 10 pmole of each primer. PCR amplification was performed as follows: pre-denaturation at 94 °C for 5 mins, denaturation at 94°C for 2 mins, annealing at 55°C for 1 min, and extension at 72°C for 2 mins. The final extension step was performed at 72 °C for 10 mins. PCR products were separated by agarose gel electrophoresis and

visualized by ethidium bromide staining and UV transilluminator and photographed.

3.2.8.6 Construction of pUC303 containing ampicillin resistant gene (pUC303-Amp)

Firstly, pBluescript® II SK^+ was digested with *Pvu*II and analyzed by agarose gel electrophoresis. 2.96 kb fragments of $pBSK^+$ were purified by Suprec^{Tm}-O1 and treated with T4 DNA Polymerase to create ***blunt ends.*** pUC303 was digested with *Xho*I and analyzed by agarose gel electrophoresis. 10.80 kb fragments of pUC303 were purified by Suprec^{Tm}-O1 and treated with T4 DNA Polymerase to create blunt ends.

The blunt end treated pUC303*/Xho*I was ligated with blunt end treated $pBSK^+$*/Pvu*II. The recombinant plasmid, pUC303-Amp, was transformed into the competent *E. coli* DH5α by heat shock method. The positive clones were selected on LB agar containing 100 $\mu g.ml^{-1}$ ampicillin, allowed to grow at 37 °C for 16 hrs and the plasmids were extracted by alkaline lysis method. To verify the insertion of DNA fragments into pUC303, the recombinant plasmid, pUC303-Amp, was digested with restriction enzyme and confirmed from the mobility of agarose electrophoresis of DNA fragments.

3.2.8.7 Construction of pUC303-Amp recombinant plasmid containing the promoter region and coding region of *ApgltS* gene containing 6xHis-tag

pBSK^{+}-promoterGltSHis and pUC303-Amp were each digested with *BamH*I and was analyzed by agarose gel electrophoresis. 1729 bp of the promoter region and coding region of *ApgltS* gene containing 6xHis-tag fragments and linearized pUC303-Amp were purified by Suprec^{Tm}-O1 and performed ***ligation*** reaction using T4 DNA ligase. The recombinant plasmid, pUC303-pGH-Amp, was transformed into the competent *E. coli* DH5α by heat shock method. The positive clones were selected on LB agar containing 100 μg.ml^{-1} streptomycin, allowed to grow at 37 °C for 16 hrs and the plasmids were extracted by alkaline lysis method. To verify the insertion of DNA fragments into pUC303-Amp, the recombinant plasmid, pUC303-pGH-Amp, was digested with restriction enzyme and confirmed from the mobility of agarose electrophoresis of DNA fragments.

Next, pUC303-Amp and pUC303-pGH-Amp were prepared and transformed to the *Synechococcus* sp. PCC 7942 competent cells by natural transformation (APPENDIX 27). The transformants were selected on BG_{11} agar containing 50 μg.ml^{-1} streptomycin and 1 μg.ml^{-1} ampicillin. The positive clones were picked and then transferred to BG_{11} liquid medium containing 50 μg.ml^{-1} streptomycin and 1 μg.ml^{-1} ampicillin. After cultivation for 2 weeks, the plasmids were extracted (APPENDIX 28). and used as template for PCR

amplification using chloramphenicol-specific primers (Table 3.3) and primer set, *ApgltS*proBamHI-F and 6XHisStopBamHI-R

Table 3.3 Oligonucleotide primers of chloramphenicol resistant gene.

Primer name	Primer sequences (5′ to 3′)	Product length (bp)	Purpose
pACYC184cm-F	ATCGGCACGTAAGAGGTTCCAACT	800	Coding region of chloramphenicol resistant gene PCR amplification
pACYC184cm-R	GCTTTCGAATTTCTGCCATTCATC		

PCR amplification of primer set, *ApgltS*proBamHI-F and 6XHisStopBamHI-R, was done as described in 3.2.6.5. For chloramphenicol resistance gene, 50 µl of reaction mixture contained 5 U of *Taq* DNA polymerase, 200 µM dNTPs, 1x PCR buffer, 2.5 mM $MgCl_2$, 50-100 pmole of DNA template, and 10 pmole of each primer. PCR amplification was performed as follows: pre-denaturation at 94 °C for 5 mins, denaturation at 94°C for 2 mins, annealing at 58°C for 1 min, and extension at 72°C for 2 mins. The final extension step was performed at 72 °C for 10 mins. PCR products were separated by agarose gel electrophoresis and visualized by ethidium bromide staining and UV transilluminator and photographed.

3.2.9 Characterization of ApGltS in *Synechococcus* sp. PCC 7942

3.2.9.1 Growth rate of *ApgltS* expressing *Synechococcus* sp. PCC 7942

Synechococcus sp. PCC 7942 transformed with pUC303-Amp (pUC303-Amp/7942) and pUC303-pGH-Amp (pUC303-pGH-Amp/7942) were grown in BG_{11} medium containing 50 μg.ml^{-1} streptomycin and 1 μg.ml^{-1} ampicillin, and indicated concentrations of NaCl (0 and 0.2 M) supplemented with 0, 1, 5 and 10 mM glutamate at 30 °C with shaking 160 rpm under continuous illumination of 40 μEm^{-2}s^{-1} with cool white fluorescent lamps. The growth was monitored by measuring optical density of culture at 750 nm.

3.2.9.2 Glutamate transport assay in *ApgltS* expressing *Synechococcus* sp. PCC 7942

Mid log phase cells at were harvested by centrifugation (3,500 *xg*, 10 min, 4°C), washed twice with 50 mM *N*-2-hydroxyethylpiperazine-*N*'-2-ethanesulfonic acid (HEPES)-KOH buffer pH 7.6, and suspended to a concentration of 0.1 mg of cell protein.ml^{-1} in the assay buffer containing various NaCl concentration. The uptake experiment was initiated by adding 0.1 mM [U-^{14}C] glutamate as described in 3.2.5.1. For K_m and V_{max} determinations, the concentrations of glutamate were varied from 0 to 100 μM. The cells suspension was withdrawn rapidly filtered through HAWP cellulose acetate filters (0.45 μm pore size; Millipore). The filters were washed twice with 3 ml of buffer (the same salinity as assay buffer) and the

radioactivity trapped in the cells was measured with scintillation fluid and determined with a liquid scintillation counter. Protein content will be determined by method of Bradford (1976) [12] using bovine serum albumin as a standard.

3.2.10 Quantification of intracellular amino acids of *A. halophytica*

Mid log phase of *A. halophytica* cells grown in the growth medium containing 0.5 and 2.0 M NaCl were harvested by centrifugation (3,500 *xg*, 10 min, 4 $^{\circ}$C), washed twice and re-suspended with 10 mM potassium phosphate citrate buffer (pH 7.6). Cell suspensions were homogenized using ultrasonic laboratory homogenizer *SONOPULS* HD 2070. The supernatant was collected by centrifugation and dried in a centrivap concentrator. The dried sample was extracted with 600 µl of a mixture of water:chloroform:methanol 3:5:12 (v:v:v), followed by 300 µl of chloroform and 450 µl of water before centrifugation at 8,000 *xg*, 4 °C for 10 min. The upper water-methanol phase was collected, dried, and dissolved in 200 µl of 0.1 N HCl. The solution was filter-sterilized through a 45-µm membrane before determination of GABA by HPLC. Quantification of intracellular amino acid content was performed using a Shimadzu Prominence Ultra-Fast Liquid Chromatography System equipped with UV-Vis detector. Intracellular amino acid was determined by derivatizing with *O*-phthalaldehyde (OPA) reagent and separated by reverse-phase high performance liquid chromatography using 4.6 x 150 mm, 5.0 µm Agilent Zorbax Eclipse AAA

analytical column and 4.6 x 12.5 mm, 5.0 μm guard column (Agilent Technologies Inc.). HPLC mobile phase conditions were modified from the gradient program described by Henderson et al. (2006) to suit our HPLC and column system. OPA-derivatized amino acids were monitored at 338 nm. Purchased standards of each individual amino acid and GABA were used for identification and quantification (external standard method). Norvaline was used as internal standard for OPA-derivative amino acids.

3.2.11 Glutamate utilization in *A. halophytica*

3.2.11.1 The $^{14}CO_2$ liberation measurement

Mid log phase *A. halophytica* cells grown in the growth medium containing 0.5 M NaCl and 2.0 M NaCl were harvested by centrifugation (3,500 *xg*, 10 min, 30 ^{o}C), washed twice and re-suspended to a concentration of 0.1 mg cell protein in 1 ml assay medium containing same NaCl concentration with the growth medium. Total volume of the reaction medium was 2 ml in the vial (10 ml) composed of cells and buffer at the bottom of vial. A filter paper, 5x5 mm diameter, was placed at the top of the vial and one drop of 1 M NaOH was applied to the paper. The reaction was initially started by adding [U-^{14}C]-glutamate. The filter paper was taken out after desired time, dried on the stainless steel, and measured with a liquid scintillation counter (model 3200C; Aloka Instruments Co., Tokyo, Japan).

3.2.11.2 Cellular ion determination

Mid log phase *A. halophytica* cells grown in the growth medium containing 0.5 M NaCl and 2.0 M NaCl were harvested by centrifugation (3,500 *xg*, 10 min, 30°C), washed twice and re-suspended with fresh medium containing 0.5 M NaCl or 2.0 M NaCl with various concentrations of exogenous glutamate. Cells were collected and re-suspended in 1 ml of distilled water. Cell suspensions were homogenized using ultrasonic laboratory homogenizer *SONOPULS* HD 2070. The supernatant was collected by centrifugation and subjected to Shimadzu PIA-1000 personal ion analyzer.

3.2.11.3 Glycine betaine determination

Mid log phase *A. halophytica* cells grown in the growth medium containing 0.5 M NaCl and 2.0 M NaCl were harvested by centrifugation (3,500 *xg*, 10 min, 30°C), washed twice and re-suspended with fresh medium containing 0.5 M NaCl or 2.0 M NaCl with various concentrations of exogenous glutamate. Cells were collected and re-suspended in extraction buffer. Cell suspensions were homogenized using ultrasonic laboratory homogenizer *SONOPULS* HD 2070. The supernatant was collected by centrifugation and concentrated with centrifugal concentrator. Dried samples were dissolved in small volume of 60% methanol and subjected to esterification step. After reaction, glycine betaine was measured after esterification with time of flight

mass spectroscopy (KOMPACT MALDI IV tDE, Shimadzu/Kratos) using D11-betaine as an internal standard.

3.2.11.4 GABA determinantion

Mid log phase *A. halophytica* cells grown in the growth medium containing 0.5 M NaCl and 2.0 M NaCl were harvested by centrifugation (3,500 *xg*, 10 min, 30°C), washed twice and re-suspended with fresh medium containing 0.5 M NaCl or 2.0 M NaCl with various concentrations of exogenous glutamate. Cells were collected and re-suspended in 10 mM potassium phosphate citrate buffer (pH 7.6). GABA extraction and GABA determination was done as described in 3.2.10.

3.2.12 Database searching of enzymes in glutamate metabolic pathways in cyanobacteria

To identify enzymes related in glutamate metabolic pathways in cyanobacteria, we searched in cyanobase using glutamate as query. In this study, we are interested only in cyanobacteria glutamate decarboxylase. Firstly, we searched in cyanobase using glutamate decarboxylase as query. The deduced amino acid sequence of *Synechocystis* sp. PCC 6803 glutamate decarboxylase (sll1641) was used as a query for domain search using InterProScan (http://www.ebi.ac.uk/InterProScan). To identify members of cyanobacteria glutamate decarboxylase, the Basic Local Alignment Search Tool (BLAST)

algorithms (BlastP and BlastN) of the NCBI database using the sequence of *Synechocystis* sp. PCC 6803 glutamate decarboxylase (sll1641) as query was conducted and we also searched for Interpro Database Matches using IPR002129 Pyridoxal phosphate-dependent decarboxylase and IPR010107 Glutamate decarboxylase as query. Nucleotide and amino acid sequences as well as information regarding each gene of interest were obtained. Deduced sequences of proteins identified by InterProScan as containing IPR002129 were subjected to phylogenetic analysis. Multiple alignments of amino acid sequences were performed by ClustalX program [109] using default settings. Alignments were carried out and protein trees were constructed using the neighbor-joining algorithm by Clustal X program [109] (default settings). Bootstrap analysis with 1000 replicates was used to evaluate the significance of the nodes. Comparison of marine cyanobacterial glutamate decarboxylase with those from *E. coli* (GenBank: NP_416010) by multiple sequence alignment was performed by ClustalW program [109].

To identify the conserved nucleotide sequences among marine cyanobacterial glutamate decarboxylase, multiple sequence alignment was performed by ClustalW program [109]. Gene-specific primers were designed based on nucleotide sequence similarity among marine cyanobacterial GAD as shown in Table 3.5.

Table 3.4 Oligonucleotide primers of *A. halophytica* glutamate decarboxylase gene.

Primer name	Primer sequences (5′ to 3′)
Apgad-F1	TGGCCACCTTTTGTCAGACC
Apgad-F2	GAACCTGATCGACAAAGACG
Apgad-F3	TGCGTTTCGATGATGG
Apgad-F4	TCCACCATTGGGAGCAG
Apgad-F5	GAAATTTGCCCGCTACTGGGA
Apgad-F6	GATGCGTGAATTAGAGATGC
Apgad-F7	GAGGCCGTGGATGAGAACA
Apgad-F8	CTCGGGGTGGATAAGAACCTGATCGAC
Apgad-F9	AAATGGCGTTGGCG
Apgad-R2	AGGCCGTGATAAGTCACC
Apgad-R3	AACGGAGCAAGAAAGCCACCACT
Apgad-R7	TCTCGACCTAACGGCACAAA
Apgad-R9	AGAGTCCAAACCACCGTGGGAAT
Apgad-R10	ATAGGCAGGCACCTGCCAAC
Apgad-R12	GCTTGCCTGATGTCTTCCA

3.2.13 Partial characterization of GABA-synthesizing enzyme glutamate decarboxylase (GAD) in *A. halophytica*

3.2.13.1 Crude enzyme preparation

Mid log phase of *A. halophytica* cells grown in the growth medium containing 0.5 M NaCl were harvested by centrifugation (3,500 *xg*, 10 min,

4 ^{o}C), washed twice and re-suspended with extraction buffer. Cell suspensions were homogenized using ultrasonic laboratory homogenizer *SONOPULS* HD 2070. The supernatant was collected by centrifugation and used as crude enzyme.

3.2.13.2 Glutamate decarboxylase activity assay using spectrophotometric method

GAD activity *in vitro* was determined using spectrophotometric method by the method of Kitaoka and Nakano (1959) [55] with some modification. The reaction mixture of GAD activity assay consisted of 50 mM Na-phosphate buffer, pH 5.8, 30 mM glutamate, 20 μM pyridoxal-5'-phosphate (PLP), 0.5 mM Ca^{2+} and crude enzyme (as described in 3.2.13.1). Reactions were incubated at 30°C, and reactions was stopped by the addition of 200 μl of 200 mM sodium borate (pH 9.0), and 1 ml of 6% phenol solution, followed by immersion in an ice-H_2O. After cooling for 2-5 min, 400 μl of sodium hypochlorite was added followed by vigorous agitation. The mixture was incubated in a boiling H_2O bath for 10 min, then immediately placed into the ice-H_2O bath for 20 min. To determine the GABA content spectrophotometrically by the Berthelot color reaction, GABA content was measured by determining the absorption at 630 nm. The reaction mixture without glutamate was also prepared. The differences of GABA concentration between substrate-contained samples and non-substrate-contained samples

were used as GAD activity to discriminate the internal GABA that was already present in the crude enzyme and synthesized GABA by glutamate application. GAD activity was defined as the amount of GABA (μmol) produced per min per mg protein.

3.2.13.3 Optimization of enzyme activity assay conditions for glutamate decarboxylase activity of *A. halophytica*

3.2.13.3.1 Optimum extraction buffer and enzyme activity assay buffer

To identify optimal method for glutamate decarboxylase activity assay, three extraction buffer, 25 mM Tris-HCl, pH 7.6, 25 mM Na-Phosphate Citrate buffer, pH 7.6 and 25 mM K-Phosphate Citrate buffer, pH 7.6, and two enzyme activity assay buffer, 50 mM Na-Phosphate Citrate buffer, pH 5.8 and 50 mM K-Phosphate Citrate buffer, pH 5.8, were compared under the standard assay condition as described in 3.2.13.1 and 3.2.13.2. The results were expressed as the percentage of relative activity. Moreover, enzyme stability in different extraction buffers was also determined. Crude enzymes were stored at 4 ^{o}C for 0, 9 and 18 day and subjected to enzyme activity assay as described in 3.2.13.2. The percentage of relative activity at day 0 of each extraction buffer is shown as 100%.

3.2.13.3.2 Optimum concentration of crude enzyme

The effect of crude enzyme concentration on GAD activity was investigated under the standard assay condition as described in 3.2.13.2. Concentrations of crude enzyme were varied from 0 to 500 μg protein. The results were expressed as the percentage of relative activity. The percentage of relative activity was plotted against the crude enzyme concentration.

3.2.13.3.3 Optimum concentration of glutamate and pyridoxal-5'-phosphate

The effect of concentration of glutamate and pyridoxal-5'-phosphate (PLP) on GAD activity was determined under the standard assay condition as described in 3.2.13.2. Glutamate and PLP concentrations were varied at 0–50 mM and 0–40 μM, respectively. The results were expressed as the percentage of relative activity. The percentage of relative activity was plotted against the glutamate and PLP concentrations, respectively.

3.2.13.3.4 Optimum $CaCl_2$ concentration

The effect of $CaCl_2$ concentration on GAD activity was investigated under the standard assay condition as described in 3.2.13.2. Concentrations of $CaCl_2$ were varied at 0–2 mM. The results were

expressed as the percentage of relative activity. The percentage of relative activity was plotted against the $CaCl_2$ concentration.

3.2.13.3.5 Optimum pH and temperature

The effect of pH and temperature on GAD activity was determined under the standard assay condition as described in 3.2.13.2. The pH and temperature of enzymatic reaction were varied at pH 4.0–8.0 and at 20 – 60 °C, respectively. The results were expressed as the percentage of relative activity. The percentage of relative activity was plotted against the final pH and temperature used in the activity assay step, respectively.

3.2.13.4 Glutamate decarboxylase activity assay using HPLC

The reaction mixture of GAD activity assay consisted of 50 mM Na-phosphate buffer, pH 5.8, 30 mM glutamate, 20 μM pyridoxal 5'-phosphate (PLP), 0.5 mM Ca^{2+} and crude enzyme (as described in 3.2.13.1). Reactions were incubated at 30°C and reactions was incubated in a boiling H_2O bath for 10 min for stop reaction. The supernatant was collected by centrifugation and dried in a centrivap concentrator. The dried sample was extracted and GABA determination was done as described in 3.2.10.

CHAPTER IV

RESULTS

4.1 The effect of salinity and amino acid supplementation on growth of *A, halophytica*

4.1.1 Effect of sodium chloride concentration on growth rate of *A. halophytica*

Growth of *Aphanothece halophytica* in BG_{11} medium, pH 7.6 plus 18 mM $NaNO_3$ and Turk Island salt solution supplemented with various NaCl concentrations was investigated. The results in Figure 4.1 showed that *A. halophytica* could adapt to a broad range of salt concentrations varying from 0.2–3.0 M NaCl. The growth rate increased with the increase in NaCl concentration up to 0.5 M, and then a decrease of growth was observed at 1.0, 2.0 and 3.0 M NaCl, respectively. The maximum growth rate of *A. halophytica* under salinity was obtained at 0.5 M NaCl. The salt stress condition that decreased growth to half of maximum growth rate was 2.0 M NaCl. The growth rate of *A. halophytica* was decreased in the presence of 0, 0.1 and 3.0 M NaCl

A. halophytica is an ellipsoidal shape cyanobacterium surrounded by mucous membrane. The cells multiply by binary fission. Cell morphology was also investigated under normal (0.5 M NaCl) and salt stress (2.0 M NaCl) conditions as shown in Figure 4.2. The cells grown under salt stress condition showed a higher longitudinal cell diameter than that of the cells grown under normal condition.

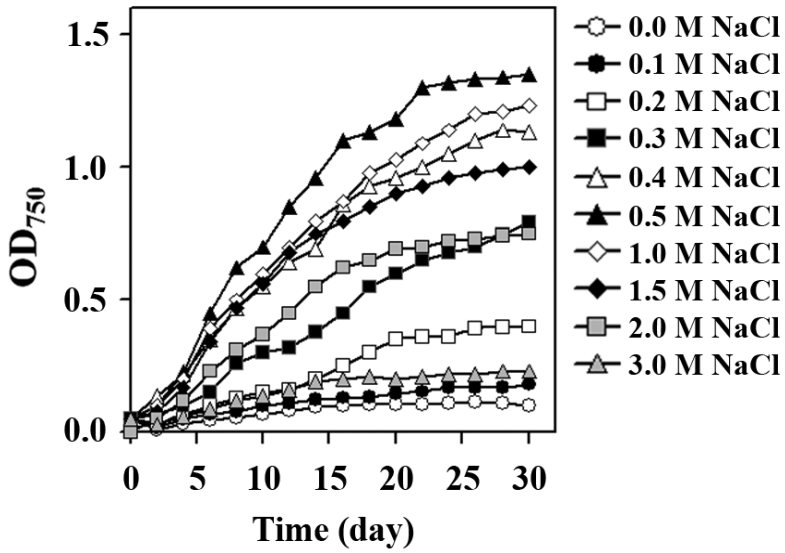

Figure 4.1 Growth curve of *A. halophytica* under various NaCl concentrations.

The data are from three independent experiments with vertical bars representing standard errors of the means, n=3. Error bars are included in the graphs where some may be smaller than the symbols.

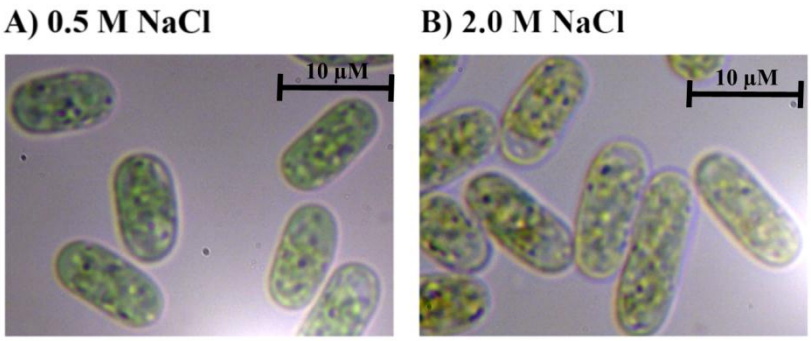

Figure 4.2 Microscopic picture of *A. halophytica* grown in BG_{11} medium supplemented with 18 mM $NaNO_3$ and Turk Island salt solution containing 0.5 M NaCl (A) or 2.0 M NaCl (B) at mid-log phase (x2,250).

4.1.2 Effect of amino acid supplementation on growth rate of *A. halophytica* under normal and salt stress conditions

Each of 20 amino acids at 1 mM was supplemented to BG_{11} liquid medium plus 18 mM $NaNO_3$ and Turk Island salt solution under normal (0.5 M NaCl) and salt stress (2.0 M NaCl) conditions. The growth rate of *A. halophytica* under each condition was determined. The results in Figure 4.3 showed that addition of glutamate, proline and glycine enhanced growth of *A. halophytica* under salt stress condition. Other amino acids had no effect on growth rate of *A. halophytica* under both normal and salt stress conditions. Interestingly, glutamate is the best amino acid to enhance growth of *A. halophytica* under salt stress condition.

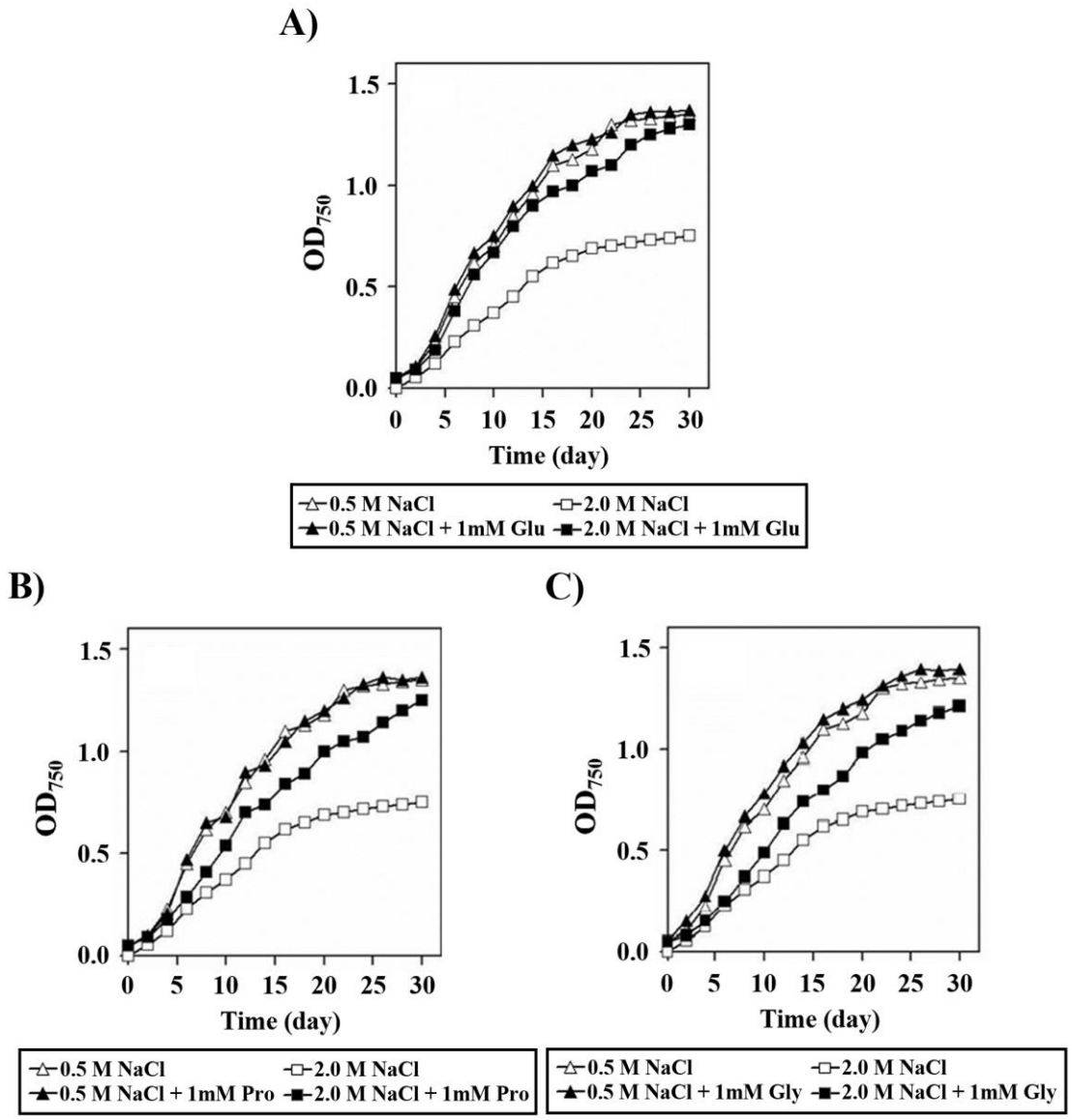

Figure 4.3 Growth curve of *A. halophytica* under normal (0.5 M NaCl) and salt stress condition (2.0 M NaCl) supplemented with 1mM glutamate (A),1 mM proline (B) and 1 mM glycine (C).

The data are from three independent experiments with vertical bars representing standard errors of the means, n=3. Error bars are included in the graphs where some may be smaller than the symbols.

4.1.3 Effect of glutamate concentration on growth rate of *A. halophytica* under normal and salt stress conditions

A. halophytica cells were grown in the growth medium containing 0.5 M NaCl (normal condition) and 2.0 M NaCl (stress condition) supplemented with 0–50 mM glutamate. The growth was monitored by measuring optical density of culture at 750 nm. *A. halophytica* cells were normally grown in growth medium containing 0.5 M NaCl, the growth rates increased upon the increase of glutamate until 50 mM as shown in Figure 4.4A. The effects of glutamate on the cell growth were prominent at high salinity (2.0 M NaCl) as shown in Figure 4.4B. The beneficial effect of glutamate on promoting the cell growth was more obvious when cells were grown at high salinity. The growth inhibitory effect of high salinity (2.0 M NaCl) was relieved in the presence of 50 mM glutamate. These indicated that glutamate was taken up by *A. halophytica* cells and enhanced the growth.

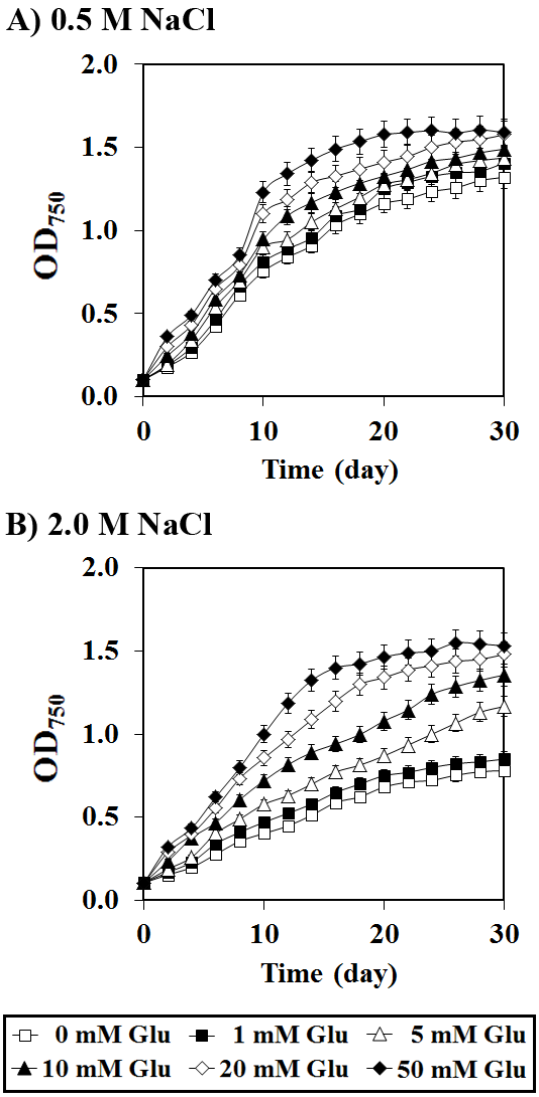

Figure 4.4 Growth curve of *A. halophytica* under normal (0.5 M NaCl) and salt stress condition (2.0 M NaCl) at various glutamate concentrations.

The data are from three independent experiments with vertical bars representing standard errors of the means, n=3. Error bars are included in the graphs where some may be smaller than the symbols.

Effects of glutamate on the growth of three cyanobacteria, freshwater cyanobacterium *Synechococcus* sp. PCC 7942, *Synechocystis* sp. PCC 6803 and *A. halophytica,* under normal and salt stress conditions supplemented with 0–50 mM glutamate were investigated. Visual appearance of the mid-log phase cultures of these three cyanobacteria was shown in Figure 4.5. The result showed that exogenous glutamate enhanced growth of *A. halophytica* at all glutamate concentrations tested in both normal and salt stress conditions and had no toxicity to the *Aphanothece* cells. The useful effects of glutamate on cell growth were clear when cells were grown under salt stress condition. In case of *Synechococcus* sp. PCC 7942 and *Synechocystis* sp. PCC 6803, growths of these two cyanobacteria were inhibited at salt. It was observed that the increase of exogenous glutamate concentration resulted in higher retardation on their growth. The high concentration of glutamate (up to 10 mM) resulted in cell death.

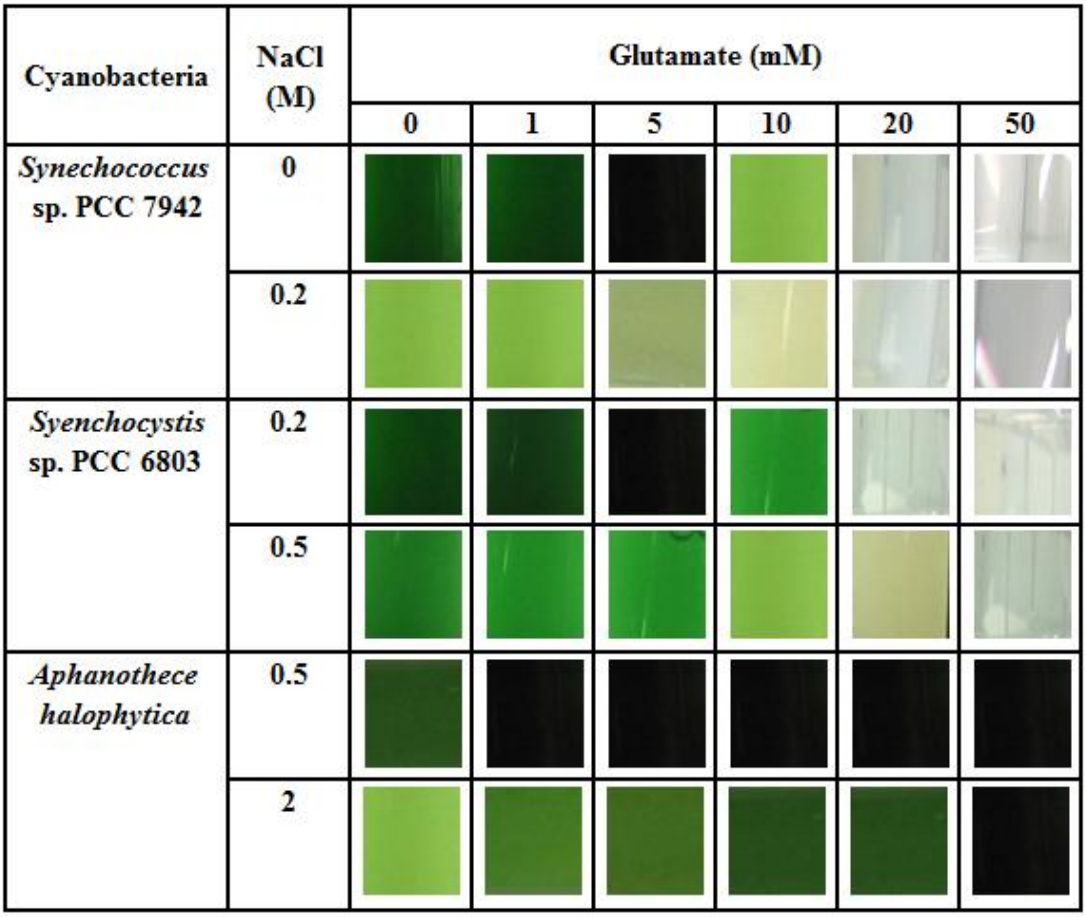

Cyanobacteria	NaCl (M)	Glutamate (mM)					
		0	1	5	10	20	50
Synechococcus sp. PCC 7942	0						
	0.2						
Syenchocystis sp. PCC 6803	0.2						
	0.5						
Aphanothece halophytica	0.5						
	2						

Figure 4.5 Visual appearance of the mid-log phase cultures of three cyanobacteria *Synechococcus* sp. PCC 7942, *Synechocystis* sp. PCC 6803 and *A. halophytica* under normal and salt stress condition supplemented with various glutamate concentrations.

4.2 Characterization of glutamate transport in *A. halophytica*

4.2.1 Time course of glutamate transport in *A. halophytica*

A. halophytica cells were grown in the growth medium containing 0.5 M NaCl. Cells at mid log phase were harvested by centrifugation, washed twice and re-suspended to a concentration of 0.1 mg cell protein in 1 ml assay medium containing either 0.5 M NaCl or 2.0 M NaCl. Glutamate transport of *Aphanothece* cells was determined at interval time for 30 min. Changes in glutamate uptake activity could be observed in the presence of 2.0 M NaCl compared to the control with 0.5 M NaCl using [U-^{14}C] glutamate (at a final concentration of 0.1 μM) as substrate. The initial rate of [U-^{14}C] glutamate uptake was observed within the first 1 min and cells showed saturated glutamate uptake after cells were exposed to glutamate for 5 min. The glutamate uptake rate was 0.28 ± 0.01 and 0.33 ± 0.02 nmol.min^{-1}.mg^{-1} protein at 0.5 M and 2 M NaCl, respectively as shown in Figure 4.6.

4.2.2 Saturation kinetics of glutamate uptake in *A. halophytica*

Incubation of *Aphanothece* cells with various glutamate concentrations ranging from 0 to 100 μM resulted in saturable uptake (Figure 4.7). The results showed that glutamate uptake of *A. halophytica* under normal and salt stress conditions exhibited the typical of Michaelis-Menten saturation kinetics with an apparent K_m of 11.76 ± 0.33 and 9.91 ± 0.24 μM, respectively, and the maximum velocity (V_{max}) of 6.67 ± 0.36 and 5.20 ± 0.25 nmol.min^{-1}.mg^{-1} protein, respectively (Table 4.1).

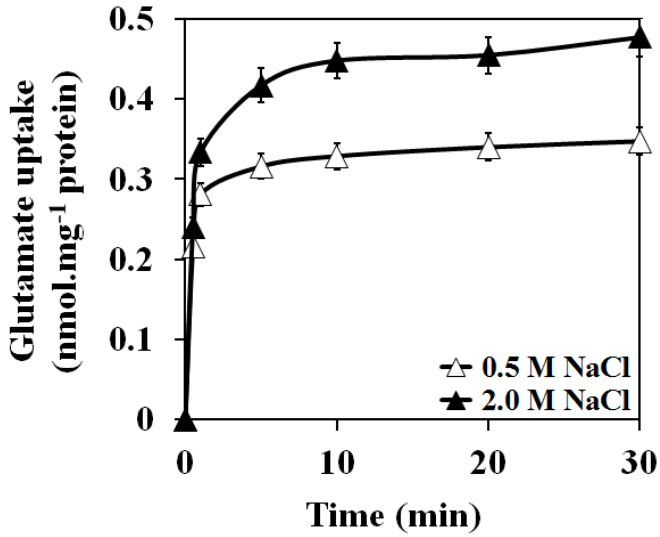

Figure 4.6 **Time intervals of glutamate uptake into *A. halophytica* in the presence of 0.5 and 2.0 M NaCl.**

The data are from three independent experiments with vertical bars representing standard errors of the means, n=3. Error bars are included in the graphs where some may be smaller than the symbols.

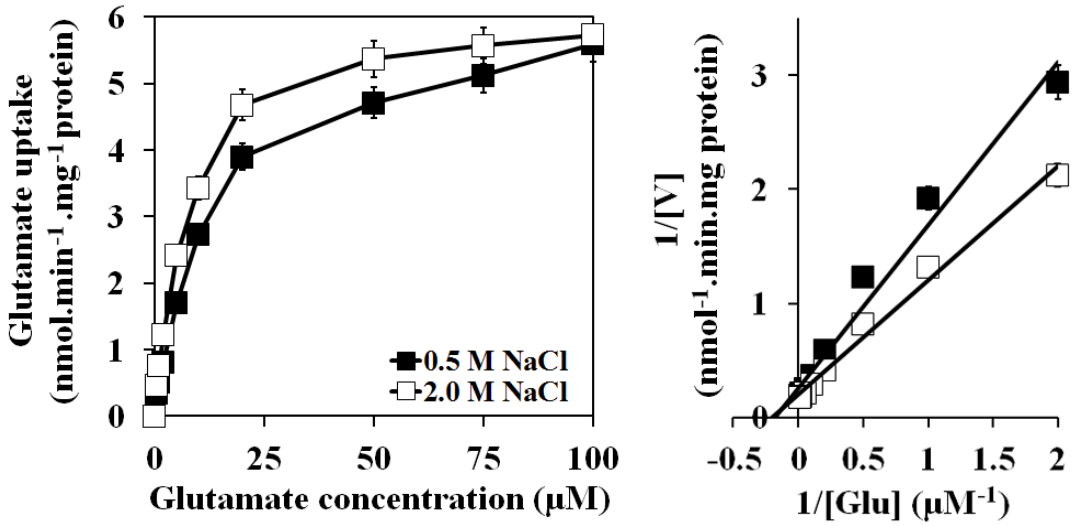

Figure 4.7 Kinetics of glutamate uptake into *A. halophytica* in the presence of 0.5 and 2.0 M NaCl.

A Lineweaver-Burk transformation of the data is shown on the right. The line drawn is that derived from regression analysis of the data. The data are from three independent experiments with vertical bars representing standard errors of the means, n=3. Error bars are included in the graphs where some may be smaller than the symbols.

Table 4.1 Kinetic values of glutamate uptake in *A. halophytica*.

NaCl concentration (M)	Kinetic value	
	K_m (µM)	V_{max} (nmol.min^{-1}.mg^{-1} protein)
0.5	11.76 ± 0.33	6.67 ± 0.36
2.0	9.91 ± 0.24	5.20 ± 0.25

4.2.3 Effect of sugars, cations, and anions on glutamate transport in *A. halophytica*

To investigate the effect of ions and osmotic agents as a coupling ion on glutamate transport, we supplemented 0.5 M of each reagent in the assay medium. As shown in Figure 4.8, sugar and alcohol sugar representing an osmotic agent slightly activated the glutamate uptake of *A. halophytica.* Monovalent cation, especially Na^+ activated the uptake to 1.5 fold of the control and NH_4^+ slightly activated the uptake up to 1.1 fold, whilst the rest had no effect on glutamate uptake of *A. halophytica.* In contrast to monovalent cation, divalent cations, Ca^{2+} and Mg^{2+}, obviously inhibited the uptake down to 0.6 fold of the control. Almost all selected anions slightly inhibited glutamate uptake of the *A. halophytica* cells, except for an activating effect of NO_3^- showing up to 1.2 fold of the control.

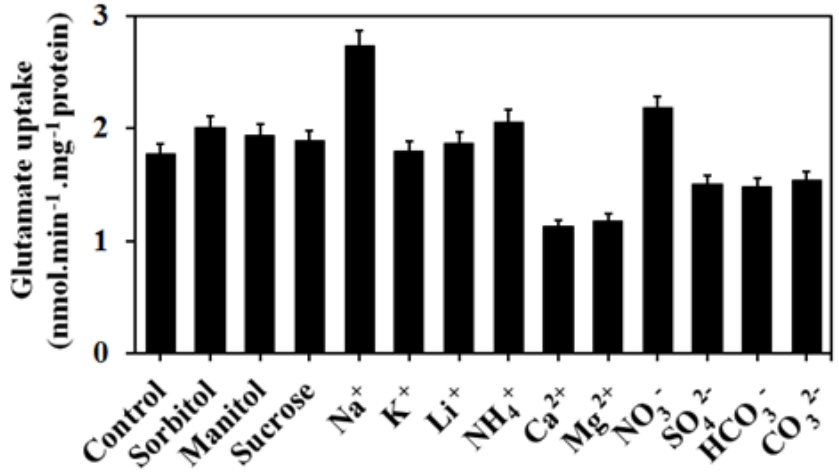

Figure 4.8 **Effect of sugars, cations, and anions on glutamate uptake in *A. halophytica*.**

Initial uptake rates were determined in assay medium containing 0.5 M NaCl supplementation with 0.5 M of each sugar, cation or anion. The data are from three independent experiments with vertical bars representing standard errors of the means, n=3.

4.2.4 Effect of NaCl concentration on glutamate transport in *A. halophytica*

The effect of NaCl on glutamate uptake was extensively studied. The results revealed that increasing NaCl concentration up to 2.0 M resulted in the stimulation of glutamate uptake in *A. halophytica.* When NaCl concentration was higher than 2.0 M, glutamate uptake in *A. halophytica* was declined as shown in Figure 4.9. The exogenous addition of NaCl to assay medium significantly increased the uptake of glutamate, with the maximum uptake observed at 1.0 M NaCl. The result suggested that the optimal concentration of NaCl for glutamate uptake was 1.0-2.0 M.

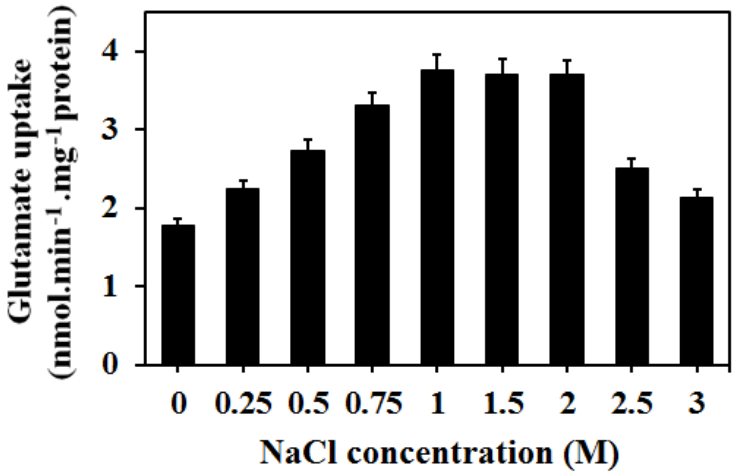

Figure 4.9 **Effect of NaCl concentration on glutamate** uptake **in *A. halophytica*.** Initial uptake rates were determined in the presence of increasing of NaCl concentration from 0-3 M. The data are from three independent experiments with vertical bars representing standard errors of the means, n=3.

4.2.5 Effect of external pH on glutamate transport in *A. halophytica*

pH is one of the parameters affecting the transport process. For accuracy and reproducibility, this parameter must be considered and optimized. The rate of glutamate uptake under various pHs ranging from 5.5 to 10.5 was monitored. The uptake assay was done with the modification using 100 mM potassium phosphate buffer pH 5.5-6.5, 100 mM Tris-HCl, pH 7.0-9.0 and 100 mM Borate buffer pH 9.5-10.5. The highest uptake of glutamate occurred at pH 9.0, an increase about 1.16 fold compared with pH 7.5 as shown in Figure 4.10.

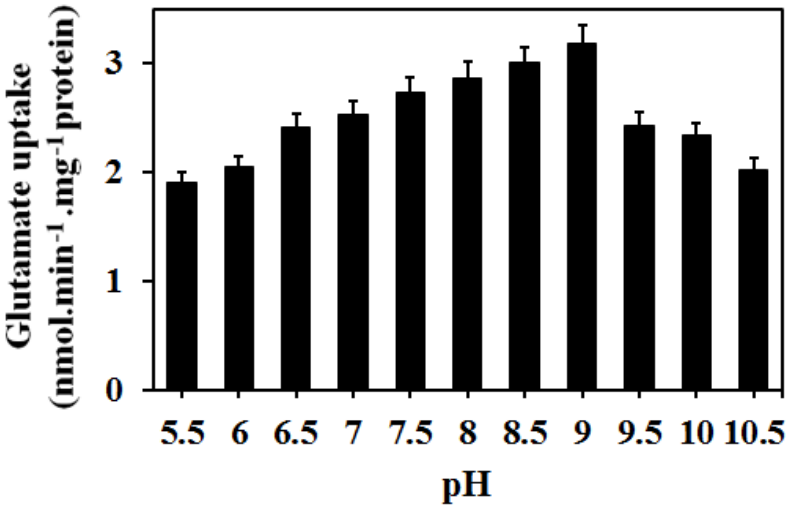

Figure 4.10 **Effect of extracellular pH on glutamate transport in *A. halophytica*.** The initial rate of glutamate uptake was determined. The uptake assay was done with the modification using different buffer systems at various pH range of 5.5–10.5. The data are from three independent experiments with vertical bars representing standard errors of the means, n=3.

4.2.6 Specificity of glutamate transport in *A. halophytica*

The specificity of glutamate uptake was determined by measuring the initial rate of [U-^{14}C] glutamate uptake in the presence of 100 folds excess of unlabeled competitive substrate. As shown in Figure 4.11, the [U-^{14}C] glutamate uptake in *A. halophytica* was inhibited by about 87% and 91% when 100-fold "cold" glutamate was added in the assay medium containing 0.5 M NaCl and 2.0 M NaCl, respectively. Aspartate showed about 72% inhibition on glutamate transport in both conditions. Moderate inhibition of the [U-^{14}C] glutamate uptake by 35-50% occurred in the presence of asparagine, glutamine and cysteine. The presence of alanine, glycine, proline, serine, betaine, choline and betaine aldehyde slightly inhibited glutamate uptake.

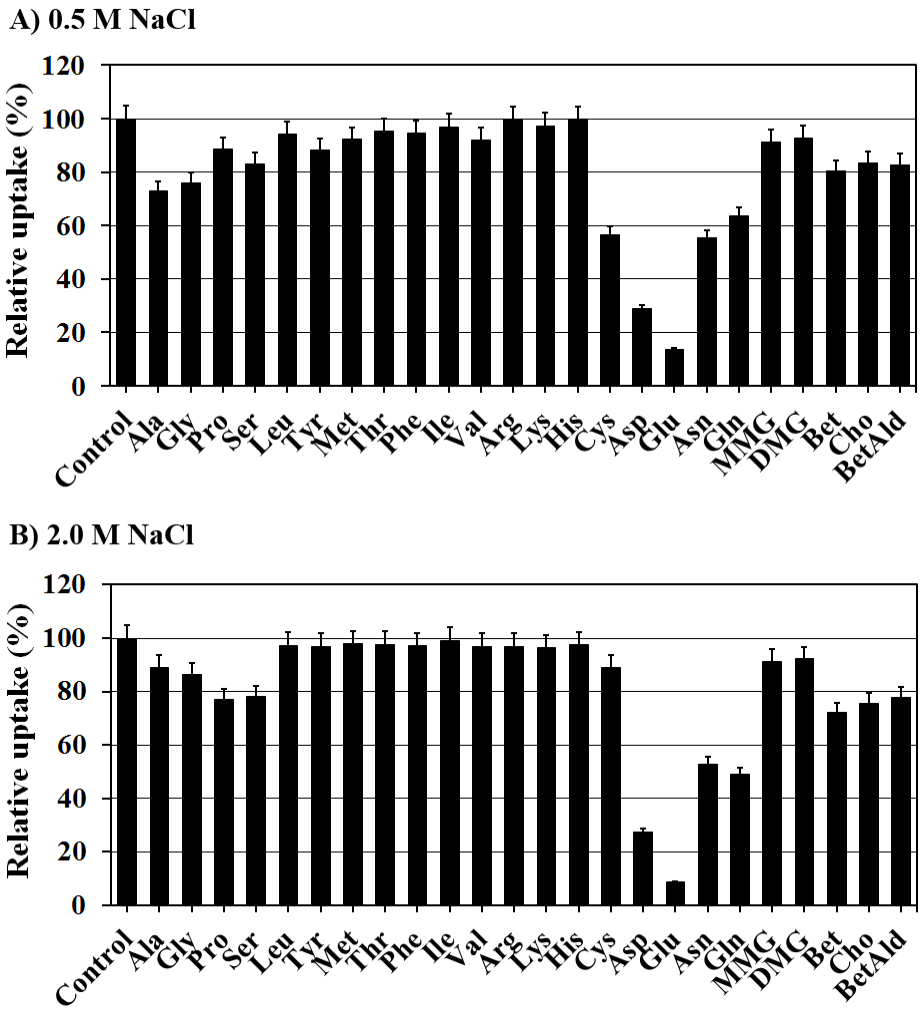

Figure 4.11 Effects of competing amino acid on [U-^{14}C] glutamate uptake of *A. halophytica* under normal and salt stress condition.

The reaction mixture contained 0.1 μM [U-^{14}C] glutamate in the presence of 0.5 M NaCl (A) and 2.0 M NaCl (B) and 10 mM of various competitor compounds. The value of the uptake in the control without competitor is shown as 100%. The data are from three independent experiments with vertical bars representing standard errors of the means, n=3.

4.2.7 Effect of different energy sources on glutamate uptake in *A. halophytica*

The ability of various energy sources to drive glutamate uptake in *A. halophytica* was investigated. *A. halophytica* cells were starved to deplete endogenous energy sources. Glutamate uptake was monitored after cell was re-energized with glucose or lactate. The results showed that both glucose and lactate could energize the uptake of glutamate in the starved cells (Table 4.2). These results indicated that glutamate uptake is an energy-dependent process. Incubation of starved cell with potassium cyanide, a respiratory inhibitor, markedly reduced glutamate uptake. Furthermore, cyanide completely inhibited glucose-supported glutamate transport and also abolished lactate-driven glutamate uptake in *A. halophytica.*

Table 4.2 Effect of energy sources on glutamate uptake[a].

Addition	Glutamate uptake (%)	
	0.5 M NaCl	**2.0 M NaCl**
None	100.00 ± 2.65	100 ± 2.17
Glucose (20 mM)	122.21 ± 3.14	127 ± 2.78
Lactate (10 mM)	110.13 ± 3.65	116 ± 3.27
KCN (20 mM)	68.14 ± 2.72	75.23 ± 3.23
Glucose + KCN	63.25 ± 3.25	72.86 ± 2.56
Lactate + KCN	56.23 ± 3.56	62.15 ± 2.89

[a]Cells were starved by suspending cells in 100 mM Tris-Cl buffer, pH 7.6 containing either 0.5 M NaCl or 2.0 M NaCl in the dark for 2 h. The starved cells were then assayed for glutamate uptake in the presence of different energy sources or respiratory inhibitor. Starved cells were pre-incubated with the tested compound(s) in the dark for 30 min before the addition of 1 μM [U-^{14}C] glutamate to initiate the uptake as described in Materials and Methods. Data are means from three independent experiments representing the percent uptake rate relative to the control rate which was 0.57 and 0.72 nmol.min^{-1}.mg^{-1} protein for 0.5 M and 2.0 M NaCl, respectively.

4.2.8 Effect of metabolic inhibitors, ionophores and ATPase inhibitors on glutamate transport in *A. halophytica*

To assess the roles of ATP and proton motive force in energizing glutamate uptake, the effects of some inhibitors on glutamate transport were investigated. *N*-ethylmaleimide (NEM); a protein structure modifier, markedly reduced glutamate transport as shown in Table 4.3. Gramicidin D, a monovalent-selective ionophore that dissipates both the pH gradient and membrane potential; Valinomycin, a potassium-selective ionophore that dissipates membrane potential; and amiloride, an inhibitor for many Na^+-coupled systems including Na^+/H^+ antiportor; all also strongly inhibited glutamate uptake activity suggesting that glutamate transport in *A. halophytica* was stimulated by ion. Slight inhibition was observed by the chemical uncouplers of electron transport and oxidative phosphorylation such as carbonyl cyanide chlorophenylhydrazone (CCCP), trifluorocarbonylcyanide phenylhydrazone (FCCP), and 2,4-dinitrophenol (DNP) and by electron transport inhibitors such as sodium azide, antimycin A and rotenone. Furthermore, potassium arsenate and potassium fluoride (glycolysis inhibitors) also slightly reduced the activity of glutamate transport.

Table 4.3 Effect of metabolic inhibitors on glutamate uptake[a].

Inhibitor	Concentration	Glutamate uptake (%)	
		0.5 M NaCl	2.0 M NaCl
None	-	100.0 ± 2.1	100.0 ± 3.0
NEM	5 mM	32.9 ± 6.5	14.2 ± 2.1
Gramicidin D	20 $\mu g.ml^{-1}$	25.3 ± 2.4	26.8 ± 2.5
Valinomycin	20 μM	20.7 ± 2.7	32.5 ± 3.5
Amiloride	5 μM	37.3 ± 3.8	28.5 ± 4.9
CCCP	20 μM	72.3 ± 3.5	82.3 ± 4.5
FCCP	20 μM	71.2 ± 2.7	83.2 ± 6.2
DNP	5 mM	77.4 ± 3.3	85.3 ± 4.7
NaN_3	20 mM	81.5 ± 4.3	84.2 ± 7.4
Antimycin A	20 mM	86.9 ± 5.7	89.3 ± 6.7
Rotenone	5 mM	89.9 ± 4.7	91.8 ± 6.5
K-arsenate	50 mM	88.1 ± 5.1	91.1 ± 5.6
KF	20 mM	93.2 ± 6.4	96.9 ± 5.9

[a]Cells were pre-incubated with inhibitors in the dark for 30 min before the addition of 1 μM [U-^{14}C] glutamate to initiate the uptake as described in Materials and Methods. Data are means from three independent experiments representing the percent uptake rate relative to the control rate which was 0.57 and 0.72 $nmol.min^{-1}.mg^{-1}$ protein for 0.5 M and 2.0 M NaCl, respectively.

4.3 Isolation of *A. halophytica* glutamate transporter gene and expression in glutamate transporter-deficient *E. coli* ME9107

4.3.1 Identification and phylogenetic analysis of *A. halophytica* Na^+/glutamate transporter gene (*ApgltS*)

Hitherto, *6803gltS-S* (*slr1145*) from *Synechocystis* sp. PCC 6803 was the only known glutamate transporter from cyanobacteria (Quintero *et al*. 2001). We searched the homologous gene in *A. halophytica* based on the shot gun sequencing of *A. halophytica*, and found that *A. halophytica* contains a gene (*ApgltS*) which exhibited a low homology to *6803gltS-S* (*slr1145*) from *Synechocystis* sp. PCC 6803. The *ApgltS* gene was 1431 bp long as shown in Figure 4.12. The nucleotide sequence of *ApgltS* gene was used for conversion to protein sequence by translation tool (http://web.expasy.org/translate/). We found that the *ApgltS* gene encoded 476 amino acid residues as shown in Figure 4.13.

Then, the deduced amino acid sequence of ApGltS was used as a query for domain search, transmembrane prediction and Blast analysis. The result of domain search using Interproscan showed that ApGltS contains Na^+/glutamate symporter domain, IPR004445. For transmembrane domain analysis, the results showed that ApGltS is a membrane protein which has 11 transmembrane helices using Hydropathy analysis (http://www.tcdb.org/progs/hydro.php) and TMHTMM Server v. 2.0 (http://www.cbs.dtu.dk/services/TMHMM/) showed that ApGltS contained 11 transmembrane segments (TMS) with the N-terminus in the periplasm and C-terminus in the cytoplasm as shown in Figure 4.14.

>ApgltS

TTGAACACCACTAACTTAGGATTAGGAGATGTTTTTGCAGCGTTTATCGTTTTAGGGCTATTCCTCCTG
ATTGGACGATTTTTAAAACAGACAATTAAGCTGTTTGATTTACTTTATTTACCAGAATCGATCCTCGCG
GGAGGCTTAGCTTTATTACTAGGAAAAGAAGGATTAGGTCATCTAGTTCCAGCTTCCAGCTTCTTGGCT
CATCAAGGGATTTTTCCAGAAAATATTGCTACCGTTTGGTCACAAGCTCCCAGTGTTTTTATTAATCTT
GTGTTTGCGACACTTTTTCTCGGGGAAACCATTCCCAGCCCCAAAGAAATTTGGCAGAAAGTTGCGCCT
CAAGTCGCGTTTTCTCAAATTTTGGCGTGGGGACAATATGTGGTTGGCTTAGGAATGACACTGCTGGTT
TTAACTCCTGTTTTTGGCATGAATCCCATTGCAGGTGCACTGATTGAAATGGCGTTTGAAGGGGGTCAT
GGAACGGCTGCAGGAATGGCTGCTGTTTTAGATGATTTTGGCTTTCAGGAAGGAGGAGAAATTGCGTTA
GGCTTAGCAACAGTCGGCTTGATTTCTGGTGTAGTGACGGGAACAATTTTGATTAATTGGGGACGGAGA
AAAGGTCATATTTCTTCAGGACATAAACCTGATTTATCTTTCGATTCTTCTCCTCAGGAAGCTGGCGAT
GATTCCCATGAGTTGCAAACGGAATATAAAAGTTTAGGGAAAAATTTATTAATCGATCCCTTATCGATT
AATTTAGGATTTGTCGCGATCGCGCTGACATTAGGCTGGCTCATTTTAGAAGGATTAAAAGAATTAGAA
GCCCTCACTTGGAGTAAAATAGACATTGAAATTATGAACTATGTCCCTTTATTTCCGATGGCGCTGATT
GGTGGGTTAATTGTTCAAATTTCTATGAGGCGTTTAGGGCTAGATGGGTTAATTCTAAGACCGCTACAG
AAAAATATTGCTGGGGTTGCTTTGGATGCCGTTATTTTCAGCGCGATCGCGTCCATTTCTCTGGGTGTA
TTGGGGACAAACCTCATCCCATTTTTAATTTTATCCGTTGCTGGTATTGCTTGGAATATTTTTGCTTTT
CTATTCTTTGCCCCGCGCATTCTTCCCACTCATTGGTTTGAACGCGGAATTGGCGATATTGGACAATCC
ATGGGAGTAACAGCAACTGGTTTATTATTGCTGCAAATGGTCGATCCAGCTAATGAAACCGAAGCGTTA
GAAAGTTTTGCCTATAAGCAATTGCTCTTTGAACCGATTATGGGAGGCGGTTTCTTTACCGCAGCAGCC
CCCATTTTGGTGTTTCAGTTAGGAGGAATGCCCGTTTTAATTTTAACAGGAGGGTTCTTAGTCTTTTGG
ATTATTTTTGGCTTATTTAATTTCAATGTTAAACCGAAAACTTTGATG***TAG***

Figure 4.12 **Nucleotide sequence of the coding region of *ApgltS* gene based on the shot gun sequencing of *A. halophytica*.**

The translation start and stop codon are indicated by boldface type and italic type, respectively.

```
>ApGltS
MNTTNLGLGDVFAAFIVLGLFLLIGRFLKQTIKLFDLLYLPESILAGGLALLLGKEGLGHLVPASSFLA
HQGIFPENIATVWSQAPSVFINLVFATLFLGETIPSPKEIWQKVAPQVAFSQILAWGQYVVGLGMTLLV
LTPVFGMNPIAGALIEMAFEGGHGTAAGMAAVLDDFGFQEGGEIALGLATVGLISGVVTGTILINWGRR
KGHISSGHKPDLSFDSSPQEAGDDSHELQTEYKSLGKNLLIDPLSINLGFVAIALTLGWLILEGLKELE
ALTWSKIDIEIMNYVPLFPMALIGGLIVQISMRRLGLDGLILRPLQKNIAGVALDAVIFSAIASISLGV
LGTNLIPFLILSVAGIAWNIFAFLFFAPRILPTHWFERGIGDIGQSMGVTATGLLLLQMVDPANETEAL
ESFAYKQLLFEPIMGGGFFTAAAPILVFQLGGMPVLILTGGFLVFWIIFGLFNFNVKPKTLM
```

Figure 4.13 Deduced amino acid sequence of ApGltS based on the shot gun sequencing of *ApgltS* gene.

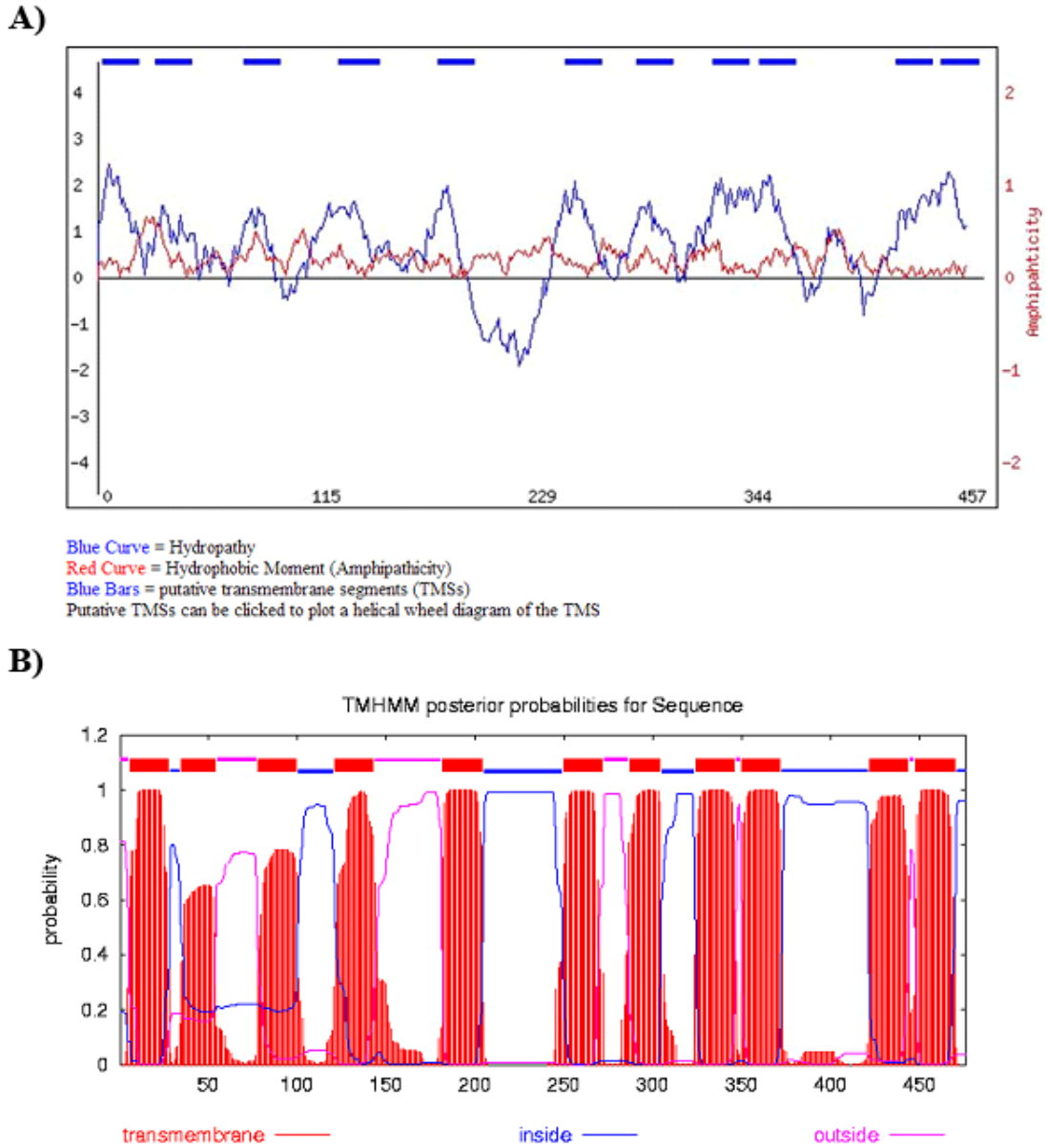

Figure 4.14 **Hydropathy profiles of ApGltS using Hydropathy analysis (A) and TMHTMM Server v. 2.0 (B).**

Transmembrane segments were represented with blue boxes in A) and red boxes in B), periplasmic loops and cytoplasmic loops were represented with pink lines and blue lines, respectively.

By functional analyses and BLAST searches of the Cyanobase and NCBI database, we used the sequence data of ApGltS as queries for BlastN and BlastP. All of these protein sequences were analyzed for Na^+/glutamate symporter domain, IPR004445 using InterProScan. Protein sequences did not have IPR004445 identifiable by InterProScan using default settings, so they were eliminated from further analysis. Totally, 37 putative IPR004445-containing proteins from cyanobacteria have been identified as shown in Table 4.4.

Next, all these protein sequences, ApGltS and also GltS of *Escherichia coli* (EcGltS) were aligned using Clustal X program [109] using default settings. Tree construction using the neighbor-joining method and bootstrap analysis was performed based on the amino acid similarities among the proteins shown in Figure 4.15. This analysis led us to separate the proteins into two groups, one is the group of ApGltS and the other is the group of 6803GltS-S (*slr1145*) which shows high homology to EcGltS (39% identity) comparing with ApGltS group. Interestingly, the numbers of amino acid residues of the members of 6803GltS-S (*slr1145*) group were 398-414 containing 10 TMS whereas those of ApGltS group were 436-501 containing 11 TMS. From Blast searches results, we found two IPR004445-containing proteins in *Synechocystis* sp. PCC 6803; 6803GltS-S (*slr1145*) and 6803GltS-L (*slr0625*) that was not mentioned previously.

Table 4.4 Characteristics of 37 putative IPR004445-containing proteins in cyanobacteria.

Name	GenBank Acc Protein	GenBank Acc Genomic	Organism	Strand	Init. - Term	Length of coding region	Length of amino acids	Interpro	% Amino acid identity (similarity) to ApGltS
CYT7424	ACK68700, YP_002375568	CP001291	*Cyanothece sp.* PCC 7424	Direct	252179.. 253648	1470	489	IPR001991 IPR004445	57.0% (72.6%)
SYNPCC7002 (SYNPCC7002 GltS)	ACA99185, YP_001734441	CP000951	*Synechococcus* sp. PCC 7002	Direct	1228209.. 1229651	1443	480	IPR004445	56.6% (71.1%)
Microco7420	EDX73739, ZP_05028277	DS989856	*Microcoleus chthonoplastes* PCC 7420	Complement	169811.. 171247	1437	478	IPR001991 IPR004445	55.6% (73.7%)
ThSynBP-1 (tlr1046GltS)	BAC08599, NP_681837	BA000039	*Thermosynechococcus elongatus* BP-1	Direct	1082543.. 1083973	1431	476	IPR004445	55.6% (70.3%)
SYNPCC7335	EDX86129, ZP_05037394	DS989904	*Synechococcus* sp. PCC 7335	Direct	1371158.. 1372594	1437	478	IPR004445	54.4% (69.7%)
Nod9414	EAW46680, ZP_01628748	AAVW 01000006	*Nodularia spumigena* CCY 9414	Complement	71436.. 72860	1425	474	IPR004445	55.3% (73.2%)
6803GltS-L (slr0625GltS)	BAA10627, NP_442557	BA000022	*Synechocystis* sp. PCC 6803	Direct	2964570.. 2966033	1464	487	IPR004445	55.0% (70.3%)

Table 4.4 (Continued)

Name	GenBank Acc Protein	GenBank Acc Genomic	Organism	Strand	Init. - Term	Length of coding region	Length of amino acids	Interpro	% Amino acid identity (similarity) to ApGltS
SYNWH7803 (SynWH7803 GltS)	CAK24571, YP_001225868	CT971583	*Synechococcus* sp. WH 7803	Direct	1966349.. 1967767	1419	472	IPR004445	39.4% (56.2%)
SYNRCC307	CAK28916, YP_001228269	CT978603	*Synechococcus* sp. RCC307	Direct	1745447.. 1746925	1479	492	IPR004445	38.6% (56.2%)
SYNWH7805	EAR19577, ZP_01122720	AAOK 01000001	*Synechococcus* sp. WH 7805	Complement	125085.. 126590	1506	501	IPR004445	36.6% (52.9%)
ProMIT9313 (PMT9313GltS)	CAE21728, NP_895380	BX548175	*Prochlorococcus marinus* str. MIT 9313	Direct	1645311.. 1646696	1386	461	IPR004445	35.6% (54.4%)
CYB7001	EDY38147, ZP_05044838	DS990556	*Cyanobium* sp. PCC 7001	Complement	2460729.. 2462099	1371	456	IPR004445	33.1% (51.9%)
SYNWH5701-L	EAQ76276, ZP_01084196	AANO 01000002	*Synechococcus* sp. WH 5701	Direct	308873.. 310300	1428	475	IPR004445	32.2% (51.2%)
ProMIT9515	ABM71903, YP_001011010	NC_008817, CP000552	*Prochlorococcus marinus* str. MIT 9515	Direct	628922.. 630301	1380	459	IPR004445	31.8% (52.2%)

Table 4.4 (Continued)

Name	GenBank Acc Protein	GenBank Acc Genomic	Organism	Strand	Init. - Term	Length of coding region	Length of amino acids	Interpro	% Amino acid identity (similarity) to ApGltS
ProCCMP1375	AAP99828, NP_875176	NC_005042, AE017126	*Prochlorococcus marinus* subsp. marinus str. CCMP1375	Direct	709152.. 710534	1383	460	IPR004445	31.0% (50.6%)
ProMIT9211	ABX08667, YP_001550621	NC_009976, CP000878	*Prochlorococcus marinus* str. MIT 9211	Direct	640465.. 641835	1371	456	IPR004445	31.0% (49.9%)
ProNATL1A	ABM75249, YP_001014514	NC_008819	*Prochlorococcus marinus* str. NATL1A	Direct	634320.. 635705	1386	461	IPR004445	30.9% (49.1%)
ProMIT9215	ABV50326, YP_001483912	NC_009840, CP000825	*Prochlorococcus marinus* str. MIT 9215	Direct	635096.. 636481	1386	461	IPR004445	30.9% (49.6%)
ProNATL2A	AAZ57559, YP_291262	NC_007335, CP000095	*Prochlorococcus marinus* str. NATL2A	Direct	621977.. 623362	1386	461	IPR004445	30.7% (49.1%)
ProCCMP1986	CAE19087, NP_892746	BX548174	*Prochlorococcus marinus* subsp. pastoris str. CCMP1986	Direct	597856.. 599229	1374	457	IPR004445	30.3% (49.9%)

Table 4.4 (Continued)

Name	GenBank Acc Protein	GenBank Acc Genomic	Organism	Strand	Init. - Term	Length of coding region	Length of amino acids	Interpro	% Amino acid identity (similarity) to ApGltS
ProHF10-11H7	ABE11173	DQ366724	*Prochlorococcus marinus* clone HF10-11H7	Complement	2130..3518	1389	462	IPR004445	30.2% (49.6%)
ProMIT9202	EEE40588, ZP_05138763	DS999537	*Prochlorococcus marinus* str. MIT 9202	Direct	1346645..1347955	1311	436	IPR004445	29.9% (48.9%)
ProMIT9301	ABO17278, YP_001090879	NC_009091, CP000576	*Prochlorococcus marinus* str. MIT 9301	Direct	582149..583537	1389	462	IPR004445	29.5% (50.3%)
ProAS9601	ABM69970, YP_001009077	NC_008816, CP000551	*Prochlorococcus marinus* str. AS 9601	Direct	607725..609113	1389	462	IPR004445	29.4% (49.1%)
ProMIT9312	ABB49689, YP_397125	CP000111	*Prochlorococcus marinus* str. MIT 9312	Direct	592523..593908	1386	461	IPR004445	28.9% (49.1%)
CYT51142	ACB52845, YP_001804911	CP000806	*Cyanothece* sp. ATCC 51142	Complement	3619098..3620306	1209	402	IPR004445	23.3% (38.6%)
CYT7425	ACL44997, YP_002483358	NC_011884, CP001344	Cyanothece sp. PCC 7425	Complement	2599171..2600379	1209	402	IPR004445	23.2% (36.8%)

Table 4.4 (Continued)

Name	GenBank Acc Protein	GenBank Acc Genomic	Organism	Strand	Init. - Term	Length of coding region	Length of amino acids	Interpro	% Amino acid identity (similarity) to ApGltS
6803GltS-S (slr1145)	BAA17303	BA000022	*Synechocystis* sp. PCC 6803	Direct	809450.. 810658	1209	402	IPR004445	22.5% (36.7%)
SYNWH5701-S	EAQ74053	AANO 01000011	*Synechococcus* sp WH 5701	Complement	100275.. 101471	1197	398	IPR004445	22.2% (35.8%)
SYNPCCBL107	EAU72115	AATZ 01000001	*Synechococcus* sp. BL107	Direct	469183.. 470418	1236	411	IPR004445	22% (35.8%)
Acaryo11017	ABW30226, YP_001519545	NC_009925, CP000828	*Acaryochloris marina* MBIC11017	Complement	5334060.. 5335250	1191	396	IPR004445	21.9% (37.3%)
Microcys7806	CAO87382	AM778946	*Microcystis aeruginosa* PCC 7806	Direct	1491.. 2699	1209	402	IPR004445	21.2% (36.9%)
Microcys843	BAG01185, YP_001656377	AP009552	*Microcystis aeruginosa* NIES-843	Direct	1221930.. 122313	1209	402	IPR004445	21.2% (36.7%)

Table 4.4 (Continued)

Name	GenBank Acc Protein	GenBank Acc Genomic	Organism	Strand	Init. - Term	Length of coding region	Length of amino acids	Interpro	% Amino acid identity (similarity) to ApGltS
RhodoCGA009	CAE27703, NP_947607	NC_005296	*Rhodopseudomonas palustris CGA009*	Complement	2565446..2566642	1197	398	IPR004445	20.9% (37.9%)
ProMIT9303	ABM78466, YP_001017731	NC_008820	*Prochlorococcus marinus* str. MIT 9303	Complement	1507190..1508434	1245	414	IPR004445	20.1% (33.5%)
SYNWH8102	CAE07397	BX569691	*Synechococcus* sp. WH 8102	Direct	847605..848834	1230	409	IPR004445	19.6% (33.6%)
Gloeo7421	BAC91665, NP_926670	BA000045	Gloeobacter violaceus PCC 7421	Complement	3935894..3937219	1326	441	IPR001991	17.2% (27.4%)

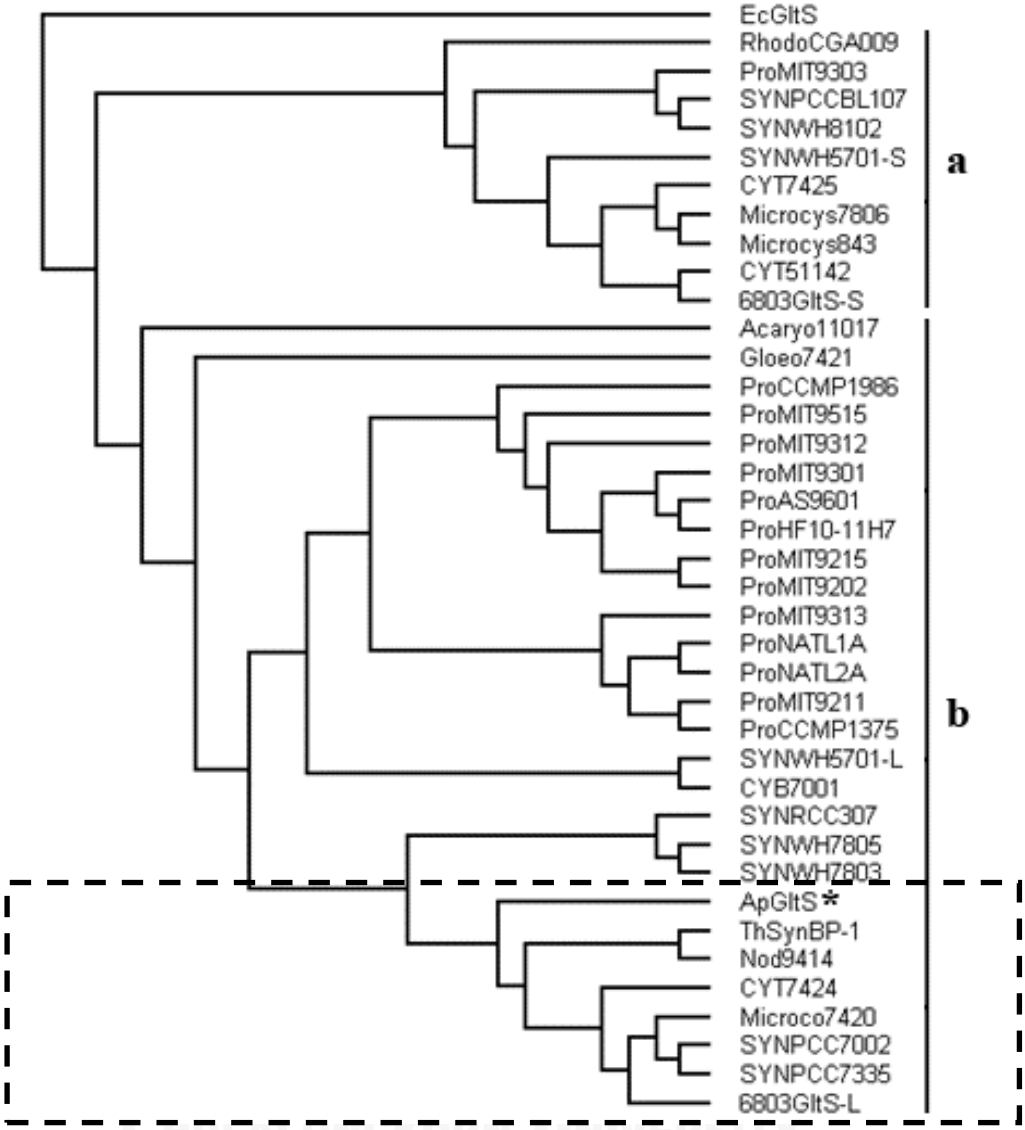

Figure 4.15 **Phylogenetic tree based on amino acid similarities showing the overall relatedness of IPR004445 containing proteins in cyanobacteria and *Escherichia coli* Na^+/glutamate transporter.**

Tree construction using the neighbor-joining method and bootstrap analysis was performed with Clustal X program [109] using default settings. Na^+/glutamate transporter of *Escherichia coli* (EcGltS; AP_004139) are used as outgroup.

In this study, by phylogenetic analysis based on amino acid sequence similarity, seven putative IPR004445-containing proteins in dash box of group b, ThSynBP-1; *ThermoSynechococcus elongatus* BP-1 (*tlr1046*), Nod9419; *Nodularia spumigena* CCY 9414, CYT7424; *Cyanothece* sp. PCC 7424, Microco7420; *Microcoleus chthonoplastes* PCC 7420, SYNPCC7002; *Synechococcus* sp. PCC 7002, SYNPCC7335; *Synechococcus* sp. PCC 7335 and 6803GltS-L; *Synechocystis* sp. PCC 6803 (*slr0625*), that showed the high degrees of amino acid sequence identity (≥ 55%) to ApGltS grouped in the bottom of tree. Multiple sequence alignment of these proteins with ApGltS as shown in Figure 4.16 indicates their high degree of sequence conservation.

```
ApgltS      LDTTNLGLGDVFAAFIVLGLFLLIGRFLKQTIKLFDLLYLPESILAGGLALLLGKEGLGH 60
SYNPCC7002  ----MFTLRDVFFAFILIALLVLAGRYVKQKVRWIQRLYLPESIVAGVLALLLGPQVLGA 56
6803GltS-L  ----MLSLINVLFAFITIAILILAGRFLKQKIKLFQKLYLPESIIAGAIALLLGPGVFGA 56
ThSynBP-1   ----MFSLMTVFWAFIFMGVLLLLGRIVRQRWALMASLYMPSSVIAGILGLLLGPGVLGA 56
SYNPCC7335  ----MLTLRDIFFAFIWIALLILAGRIIKQKVGWIQRLYLPESIVAGVLALLLGPQVLGA 56
Microco7420 ----MSSLKDALFAFILVVLLILVGRFIHQKIRWIQKLYIPESIVAGVVALVLGPQVLGA 56
CYT7424     ----MFSLKDAFFAFTLLALLLLVGRWLKHKIGLFQQLYLPSSIIAGVVGLLLGPQILGA 56
Nod9414     ----MFKLIDVFWAYILIAILILVGRLIRQRLGILRSLYIPSSIVAGIIALLLGKSALGA 56
                   *   : *:  : :::* ** :::    :  **:*.*::** :.*:**   :*

ApgltS      LVPASSFLAH----QGIFPENIATVWSQAPSVFINLVFATLFLGETIPSPKEIWQKVAPQ 116
SYNPCC7002  IATAISGGTS-ILSDGLFSEPIRAVWSQSPGIFINIVFAALFLGEAIPRPKDIWTKTAPQ 115
6803GltS-L  IAVALGVPADGYLAGGVFSETTRAVWAQSPGVFINIVFAALFLGETIPKPKEIWRKTAPQ 116
ThSynBP-1   IASHIAPDSD--LVNGLFAEEIREVWKQSPSIFINIVFACLFLGEIIPSPREIWQKAAPQ 114
SYNPCC7335  ITTAVAGEGA-FLSEGLFSEPIRETWSSSPGIFINIVFAALFLGETIPSPKQIWRRAAPQ 115
Microco7420 IANPNS-----PLANGVFPESIRDVWSQSPGVFINIVFAALFLGESIPHPRDIWNKAAPQ 111
CYT7424     IATNLGYEGSYLAENGLFTEPIREVWKQSPGVFINIVFAALFLGETIPSPRDIWRKAAPQ 116
od9414      IVKLINPESP--LVQGIFTENVQAVWSQSPGIFINIVFATLFLGQYVPTLREFWRKAAPQ 114
            :.            *:*.*    .* .:*.:***:*** ****: :*  :::* :.***

ApgltS      VAFSQILAWGQYVVGLGMTLLVLTPVFGMNPIAGALIEMAFE**GGHGT**AAGMAAVLDDFGF 176
SYNPCC7002  VVFGQTLAWGQYVVGILVTLLILMPLFGVNPIAACLIEIGFE**GGHGT**AGGMAETFTELGF 175
6803GltS-L  VAFGQTLAWGQYVLPILVTLLILIPLFDVDPIIATLVEISFE**GGHGT**AAGMAETFNRLNF 176
ThSynBP-1   VAFGQILAWGQYVVGLLLTGLILTPIFGMDPVAGALIEITFE**GGHGT**AAGMADTFRELNF 174
SYNPCC7335  VVFGQSLAWGQYVVGILATLFILIPLFDANPISGALIEIGFE**GGHGT**AGGMASTFADLGF 175
Microco7420 VVFGQSLAWGQYVVGILLTLLILIPVFGIDPTAAALIEIAFE**GGHGT**AAGMAGTFQELGF 171
CYT7424     VAFGQTLAWGQYVVGILLTLLILTPLFGINPMAGALIEMTFE**GGHGT**AAGMGDTLRELGF 176
Nod9414     VALGQSIAWGQYVVGLILAITILTPVFGLPPIAACLIEVAFE**GGHGT**SAGMAATFTELGF 174
            *.:.* :******: :  :  :* *:*.  *  . *:*: *******:.**. .:  :.*

ApgltS      QEGGEIALGLATVGLISGVVTGTILINWGRRKGHISSGHKPDLSFDS----SPQEAGDDS 232
SYNPCC7002  EAGADLALGIATVGIVGGIVAGTALADWGRRKGHVTSFQKAVEDLDG----VPELTETES 231
6803GltS-L  PDGGDLALGLATVGIVTGVIAGTILADWGRKNNYIQEIPTEVPSGDAQ---FQPTAHLES 233
ThSynBP-1   GAGADMALGLATVGLVSGVVFGVALINWARRTGRLQIQPLADFKAEE----NPDPHPHDD 230
SYNPCC7335  EEGADLALGLATVGIVTGIISGTLLADWARKKQHISVSRAPEDTEDD----VPQLSHDDN 231
Microco7420 PDGADLAVGLATVGIVSGIVTGTVLANWGRRQGYVQGVQQNVAEPEW----FEDYTHSET 227
CYT7424     PEGADMALGLATVGIVSGIVAGVFLTNWGRRRDYLAFPNEGTQPEDPDSEIIPEMIPPED 236
Nod9414     TAGPDLSLALATVGLVSGVVSGTILIHWGRRTGRIKVSSEPLYRVED----TENQHPEEE 230
              * ::::.:****:: *:: *. * .*.*:   :        :           :

ApgltS      HELQTEYKSLGKNLLIDPLSINLGFVAIALTLGWLILEGLKELEALTWSKIDIEIMNYVP 292
SYNPCC7002  PEVRRRRAQLMRNLLIDPLSINFGIVGAAIVIGWLILEALVWVESVTWGQTGFEVISYVP 291
6803GltS-L  DRVLTRRARLMQNLLVDPLSLNFGFTALAVLIGWIILELLRLLEFFTWGKTGFELAGAIP 293
ThSynBP-1   VETRRRRQQLLRELLIDPLSLNFCFVGLAILVGWVILEALRLLERVTWGHTGLKLMAYVP 290
SYNPCC7335  ERVRERRAHLTRGLLIDPLSLNFGFVGIAVIFGWLIQQALILIENLTWASTGFTVMEYIP 291
Microco7420 PQIRRARSRLMRNMLIDPLSLNFGFVGLAIAIGWLLLQGLIWIESVTWGVGGFEMMSYVP 287
CYT7424     RETRLARARLMRNLLIDPLSLNFGFVALAVVIGWLILQILGQVEALTWGRTGFILVEYIP 296
Nod9414     PSVTIARKNLFRNLLIDPLSLNFGFVGLAIAFGWLILEALRLLESITWGRGGVELISYVP 290
                     * : :*:****:*: :.. *: .**:: : *  :* .**.  .. :   :*

ApgltS      LFPMALIGGLIVQISMRRLGLDGLILRPLQKNIAGVALDAVIFSAIASISLGVLGTNLIP 352
SYNPCC7002  LFPMALIGGIIVQLVMERLGLAPLIIRSLMSNIAGLALDVVVVTALASISLSVIGSNLGV 351
6803GltS-L  LFPMALIGGIIVQLIMKKLDLDTLIIRNLQERIAGVALDLVVVTALASIKLQVLGANLPV 353
ThSynBP-1   LFPLALIGGIIVQLILTRWRKQYLISRPLINHIGGVALDVTIITALATLSLAAIGENLIP 350
SYNPCC7335  LFPMALIGGILVQLIMVRLNLDALVIPRLTKNIAGTALDVVVVTALASISLQVLGGNLGI 351
Microco7420 LFPMALVGGIIVQLLMERLGLHPLIIRPLMNNIAGVALDIVVVTALATISLTVLGENFGS 347
CYT7424     LFPMALIGGVIVQLFMKSRRLSPLIMRPLQGHIAGLALDVVIVSALASLSLAVLGENLVP 356
Nod9414     LFPIALIGGMIVQYILMRTRRTYLISRPLMENIGGLALDITIVTALASISLSVLGDNLAP 350
            ***:**:**::**  :       *:   *  .*.* *** .:.:*:*::.* .:* *:
```

```
ApgltS      FLILSVAGIAWNIFAFLFFAPRILPTHWFERGIGDIGQSMGVTATGLLLLQMVDPANETE 412
SYNPCC7002  FTILSVVGITWNVVMFLYFAPRIFPSHWFEKGIGDMGQSMGVTATGILLLRMVDPENRTG 411
6803GltS-L  FLSLSLVGIVWNIVAFVYLAPKILPSYWFERGIGDMGQSMGVTATGILLIKMVDPHNRTG 413
ThSynBP-1   FLLLSLGGIGWNLFVMLYLAPRILPMFWFERGIGDMGQSMGVTSTGLLLIRMVDPHNQSG 410
SYNPCC7335  FLTLSILGIAWNIAFFLWFAPRLFPDYWFEKGIGDLGQSMGVTATGILLMRMVDPENRSG 411
Microco7420 FLLLSVAGITWNIFAFLYLAPRVIPSYWFERGLGDLGQSMGVTATGILLLRMVDPDNRSG 407
CYT7424     FVVLSLGGIIWNIWAFVYLGPRLLPSYWFERGIGDMGQSMGVTATGILLIRMVDPYNRTG 416
Nod9414     FLILSVAGIAWNVCAFVFLGPHLLPFYWFERGIGDMGQSMGVTSTGLLLLRMVDPDNRSG 410
            *  **: ** **:  :::::.*:::* .***:*:**:*******:**:**::**** *.:

ApgltS      ALESFAYKQLLFEPIMGGGFFTAAAPILVFQLGGMPVLILTGGFLVFWIIFGLFNFNVKP 472
SYNPCC7002  AFESFAYKQLFFEPIVGGGLFTAAAPALVVRFGLVPVLLLTGGLLIFWLAMGFLII-RQN 470
6803GltS-L  AFESFAYKQLFFEPIVGGGLFTAAAPTLIRQFGLVPMLISTSGLLAFWLIFGFWNYKVIK 473
ThSynBP-1   ALESFAYKQILFEPIVGGGLFTAAAPILIRNFGLAPVLGLTSGLLLLWLWFGFWNYGQIR 470
SYNPCC7335  AFESFAYKQLFFEPIVGGGLFTAASPALIASFGLTTTLLITAGLLVFWIVAGLFLV-RQD 470
Microco7420 AFESFAYKQLFFEPIVGGGLFTAAAPSLIARFGLVSILFLTSGILVAWLIFGFLAFGKQA 467
CYT7424     AFESFAYKQLFFEPIVGGGLFTAAAPALIVNFGAIPVLILTGGLLIFWIVLGFYLYKKLK 476
Nod9414     AFESFAYKQLLFEPIVGGGLFTAAAPLLIYNFGPIPILLLTSFILAFWLIFGFYNCKQIR 470
            *:*******::****:***:****:* *:  :*  . *  *. :*  *:  *:

ApgltS      KTLM---------- 476
SYNPCC7002  QQQRRRSPSL---- 480
6803GltS-L  REMIAEANSPNPIT 487
ThSynBP-1   RSLVQN-------- 476
SYNPCC7335  KRAAGANR------ 478
Microco7420 RRARKAEKGIE--- 478
CYT7424     PPQKTGYTEVIRR- 489
Nod9414     KQSA---------- 474
```

Figure 4.16 **Multiple sequence alignment of 8 cyanobacterial Na^+/glutamate transporters.**

The identical residues in other sequences are indicated by a dash (*).

4.3.2 Comparative analysis of marine cyanobacterial GltS and bacterial glutamate transporter

Unrooted phylogenetic tree of some marine cyanobacterial GltS such as SYNPCC7002 (*Synechococcus* sp. PCC 7002), SYNWH7803 (*Synechococcus* sp. WH7803), and ProMIT9313 (*Prochlorococcus marinus* MIT9313), and also in 6803GltS-S *and* 6803GltS-L (*Synechocystis* sp. PCC 6803), ThSynBP-1 (*ThermoSynechococcus elongatus* BP-1) and CYT51142 (*Cyanothece* sp. ATCC 51142) together with Na^+/glutamate transporter of *Escherichia coli* (EcGltS; [GenBank: AP_004139]), proton coupled glutamate/aspartate transporters from *E.coli* (EcGltP; [GenBank: AAA24323]) and from *Bacillus stearothermophilus* (BsGltP; [UniProtKB/Swiss-Prot: P24943]), proton/glutamate symport protein from *Pyrococcus horikoshi* (PhGltP; [GenBank: NP_143181]) and from *Bacillus caldotenax* (BsGltT; [UniProtKB/Swiss-Prot: P24944]), was performed with Clustal X program [109] using default settings based on the amino acid similarities among the proteins. Among cyanobacteria glutamate transporter proteins, ApGltS exhibited the highest homology to SYNPCC7002 (57% identity), followed by 6803GltS-L and ThSynBP-1 (56% identity), SYNWH7803 (40% identity), ProMIT9313 (34% identity), 6803GltS-S (19% identity), and CYT51142 (*Cyanothece* sp. ATCC 51142) (17% identity) and only 18% identity to EcGltS. Moreover, ApGltS belongs to a different group from those of proton coupled glutamate/aspartate transporters, EcGltP and BsGltP, and proton/glutamate symport proteins PhGltP and BsGltT as shown in Figure 4.17.

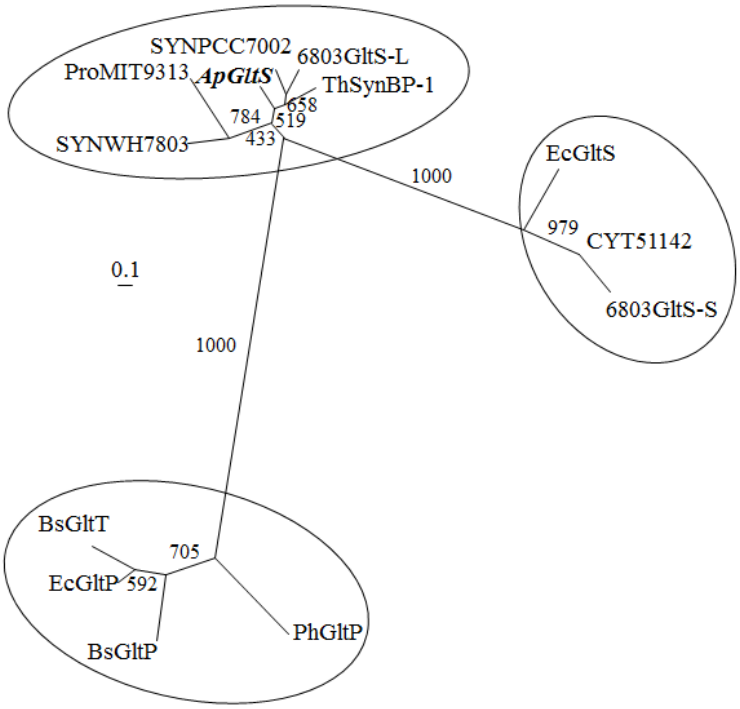

Figure 4.17 Unrooted phylogenetic tree of marine cyanobacterial GltS and bacterial glutamate transporter.

Tree construction using the neighbor-joining method and bootstrap analysis was performed with ClustalX program [109] using default settings based on the amino acid similarities among the proteins. The accession numbers of glutamate transporters are SYNPCC7002 (GenBank: ACA99185), ThSynBP-1 (GenBank: BAC08599), 6803GltS-L (GenBank: BAA10627), SYNWH7803 (GenBank: CAK24571), ProMIT9313 (GenBank: CAE21728), 6803GltS-S (GenBank: BAA17303), CYT51142 (GenBank: ACB52845), EcGltS (GenBank: AP_004139), EcGltP (GenBank: AAA24323), PhGltP (GenBank: NP_143181), BsGltP (UniProtKB/Swiss-Prot: P24943) and BsGltT (UniProtKB/Swiss-Prot: P24944).

4.3.3 Membrane topology of ApGltS

Three amino acid sequences of ApGltS, SYNPCC7002, and EcGltS were aligned using Clustal X program [109] using default settings. Cyanobacteria and *Escherichia coli* Na^+/glutamate transporter possess significant amino acid sequence relationships especially in pore-loop regions as shown in Figure 4.18. The GGHGT motif in the putative pore-loop between the fourth and fifth TMS in the N-terminus (loop Vb) was completely conserved among the three transporters whereas the GVTAT motif in the putative pore-loop between the ninth and tenth TMS in the C-terminal half (loop Xa) matched well between SYNPCC7002 and ApGltS but not EcGltS. Hydropathy analysis showed that ApGltS and SYNPCC7002 contained 11 transmembrane segments (TMS) with the N-terminus in the periplasm and C-terminus in the cytoplasm (Figure 4.19) but EcGltS contained only 10 transmembrane segments (TMS) with the N-terminus and C-terminus in the periplasm.

```
                I                   II
Ap      1 LNTTNLGLGDVFAAFIVLGLFLLIGRFLKQTIKLFDLLYLPESILAGGLALLLGKEGLGHLVPASS---FLAHQGIFPENI
7002    1     MFTLRDVFFAFILIALLVLAGRYVKQKVRWIQRLYLPESIVAGVLALLLGPQVLGAIATAISGGTSILSDGLFSEPI
Ec      1      MFHLDTLATLVAATLTLLLGRKLVHSVSFLKKYTIPEPVAGGLLVALALLVLKKSMGWEVN----------FDMSL
                :   * : :::   * :* ** : : :  :    :** :  * *  * :                      *   :

                III                 IV
Ap     79 ATVWSQAPSVFINLVFATLFLGETIPSPKEIWQKVAPQVAFSQILAWGQYVVGLGMTLLVLTPVFGMNPIAGALI-EMAFE
7002   78 RAVWSQSPGIFINIVFAALFLGEAIPRPKDIWTKTAPQVVFGQTLAWGQYVVGILVTLLILMPLFGVNPIAACLI-EIGFE
Ec     66 R-------DPLMLAFFATIGLNANIASLRAGGRVVGIFLIVVVGLLVMQNAIGIG-----MASLLGLDPLMGLLAGSITLS
                     ::   **:: *   *   :         :     *   *  :*:      :  ::*::*:   *   : :
       Pore-loop region
                ---Vb---          V
Ap    159 GGHGTAAGMAAVLDD-FGFQEGGEIALGLATVGLISGVVTGTILINWGRRKGHISSGHKPDLSFDSSPQEAGDDSHELQTEY
7002  158 GGHGTAGGMAETFTE-LGFEAGADLALGIATVGIVGGIVAGTALADWGRRKGHVTSFQKAVEDLDGVPELTETESPEVRRRR
Ec    136 GGHGTGAAWSKLFIERYGFTNATEVAMACATFGLVLGGLIGGPVARYLVKHSTTP---------NGIPD---DQEVPTAFEK
          *****    :  : :  **    ::*:  ** *:: * : *  :  :  ::             :  *:    :

                VI                  VII
Ap    240 KSLGKNLLIDPLSINLGFVAIALTLGWLILEGLKELEALTWSKIDIEIMNYVPLFPMALIGGLIVQISMRRLGLDGLILRPL
7002  239 AQLMRNLLIDPLSINFGIVGAAIVIGWLILEALVWVESVTWGQTGFEVISYVPLFPMALIGGIIVQLVMERLGLAPLIIRSL
Ec    206 PDVGRMITSLVLIETIALIAICLTVGKIVAQLLAG------------TAFELPTFVCVLFVGVILSNGLSIMGFYRVFER-A
            : : :    *   : ::   : :* :: : *                :* *   *: *:*:   :  :*:  :: *
                                                                                Pore-loop region
                VIII                IX                                          ---------Xa---------
Ap    322 QKNIAGVALDAVIFSAIASISLGVLGTNLIPFLILSVAGIAWNIFAFLFFAPRILPTHWFERGIGDIGQSMGVTATGLLLLQ
7002  321 MSNIAGLALDVVVVTALASISLSVIGSNLGVFTILSVVGITWNVVMFLYFAPRIFPSHWFEKGIGDMGQSMGVTATGILLLR
Ec    275 VSVLGNVSLSLFLAMALMGLKLWELASLALPMLAILVVQTIFMALYAIFVTWRMMGKNYDAAVLAAGHCGFGLGATPTAIAN
             :  ::*   :  *:  : *  : :    : :  *    :     : : : *::  ::    :      :*: **   :

                X                   XI
Ap    404 MVDPANETEALESFAYKQLLFEPIMGGGFFTAAAPILVFQLGGMPVLILTGGFLVFWIIFGLFNFNVKPKTLM        476
7002  403 MVDPENRTGAFESFAYKQLFFEPIVGGGLFTAAAPALVVRFGLVPVLLLTGGLLIFWLAMGFLIIRQNQQQRRRSPSL 480
Ec    357 MQAITERFGP----SHMAFLVVPMVG-AFFIDIVNALVIKLYLMLPIFAG                              401
          *    :        ::  ::  *::*  :*      ** ::  :  ::
```

Figure 4.18 **Amino acid sequence alignment of three Na^+/glutamate transporter, ApGltS, SYNPCC7002, and EcGltS.**

Boxes above the alignment correspond to transmembrane regions according to Figure 4.19. Sequence highlights regions show pore-loop regions, Vb containing GGHGT motif and Xa containing GVTAT motif. Dash box represents the XI transmembrane that is missing in *E. coli* GltS.

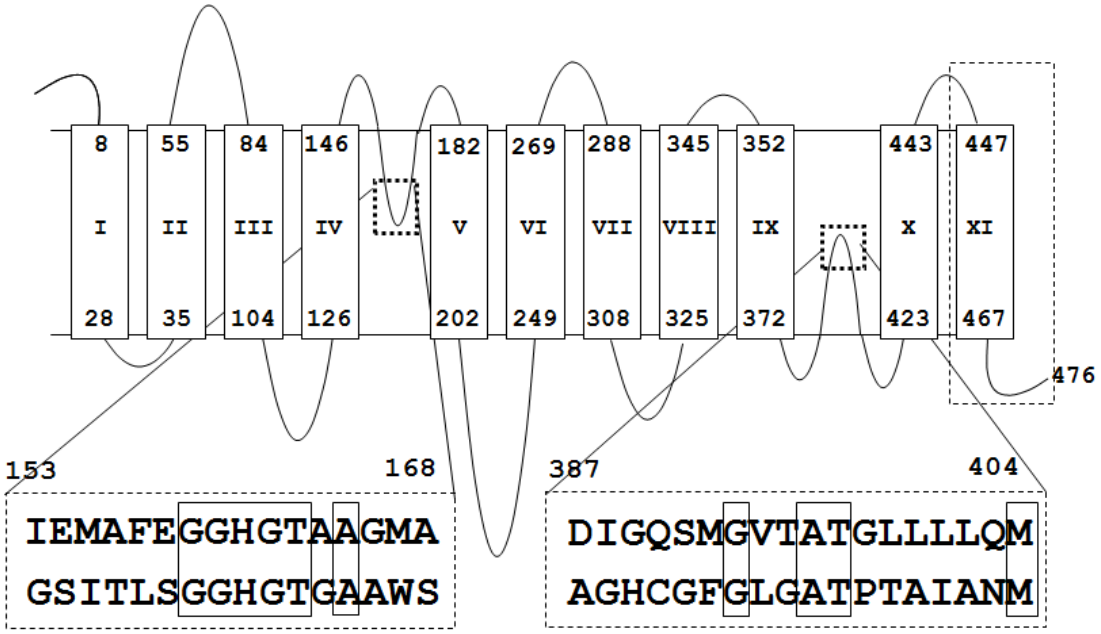

Figure 4.19 Topology model of ApGltS.

Position numbers correspond to the residue numbers in ApGltS. Dash boxes indicate the pore-loop structures. Upper amino acid residues represent the residues in ApGltS and lower amino acid residues represent the residues in *E. coli* GltS.

4.3.4 Amplification of *A. halophytica* Na^+/glutamate transporter gene (*ApgltS*) and construction of pBluescript® II SK^+ recombinant plasmid containing *ApgltS* gene

A. halophytica genomic DNA was used as template for PCR amplification of the *gltS* gene. Primers *ApgltS*NcoI-F and *ApgltS*SalI-R were used to amplify the coding sequence of *ApgltS* with the size of 1,400 bp as shown by agarose gel electrophoresis in Figure 4.20. The purified PCR product was cloned into the *Eco*RV restriction site of pBluescript® II SK^+ ($pBSK^+$) vector and the recombinant plasmid, $pBSK^+$-*ApgltS*, was transformed into the *E. coli* DH5α competent cells. The transformants were selected by blue-white screening on ampicillin agar plates containing X-gal. White colonies were randomly selected and cultured in 1 ml LB broth containing 100 $\mu g.ml^{-1}$ ampicillin at 37 °C for overnight and the cultures were subjected to plasmid extraction. To verify the insertion of PCR products, the recombinant plasmid, $pBSK^+$-*ApgltS*, was restricton digested with *Pst*I, *Hinc*II, *Nco*I + *EcoR*I, *Mun*I + *SalI,* and *Nco*I + *Sal*I and analyzed by 1% agarose gel electrophoresis. The expected sizes of DNA fragments are shown in Table 4.5 that corresponded to the results in Figure 4.21.

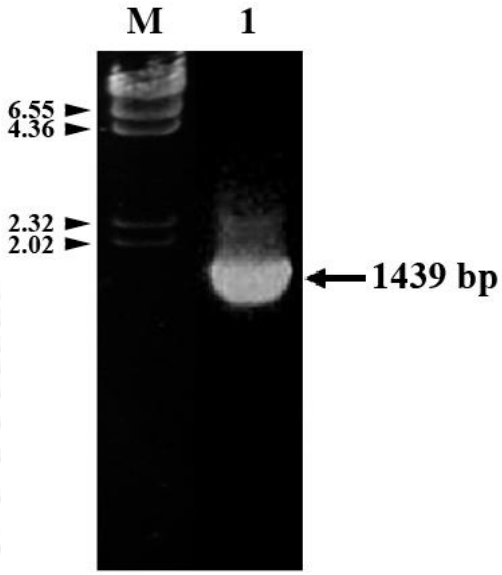

Figure 4.20 **Agarose gel electrophoresis of the amplified coding sequence of *ApgltS*.**

The PCR products were separated on 1% agarose gels and visualized by ethidium bromide staining.

Lane M DNA Marker: λ/*Hind*III

Lane 1 PCR product of *ApgltS*

Table 4.5 Restriction enzymes used for the digestion of pBSK^{+}-*ApgltS* and expected size of DNA fragments.

Restriction Enzymes	Expected DNA Fragments (bp)
*Pst*I	3446, 955
*Hinc*II	2945, 1456
*Nco*I + *EcoR*I	2960, 1173, 268
*Mun*I + *Sal*I	2945, 1288, 168
*Nco*I + *Sal*I	2945, 1173, 257, 260

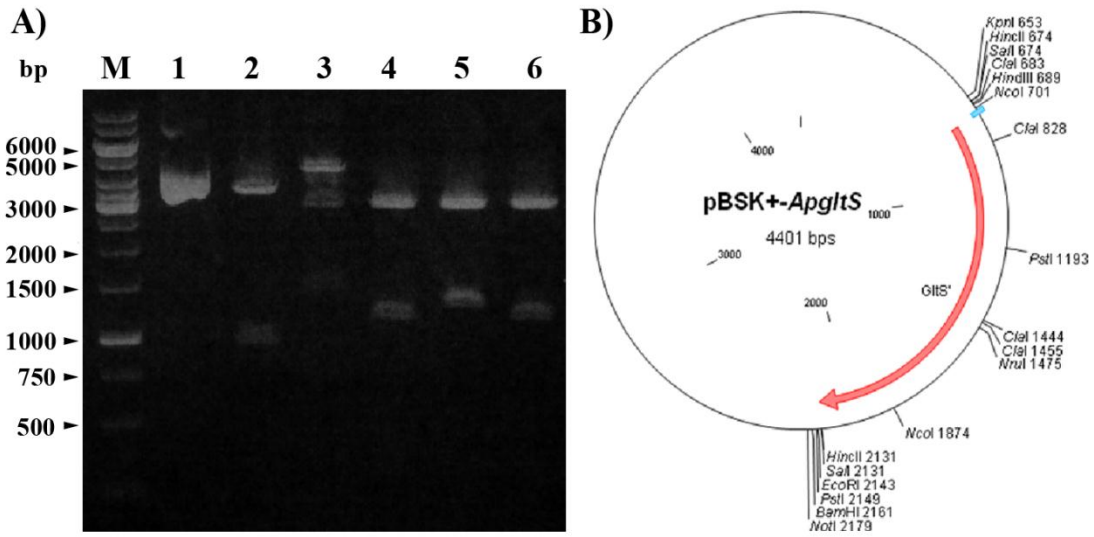

Figure 4.21 **Agarose gel electrophoresis of restriction digestion of the recombinant plasmid pBSK^{+}-*ApgltS*.**

The DNA was separated on 1% agarose gels and visualized by ethidium bromide staining.

A) Lane M GeneRuler™ 1 kb DNA ladder

Lane 1 undigested pBSK^{+}-*ApgltS*

Lane 2 pBSK^{+}-*ApgltS* digested with *Pst*I

Lane 3 pBSK^{+}-*ApgltS* digested with *Hinc*II

Lane 4 pBSK^{+}-*ApgltS* digested with *Nco*I and *EcoR*I

Lane 5 pBSK^{+}-*ApgltS* digested with *Mun*I and *Sal*I

Lane 6 pBSK^{+}-*ApgltS* digested with *Nco*I and *Sal*I

B) Map of the recombinant plasmid pBSK^{+}-*ApgltS*

To verify the sequence of *ApgltS* gene, the recombinant plasmids were subjected to DNA sequencing. DNA sequences of pBSK^{+}-*ApgltS* are shown in Figure 4.22. The nucleotide sequence revealed a single reading frame of 1,439 bp which TTG start codon of *A. halophytica* was changed to ATG for improving the expression efficiency in *E. coli* and TAG stop codon was changed to TCG for using 6xHis-tag stop codon in expression vector (pTrcHis2_C). The resulted pBSK^{+}-*ApgltS* DNA sequences was compared with data from genome sequence using the EMBOSS Pairwise Alignment Algorithms. The results revealed that the *ApgltS* sequence shared 99.6% identity with the coding sequence of *ApgltS* from the genome sequence data as shown in Figure 4.23. Furthermore, the deduced amino acid sequences alignment of ApGltS from genome sequences (ApGltS-G) and from the recombinant plasmid (result of DNA sequencing of pBSK^{+}-*ApgltS*; ApGltS-S) showed that they have a single-amino acid differences between them. Leucine was substituted with methionine in recombinant ApGltS for cloning purpose as shown in Figure 4.24.

>pBSK^{+}-*ApgltS*

TCCC**ATG**GACACCACTAACTTAGGATTAGGAGATGTTTTTGCAGCGTTTATCGTTTTAGGGCTATTCCT
CCTGATTGGACGATTTTTAAAACAGACAATTAAGCTGTTTGATTTACTTTATTTACCAGAATCGATCCT
CGCGGGAGGCTTAGCTTTATTACTAGGAAAAGAAGGATTAGGTCATCTAGTTCCAGCTTCCAGCTTCTT
GGCTCATCAAGGGATTTTTCCAGAAAATATTGCTACCGTTTGGTCACAAGCTCCCAGTGTTTTTATTAA
TCTTGTGTTTGCGACACTTTTTCTCGGGGAAACCATTCCCAGCCCCAAAGAAATTTGGCAGAAAGTTGC
GCCTCAAGTCGCGTTTTCTCAAATTTTGGCGTGGGGACAATATGTGGTTGGCTTAGGAATGACACTGCT
GGTTTTAACTCCTGTTTTTGGCATGAATCCCATTGCAGGTGCACTGATTGAAATGGCGTTTGAAGGGGG
TCATGGAACGGCTGCAGGAATGGCTGCTGTTTTAGATGATTTTGGCTTTCAGGAAGGAGGAGAAATTGC
GTTAGGCTTAGCAACAGTCGGCTTGATTTCTGGTGTAGTGACGGGAACAATTTTGATTAATTGGGGACG
GAGAAAAGGTCATATTTCTTCAGGACATAAACCTGATTTATCTTTCGATTCTTCTCCTCAGGAAGCTGG
CGATGATTCCCATGAGTTGCAAACGGAATATAAAAGTTTAGGGAAAAATTTATTAATCGATCCCTTATC
GATTAATTTAGGATTTGTCGCGATCGCGCTGACATTAGGCTGGCTCATTTTAGAAGGATTAAAAGAATT
AGAAGCCCTCACTTGGAGTAAAATAGACATTGAAATTATGAACTATGTCCCTTTATTTCCGATGGCGCT
GATTGGTGGGTTAATTGTTCAAATTTCTATGAGGCGTTTAGGGCTAGATGGGTTAATTCTAAGACCGCT
ACAGAAAAATATTGCTGGGGTTGCTTTGGATGCCGTTATTTTCAGCGCGATCGCGTCCATTTCTCTGGG
TGTATTGGGGACAAACCTCATCCCATTTTTAATTTTATCCGTTGCTGGTATTGCTTGGAATATTTTTGC
TTTTCTATTCTTTGCCCCGCGCATTCTTCCCACTCATTGGTTTGAACGCGGAATTGGCGATATTGGACA
ATCCATGGGAGTAACAGCAACTGGTTTATTATTGCTGCAAATGGTCGATCCAGCTAATGAAACCGAAGC
GTTAGAAAGTTTTGCCTATAAGCAATTGCTCTTTGAACCGATTATGGGAGGCGGTTTCTTTACCGCAGC
AGCCCCCATTTTGGTGTTTCAGTTAGGAGGAATGCCCGTTTTAATTTTAACAGGAGGGTTCTTAGTCTT
TTGGATTATTTTTGGCTTATTTAATTTCAATGTTAAACCGAAAACTTTGATGGTCGACAG

Figure 4.22 DNA sequences of *ApgltS* gene in the recombinant plasmid pBSK^{+}-*ApgltS*.

The underlined letters represent primer binding sites.

```
ApgltSgeno   1 TCAATTGAACACCACTAACTTAGGATTAGGAGATGTTTTTGCAGCGTTTA  50
pBSKApgltS   1 --CCA--G-------------------------------------------  50

ApgltSgeno  51 TCGTTTTAGGGCTATTCCTCCTGATTGGACGATTTTTAAAACAGACAATT 100
pBSKApgltS  51 ---------------------------------------------------- 100

ApgltSgeno 101 AAGCTGTTTGATTTACTTTATTTACCAGAATCGATCCTCGCGGGAGGCTT 150
pBSKApgltS 101 ---------------------------------------------------- 150

ApgltSgeno 151 AGCTTTATTACTAGGAAAAGAAGGATTAGGTCATCTAGTTCCAGCTTCCA 200
pBSKApgltS 151 ---------------------------------------------------- 200

ApgltSgeno 201 GCTTCTTGGCTCATCAAGGGATTTTTCCAGAAAATATTGCTACCGTTTGG 250
pBSKApgltS 201 ---------------------------------------------------- 250

ApgltSgeno 251 TCACAAGCTCCCAGTGTTTTTATTAATCTTGTGTTTGCGACACTTTTTCT 300
pBSKApgltS 251 ---------------------------------------------------- 300

ApgltSgeno 301 CGGGGAAACCATTCCCAGCCCCAAAGAAATTTGGCAGAAAGTTGCGCCTC 350
pBSKApgltS 301 ---------------------------------------------------- 350

ApgltSgeno 351 AAGTCGCGTTTTCTCAAATTTTGGCGTGGGGACAATATGTGGTTGGCTTA 400
pBSKApgltS 351 ---------------------------------------------------- 400

ApgltSgeno 401 GGAATGACACTGCTGGTTTTAACTCCTGTTTTTGGCATGAATCCCATTGC 450
pBSKApgltS 401 ---------------------------------------------------- 450

ApgltSgeno 451 AGGTGCACTGATTGAAATGGCGTTTGAAGGGGGTCATGGAACGGCTGCAG 500
pBSKApgltS 451 ---------------------------------------------------- 500

ApgltSgeno 501 GAATGGCTGCTGTTTTAGATGATTTTGGCTTTCAGGAAGGAGGAGAAATT 550
pBSKApgltS 501 ---------------------------------------------------- 550

ApgltSgeno 551 GCGTTAGGCTTAGCAACAGTCGGCTTGATTTCTGGTGTAGTGACGGGAAC 600
pBSKApgltS 551 ---------------------------------------------------- 600

ApgltSgeno 601 AATTTTGATTAATTGGGGACGGAGAAAAGGTCATATTTCTTCAGGACATA 650
pBSKApgltS 601 ---------------------------------------------------- 650

ApgltSgeno 651 AACCTGATTTATCTTTCGATTCTTCTCCTCAGGAAGCTGGCGATGATTCC 700
pBSKApgltS 651 ---------------------------------------------------- 700

ApgltSgeno 701 CATGAGTTGCAAACGGAATATAAAAGTTTAGGGAAAAATTTATTAATCGA 750
pBSKApgltS 701 ---------------------------------------------------- 750

ApgltSgeno 751 TCCCTTATCGATTAATTTAGGATTTGTCGCGATCGCGCTGACATTAGGCT 800
pBSKApgltS 751 ---------------------------------------------------- 800

ApgltSgeno 801 GGCTCATTTTAGAAGGATTAAAAGAATTAGAAGCCCTCACTTGGAGTAAA 850
pBSKApgltS 801 ---------------------------------------------------- 850

ApgltSgeno 851 ATAGACATTGAAATTATGAACTATGTCCCTTTATTTCCGATGGCGCTGAT 900
pBSKApgltS 851 ---------------------------------------------------- 900
```

```
ApgltSgeno 901 TGGTGGGTTAATTGTTCAAATTTCTATGAGGCGTTTAGGGCTAGATGGGT 950
pBSKApgltS 901 -------------------------------------------------- 950

ApgltSgeno 951 TAATTCTAAGACCGCTACAGAAAAATATTGCTGGGGTTGCTTTGGATGCC1000
pBSKApgltS 951 ---------------------------------------------------1000

ApgltSgeno1001 GTTATTTTCAGCGCGATCGCGTCCATTTCTCTGGGTGTATTGGGGACAAA1050
pBSKApgltS1001 ---------------------------------------------------1050

ApgltSgeno1051 CCTCATCCCATTTTTAATTTTATCCGTTGCTGGTATTGCTTGGAATATTT1100
pBSKApgltS1051 ---------------------------------------------------1100

ApgltSgeno1101 TTGCTTTTCTATTCTTTGCCCCGCGCATTCTTCCCACTCATTGGTTTGAA1150
pBSKApgltS1101 ---------------------------------------------------1150

ApgltSgeno1151 CGCGGAATTGGCGATATTGGACAATCCATGGGAGTAACAGCAACTGGTTT1200
pBSKApgltS1151 ---------------------------------------------------1200

ApgltSgeno1201 ATTATTGCTGCAAATGGTCGATCCAGCTAATGAAACCGAAGCGTTAGAAA1250
pBSKApgltS1201 ---------------------------------------------------1250

ApgltSgeno1251 GTTTTGCCTATAAGCAATTGCTCTTTGAACCGATTATGGGAGGCGGTTTC1300
pBSKApgltS1251 ---------------------------------------------------1300

ApgltSgeno1301 TTTACCGCAGCAGCCCCCATTTTGGTGTTTCAGTTAGGAGGAATGCCCGT1350
pBSKApgltS1301 ---------------------------------------------------1350

ApgltSgeno1351 TTTAATTTTAACAGGAGGGTTCTTAGTCTTTTGGATTATTTTTGGCTTAT1400
pBSKApgltS1351 ---------------------------------------------------1400

ApgltSgeno1401 TTAATTTCAATGTTAAACCGAAAACTTTGAT.GTAGACAG1439
pBSKApgltS1401 -------------------------------G--C-----1440
```

Figure 4.23 **Nucleotide sequence alignment of the coding sequence of *ApgltS* gene from genome sequences (*ApgltS*geno) and from the result of DNA sequencing of pBSK^{+}-*ApgltS* using EMBOSS Pairwise Alignment Algorithms.**

The identical residues in other sequences are indicated by a dash (-), and a gap introduced for alignment purposes is indicated by a dot (.).

```
ApGltS-G LDTTNLGLGDVFAAFIVLGLFLLIGRFLKQTIKLFDLLYLPESILAGGLALLLGKEGLGH
ApGltS-S MDTTNLGLGDVFAAFIVLGLFLLIGRFLKQTIKLFDLLYLPESILAGGLALLLGKEGLGH
          ************************************************************

ApGltS-G LVPASSFLAHQGIFPENIATVWSQAPSVFINLVFATLFLGETIPSPKEIWQKVAPQVAFS
ApGltS-S LVPASSFLAHQGIFPENIATVWSQAPSVFINLVFATLFLGETIPSPKEIWQKVAPQVAFS
         ************************************************************

ApGltS-G QILAWGQYVVGLGMTLLVLTPVFGMNPIAGALIEMAFEGGHGTAAGMAAVLDDFGFQEGG
ApGltS-S QILAWGQYVVGLGMTLLVLTPVFGMNPIAGALIEMAFEGGHGTAAGMAAVLDDFGFQEGG
         ************************************************************

ApGltS-G EIALGLATVGLISGVVTGTILINWGRRKGHISSGHKPDLSFDSSPQEAGDDSHELQTEYK
ApGltS-S EIALGLATVGLISGVVTGTILINWGRRKGHISSGHKPDLSFDSSPQEAGDDSHELQTEYK
         ************************************************************

ApGltS-G SLGKNLLIDPLSINLGFVAIALTLGWLILEGLKELEALTWSKIDIEIMNYVPLFPMALIG
ApGltS-S SLGKNLLIDPLSINLGFVAIALTLGWLILEGLKELEALTWSKIDIEIMNYVPLFPMALIG
         ************************************************************

ApGltS-G GLIVQISMRRLGLDGLILRPLQKNIAGVALDAVIFSAIASISLGVLGTNLIPFLILSVAG
ApGltS-S GLIVQISMRRLGLDGLILRPLQKNIAGVALDAVIFSAIASISLGVLGTNLIPFLILSVAG
         ************************************************************

ApGltS-G IAWNIFAFLFFAPRILPTHWFERGIGDIGQSMGVTATGLLLLQMVDPANETEALESFAYK
ApGltS-S IAWNIFAFLFFAPRILPTHWFERGIGDIGQSMGVTATGLLLLQMVDPANETEALESFAYK
         ************************************************************

ApGltS-G QLLFEPIMGGGFFTAAAPILVFQLGGMPVLILTGGFLVFWIIFGLFNFNVKPKTLM--
ApGltS-S QLLFEPIMGGGFFTAAAPILVFQLGGMPVLILTGGFLVFWIIFGLFNFNVKPKTLMVD
         *******************************************************
```

Figure 4.24 Amino acid sequence alignment of ApGltS from genome sequences (ApGltS-G) and from recombinant plasmid (result of DNA sequencing; ApGltS-S).

4.3.5 Construction of pTrcHis2_C recombinant plasmid containing *ApgltS* gene

The recombinant plasmid, pBSK^{+}-*ApgltS*, was digested with *Nco*I and *Sal*I to obtained 1.439 kb fragment of *gltS* gene from *A. halophytica* and then this fragment was eluted and purified. The purified fragment of *ApgltS* was subcloned into *Nco*I-*Sal*I sites of pTrcHis2_C expression vector. The resulting plasmid, p*ApgltS* harboring *ApgltS gene*, was transformed to *E. coli* DH5α. The transformants were selected and screening on ampicillin agar plates. White colonies were randomly selected and cultured in 1 ml LB broth containing 100 μg.ml^{-1} of ampicillin at 37 °C overnight and the cultures were subjected to plasmid extraction. To confirm the insertion of purified *ApgltS* fragment into pTrcHis2_C, p*ApgltS* was digested with restriction enzyme as shown in Table 4.6. Subsequently, the products were analyzed by 1% agarose gel electrophoresis as shown in Figure 4.25. Positive clone was selected and subjected to DNA sequencing. The result of DNA sequencing showed that *ApgltS* was in-frame ligated with 6xHis-tag at the C-terminus. The p*ApgltS* was transformed into ME9107 cell.

Table 4.6 Restriction enzymes used for the digestion of p*ApgltS* and expected sizes of DNA fragments.

Restriction Enzymes	Expected DNA Fragments (bp)
*Hinc*II	1885,1649,935,809,459
*Nco*I+*Sal*I	4307,1173,257
*Pst*I	5737

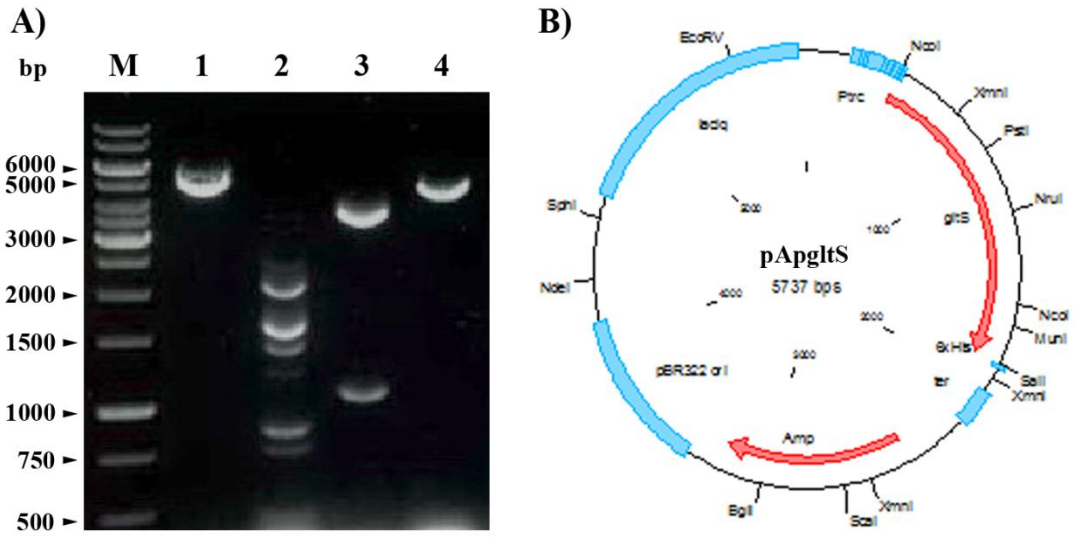

Figure 4.25 Agarose gel electrophoresis of restriction digestion of the recombinant plasmid p*ApgltS*.

The DNA was separated on agarose gels and visualized by ethidium bromide staining.

a) Lane M GeneRuler™ 1 kb DNA ladder

Lane 1 undigested p*ApgltS*

Lane 2 pTrcHis2_C-*ApgltS* digested with *Hinc*II

Lane 3 pTrcHis2_C-*ApgltS* digested with *Nco*I and *Sal*I

Lane 4 pTrcHis2_C-*ApgltS* digested with *Pst*I

b) Map of the recombinant plasmid p*ApgltS*

4.3.6 Expression of *ApgltS* in *E. coli* ME9107 under trc promoter using anti-His-tag antibodies

To express the ApGltS in *E. coli* system, the recombinant plasmid, p*ApgltS*, was transformed into GltS-deficient *E. coli* mutant ME9107 cells which were deficient in glutamate uptake. The *ApgltS* expressing *E. coli* ME9107 were grown at 37 °C in Minimal Medium A (MMA), pH 7.5 containing 0.2% glucose, ampicillin (50 μg.ml^{-1}) until optical density at 620 nm reached 0.3 and then isopropyl-D-thiogalactoside (IPTG) was added to final concentration of 1 mM. After induction with 1 mM IPTG for 5 hrs, cells were harvested, sonicated, and membrane fractions were used for Western blotting by 12.0% SDS-PAGE using anti-6xHis as primary antibody and anti-mouse immunoglobulin G as secondary antibody. As shown in Figure 4.26, ApGltS could be expressed in *E. coli* ME9107 cells transformed with p*ApgltS* in membrane fraction after induction by 1 mM IPTG, however no detectable band was observed in *E. coli* ME9107 transformed with pTrcHis2_C. Its molecular mass was ≈ 52 kDa which corresponded to the calculated value of 50,976 Da.

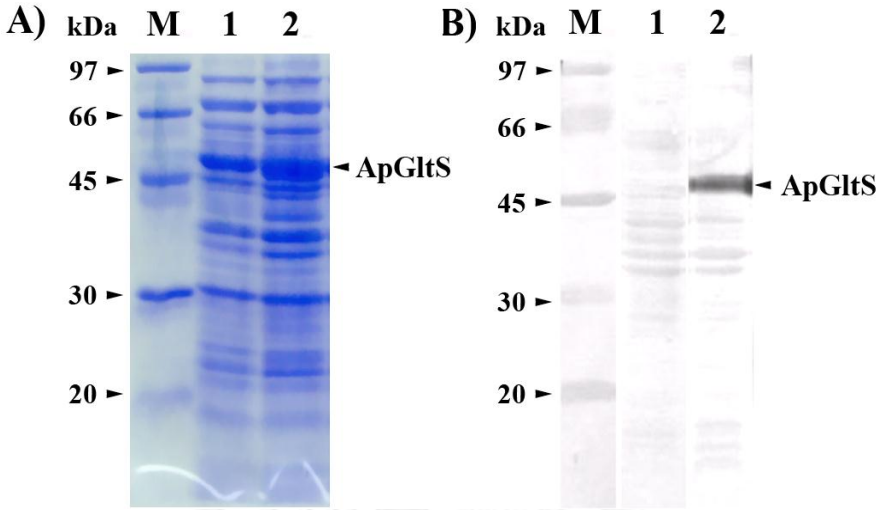

Figure 4.26 Immunoblotting analyses of *ApgltS* expressing *E. coli* ME9107 probing with anti-6xHis.

The membrane fractions of *E. coli* were prepared. Equal amounts of proteins (20 µg) were applied on SDS-PAGE and visualized by Coomassie blue-stained (A) and using the antibodies raised against 6×His tag (B). The plasmids used for the transformation of ***E. coli*** were follows:

Lane M Molecular weight marker

Lane 1 pTrcHis2_C

Lane 2 p*ApgltS*

4.3.6.1 Effect of IPTG concentration on the expression of ApGltS in *E. coli* ME9107

The transformant cells were in MMA, pH 7.5 containing 0.2% glucose, ampicillin (50 μg.ml^{-1}) until optical density at 620 nm reached 0.3 then the indicated concentrations of IPTG were added. After 5 hrs incubation, the membrane fractions were prepared and analyzed by Western blotting. The results showed that the optimal concentration of IPTG is at 1 mM. Increasing IPTG concentration slightly increased the expression level of ApGltS (Figure 4.27A).

4.3.6.2 Effect of NaCl in the growth medium on the expression of ApGltS in *E. coli* ME9107

The transformant cells were in MMA, pH 7.5 containing 0.2% glucose, ampicillin (50 μg.ml^{-1}), and indicated concentrations of NaCl (0, 0.25 and 0.5 M) until optical density at 620 nm reached 0.3 and then IPTG was added to final conc. of 1 mM. After 5 hrs induction, the membrane fractions were prepared and analyzed by Western blotting. The results showed that the expression of ApGltS was hardly affected by the concentrations of NaCl in growth medium (Figure 4.27B).

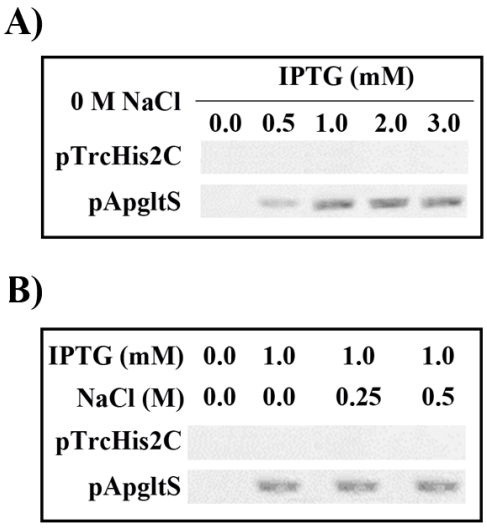

Figure 4.27 Effect of IPTG concentration (A) and NaCl in the growth medium (B) on the expression of ApGltS in *E. coli* ME9107.

The membrane fractions of ***E. coli*** were prepared. Equal amounts of proteins (20 μg) were applied on SDS-PAGE and visualized by using the antibodies raised against 6×-His tag.

4.4 Characterization of *ApgltS* expressing *E. coli* ME9107

4.4.1 Complementation tests of *ApgltS* expressing *E. coli* ME9107

For the complementation test on liquid medium, *E. coli* ME9107 transformed with pTrcHis2_C and transformed with p*ApgltS* were grown in MMA, pH 7.5 containing 0.2% glucose, ampicillin (50 $\mu g.ml^{-1}$), and indicated concentrations of NaCl (0, 0.25 and 0.5 M) supplemented with 0, 1 and 5 mM glutamate. The growth was monitored by measuring optical density of culture at 620 nm as shown in Figure 4.28. The results showed that both pTrcHis2_C control vector and *ApgltS*-expressing transformants exhibited similar growth patterns when grown in MMA medium in the absence of NaCl. The increase of NaCl concentration up to 0.25 and 0.5 M NaCl resulted in slower growth of the cells. However, the growth rate of *ApgltS*-expressing cells was slightly higher than that of control. Glutamate supplementation enhanced growth of *ApgltS*-expressing cells only under salt stress condition at all glutamate concentrations tested. The growth inhibitory effect of 0.25 and 0.5 M NaCl was relieved in the presence of 1 and 5 mM glutamate, respectively.

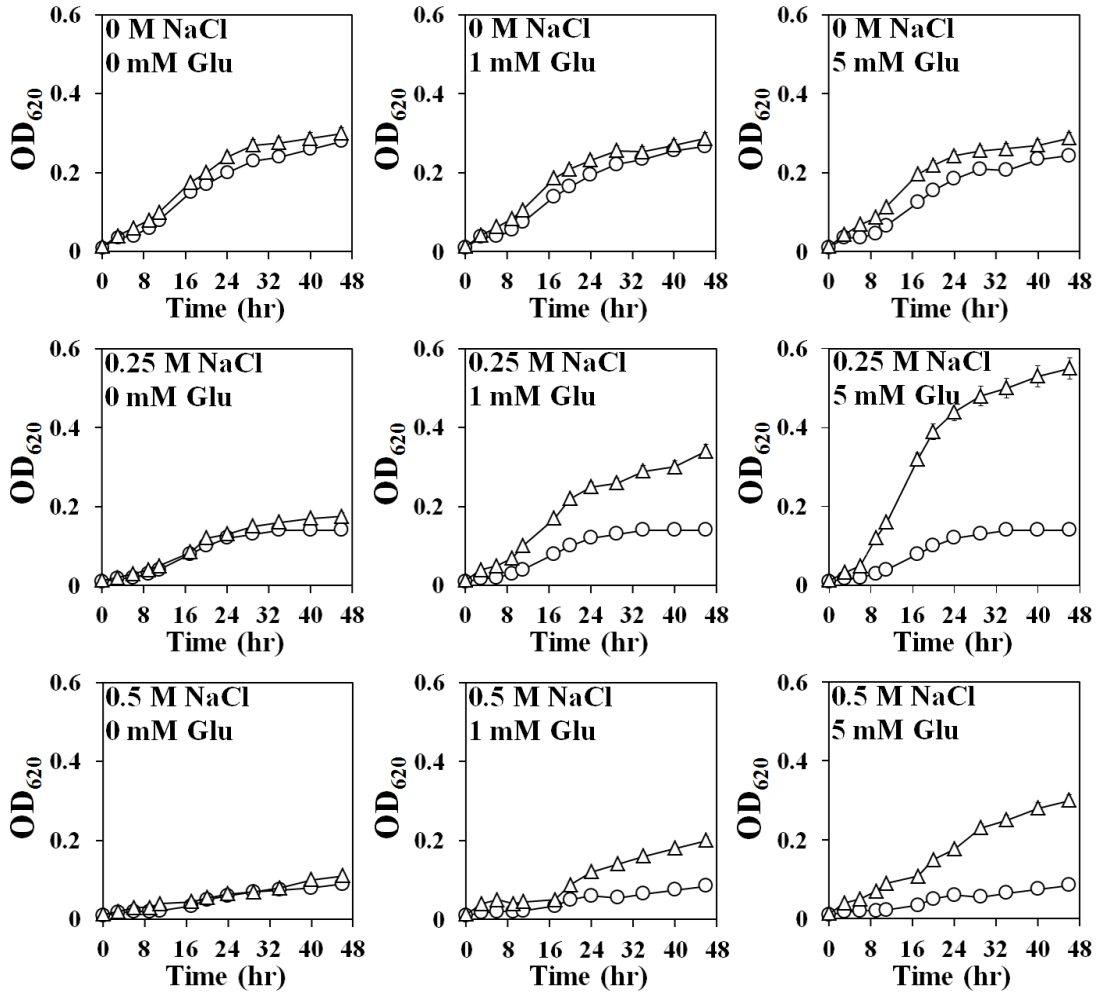

Figure 4.28 Growth curve of *ApgltS* expressing *E. coli* ME9107.

E. coli ME9107 transformed with pTrcHis2_C and p*ApgltS* were grown in MMA medium containing 0.0 M NaCl, 0.25 M NaCl or 0.5 M NaCl supplemented with 0, 1 and 5 mM glutamate. (○) represents *E. coli* ME9107 cells transformed with pTrcHis2_C, whereas (△) represents *E. coli* ME9107 cells transformed with p*ApgltS*. The data are from three independent experiments with vertical bars representing standard errors of the means, n=3

4.4.2 Glutamate transport assay in *ApgltS* expressing *E. coli* ME9107

4.4.2.1 Glutamate uptake into *E. coli* ME9107, *E. coli* ME9107 cells transformed with pTrcHis2_C (pTrcHis2_C/ME9107) and *E. coli* ME9107 cells transformed with p*ApgltS* (p*ApgltS*/ME9107)

The *E. coli* ME9107 transformed with pTrcHis2_C or p*ApgltS* were grown overnight at 37 °C in MMA (pH 7.5) containing 0.2% glucose and ampicillin (50 μg.ml^{-1}) and were inoculated into the same fresh medium with an OD_{620} of 0.05. Isopropyl 1 mM β-D-1thiogalactopyranoside (IPTG) was added. After 3 h of incubation, cells were harvested, washed twice, and suspended to an OD_{620} of 1.0 in 100 mM Tris HCl, pH 7.5 or 100 mM sodium phosphate buffer pH 7.5. Subsequently, the cell suspension was shaken for 5 min at 37 °C, and the uptake was initiated by the addition of 0.1 mM [U-^{14}C] glutamate.

The *E. coli* ME9107 transformed with p*ApgltS* (p*ApgltS*/ME9107) could take up glutamate in 100 mM sodium phosphate buffer. No measurable uptake of [U-^{14}C] glutamate was observed for the *E. coli* ME9107 transformed with pTrcHis2_C (pTrcHis2_C /ME9107) and also *E. coli* ME9107 as shown in Figure 4.29B. The initial rate of [U-^{14}C] glutamate uptake was observed within 1 min and cells showed saturated glutamate uptake after cells were exposed to glutamate for 10 min. The glutamate uptake rate was 0.72 ± 0.06 nmol.min^{-1}.mg^{-1} protein. In addition, using Tris-HCl buffer instead of sodium phosphate buffer resulted in a complete loss of glutamate uptake

activity (Figure 4.29A). This was due to the fact that ApGltS, a Na^+/glutamate symporter, needs Na^+ to stimulate glutamate uptake and 100 mM sodium phosphate buffer contains 161 mM Na^+.

4.4.2.2 Saturation kinetics of glutamate uptake in *ApgltS* expressing *E. coli* ME9107

The kinetic properties of ApGltS in the *E. coli* ME9107 cells transformed with p*ApgltS* were examined. Figure 4.30 shows the effects of glutamate concentration ranging from 0 to 100 μM on the uptake rate. The glutamate uptake rates were increased with the increase of glutamate and showed the saturation curves. The glutamate uptake at pH 7.5 increased upon the increase of the concentrations of NaCl (0-0.5 M NaCl). From the double reciprocal plots of glutamate transport kinetics by p*ApgltS*/ME9107 cells, K_m and V_{max} values were determined. The results showed that glutamate uptake of *ApgltS* expressing *E. coli* ME9107 under 0, 0.25 and 0.5 M NaCl exhibited the typical of Michaelis-Menten saturation kinetics with an apparent K_m of 5.29 ± 0.21, 4.96 ± 0.31 and 5.16 ± 0.28 μM and the maximum velocity (V_{max}) of 17.73 ± 0.65, 25.64 ± 0.78 and 46.51 ± 1.09 $nmol.min^{-1}.mg^{-1}$ protein, respectively (Table 4.7). The V_{max} values increased upon the increase of NaCl concentrations whereas K_m values were slightly affected. It should be pointed out that an extra 161 mM Na^+ was present due to the use of 100 mM sodium phosphate buffer, pH 7.5 in the uptake assay at each indicated concentration of NaCl.

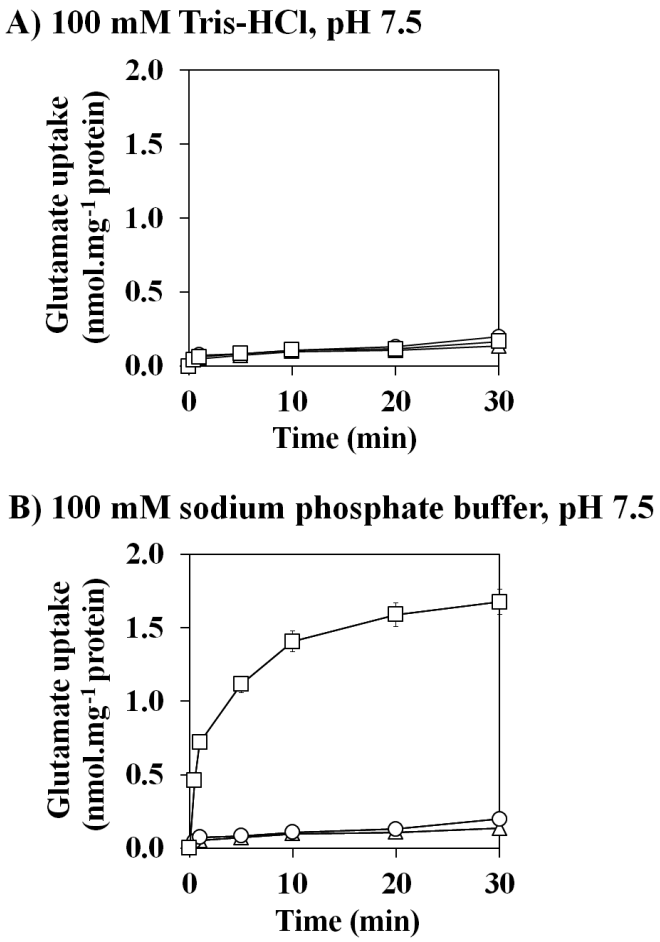

Figure 4.29 Time intervals of glutamate uptake into *E. coli* ME9107, pTrcHis2_C/ME9107 and p*ApgltS*/ME9107 under in the assay medium: 100 mM Tris HCl, pH 7.5 (A) and 100 mM sodium phosphate buffer pH 7.5 (B).

(△) represents *E. coli* ME9107, (○) represents pTrcHis2_C/ME9107 and whereas (□) represents p*ApgltS*/ME9107. The data are from three independent experiments with vertical bars representing standard errors of the means, n=3. Error bars are included in the graphs where some may be smaller than the symbols.

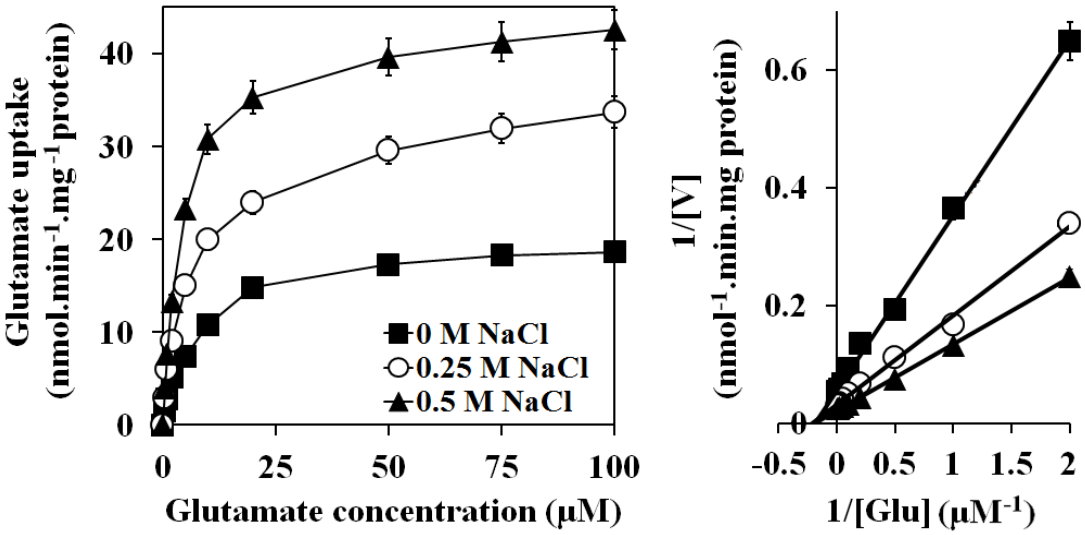

Figure 4.30 **Kinetics of glutamate uptake by *ApgltS* expressing *E. coli* ME9107.** Saturation curve and double reciprocal plots of glutamate uptake by *ApgltS* expressing *E. coli* ME9107 cells assayed in the presence of 0, 0.25 or 0.5 M NaCl at pH 7.5. An extra 161 mM Na^+ contributed by 100 mM sodium phosphate buffer, pH 7.5 was present at each indicated NaCl concentration. The data are from three independent experiments with vertical bars representing standard errors of the means, n=3. Error bars are included in the graphs where some may be smaller than the symbols.

Table 4.7 Kinetic values of glutamate uptake in *ApgltS* expressing *E. coli* ME9107.

NaCl concentration (M)	Kinetic value	
	K_m (μM)	V_{max} (nmol.min^{-1}.mg^{-1} protein)
0	5.29 ± 0.21	17.73 ± 0.65
0.25	4.96 ± 0.31	25.64 ± 0.78
0.5	5.16 ± 0.28	46.51 ± 1.09

4.4.2.3 Effect of sugar, cations, and anions on glutamate transport in *ApgltS* expressing *E. coli* ME9107

We also examined the effect of ions and osmotic agents as a coupling ion on glutamate transport by supplementation with 0.5 M of each agent in the assay medium. Figure 4.31 shows that Na^+ activated the uptake to 3.2 fold of the control whereas NH_4^+ and NO_3^- slightly activated the uptake up to 1.2 and 1.5 fold, respectively. Sugar and alcohol sugar, cations such as K^+, Li^+, Ca_2^+ and Mg_2^+ and anions such as SO_4^{2-}, HCO_3^- and CO_3^{2-} were also ineffective, indicating that ApGltS is a Na^+-dependent glutamate transporter.

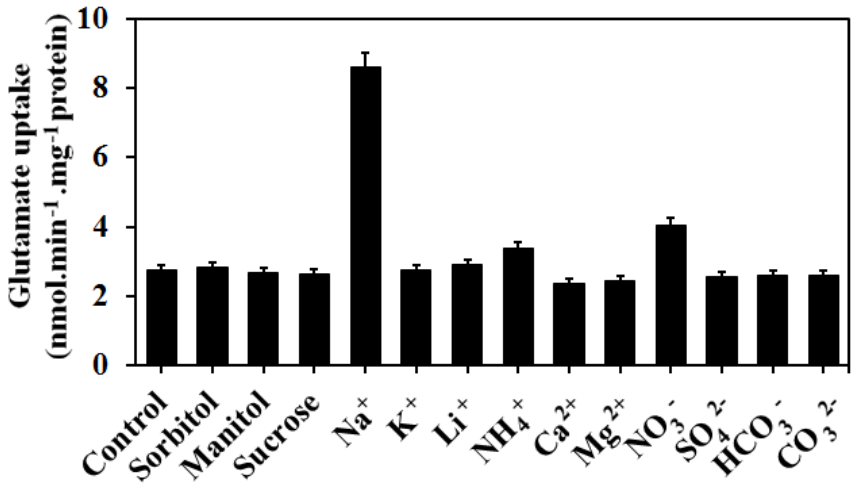

Figure 4.31 **Effect of sugar, cations, and anions on glutamate uptake in *ApgltS* expressing *E. coli* ME9107.**

Initial uptake rates were determined in assay medium supplementation with 0.5 M of each sugar, cation or anion. The data are from three independent experiments with vertical bars representing standard errors of the means, n=3.

4.4.2.4 Effect of NaCl concentration on glutamate transport in *ApgltS* expressing *E. coli* ME9107

The effect of NaCl concentration on glutamate uptake was examined. The results revealed that the exogenous addition of NaCl to assay medium significantly increased the uptake of glutamate, with the maximum uptake at 0.5 M NaCl and NaCl ≥ 1 M decreased glutamate uptake compared to the control with no NaCl as shown in Figure 4.32. Since the assay medium contained 100 mM sodium phosphate, the concentration of Na^+ would be 161 mM higher at pH 7.0 in the assay medium than the indicated values.

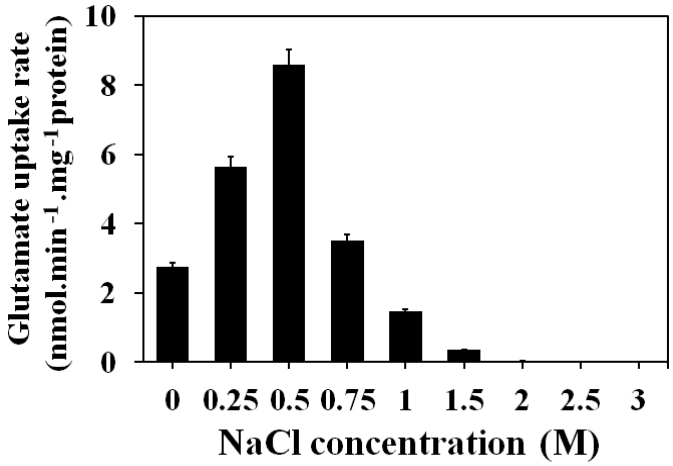

Figure 4.32 Effect of NaCl concentration on glutamate uptake in *ApgltS* expressing *E. coli* ME9107.

Initial uptake rates were determined in the presence of increasing of NaCl concentration from 0-3 M. The data are from three independent experiments with vertical bars representing standard errors of the means, n=3.

4.4.2.5 Effect of pH on glutamate transport in *ApgltS* expressing *E. coli* ME9107

The effect of pH on glutamate uptake by *ApgltS* expressing *E. coli* ME9107 cells was determined in various pH ranging from 5.5 to 10.5. The results showed that ApGltS took up glutamate at a wide range of pH 5.5-10.5 irrespective of the concentrations of NaCl in the assay medium (Figure 4.33). The optimum pH was around 8.5.

4.4.2.6 Specificity of glutamate transport in *ApgltS* expressing *E. coli* ME9107

To determine the specificity of the uptake by ApGltS, we performed the competition experiments. The initial rate of [U-^{14}C] glutamate uptake in the presence of 100 folds excess of unlabeled competitive substrate was examined. The [U-^{14}C] glutamate uptake by ApGltS in *E. coli* ME9107 cells was inhibited by about 90% when 100-fold "cold" glutamate was included in the assay medium containing 0.5 M NaCl as shown in Figure 4.34. Aspartate strongly inhibited glutamate uptake by 80%. Asparagine and glutamine moderately inhibited glutamate uptake about 40-50%. By contrast, no other compounds tested inhibited the glutamate uptake by ApGltS.

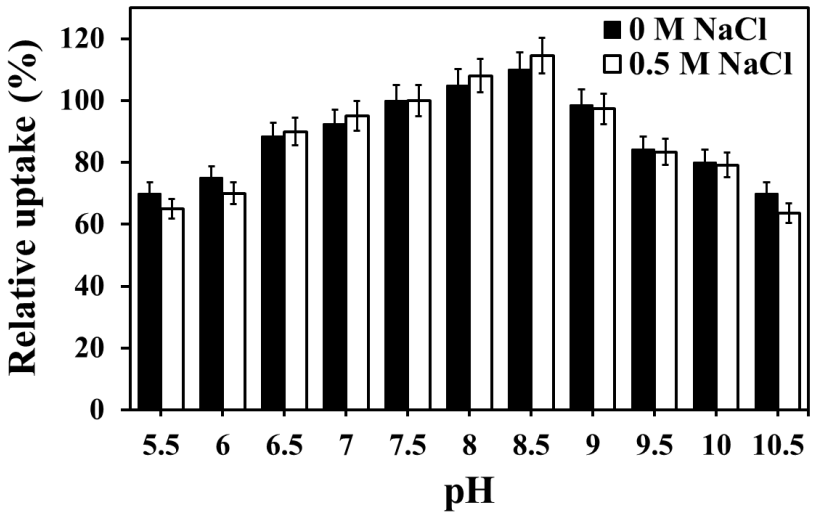

Figure 4.33 Effect of extracellular pH on glutamate transport in *ApgltS* expressing *E. coli* ME9107.

The initial rate of glutamate uptake was determined in assay medium containing 0 and 0.5 M NaCl. The uptake assay was done with the modification using various pH range of 5.5 – 10.5. Uptake rates were normalized with respect to the values at pH 7.5 which is shown as 100%. The data are from three independent experiments with vertical bars representing standard errors of the means, n=3.

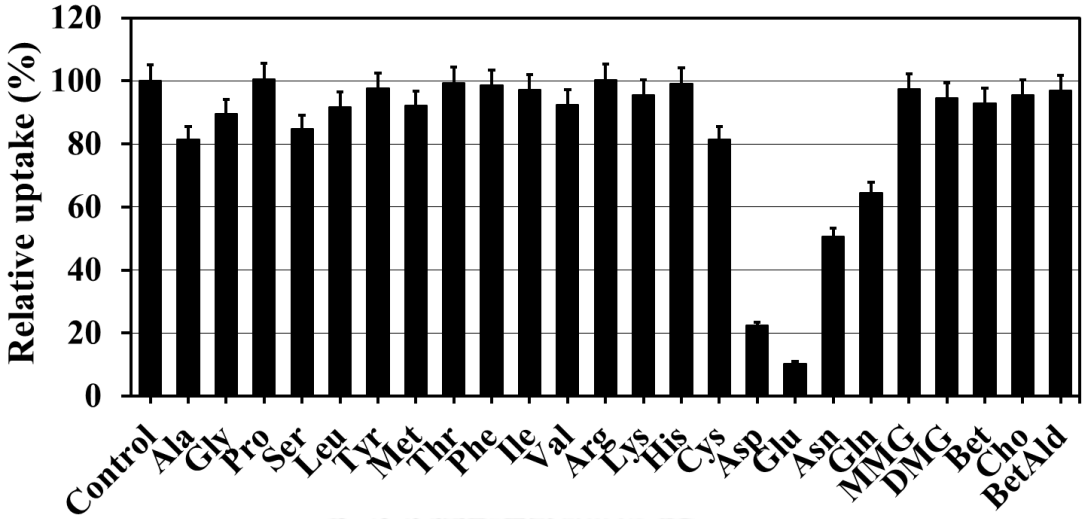

Figure 4.34 Effects of competing amino acid on [U-^{14}C] glutamate uptake in *ApgltS* expressing *E. coli* ME9107.

The reaction mixture contained 0.1 mM [U-^{14}C] glutamate in the presence of 0.5 M NaCl and 10 mM of various competitor compounds. The value of the uptake in the control without competitor is shown as 100%. The data are from three independent experiments with vertical bars representing standard errors of the means, n=3.

4.5 Construction of pUC303 containing *ApgltS* gene for the expression of ApGltS in a freshwater cyanobacterium *Synechococcus* sp. PCC 7942

4.5.1 Construction of pBluescript® II SK+ recombinant plasmid containing promoter region of *ApgltS* gene fused with the coding region of ApgltS gene containing 6xHis-tag

4.5.1.1 Promoter analysis

From the shot gun sequencing of *A. halophytica*, we found the 262-bp of non-coding region within 5' upstream region of the *ApgltS* gene. The putative promoter sequence of *ApgltS* gene was used as a query for promoter analysis. First, transcription start site and promoter prediction was performed using The Berkeley Drosophila Genome Project (BDGP: http://www.fruitfly.org/seq_tools/promoter.html). The results (APPENDIX 23) showed that the *A. halophytica* Na^+/glutamate transporter promoter region occurred between positions 117 and 162. Transcription start site of this promoter was at sequence position 157 and set as +1 as shown in Figure 4.35. Next, the consensus sequence at -10 and -35 regions were predicted by GENETYX7. The -35 and -10 consensus for these promoters is 5'-TTGAAC-N19-AATAAT at positions 124-129 and 149-154, respectively as shown in APPENDIX 24. Moreover, the putative lactococcal-like sigmaA binding domain was identified using Prokaryotic Promoter Prediction (PPP: http://bioinformatics.biol.rug.nl/websoftware/ppp/ppp_start.php) as shown in APPENDIX 25. The putative lactococcal-like sigmaA binding domain found in the region between positions 25 and 58 represented AT-rich recognition element,

called the UP (upstream promoter) element. Putative ribosome binding site (GAAGGA) was observed in the region between positions 253 and 258 (about 10-16 bp upstream of TTG start codon as shown in Figure 4.35.

AT-rich recognition element (UP element)

CTTAATCCAGTAACTTAATCTAGA**TTTTTAGGTGATTAAAAGCATTATATAATATACT**ATAAATCACTT

TTACGGGCAAAAAGGGAAGTTTTTTCTCTATCTTAGGTCAGATTCAATACATTA**TTGAAC**CTTTGCATC

-10 region +1

CCTGAAATGT**AATAAT**TG**C**TACTACTTGCTGACAGGAAAGCTCCCACACTGTAACCTGTCTCTACTGC

RBS *ApgltS* M D T

ACTCATCTAGAAGTAGGGACTGTCTTATATCGTAGTTCAGAAGAG**GAAGGA**TTATAGTCAA***TTG*AACAC**

Figure 4.35 Nucleotide sequence of the putative promoter of *ApgltS* gene based on the shot gun sequencing of *A. halophytica*.

The transcriptional start point is marked by an arrow and indicated by +1. The -35 (gray ellipse) and -10 (gray rectangle) boxes of the *ApgltS* basic promoter are highlighted. Sequences of putative UP element are bolded and underlined. Translation start codon is indicated by italic type.

4.5.1.2 Amplification of promoter region of *A. halophytica* Na^+/glutamate transporter gene (*ApgltS*) and construction of *ApgltS* promoter-probe vector

A. halophytica genomic DNA was used as template for PCR amplification. Primers *ApgltS*proBamHI-F and *ApgltS*proNcoI-R were used to amplifiy the promoter region of *ApgltS* gene with the size of 240 bp as shown by agarose gel electrophoresis in Figure 4.36. To study the activity and regulation of the *ApgltS* promoter with transcriptional lacZ fusions, the promoter probe vector pQF50 was used. The 240 bp PCR product was cloned into cloning plasmid pCR®2.1 and the recombinant plasmid, pCR®2.1-progltS, was transformed into the *E. coli* DH5α competent cells. The transformants were selected on ampicillin agar plates. Colonies were randomly selected and cultured in 1 ml LB broth containing 100 $\mu g.ml^{-1}$ ampicillin at 37 °C overnight and the cultures were subjected to plasmid extraction. To verify the insertion of PCR products, the recombinant plasmid, pCR®2.1-progltS, was double restriction digested with *Nco*I + *Sph*I and analyzed by 1% agarose gel electrophoresis. The expected sizes of DNA fragments are 2348, 1509, 318 and 27 that corresponded to the results in Figure 4.37.

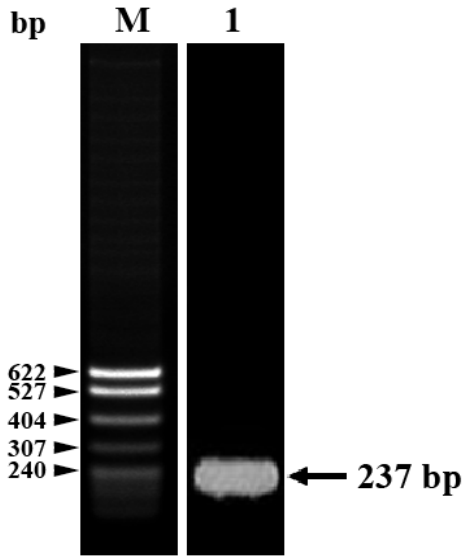

Figure 4.36 Agarose gel electrophoresis of the amplified promoter region of *ApgltS*.

The PCR products were separated on 1% agarose gels and visualized by ethidium bromide staining.

Lane M DNA Marker: λ/*Hind*III

Lane 1 PCR product of promoter region of *ApgltS*

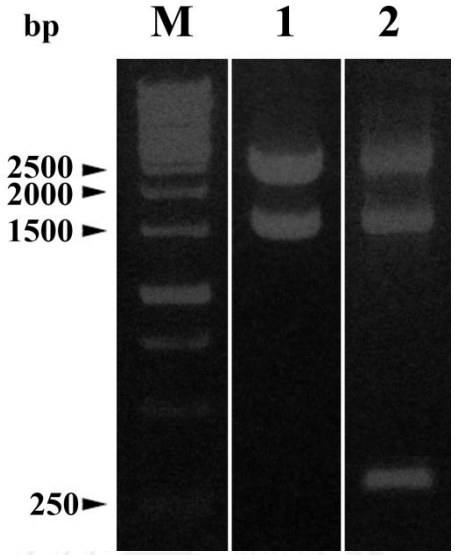

Figure 4.37 Agarose gel electrophoresis of restriction digestion of the recombinant plasmid pCR2.1-progltS.

The DNA was separated on 1% agarose gels and visualized by ethidium bromide staining.

Lane M GeneRuler™ 1 kb DNA ladder

Lane 1 pCR®2.1 digested with *Nco*I+*Sph*I

Lane 2 pCR®2.1-progltS digested with *Nco*I+*Sph*I

The 318-bp promoter region of *ApgltS* gene was purified and ligated into the *NcoI*/*Sph*I sites of pQF50. The recombinant plasmid, pQF50-promotergltS was transformed into the *E. coli* DH5α competent cells. The transformants were selected by blue-white colony screening on ampicillin agar plates containing X-gal. Blue colonies were randomly selected and cultured in 1 ml LB broth containing 100 μg.ml^{-1} ampicillin and X-gal at 37 °C overnight and the cultures were subjected to plasmid extraction. To verify the insertion of DNA fragments into pQF50, the recombinant plasmid, pQF50-promotergltS, was used as template for PCR amplification using primer pair specific to promoter region of *ApgltS* gene and analyzed by 1% agarose gel electrophoresis. Figure 4.38 shows that only pQF50-promotergltS transformants could amplify the promoter region of *ApgltS* gene with the size of 240-bp.

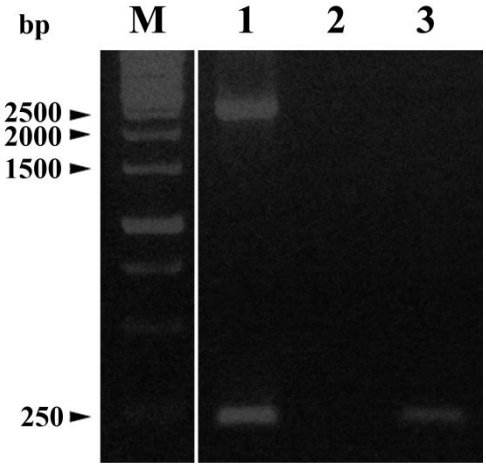

Figure 4.38 Agarose gel electrophoresis of the amplified promoter region of *ApgltS* from recombinant plasmid pQF50-promotergltS.

The PCR products were separated on 1% agarose gels and visualized by ethidium bromide staining.

Lane M GeneRuler™ 1 kb DNA ladder

Lane 1 PCR product of pCR2.1-progltS

Lane 2 PCR product of pQF50

Lane 3 PCR product of pQF50-promotergltS

4.5.1.3 Promoter activity characterization of pQF50-promotergltS

Promoter-probe vector, pQF50-promotergltS, was constructed and used to monitor activity of *ApgltS* promoter. With various concentrations of KCl and NaCl, promoter activity was significantly increased with increasing concentration of NaCl. In contrast, induction of promoter activity was not changed at all KCl concentration tested comparing with control as shown in Figure 4.39. The highest promoter activity (4-fold) was obtained at 0.5 mM NaCl. The effect of exogenous glutamate on promoter activity was also examined as shown in Figure 4.40. Exogenous glutamate slightly induced promoter activity. The activity of *ApgltS* promoter showed similar induction pattern in response to exogenous glutamate in all NaCl concentrations tested. The highest promoter activity was observed at 0.5 mM glutamate.

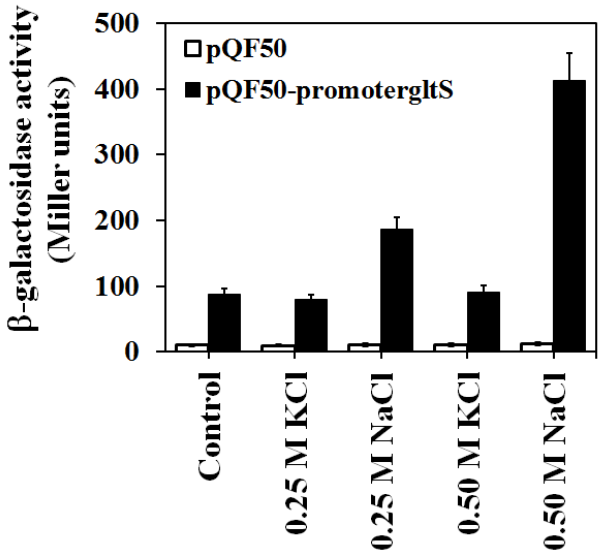

Figure 4.39 Promoter activities of control vector (pQF50) and pQF50-promotergltS in *E. coli* DH5α after induction with 0, 0.25 and 0.50 mM KCl or NaCl.

The data are from three independent experiments with vertical bars representing standard errors of the means, n=3.

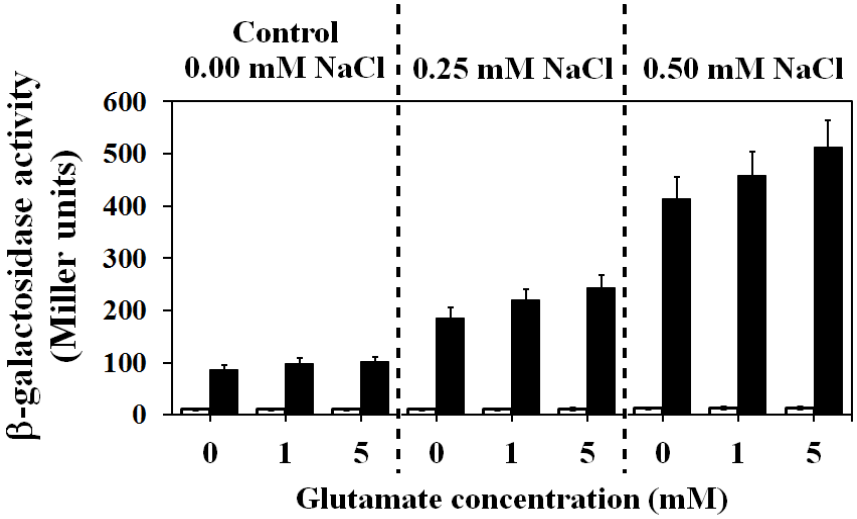

Figure 4.40 Promoter activities of control vector (pQF50) represented with (□) and and pQF50-promotergltS represented with (■) in *E. coli* DH5α after induction with 0, 0.25 and 0.50 mM NaCl supplemented with 0, 1 and 5 mM glutamate.

The data are from three independent experiments with vertical bars representing standard errors of the means, n=3.

4.5.1.4 Construction of pBluescript® II SK$^+$ recombinant plasmid containing promoter region of *ApgltS* gene

The purified PCR product of promoter region of *ApgltS* gene was ligated into the *Eco*RV restriction site of pBluescript® II SK$^+$ (pBSK$^+$) vector and the recombinant plasmid, pBSK$^+$-promoter*ApgltS*, was transformed into the *E. coli* DH5α competent cells. The transformants were selected by blue-white screening on ampicillin agar plates containing X-gal. White colonies were randomly selected and cultured in 1 ml LB broth containing 100 μg.ml^{-1} ampicillin at 37 °C overnight and the cultures were subjected to plasmid extraction. To verify the insertion of PCR products, the recombinant plasmid, pBSK$^+$-promoter*ApgltS*, was restriction digested with *BamH*I, *Xba*I, and *Nco*I + *Sal*I and analyzed by 1% agarose gel electrophoresis. The expected sizes of DNA fragments are shown in Table 4.8 that corresponded to the results in Figure 4.41.

Then, the recombinant plasmids were subjected to DNA sequencing. DNA sequences of pBSK$^+$-promoter*ApgltS* are shown in Figure 4.42. The resulting pBSK$^+$-promoter*ApgltS* DNA sequence was compared with data from genome sequence using the EMBOSS Pairwise Alignment Algorithms. The results revealed that the promoter*ApgltS* sequence shared 97.8% identity with the promoter region of *ApgltS* from the genome sequence data as shown in Figure 4.43.

Table 4.8 Restriction enzymes used for the digestion of pBSK^{+}-promoter*ApgltS* and expected size of DNA fragments.

Restriction Enzymes	Expected DNA Fragments (bp)
*BamH*I	3205, 29
*Xba*I	2984, 193, 57
*Nco*I+*Sal*I	3208, 26

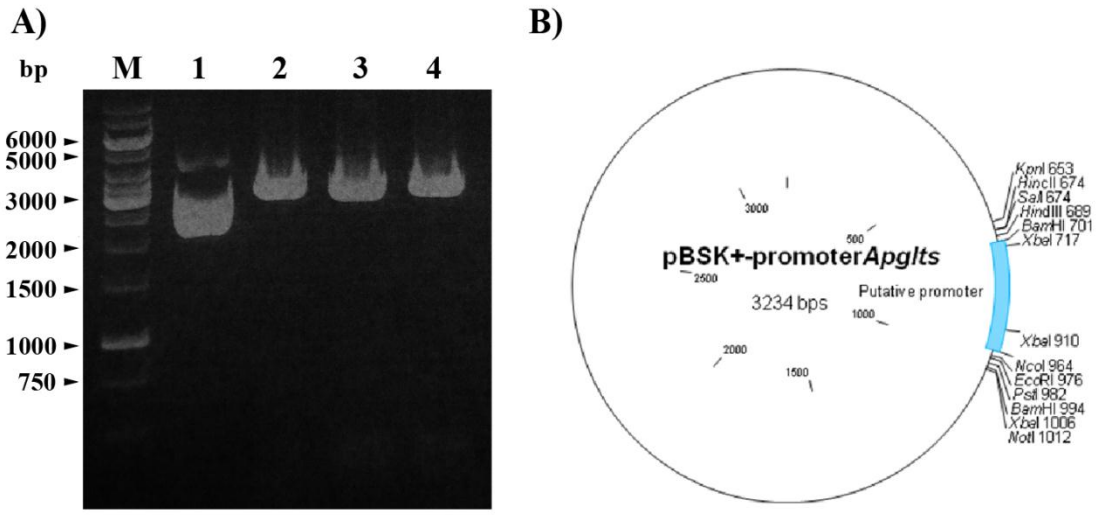

Figure 4.41 **Agarose gel electrophoresis of restriction digestion of the recombinant promoter region of *ApgltS* gene inserted in pBluescript® II SK$^+$ (pBSK$^+$-promoter*ApgltS*).**

The DNA was separated on 1% agarose gels and visualized by ethidium bromide staining.

a) Lane M GeneRuler™ 1 kb DNA ladder

Lane 1 undigested pBSK$^+$-promoter*ApgltS*

Lane 2 pBSK$^+$-promoter*ApgltS* digested with *Bam*HI

Lane 3 pBSK$^+$-promoter*ApgltS* digested with *Xba*I

Lane 4 pBSK$^+$-promoter*ApgltS* digested with *Nco*I and *Sal*I

b) Plasmid map of the recombinant promoter region of *ApgltS* gene inserted in pBluescript® II SK$^+$ (pBSK$^+$-promoter*ApgltS*)

>pBSK^{+}-promoter*ApgltS*

CTTGGTCCAGTAACTTAATCTAGATTTTTAGGTGATTAAAAGCATTATATAATATACTATAAATCACTT
TTACGGGCAAAAAGGGAAGTTTTTTCTCTATCTTAGGTCAGATTCAATACATTATTGAACCTTTGCATC
CCTGAAATGTAATAATTGCTACTACTTGCTGACAGGAAAGCTCCCACACTGTAACCTGTCTCTACTGCA
CTCATCTAGAAGTAGGGACTGTCTTATATCGTAGTTCAGAAGAGGAAGGATTATAGTCCCATGGAC

Figure 4.42 **DNA sequences of promoter region of *ApgltS* gene in the recombinant plasmid pBSK^{+}-promoter*ApgltS*.**

The underlined letters represent primer binding sites.

```
proApgltS-GEN   1 CTTAATCCAGTAACTTAATCTAGATTTTTAGGTGATTAAAAGCAT  45
pBSK+proApglt   1 ---GG----------------------------------------  45

proApgltS-GEN  46 TATATAATATACTATAAATCACTTTTACGGGCAAAAAGGGAAGTT  90
pBSK+proApglt  46 ----------------------------------------------  90

proApgltS-GEN  91 TTTTCTCTATCTTAGGTCAGATTCAATACATTATTGAACCTTTGC 135
pBSK+proApglt  61 --------------------------------------------- 135

proApgltS-GEN 136 ATCCCTGAAATGTAATAATTGCTACTACTTGCTGACAGGAAAGCT 180
pBSK+proApglt 121 --------------------------------------------- 180

proApgltS-GEN 181 CCCACACTGTAACCTGTCTCTACTGCACTCATCTAGAAGTAGGGA 225
pBSK+proApglt 181 --------------------------------------------- 225

proApgltS-GEN 226 CTGTCTTATATCGTAGTTCAGAAGAGGAAGGATTATAGTCAATTG 270
pBSK+proApglt 226 ----------------------------------------CCA-

proApgltS-GEN 271 AAC 273
pBSK+proApglt 271 G-- 273
```

Figure 4.43 **Nucleotide sequence alignment of promoter region of *ApgltS* gene from genome sequences (pro*ApgltS*-GEN) and from the result of DNA sequencing of pBSK^{+}-promoter*ApgltS* (pBSK^{+}-pro*ApgltS*) used EMBOSS Pairwise Alignment Algorithms.**

The identical residues in other sequences are indicated by a dash (-), and a gap introduced for alignment purposes is indicated by a dot (.).

4.5.1.5 Amplification of the coding region of *ApgltS* gene containing 6xHis-tag and construction of pBluescript® II SK$^+$ recombinant plasmid containing the coding region of *ApgltS* gene containing 6xHis-tag

p*ApgltS* was used as template for PCR amplification of the coding region of *ApgltS* gene containing 6xHis-tag. Primers *ApgltS*NcoI-F and 6XHisStopBamHI-R were used to amplify the promoter region of *ApgltS* with the size of 1500 bp as shown by agarose gel electrophoresis in Figure 4.44. The purified PCR product was cloned into the *Eco*RV restriction site of pBluescript® II SK$^+$ (pBSK$^+$) vector and the recombinant plasmid, pBSK$^+$-*gltSHis-F*, was transformed into the competent *E. coli* DH5α cells. The transformants were selected by blue-white colony screening on ampicillin agar plates containing X-gal. White colonies were randomly selected and cultured in 1 ml LB broth containing 100 μg.ml^{-1} ampicillin at 37 °C overnight and the cultures were subjected to plasmid extraction. To verify the insertion of PCR products into pBSK$^+$, the recombinant plasmid, pBSK$^+$-*gltSHis-F*, was digested with *Pst*I and *Nco*I + *Sac*I and analyzed by 1% agarose gel electrophoresis. The expected sizes of DNA fragments are shown in Table 4.9 that corresponded to the results in Figure 4.45.

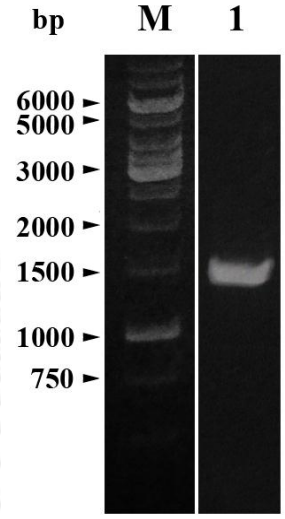

Figure 4.44 **Agarose gel electrophoresis of the amplified coding region of *ApgltS* gene containing 6xHis-tag.**

The PCR products were separated on 1% agarose gels and visualized by ethidium bromide staining.

Lane M GeneRuler™ 1 kb DNA ladder

Lane 1 PCR product of the coding region of *ApgltS* gene containing 6xHis-tag

Table 4.9 **Restriction enzymes used for the digestion of pBSK^{+}-gltSHis-F and expected size of DNA fragments.**

Restriction Enzymes	Expected DNA Fragments (bp)
*Pst*I	3446, 982
*Nco*I+*Sac*I	2902, 1526*, 1173, 353 (Partial digestion)

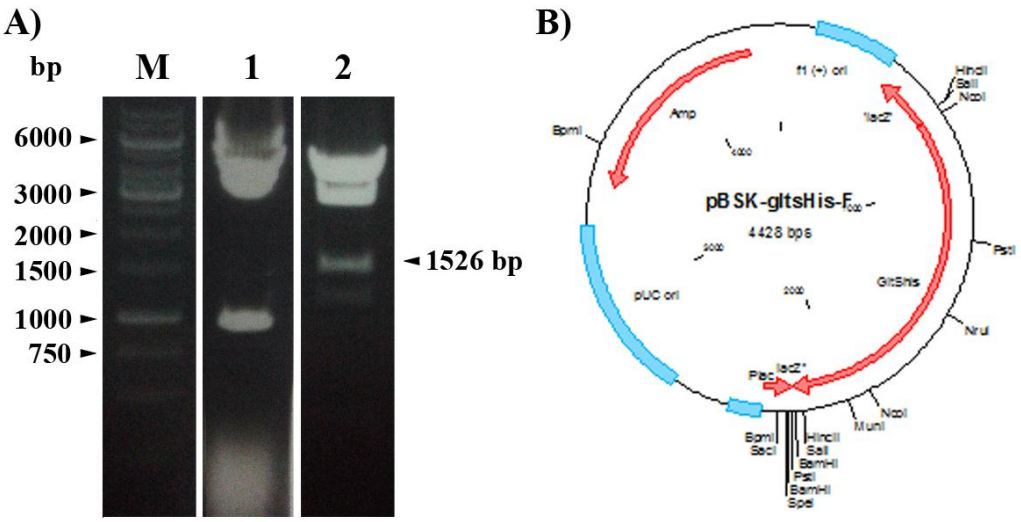

Figure 4.45 **Agarose gel electrophoresis of restriction digestion of the recombinant plasmid pBSK^{+}-gltSHis-F.**

The DNA was separated on 1% agarose gels and visualized by ethidium bromide staining.

A) Lane M GeneRuler™ 1 kb DNA ladder

Lane 1 pBSK^{+}-*gltSHis-F* digested with *Pst*I

Lane 2 pBSK^{+}-*gltSHis-F* partial digested with *Nco*I and *Sac*I

B) Map of the recombinant plasmid pBSK^{+}-*gltSHis-F*.

4.5.1.6 Construction of pBluescript® II SK$^+$ recombinant plasmid containing the promoter region and coding region of *ApgltS* gene containing 6xHis-tag

pBSK$^+$-*gltSHis-F* was digested with *Nco/Sac*I and was analyzed by agarose gel electrophoresis. 1526-bp coding region of *ApgltS* gene containing 6xHis-tag fragments were purified and ligated into the *Nco*I/*Sac*I sites of pBSK$^+$-promoter*ApgltS.* The recombinant plasmid, pBSK$^+$-promoterGltSHis, was transformed into the competent *E. coli* DH5α as shown in Figure 4.46. The transformants were selected by blue-white colony screening on ampicillin agar plates containing X-gal. White colonies were randomly selected and cultured in 1 ml LB broth containing 100 μg.ml^{-1} ampicillin at 37 °C overnight and the cultures were subjected to plasmid extraction. To verify the insertion of DNA fragments into pBSK$^+$, the recombinant plasmid, pBSK$^+$-promoterGltSHis, was amplified using primers *ApgltS*proBamHI-F and 6XHisStopBamHI-R. The expected size of PCR product is approximately 1700 bp as shown in Figure 4.47.

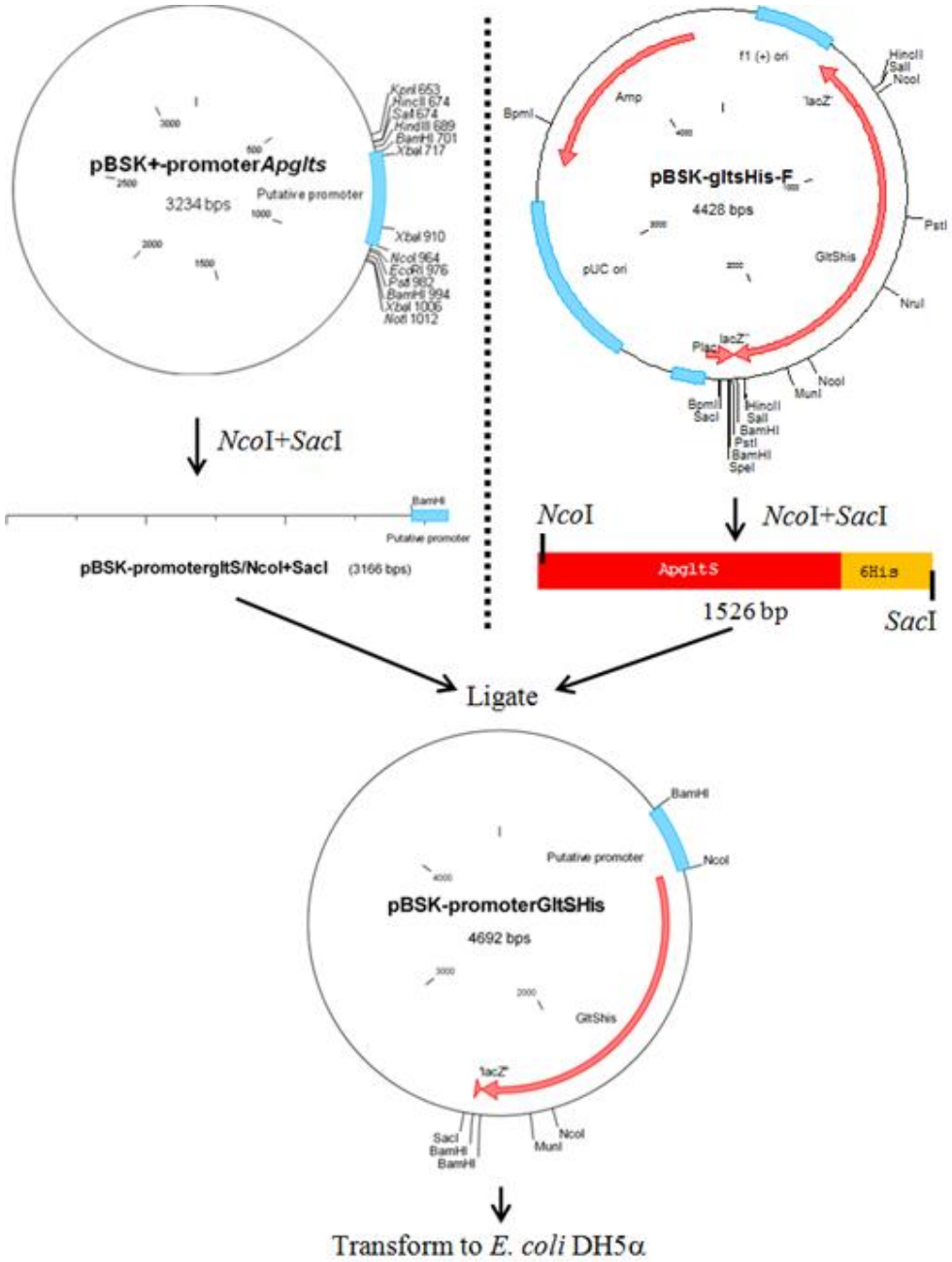

Figure 4.46 **Construction of plasmid pBSK$^+$-promoterGltSHis.**

The 1526-bp coding region of *ApgltS* gene containing 6xHis-tag fragments were purified and ligated into the NcoI/SacI sites of pBSK$^+$-promoter*ApgltS* and then transformed into *E. coli* DH5α.

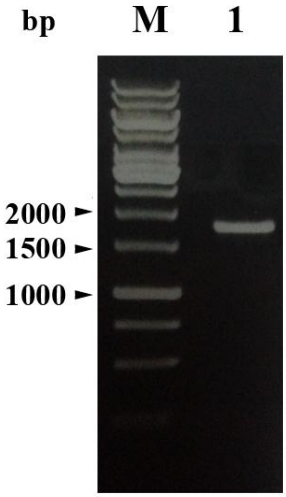

Figure 4.47 Agarose gel electrophoresis of the amplified promoter region and coding region of *ApgltS* gene containing 6xHis-tag using pBSK^{+}-promoterGltSHis as template.

The PCR products were separated on 1% agarose gels and visualized by ethidium bromide staining.

Lane M GeneRuler™ 1 kb DNA ladder

Lane 1 PCR product of the promoter region and coding region of *ApgltS* gene containing 6xHis-tag

4.5.2 Construction of pUC303 containing ampicillin resistant gene (pUC303-Amp)

pBluescript® II SK$^+$ was digested with *Pvu*II and was analyzed by agarose gel electrophoresis. 2.96 kb fragment of pBSK$^+$ was purified and ligated with blunt end treated pUC303*/Xho*I. The recombinant plasmid, pUC303-Amp, was transformed into the competent *E. coli* DH5α as shown in Figure 4.48. The pUC303-Amp was cut check with *Hind*III and analyzed by 1% agarose gel electrophoresis. The recombinant plasmid pUC303-Amp was digested with *Hind*III to obtain 8923 and 4394-bp whereas pUC303 was digested with *Hind*III to obtain 6406 and 4394-bp as shown in Figure 4.49

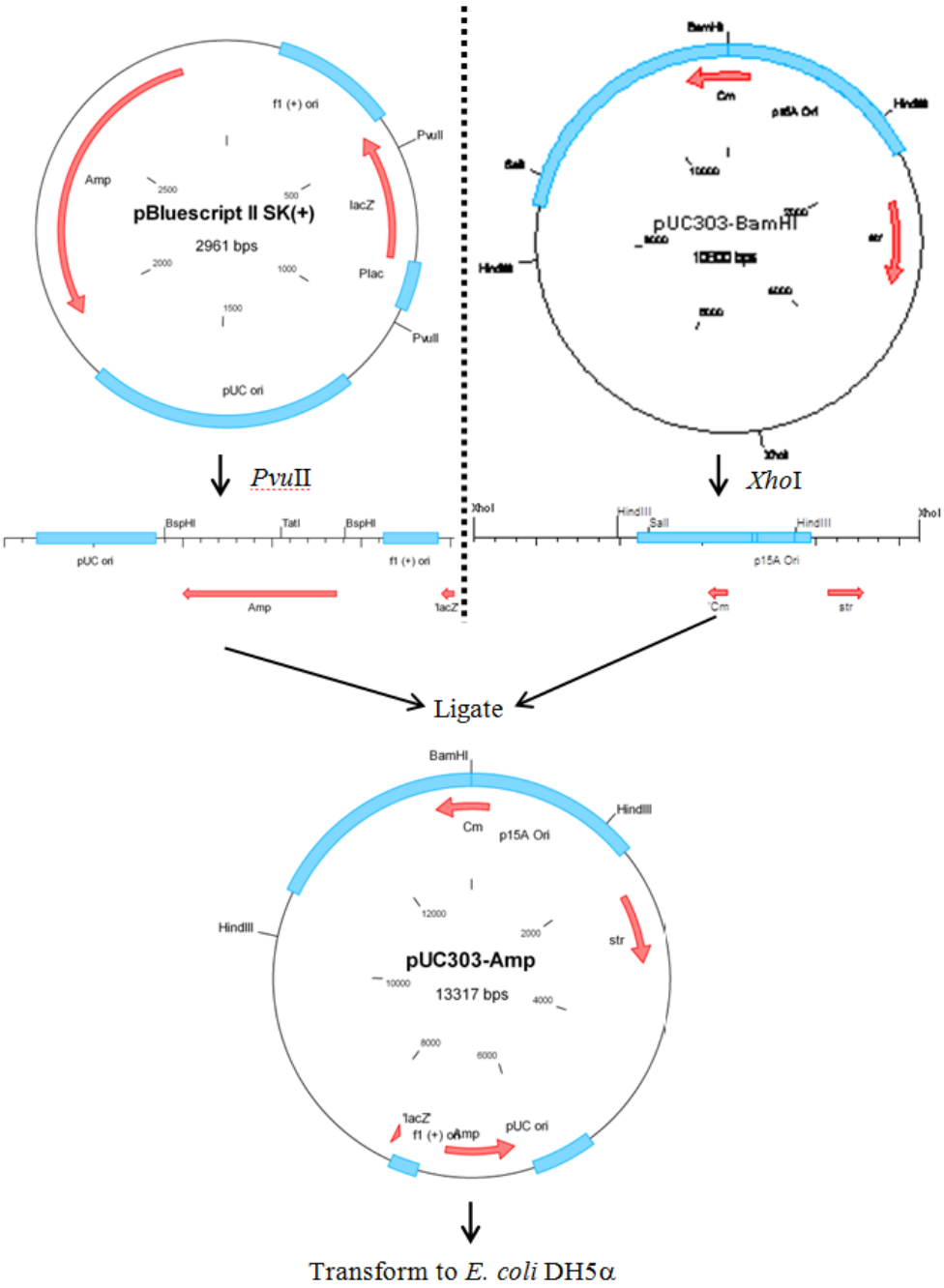

Figure 4.48 **Construction of plasmid pUC303-Amp.**

The 2961 bp of pBSK^{+} fragments containing ampicillin resistant gene were purified and ligated with blunt end treated pUC303/XhoI and then transformed into *E. coli* DH5α.

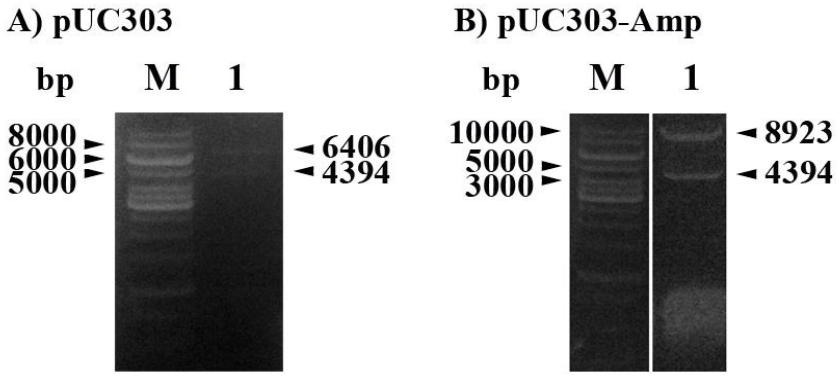

Figure 4.49 Agarose gel electrophoresis of pUC303 and pUC303-Amp digested with HindIII.

The DNA was separated on 1% agarose gels and visualized by ethidium bromide staining.

A) Lane M GeneRuler™ 1 kb DNA ladder

Lane 1 plasmid pUC303 digested with *Hind*III

B) Lane M GeneRuler™ 1 kb DNA ladder

Lane 1 plasmid pUC303-Amp digested with *Hind*III

4.5.3 Construction of pUC303-Amp recombinant plasmid containing the promoter region and coding region of *ApgltS* gene containing 6xHis-tag for the expression of ApGltS in a freshwater cyanobacterium *Synechococcus* sp. PCC 7942

The expression plasmid designated as pUC303-pGH-Amp, was constructed under the *ApgltS* promoter. Firstly, pBSK^{+}-promoterGltSHis was digested with *BamH*I and was analyzed by agarose gel electrophoresis. 1729 bp of the promoter region and coding region of *ApgltS* gene containing 6xHis-tag fragments were harvested, purified and then ligated into the *BamH*I sites of pUC303-Amp as shown in Figure 4.50. The pUC303-Amp containing chloramphenicol, streptomycin and ampicillin resistant gene was used as control plasmid. The recombinant plasmid, pUC303-pGH-Amp whose insert DNA fragment is ***inserted*** into the middle of the chloramphenicol resistance gene was constructed. Each plasmid was transformed into *E. coli* DH5α cells. The positive transformants were primarily screened on LB agar containing 100 µg.ml^{-1} streptomycin for pUC303-pGH-Amp and pUC303-Amp. To verify the insertion of DNA fragments into pUC303-Amp, the recombinant plasmid, pUC303-pGH-Amp, was restriction digested with *BamH*I and analyzed by 1% agarose gel electrophoresis. The expected sizes of DNA fragments are shown in Table 4.10 that corresponded to the results in Figure 4.51.

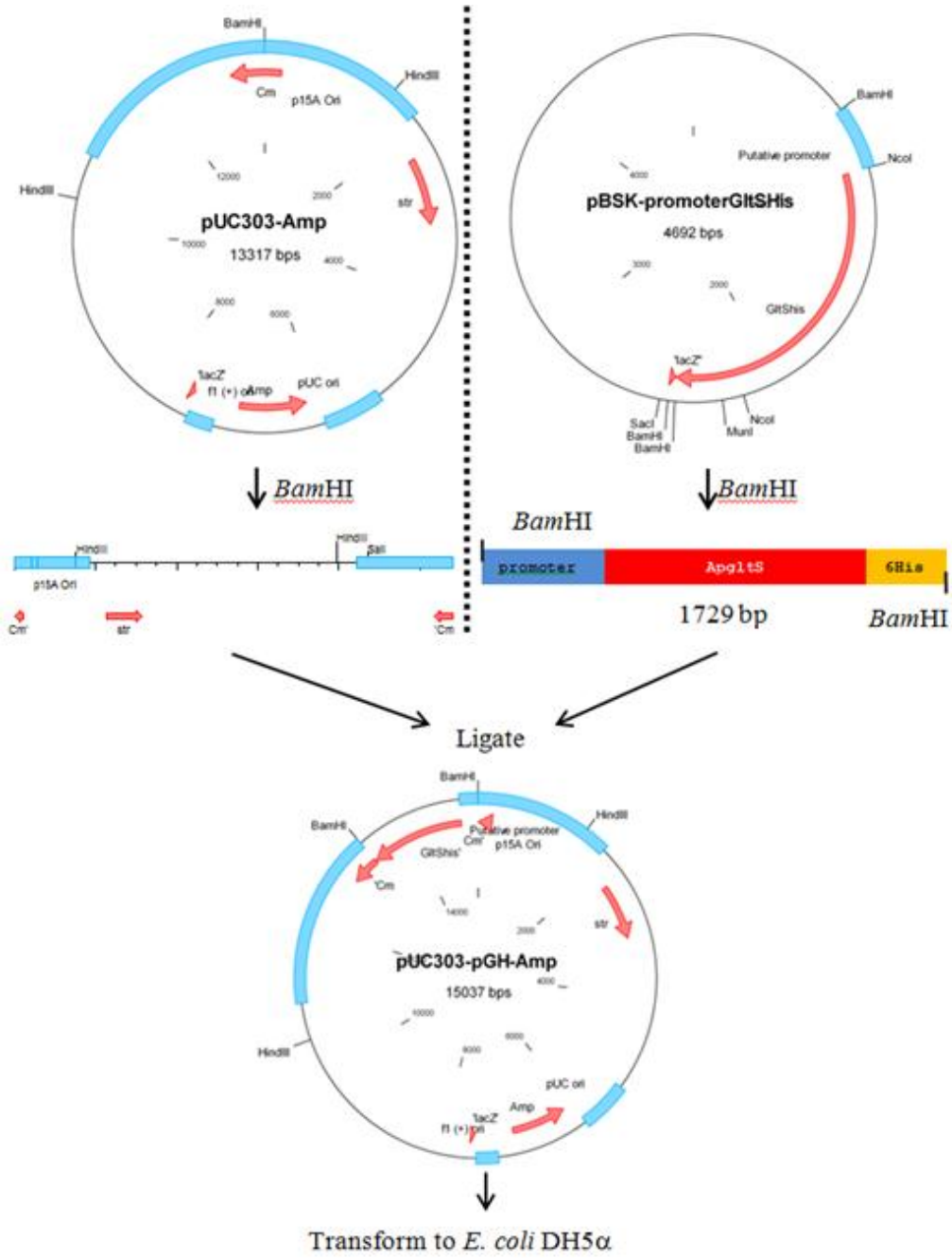

Figure 4.50 Construction of plasmid pUC303-pGH-Amp.

The 1729 bp of the promoter region and coding region of *ApgltS* gene containing 6xHis-tag fragments were purified and ligated into the BamHI sites of pUC303-Amp and then transformed into *E. coli* DH5α.

Table 4.10 Restriction enzyme used for the digestion of pUC303-pGH-amp-F and expected size of DNA fragments.

Restriction Enzymes	Plasmid	Expected DNA Fragments (bp)
*Bam*HI	pUC303-Amp	13317
	pUC303-pGH-Amp	13308, 1729
*Hind*III	pUC303-Amp	8923, 4349
	pUC303-pGH-Amp	8923, 6114

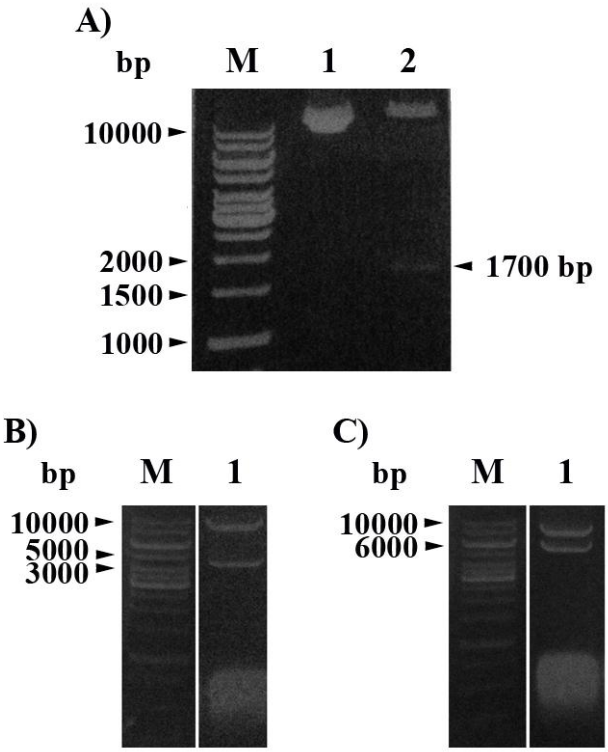

Figure 4.51 Agarose gel electrophoresis of restriction digestion of the recombinant plasmid pUC303-pGH-Amp.

The DNA was separated on 1% agarose gels and visualized by ethidium bromide staining.

A) Lane M GeneRuler™ 1 kb DNA ladder

Lane 1 plasmid pUC303-Amp digested with *Bam*HI

Lane 2 plasmid pUC303-pGH-amp digested with *Bam*HI

B) Lane M GeneRuler™ 1 kb DNA ladder

Lane 1 plasmid pUC303-Amp digested with *Hind*III

C) Lane M GeneRuler™ 1 kb DNA ladder

Lane 1 plasmid pUC303-pGH-Amp digested with *Hind*III

4.5.4 Transformation of *Synechococcus* sp. PCC 7942 with *ApgltS*

To examine functional properties of ApGltS, a fresh water cyanobacterium *Synechococcus* sp. PCC 7942 was transformed with *ApgltS* gene comparing with pUC303-Amp transformants. The plasmids pUC303-Amp and pUC303-pGH-Amp were prepared and transformed to the *Synechococcus* sp. PCC 7942 cells. The transformants were selected on BG_{11} agar containing 50 $\mu g.ml^{-1}$ streptomycin and 1 $\mu g.ml^{-1}$ ampicillin. The positive clones were picked and then transferred to BG_{11} liquid medium containing 50 $\mu g.ml^{-1}$ streptomycin and 1 $\mu g.ml^{-1}$ ampicillin. After cultivation for 2 weeks, the plasmids were extracted and used as template for PCR amplification using chloramphenicol-specific primers and specific primers for the promoter region and coding region of *ApgltS* gene containing 6xHis-tag fragment. Figure 4.52A shows that both of pUC303-Amp and pUC303-pGH-Amp transformants could be amplified with chloramphenicol-specific primers with the sizes of 800 and 2500 bp, respectively. Figure 4.52B shows only pUC303-pGH-Amp transformants could be amplified with coding region of *ApgltS* gene-specific primers with the size of 1700 *bp.*

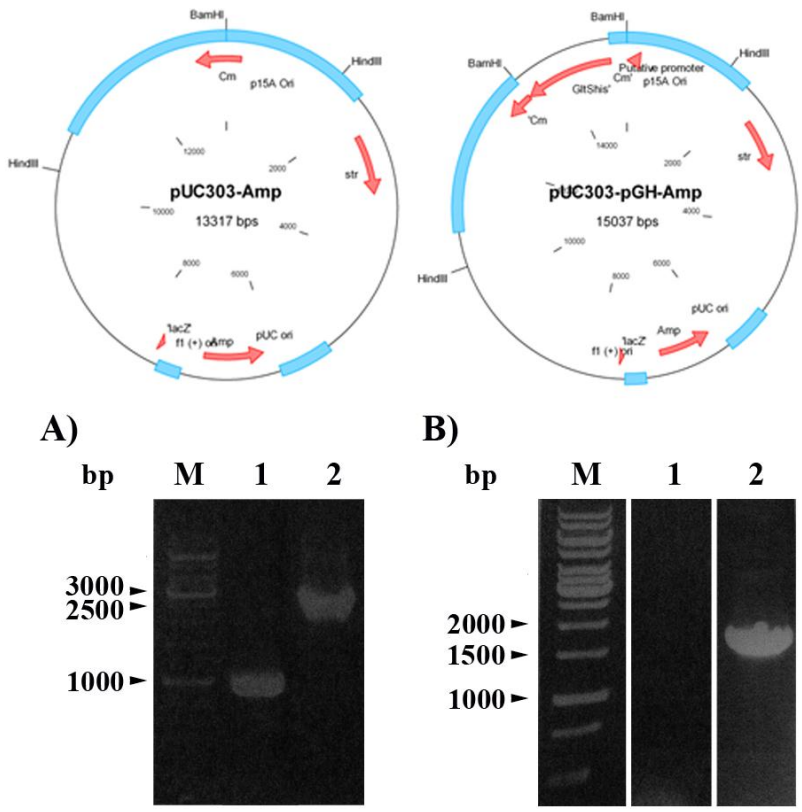

Figure 4.52 Maps of pUC303-Amp and pUC303-pGH-Amp and agarose gel electrophoresis of the PCR products from chloramphenicol-specific primers (A) and specific primers for the promoter region and coding region of *ApgltS* gene containing 6xHis-tag fragment (B) using DNA from pUC303-Amp and pUC303-pGH-Amp *Synechococcus* sp. PCC 7942 transformants as template.

The DNA was separated on 1% agarose gels and visualized by ethidium bromide staining.

Lane M GeneRuler™ 1 kb DNA ladder

Lane 1 7942 transformed with pUC303-Amp

Lane 2 7942 transformed with pUC303-pGH-Amp

4.6 Characterization of ApGltS in *Synechococcus* sp. PCC 7942

4.6.1 Growth rate of *ApgltS* expressing *Synechococcus* sp. PCC 7942

Synechococcus sp. PCC 7942 transformed with pUC303-Amp (pUC303-Amp/7942) and pUC303-pGH-Amp (pUC303-pGH-Amp/7942) were grown in BG_{11} medium containing 50 μg.ml^{-1} streptomycin and 1 μg.ml^{-1} ampicillin, and indicated concentrations of NaCl (0 and 0.2 M) supplemented with 0, 1, 5 and 10 mM glutamate. The growth was monitored by measuring optical density of culture at 750 nm as shown in Figure 4.53. The results showed that both pUC303-Amp control vector and pUC303-pGH-Amp transformants exhibited similar growth patterns when grown in BG_{11} medium in the absence of NaCl. The increase of NaCl concentration up to 0.2 M NaCl resulted in slower growth of the cells. However, the growth rate of control vector transformants was slightly higher than that of *ApgltS*-expressing cells. Glutamate supplementation decreased growth of both transformants especially in pUC303-pGH-Amp transformants under salt stress condition.

Growth of pUC303-pGH-Amp transformant was inhibited by glutamate supplementation. The high concentration of glutamate (10 mM) decreased growth to half of growth rate in normal condition and inhibited growth in 0.2 M NaCl. Growth of pUC303-Amp did not significantly change in BG_{11} medium in the absence of NaCl supplemented with 0, 1 and 5 mM glutamate and in BG_{11} medium containing 0.2 M NaCl supplemented with 0 and 1 mM glutamate. Glutamate supplementation at 10 mM decreased growth of pUC303-Amp in BG_{11}

medium in the absence of NaCl to the same level of the growth of that under salt stress condition.

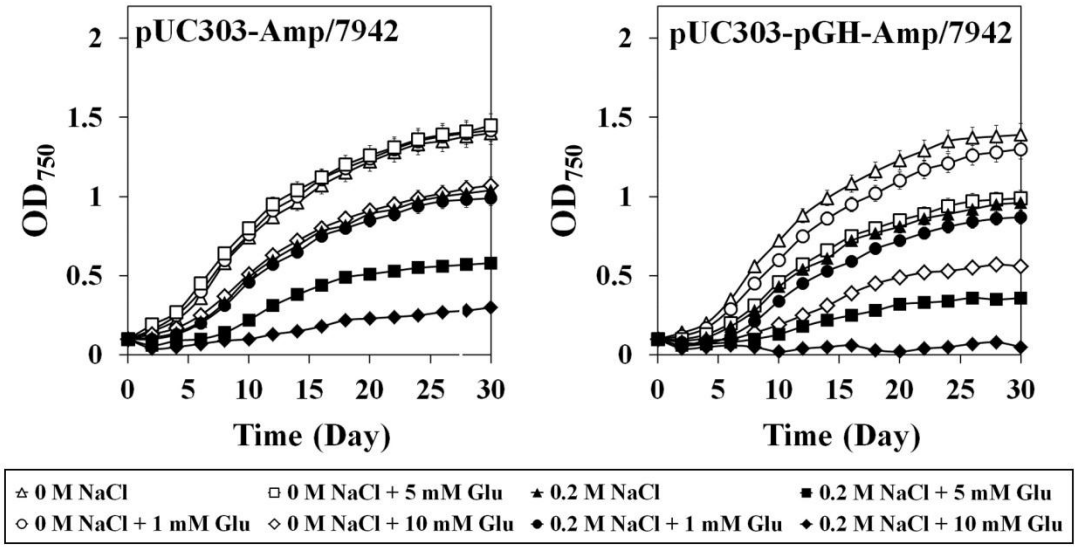

Figure 4.53 **Growth curves of *ApgltS* expressing *Synechococcus* sp. PCC 7942.** pUC303-Amp and pUC303-pGH-Amp *Synechococcus* sp. PCC 7942 transformants were grown in BG_{11} medium containing 0.0 M NaCl or 0.2 M NaCl supplemented with 0, 1, 5 and 10 mM glutamate. The data are from three independent experiments with vertical bars representing standard errors of the means, n=3. Error bars are included in the graphs where some may be smaller than the symbols.

4.6.2 Glutamate transport assay in *ApgltS* expressing *Synechococcus* sp. PCC 7942

4.6.2.1 Time course of glutamate transport in pUC303-Amp and pUC303-pGH-Amp *Synechococcus* sp. PCC 7942 transformants.

Synechococcus sp. PCC 7942 transformed with pUC303-Amp (pUC303-Amp/7942) and *Synechococcus* sp. PCC 7942 transformed with pUC303-pGH-Amp (pUC303-pGH-Amp/7942) were grown in BG_{11} medium. Cells at mid-log phase were harvested by centrifugation, washed twice and re-suspended to a concentration of 0.1 mg cell protein in 1 ml assay medium (100 mM Tris HCl, pH 7.5) containing various NaCl concentrations (0–500 mM). The uptake was initiated by the addition of 5 μM [U-^{14}C] glutamate. Glutamate transport of cells was determined at interval time for 90 min. The initial rate of [U-^{14}C] glutamate uptake was observed within 5 min and cells showed saturated glutamate uptake after cells were exposed to glutamate for 10 min. The glutamate uptake rate of pUC303-pGH-Amp/7942 was 0.023 ± 0.01, 0.092 ± 0.02, 0.117 ± 0.04, 0.138 ± 0.03, 0.106 ± 0.05 and 0.088 ± 0.03 nmol.min^{-1}.mg^{-1} protein, whereas that of pUC303-Amp/7942 was 0.021 ± 0.02, 0.075 ± 0.03, 0.085 ± 0.05, 0.087 ± 0.04, 0.088 ± 0.04 and 0.091 ± 0.04 nmol.min^{-1}.mg^{-1} protein at 0, 10, 50, 100, 200 and 500 mM NaCl, respectively as shown in Figure 4.54. Interestingly, the glutamate uptake rate of *ApgltS*-expressing *Synechococcus* sp. PCC 7942 cells increased when NaCl concentration increased but that of control vector transformants did not significantly change in all NaCl concentrations.

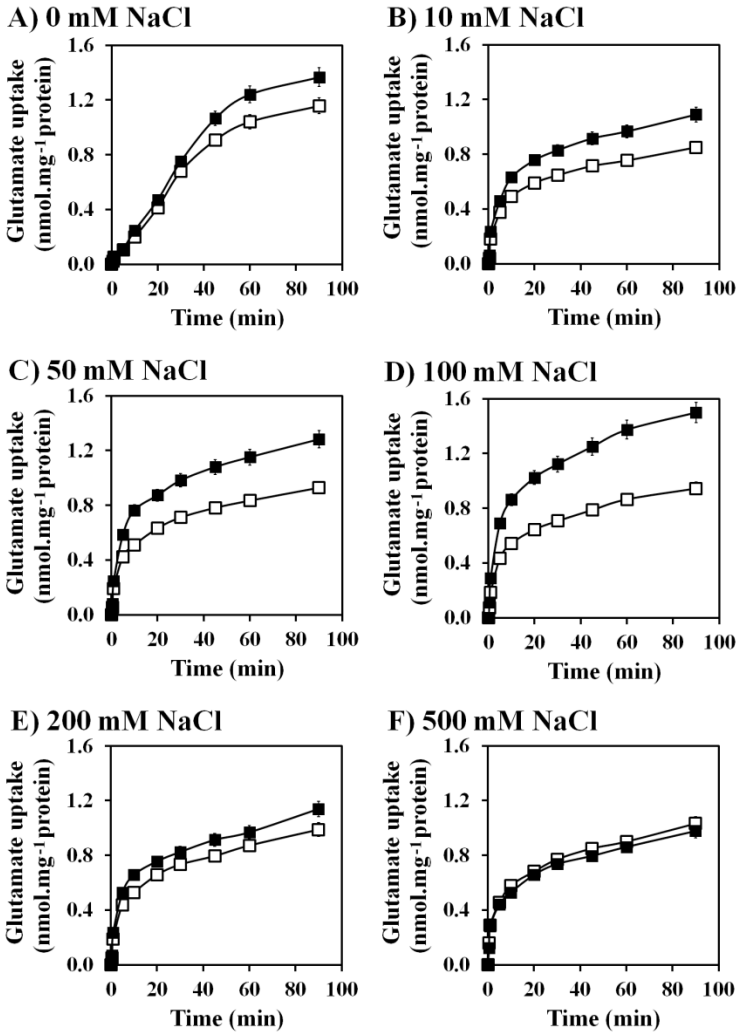

Figure 4.54 Time intervals of glutamate uptake into *Synechococcus* sp. PCC 7942 transformed with pUC303-Amp (pUC303-Amp/7942) represented with (□) and pUC303-pGH-Amp (pUC303-pGH-Amp/7942) represented with (■) under various NaCl concentration (0-500 mM).

The data are from three independent experiments with vertical bars representing standard errors of the means, n=3. Error bars are included in the graphs where some may be smaller than the symbols.

4.6.2.2 Saturation kinetics of glutamate uptake in *Synechococcus sp.* PCC 7942 transformed with pUC303-Amp and pUC303-pGH-Amp

The kinetic properties of pUC303-pGH-Amp/7942 were determined. Figure 4.55 shows the effects of glutamate concentration ranging from 0 to 100 μM on the uptake rate under various NaCl concentrations (0–100 mM). Incubation of *Synechococcus* sp. PCC 7942 transformant cells with various glutamate concentrations ranging from 0 to 100 μM resulted in saturable uptake. The saturation curve of glutamate uptake at pH 7.5 increased upon the increase of the concentrations of NaCl (0-100 mM NaCl). From the double reciprocal plots of glutamate transport kinetics *Synechococcus* sp. PCC 7942 transformant cells, K_m and V_{max} values were determined.

Figure 4.55A shows that glutamate uptake of pUC303-Amp/7942 in assay buffer containing 0, 10, 50 and 100 mM NaCl exhibited the typical of Michaelis-Menten saturation kinetics with an apparent K_m of 7.72 ± 0.34, 7.53 ± 0.53, 7.69 ± 0.34 and 7.66 ± 0.33 μM, respectively, and the maximum velocity (V_{max}) of 0.0559 ± 0.00063, 0.2237 ± 0.00371, 0.2227 ± 0.00246 and 0.2266 ± 0.00246 nmol.min^{-1}.mg^{-1} protein, respectively. Figure 4.55B shows that glutamate uptake of pUC303-pGH-Amp/7942 in assay buffer containing 0, 10, 50 and 100 mM NaCl exhibited the typical of Michaelis-Menten saturation kinetics with an apparent K_m of 7.70 ± 0.44, 7.72 ± 0.34, 7.69 ± 0.32 and 7.66 ± 0.36 μM, respectively, and the maximum velocity (V_{max}) of 0.0577 ±

0.00093, 0.2667 ± 0.00299, 0.3364 ± 0.00341 and 0.3597 ± 0.00391 nmol.min^{-1}.mg^{-1} protein, respectively (Table 4.11). The V_{max} values slightly increased upon the increase of NaCl concentrations whereas K_m values of both transformants did not significantly change.

Table 4.11 Kinetic values of glutamate uptake in *ApgltS* expressing *Synechococcus* sp. PCC 7942.

NaCl concentration (mM)	Kinetic value	
	K_m (μM)	V_{max} (nmol.min^{-1}.mg^{-1} protein)
pUC303-Amp/7942		
0	7.72 ± 0.34	0.0559 ± 0.00063
10	7.53 ± 0.53	0.2237 ± 0.00371
50	7.69 ± 0.34	0.2227 ± 0.00246
100	7.66 ± 0.33	0.2266 ± 0.00246
pUC303-pGH-Amp/7942		
0	7.70 ± 0.44	0.0577 ± 0.00093
10	7.72 ± 0.34	0.2667 ± 0.00299
50	7.69 ± 0.32	0.3364 ± 0.00341
100	7.66 ± 0.36	0.3597 ± 0.00391

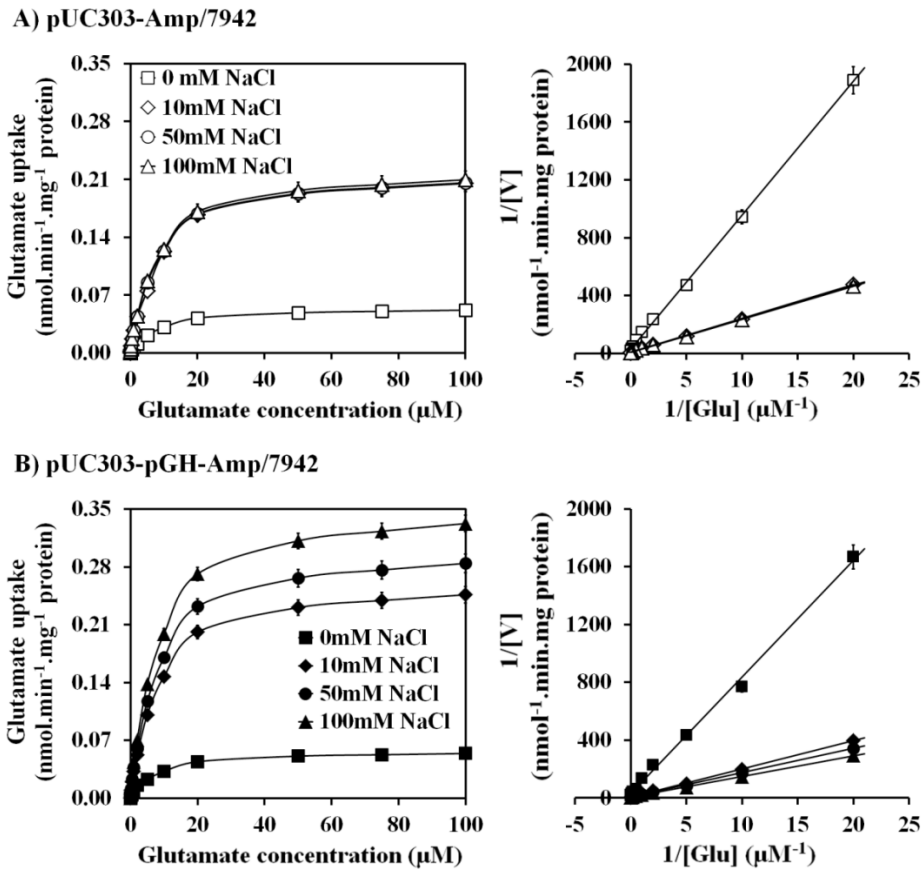

Figure 4.55 Kinetics of glutamate uptake by *Synechococcus* sp. PCC 7942 transformed with pUC303-Amp (pUC303-Amp/7942) represented with (□) and pUC303-pGH-Amp (pUC303-pGH-Amp/7942) represented with (■).

Saturation curves and double reciprocal plots of glutamate uptake by pUC303-Amp/7942 and pUC303-pGH-Amp/7942 assayed in the presence of various NaCl concentrations are shown. The data are from three independent experiments with vertical bars representing standard errors of the means, n=3. Error bars are included in the graphs where some may be smaller than the symbols.

4.7 Intracellular amino acid composition of *A. halophytica* under normal (0.5 M NaCl) and salt stress condition (2.0 M NaCl).

A. halophytica cells were grown in the growth medium containing 0.5 and 2.0 M NaCl. Cells at mid log phase were harvested and subjected to intracellular amino acid determination. Quantification of intracellular amino acids was performed using a Shimadzu Prominence Ultra-Fast Liquid Chromatography System with Agilent Zorbax Eclipse AAA analytical column as described in Materials and Methods. The amino acid showing highest content detected in *A. halophytica* is glutamate as shown in Table 4.12. Under salt stress condition, cells accumulated higher content of some amino acids such as glutamate, asparagine, GABA, valine, methionine, phenylalanine, ornithine and leucine than that of under normal condition.

Table 4.12 Intracellular amino acid composition of *A. halophytica* under normal (0.5 M NaCl) and salt stress condition (2.0 M NaCl).

Amino acid	Intracellular amino acid content (nmol. mg^{-1} protein)	
	Normal growth condition (0.5 M NaCl, pH 7.6)	Salt stress condition (2.0 M NaCl, pH 7.6)
Aspartate	4.0995 ± 0.0943	3.8695 ± 0.1470
Glutamate	29.9507 ± 0.9285	60.1061 ± 2.3441
Asparagine	0.0930 ± 0.0011	0.3622 ± 0.0043
Serine	0.0740 ± 0.0005	0.0908 ± 0.0002
Glutamine	2.9616 ± 0.0651	0.7239 ± 0.0232
Histidine	0.2924 ± 0.0044	0.2282 ± 0.0114
Glycine	0.2462 ± 0.0019	0.2849 ± 0.0042
Threonine	0.9549 ± 0.0134	1.4979 ± 0.0344
Arginine	0.0373 ± 0.0006	0.0528 ± 0.0016
Alanine	0.2612 ± 0.0036	0.0542 ± 0.0012
γ-aminobutyric acid	0.0958 ± 0.0012	0.1905 ± 0.0027
Tyrosine	0.1202 ± 0.0038	0.0775 ± 0.0022
Cysteine	0.3561 ± 0.0075	0.2488 ± 0.0092
Valine	0.0559 ± 0.0009	0.1525 ± 0.0038
Methionine	0.0057 ± 0.0004	0.1699 ± 0.0054
Phenylalanine	0.0549 ± 0.0017	0.1501 ± 0.0034
Isoleucine	0.0161 ± 0.0001	0.0041 ± 0.0001
Ornithine	0.0251 ± 0.0001	0.1818 ± 0.0053
Leucine	0.0767 ± 0.0008	0.3541 ± 0.0117
Lysine	0.7351 ± 0.0353	0.9693 ± 0.0436

4.8 Glutamate utilization in *A. halophytica*

From Figure 4.5, we suggested that *A. halophytica* may be used exogenous glutamate as an energy source and also as an intermediate in nitrogen assimilation via GDH and GS-GOGAT pathways. In addition, the possible roles of glutamate are signaling molecule and also precursor for the synthesis of other main osmoprotectants such as glycine betaine, glutamate betaine, gamma-aminobutyric acid (GABA), arginine and proline etc. In this study, we focused on utilization of glutamate in *A. halophytica*.

4.8.1 The $^{14}CO_2$ liberation measurement

A. halophytica cells were grown in the growth medium containing 0.5 M NaCl and 2.0 M NaCl. Cells at mid log phase were harvested by centrifugation, washed twice and re-suspended to a concentration of 0.1 mg cell protein in 1 ml assay medium containing either 0.5 M NaCl or 2.0 M NaCl. Briefly, the total volume of the reaction medium was 2 ml in the vial (10 ml) composed of cells and buffer at the bottom of vial. A filter paper, 5x5 mm diameter, was placed at the top of the vial and one drop of 1 M NaOH was applied to the paper. The reaction was initially started by adding [U-^{14}C]-glutamate. The filter paper was taken out after desired time, dried on the stainless steel, and measured with a liquid scintillation counter as shown in Figure 4.56A. The results showed that the $^{14}CO_2$ production was increased about 4.6 folds under salt stress condition comparing with normal condition (Figure 4.56B). The initial rate of $^{14}CO_2$

production was observed within the first 5 min and cells showed saturated glutamate uptake after cells were exposed to glutamate for 20 min. This results suggested that [U-^{14}C]-glutamate was taken up into the *A. halophytica* cell and can be used as the carbon source.

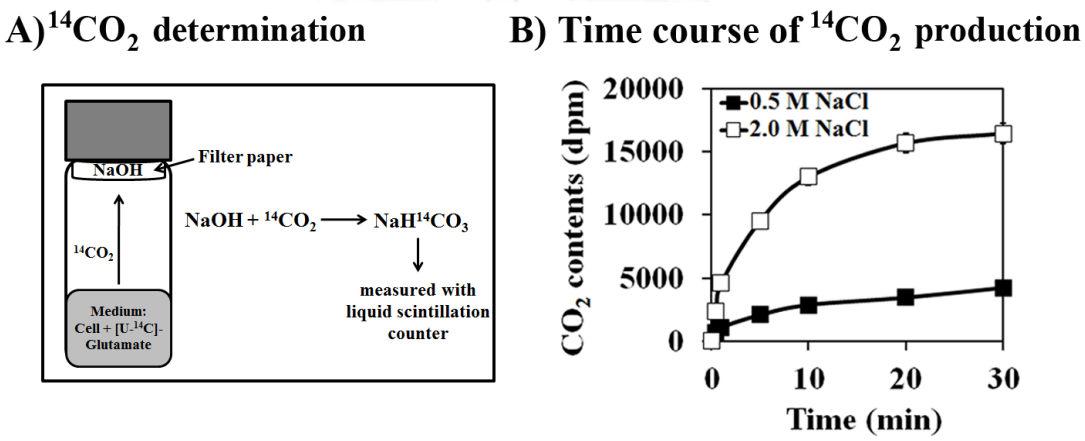

Figure 4.56 The release of $^{14}CO_2$ from the *A. halophytica*.

(A) $^{14}CO_2$ determination follows materials and methods. (B) Time course of $^{14}CO_2$ production. The data are from three independent experiments with vertical bars representing standard errors of the means, n=3. Error bars are included in the graphs where some may be smaller than the symbols.

3.8.2 Cellular ion determination

We also determined the effect of exogenous glutamate on the content of cellular ions. In this experiment, *A. halophytica* cells were cultured under 0.5 and 2.0 M NaCl until mid-log phase before harvesting the cells by centrifugation, washed twice with fresh medium and re-suspended in desired medium containing various concentrations of exogenous glutamate. Cellular ions of *Aphanothece* cells were determined at interval time for 60 min with a Shimadzu PIA-1000 personal ion analyzer. Changes in cellular ion contents could be observed in the presence of 2.0 M NaCl compared to the control with 0.5 M NaCl. The initial rate of ammonium ion (NH_4^+), sodioum ion (Na^+) and potassioum ion (K^+) production were observed within the first 5 min.

Figure 4.57 shows contents of ammonium ion, sodioum ion and potassioum ion from *A. halophytica* cells under normal and salt stress condition with various exogenous glutamate concentrations. The results showed that the contents of ammonium ion and sodioum ion were increased about 1.6 and 3 folds under salt stress condition. As expected, an increased exogenous glutamate under salt stress resulted in an increased ammonium ion and Na^+ contents. In contrast, the contents of potassioum ion were decreased at all glutamate concentrations tested in both normal and salt stress.

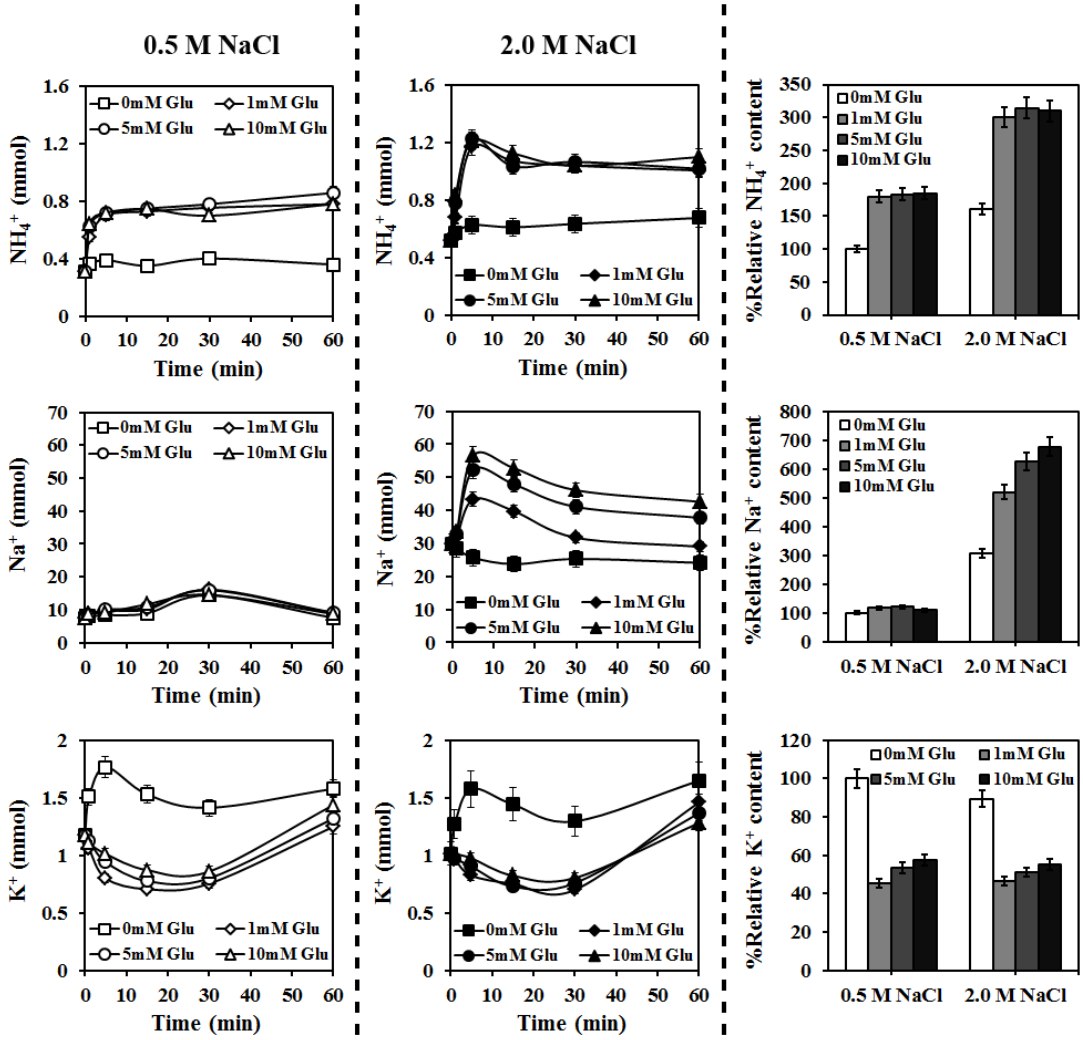

Figure 4.57 Cellular ion contents of *A. halophytica* under normal and salt stress condition with various exogenous glutamate concentrations. The data are from three independent experiments with vertical bars representing standard errors of the means, n=3. Error bars are included in the graphs where some may be smaller than the symbols.

4.8.3 Glutamate as glycine betaine precursor

A. halophytica were cultured under 0.5 and 2.0 M NaCl until mid-log phase before harvesting the cells by centrifugation at 5000 rpm for 10 min at room temperature, washed twice with fresh medium and re-suspended in desired medium containing various concentrations of exogenous glutamate. Glycine betaine content of *Aphanothece* cells was determined at interval time for 60 min with a time of flight mass spectroscopy (KOMPACT MALDI IV tDE, Shimadzu/Kratos, Japan). Changes in glycine betaine contents could be observed in the presence of 2.0 M NaCl compared to the control with 0.5 M NaCl. The initial rate of glycine betaine production was observed within the first 5 min and cells showed saturated glutamate uptake after cells were exposed to glutamate for 30 min. Figure 4.58 shows the contents of glycine betaine in *A. halophytica* adapted in normal and salt stress condition supplemented with different glutamate concentrations. The result showed that glycine betaine was increased about 2.8 fold in mid-log phase cells grown under salt stress condition. Increasing glutamate concentration resulted in a slight increase of glycine betaine in *A. halophytica* when grown under normal condition. In contrast, increasing glutamate concentration caused a large increase of glycine betaine in cells grown under high salinity. The highest glycine betaine content was observed under salt stress condition supplemented with 5 mM glutamate showing about 4.8 folds increase comparing with normal condition.

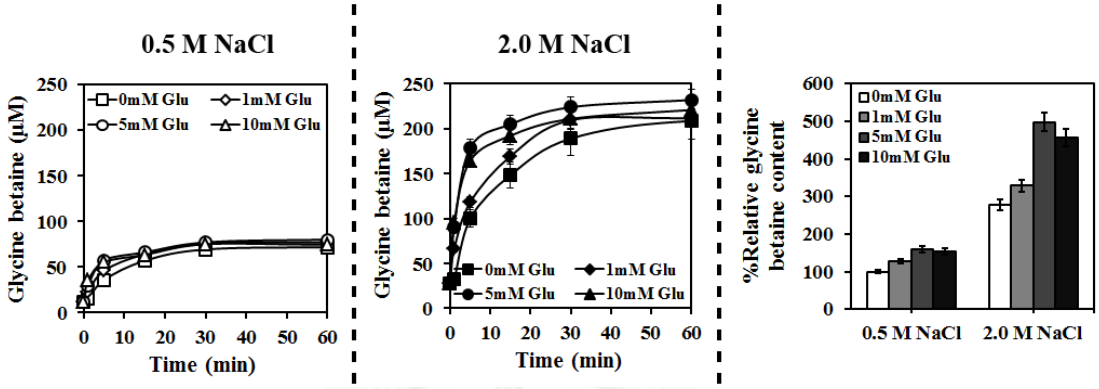

Figure 4.58 Glycine betaine contents of *A. halophytica* under normal and salt stress condition with various exogenous glutamate concentrations. The data are from three independent experiments with vertical bars representing standard errors of the means, n=3. Error bars are included in the graphs where some may be smaller than the symbols.

4.8.4 Glutamate as a substrate for gamma-aminobutyric acid (GABA) synthesis

A. halophytica were cultured under 0.5 and 2.0 M NaCl until mid-log phase before harvesting the cells by centrifugation at 5000 rpm for 10 min at room temperature, washed twice with fresh medium and re-suspended in desired medium containing various concentrations of exogenous glutamate. GABA content of *Aphanothece* cells was determined at interval time for 4 hrs using a Shimadzu Prominence Ultra-Fast Liquid Chromatography System with Agilent Zorbax Eclipse AAA analytical column. Changes in GABA contents could be observed in the presence of 2.0 M NaCl compared to the control with 0.5 M NaCl. The initial rate of GABA production was observed within the first 1 hr and cells showed saturated glutamate uptake after cells were exposed to glutamate for 2 hrs. Figure 4.59 shows the contents of GABA in *A. halophytica* adapted in normal and salt stress condition supplemented with different glutamate concentrations. The result showed that GABA accumulation was increased about 2 fold in mid-log phase cells grown under salt stress condition. Increasing glutamate concentration resulted in a slight increase of GABA accumulation in *A. halophytica* under both conditions. The highest GABA content was observed under salt stress condition supplemented with 5 mM glutamate showing about 2.2 fold increased comparing with normal condition.

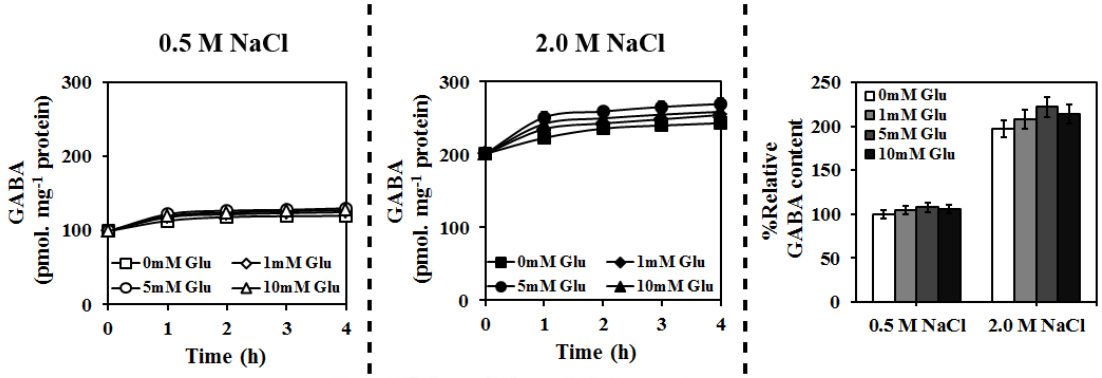

Figure 4.59 GABA contents of *A. halophytica* under normal and salt stress condition with various exogenous glutamate concentrations.

The data are from three independent experiments with vertical bars representing standard errors of the means, n=3. Error bars are included in the graphs where some may be smaller than the symbols.

4.9 Enzymes in glutamate metabolic pathways in cyanobacteria

4.9.1 Database searching

To identify enzymes in glutamate metabolic pathways, we searched in cyanobase using glutamate as query. 430 genes were matched containing glutamate transporters, enzymes in glutamate metabolic pathways such as glutamate decarboxylase, glutamate dehydrogenase, glutamate synthase, glutamine synthetase, etc. and also enzymes in glutamate derivatives synthetic pathways such as folylpolyglutamate synthase, *N*-acetylglutamate synthase, etc. Enzymes in glutamate metabolic pathways were selected for further study. Totally, a maximum of 10 groups of enzymes related in glutamate metabolic pathways have been identified as shown in Table 4.13.

γ-aminobutyric acid (GABA) is a valuable compound of the free amino acid pool that is widely distributed in nature among prokaryotes and eukaryotes. In plants, GABA is an intermediate for amino acid metabolism and also is accumulated in response to a wide range of environmental stress. GABA is mainly synthesized from glutamate by glutamate decarboxylase (GAD). However, the role of GAD and GABA production in cyanobacteria has not been reported. Unfortunately, the *A. halophytica* genome sequence was not reported.

Table 4.13 List of enzymes related in glutamate metabolic pathways in cyanobacteria.

Enzyme	Description	Reaction	Number of gene in Cyanobase	Interpro	Number of protein in EBI database
1. Glutamate decarboxylase (EC 4.1.1.15)	An enzyme that catalyzes the decarboxylation of glutamate to GABA and CO_2. **Cofactor:** pyridoxal-5'-phosphate (PLP)	glutamate → CO_2 + GABA	6	IPR010107	27
2. γ-Glutamylcysteine synthetase (Glutamate-cysteine ligase; EC 6.3.2.2)	An enzyme that catalyses the ATP-dependent condensation of cysteine and glutamate to form the dipeptide γ-glutamylcysteine.	ATP + L-glutamate + L-cysteine ⇌ ADP + phosphate + γ-L-glutamyl-L-cysteine	23	IPR006336	153
3. Glutamate synthase (Glutamate-ammonia ligase; EC 1.4.1.13)	An enzyme that catalyzes the single-step conversion of L-glutamine and alpha-ketoglutarate into two molecules of L-glutamate. **Cofactors:** FAD, Iron, FMN, Sulfur, and Iron-sulfur	L-glutamine + 2-oxoglutarate + 2 reduced ferredoxin + 2 H^+ ⇌ 2 L-glutamate + 2 oxidized ferredoxin or L-glutamine + 2-oxoglutarate + NADPH + H^+ ⇌ 2 L-glutamate + $NADP^+$	98	IPR002489 or IPR006005	179 or 45

Table 4.13 (Continued)

Enzyme	Description	Reaction	Number of genes in Cyanobase	Interpro	Number of proteins in EBI database
4. Glutamine synthetase (EC 6.3.1.2)	An enzyme that catalyzes the production of *glutamine* from glutamate.	Glutamate + ATP + NH_3 → Glutamine + ADP + phosphate	76	IPR004809	148
5. Glutamate dehydrogenase (EC 1.4.1.4)	An enzyme that catalyzes the reversible inter-conversion of glutamate to α-ketoglutarate and ammonia.	L-glutamate + H_2O + $NADP^+$ ⇌ 2-oxoglutarate + NH_3 + NADPH + H^+	35	IPR006095	124
6. N-Acetylglutamate synthase (EC 2.3.1.1, EC 2.3.1.35)	An enzyme that catalyses the production of N-acetylglutamate from acetyl-CoA and glutamate.	acetyl-CoA + L-glutamate ⇌ CoA + N-acetyl-L-glutamate	17	IPR002813	134
7. 1-Pyrroline-5-carboxylate dehydrogenase (EC 1.5.1.12)	An enzyme that catalyzes the NAD^+-dependent oxidation of 1-pyrroline-5-carboxylate to glutamate.	1-pyrroline-5-carboxylate + NAD^+ + 2 H_2O ⇌ L-glutamate + NADH + H^+	10	IPR005932	90
8. Glutamate 5-kinase (Glutamate 5-phosphotransferase ; EC 2.7.2.11)	An enzyme that the ATP-dependent phosphorylation of glutamate to glutamate 5-phosphate.	ATP + L-glutamate ⇌ ADP + L-glutamate 5-phosphate	26	IPR001057	256

Table 4.13 (Continued)

Enzyme	Description	Reaction	Number of gene in Cyanobase	Interpro	Number of protein in EBI database
9. Glutamate racemase (EC 5.1.1.3)	An enzyme that catalyzes the stereoinversion of D-glutamate and L-glutamate.	L-glutamate ⇌ D-glutamate	39	IPR004391	133
10. Transaminase a) Succinyldiaminopimelatetransaminase (EC 2.6.1.17) This enzyme participate in lysine biosynthesis	An enzyme that catalyzes the transfer amino group from N-succinyl-L-2,6-diaminoheptanedioate to 2-oxoglutarate in order to generate N-succinyl-2-L-amino-6-oxoheptanedioate and L- glutamate. **Cofactor:** pyridoxal-5'-phosphate (PLP)	N-succinyl-L-2,6-diaminoheptanedioate + 2-oxoglutarate ⇌ N-succinyl-L-2-amino-6-oxoheptanedioate + L-glutamate	6	IPR015424	4080

Table 4.13 (Continued)

Enzyme	Description	Reaction	Number of gene in Cyanobase	Interpro	Number of protein in EBI database
b) Acetylornithine transaminase (EC 2.6.1.11) This enzyme participates in urea cycle and metabolism of amino groups	An enzyme that catalyzes the transfer amino group from N_2-acetyl-L-ornithine to 2-oxoglutarate in order to generate N-acetyl-L-glutamate 5-semialdehyde and L-glutamate. **Cofactor:** pyridoxal-5'-phosphate (PLP)	N_2-acetyl-L-ornithine + 2-oxoglutarate $\rightleftharpoons$ N-acetyl-L-glutamate 5-semialdehyde + L-glutamate	1	IPR005814	690
c) Aspartate aminotransferase (EC 2.6.1.1)	An enzyme that catalyzes the reversible transfer of an α-amino group between aspartate and glutamate. **Cofactor:** pyridoxal-5'-phosphate (PLP)	Aspartate + α-ketoglutarate $\rightleftharpoons$ oxaloacetate + glutamate	6	IPR004839	1251

Table 4.13 (Continued)

Enzyme	Description	Reaction	Number of gene in Cyanobase	Interpro	Number of protein in EBI database
d) Glutamine fructose-6-phosphate transaminase (EC 2.6.1.16) This enzyme participates in glutamate metabolism and aminosugars metabolism.	An enzyme that catalyzes the synthesis of D-glucosamine 6-phosphate and L- glutamate from D-fructose 6-phosphate and L-glutamine.	L-glutamine + D-fructose 6-phosphate ⇌ L-glutamate + D-glucosamine 6-phosphate	7	IPR005855	135
e) 2,4-diaminobutyrate -2-oxoglutarate transaminase (EC 2.6.1.76) This enzyme participates in glycine, serine and threonine metabolism.	An enzyme that catalyzes the synthesis of L-aspartate 4-semialdehyde and L- glutamate from L-2,4-diaminobutanoate and 2-oxoglutarate.	L-2,4-diaminobutanoate + 2-oxoglutarate ⇌ L-aspartate 4-semialdehyde + L-glutamate	1	IPR004637	18

4.9.2 Database searching of glutamate decarboxylase in cyanobacteria

To identify cyanobacterial glutamate decarboxylase, firstly, we searched in cyanobase using glutamate decarboxylase as query. Six genes from six cyanobacterial strains were matched: *Synechocystis* sp. PCC 6803, *Microcystis aeruginosa* NIES-843, *Prochlorococcus marinus* MIT9313, *Synechococcus* sp. CC9311, *Prochlorococcus marinus* str. MIT 9303, *Synechococcus* sp. RCC307. Secondly, we searched using the amino acid sequences of *Synechocystis* sp. PCC 6803 glutamate decarboxylase (sll1641) as query in the programs BlastP, PSI-BLAST and DELTA-BLAST, and nucleotide sequences of *Synechocystis* sp. PCC 6803 as query in the programs BlastN. Moreover, IPR002129 Pyridoxal phosphate-dependent decarboxylase and IPR010107 Glutamate decarboxylase were used as query in the InterPro database. The protein sequences that were not found by the domain searches were added to the list. Totally, a maximum of 87 pyridoxal phosphate-dependent decarboxylase containing proteins in cyanobacteria have been identified.

Next, sequences of all the proteins identified by the InterProScan were aligned using Clustal X program [109]. Tree construction using the neighbor-joining method and bootstrap analysis was performed based on the amino acid similarities among the proteins shown in Figure 4.60. This analysis led us to catagorized the proteins into three main groups: glutamate decarboxylase, ornithine/lysine/arginine decarboxylase and aspartate decarboxylase. In this study, glutamate decarboxylase or IPR010107-containing proteins were further analyzed.

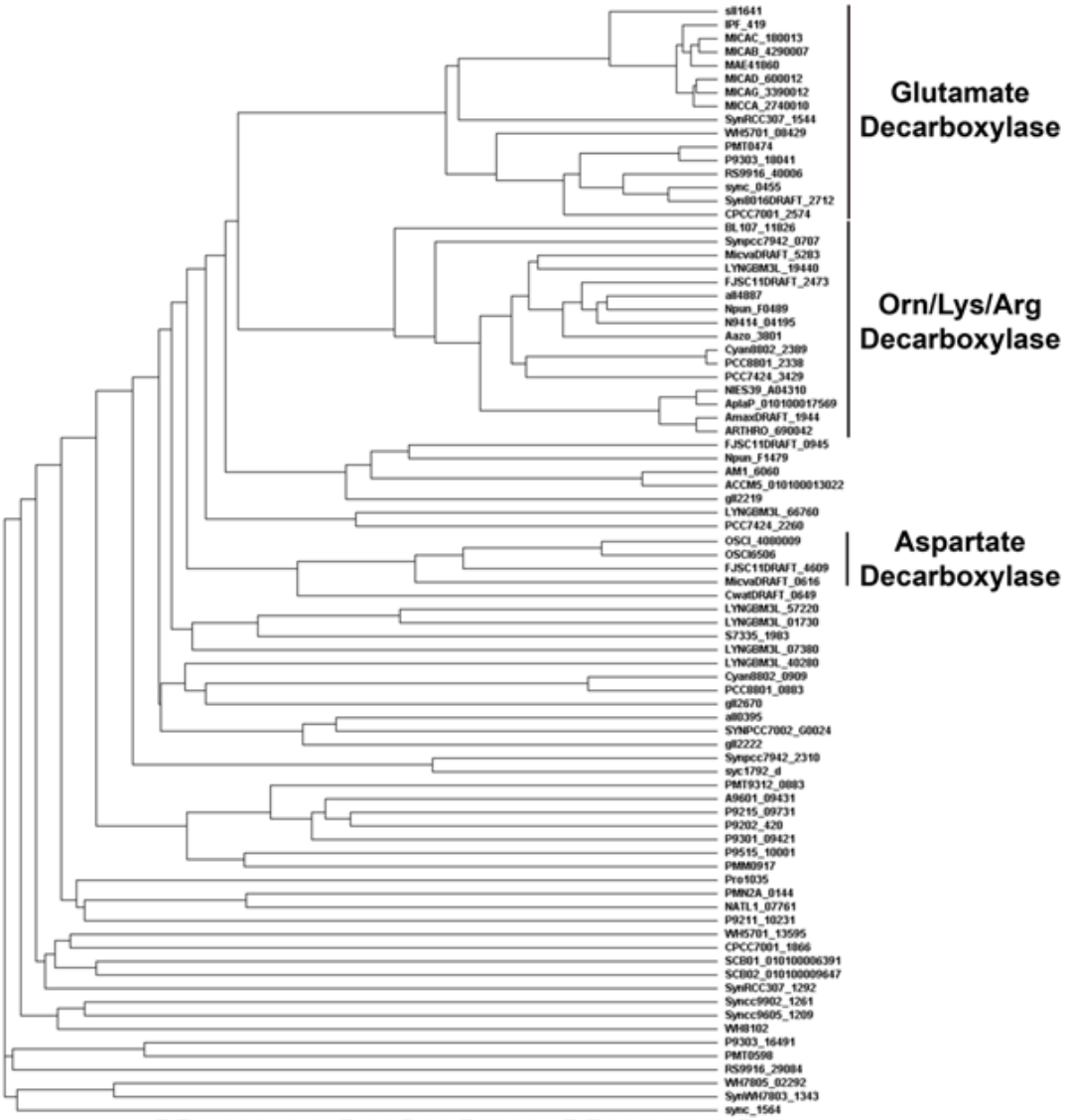

Figure 4.60 Phylogenetic tree showing the overall relatedness of pyridoxal phosphate-dependent decarboxylase (IPR002129-containing proteins) in cyanobacteria.

Alignment of full-length protein sequences and phylogenetic analysis were performed as described in the “Materials and Methods” section.

4.9.3 Comparative analysis of marine glutamate decarboxylase and *E. coli* glutamate decarboxylase

Totally, 16 putative IPR010107-containing proteins from cyanobacteria have been identified as shown in Table 4.14. Rooted phylogenetic tree of 16 marine cyanobacterial glutamate decarboxylase and glutamate decarboxylase from *E. coli* (NP_416010) was performed with Clustal X program [109] using default settings based on the amino acid similarities among the proteins. *E. coli* glutamate decarboxylase was used as outgroup. These proteins were classified to two main groups: glutamate decarboxylase of marine cyanobacteria and that of freshwater cyanobacteria as shown in Figure 4.83.

Six marine cyanobacterial glutamate decarboxylases such as *Cyanobium* sp. PCC 7001 (ZP_05046384), *Prochlorococcus marinus* MIT9313 (NP_894307), *Prochlorococcus marinus* str. MIT 9303 (YP_001017811), *Synechococcus* sp. RS9916 (ZP_01473044), *Synechococcus* sp. CC9311 (YP_729684) and *Synechococcus* sp. WH 8016 (ZP_08957365) were compared to glutamate decarboxylase from *E. coli* (NP_416010) and *Arabidopsis thaliana* (NP_197235). The marine cyanobacterial glutamate decarboxylases have identity in range 52-54% with EcGAD and 37-39% with AtGAD (Table 4.17). It should be mentioned that marine cyanobacterial glutamate decarboxylases showed the high degrees of amino acid sequence identity ($\geq$ 50%) to EcGAD.

Table 4.14 Characteristics of 16 putative IPR010107-containing proteins (glutamate decarboxylase) in cyanobacteria.

GenBank Acc Protein	GenBank Acc nucleotide	Locus_tag (XXXXXX = cyanobase ID	Description	Organism	Length of coding region	Length of amino acids	Interpro	% Amino acid identity (similarity) to 6803GAD
NP_440384 (YP_005382250, YP_005385420, YP_005408127, YP_005650441, BAA17064, BAK49236, BAL28235, BAL31405, BAL34574)	NC_000911 (BA000022)	sll1641 (F7ULE4_SYNYG, H0P291_9SYNC, H0PEK7_9SYNC, H0PJX2_9SYNC, P73043_SYNY3)	Glutamate decarboxy-lase	*Synechocys-tis* sp. PCC 6803	1404	467	IPR002129 **IPR010107** IPR015421 IPR015424 PTHR11999	100.0% (100.0%) [to EcGAD 48.7% (66.9%); to AtGAD 45.9% (63.7%)]
CAO87476	AM778946	IPF_419 A8YIA1_MICAE	unnamed protein product	*Microcystis aeruginosa* PCC 7806	1404	467	IPR002129 **IPR010107** IPR015421 IPR015424 PTHR11999	78.6% (89.9%) [to EcGAD 47.6% (65.3%); to AtGAD 45.4% (62.0%)]

Table 4.14 (Continued)

GenBank Acc Protein	GenBank Acc nucleotide	Locus_tag (XXXXXX = cyanobase ID	Description	Organism	Length of coding region	Length of amino acids	Interpro	% Amino acid identity (similarity) to 6803GAD
CCI01250	CAIJ01000090	MICAC_180013	Glutamate decarboxy-lase A	*Microcystis aeruginosa* PCC 9443	1404	467	IPR002129 **IPR010107** IPR015421 IPR015424 PTHR11999	78.6% (89.7%) [to EcGAD 47.1% (64.7%); to AtGAD 45.3% (61.5%)]
CCH98079	CAII01000367	MICAB_4290007	Glutamate decarboxy-lase A	*Microcystis aeruginosa* PCC 9717	1404	467	IPR002129 **IPR010107** IPR015421 IPR015424 PTHR11999	77.7% (89.3%) [to EcGAD 47.1% (64.7%); to AtGAD 45.3% (61.5%)]
CCI09506	CAIK01000391	MICAD_600012	Glutamate decarboxy-lase A	Microcystis aeruginosa PCC 7941	1404	467	IPR002129 **IPR010107** IPR015421 IPR015424 PTHR11999	78.6% (89.1%) [to EcGAD 47.6% (64.7%); to AtGAD 44.3% (60.7%)]

Table 4.14 (Continued)

GenBank Acc Protein	GenBank Acc nucleotide	Locus_tag (XXXXXX = cyanobase ID	Description	Organism	Length of coding region	Length of amino acids	Interpro	% Amino acid identity (similarity) to 6803GAD
CCI27064	CAIN01000267	MICAG_3390012	Glutamate decarboxy-lase A	Microcystis aeruginosa PCC 9808	1404	467	IPR002129 **IPR010107** IPR015421 IPR015424 PTHR11999	77.9% (88.2%) [to EcGAD 47.6% (64.5%); to AtGAD 44.3% (60.3%)]
ZP_01085038	NZ_AANO01000005	WH5701_08429 A3YYB2_9SYNE	Glutamate decarboxy-lase	*Synechococ-cus* sp. WH 5701	1401	466	IPR002129 **IPR010107** IPR015421 IPR015424 PTHR11999	53.7% (67.9%) [to EcGAD 55.6% (71.5%); to AtGAD 40.5% (55.9%)]
NP_894307	NC_005071	PMT0474 Q7V891_PROMM	Glutamate decarboxy-lase	*Prochloro-coccus marinus* MIT9313	1440	479	IPR002129 **IPR010107** IPR015421 IPR015424 PTHR11999	48.0% (64.0%) [to EcGAD 52.6% (67.3%); to AtGAD 39.2% (57.1%)]

Table 4.14 (Continued)

GenBank Acc Protein	GenBank Acc nucleotide	Locus_tag (XXXXXX = cyanobase ID	Description	Organism	Length of coding region	Length of amino acids	Interpro	% Amino acid identity (similarity) to 6803GAD
YP_001227800	NC_009482	SynRCC307_1544 A5GU88_SYNR3	Glutamate decarboxy-lase	*Synechococ-cus* sp. RCC307	1395	464	IPR002129 **IPR010107** IPR015421 IPR015424 PTHR11999	52.5% (65.7%) [to EcGAD 42.8% (58.2%); to AtGAD 38.9% (53.2%)]
ZP_01473044	NZ_AAUA0100 0004	RS9916_40006 Q05Q95_9SYNE	Glutamate decarboxy-lase	*Synechococ-cus* sp. RS9916	1395	464	IPR002129 **IPR010107** IPR015421 IPR015424 PTHR11999	48.0% (64.9%) [to EcGAD 54.9% (71.0%); to AtGAD 37.0% (56.6%)]
YP_001017811	NC_008820	P9303_18041 A2CAN6_PROM3	Glutamate decarboxy-lase	*Prochloro-coccus marinus* str. MIT 9303	1440	479	IPR002129 **IPR010107** IPR015421 IPR015424 PTHR11999	47.8% (64.1%) [to EcGAD 52.6% (66.9%); to AtGAD 39.4% (58.0%)]

Table 4.14 (Continued)

GenBank Acc Protein	GenBank Acc nucleotide	Locus_tag (XXXXXX = cyanobase ID	Description	Organism	Length of coding region	Length of amino acids	Interpro	% Amino acid identity (similarity) to 6803GAD
YP_729684	NC_008319	sync_0455 Q0ICY8_SYNS3	Glutamate decarboxy-lase	*Synechococ-cus* sp. CC9311	1332	443	IPR002129 **IPR010107** IPR015421 IPR015424 PTHR11999	48.9% (63.4%) [to EcGAD 53.5% (68.7%); to AtGAD 38.0% (56.7%)]
ZP_08957365	NZ_AGIK0100 0006	Syn8016DRAFT _2712 G4FPV8_9SYNE	Glutamate decarboxy-lase	*Synechoco-ccus* sp. WH 8016	1395	464	IPR002129 **IPR010107**	48.4% (64.7%) [to EcGAD 54.1% (70.3%); to AtGAD 37.5% (56.9%)]
ZP_05046384	-	CPCC7001_2574 B5IMY2_9CHRO	Glutamate decarboxy-lase	*Cyanobium* sp. PCC 7001	-	449	IPR002129 **IPR010107** IPR015421 IPR015424 PTHR11999	47.5% (62.9%) [to EcGAD 54.2% (69.1%); to AtGAD 37.1% (54.8%%)]

Table 4.14 (Continued)

GenBank Acc Protein	**GenBank Acc nucleotide**	**Locus_tag (XXXXXX = cyanobase ID**	**Description**	**Organism**	**Length of coding region**	**Length of amino acids**	**Interpro**	**% Amino acid identity (similarity) to 6803GAD**
CCH93070	CAIH01000195	MICCA_2740010	Glutamate decarboxy-lase	*Microcystis aeruginosa* PCC 9432	1599	532	IPR002129 **IPR010107** IPR015421 IPR015424 PTHR11999	67.9% (77.4%) [to EcGAD 39.4% (53.0%); to AtGAD 37.5% (50.4%)]
YP_001659200	NC_010296	MAE41860 B0JS50_MICAN	Glutamate decarboxy-lase	*Microcystis aeruginosa* NIES-843	558	185	IPR002129 **IPR010107** IPR015421 IPR015424 PTHR11999	31.9% (36.4%) [to EcGAD 19.6% (26.4%); to AtGAD 18.8% (25.9%)]

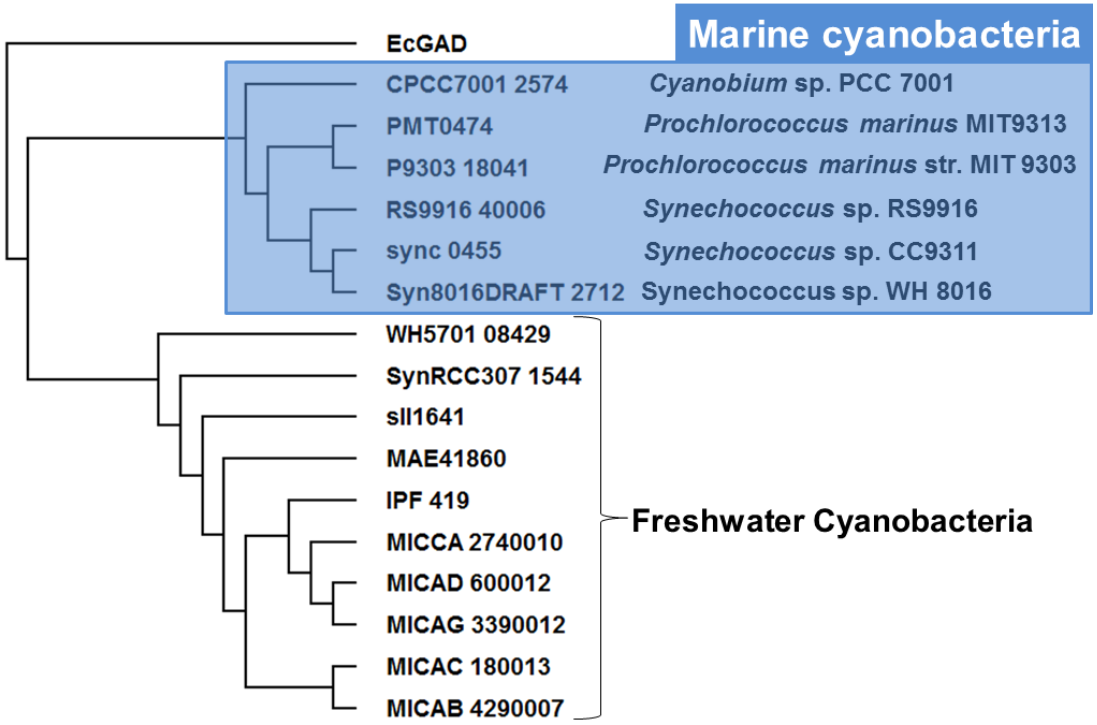

Figure 4.61 Neighbor-joining tree based on amino acid similarities among 16 putative IPR010107-containing proteins in cyanobacteria and glutamate decarboxylase from *E. coli* (NP_416010).

Tree construction using the neighbor-joining method and bootstrap analysis was performed with ClustalX program [109] as described in the "Materials and Methods" section.

Multiple sequence alignment of these proteins with EcGAD shown in Figure 4.62 indicates their high degree of sequence conservation especially in PLP-binding domain and substrate-binging region. The alignment of the GAD sequences allowed us to establish the conserved residue in GAD. Amino acid residues in contact with PLP in active sites of GAD are presented. These amino acids form the direct environment of the cofactor. Mainly G, A, and S amino acid residues in position 1-3, bind the phosphate moiety of PLP. H or W in position 4 is found near PLP. The sequence DAA in position 5-7 forms the environment of the pyridinium ring nitrogen. W or S in position 8 forms a hydrogen bond with the hydroxyl of phosphate moiety. H and K in position 9 and 10 form the Schiff base with the PLP. Glycine-rich fragments (GG), common for all GAD, were found in sequences of marine cyanobacterial glutamate decarboxylases.

Glutamate is the common substrate for glutamate decarboxylase. Substrate-binding regions of GAD are 2 domains: the sequence FV**R**LG and E**R**L as shown in underlined alphabets in Figure 4.62. Arginine (R) residue is proposed for glutamate binding. We found these 2 domains in marine cyanobacterial glutamate decarboxylase. The arginine residue in FV**R**LG binds with γ-carboxyl, whereas arginine residue in the small domain E**R**L binds with α-carboxyl.

```
PMT0474       MALHRSNPRSNDLEEHAIGETVDALVSPLPRTTFPQEYRPALTTFNLLKEELLLDGNSKQ 60
P9303_18041   MALHRSNPRSNDLEEHAIWETVDALVSPLPRATFPQECRPALTTFNLLKEELLLDGNSKQ 60
sync_0455     ------------------------MLTPLPKHHFPGEGREGNSTVQLLREELLLDGNSKQ 36
Syn8016DRAFT  MALHQSRHHLRDSEEQAL---VDAMLSPLPKHHFPGVGREGNSTVQLLKEELLLDGNSKQ 57
RS9916_40006  MGIHRSRHHLIDSGEQAL---VDAMVDPLPRDHFPVDGRAADTTVQLLKEELLLDGNSKQ 57
CPCC7001_2574-MLHS-----------------EESTRPLPRDRFPQHGQEPAATAEIISDELLLDGNSKQ 42
EcGAD         MDKKQVTDLRSELLDSRFG--AKSISTIAESKRFPLHEMRDDVAFQIINDELYLDGNARQ 58
                                            **        : ::: :** ****::*

PMT0474       NLATFCQTYESQQVAELMALAVDKNLIDKDEYPQTAEIERRCVSMMADLWHAPG----EA116
P9303_18041   NLATFCQTYESHQVADLMALAVDKNLIDKDEYPQTAEIERRCVSMMADLWHAPG----EA116
sync_0455     NLATFCQTYQAQSAMELMTLGVDKNLIDKDEYPQTAELEGRCVSMMADLWNAPG----AA 92
Syn8016DRAFT  NLATFCQTYQAQSAMELMALGVDKNLIDKDEYPQTAELESRCVSMMADLWNAPG----AA113
RS9916_40006  NLATFCQTYQGSAAMELMALGVDKNLIDKDEYPQTAEVERRCVSMMADLWNAPG----EA113
CPCC7001_2574NLATFCQTTEGAQVHALMDLAMDKNLIDKDEYPQTAELERRCVALLADLWHAPA----GA 98
EcGAD         NLATFCQTWDDENVHKLMDLSINKNWIDKEEYPQSAAIDLRCVNMVADLWHAPAPKNGQA118
              ******** :   .  ** *.::** ***:****:* :: *** ::****:**.     *

                                          PLP-binding region
                        12 3                                    4
PMT0474       VGCSTIGSSEAAMLGGLAAKWRWREHRKAAGQSIDRPNMVCGSVQICWTKFARYWDVELR176
P9303_18041   VGCSTIGSSEAAMLGGLAAKWRWREHRKAAGQSIDRPNMVCGSVQICWTKFARYWDVELR176
sync_0455     VGCSTIGSSEAAMLGGMAAKWRWRKRREAAGLPTDKPNMVCGSVQICWKKFARYWDIEMR152
Syn8016DRAFT  VGCSTIGSSEAAMLGGMAAKWRWRKRREAAGLPTDKPNMVCGSVQICWKKFARYWDIEMR173
RS9916_40006  IGCSTIGSSEASMLGGMAAKWRWRKKRQQAGLPTDQPNMVCGSVQICWKKFARYWDIEMR173
CPCC7001_2574IGCSTIGSSEAAMLGGMAAKWRWRARQQAAGRPTDNPNMVCGSVQICWHKFARYWDIELR158
EcGAD         VGTNTIGSSEACMLGGMAMKWRWRKRMEAAGKPTDKPNLVCGPVQICWHKFARYWDVELR178
              :* .*******.****:* ***** : : ** . *.**:***.***** *******:*:*

PMT0474       EVEMTSGELCMSPERMLEQVDENTIVVVPTLGVTYHGLYEDVQAVSQALDELQQRKGLDI236
P9303_18041   EVEMTSGELCMSPERMLEQVDENTIVVVPTLGVTYHGLYEDVQAISQALDELQQRKGLDI236
sync_0455     ELEMLTGELCVSPERVLEAVDENTIFVVPTLGVTYHGLYEDIESISKALDDLQARTGLDV212
Syn8016DRAFT  ELEMLAGELCISPERVIEAVDENTIFVVPTLGVTYHGLYEDIESISKALDDLQARTGLDV233
RS9916_40006  ELEMRPGDLCITPERVLEAVDENTIFVVPTLGVTYHGLYEDVEAISRALDDYQARTGIDI233
CPCC7001_2574EITMEPGKLCLTPEDVLSQVDENTIMVVPTLGVTYHGLYEDVASLSAALDGLQQRSGLDI218
EcGAD         EIPMRPGQLFMDPKRMIEACDENTIGVVPTFGVTYTGNYEFPQPLHDALDKFQADTGIDI238
              *: * .*.* : *: ::.  ***** ****:**** * **   .:  ***  *  .*:*:

                    Bind with hydrogen bond
                 5678                          910
PMT0474       PIHVDAASGGFLAPFCAPDLAPWDFRLPRVKSINSSGHKFGLAPLGVGWVLWRESRDLPE296
P9303_18041   PIHVDAASGGFLAPFCAPDLAPWDFRLPRVKSINSSGHKFGLAPLGVGWVLWRESSDLPE296
sync_0455     PIHVDAASGGFLAPFCAPDLPLWDFRLERVKSINASGHKFGLAPLGVGWVLWRSQEDLPD272
Syn8016DRAFT  PIHVDAASGGFLAPFCAPDLPLWDFRLERVKSINASGHKFGLAPLGVGWVLWRSQDDLPD293
RS9916_40006  PIHVDGASGGFLAPFCAPDLPPWDFRLERVKSINASGHKFGLAPLGVGWVMWRSPEDLPD293
CPCC7001_2574PIHVDAASGGFLAPFTAPHLPPWDFRLERVKSINASGHKFGLAPLGVGWVLWRQASDLPS278
EcGAD         DMHIDAASGGFLAPFVAPDIV-WDFRLPRVKSISASGHKFGLAPLGCGWVIWRDEEALPQ297
              :*:*.********* **.:  ***** *****.:*********** ***:**.   **.
```

```
                                      Glutamate binding residue 1
                                                   #
PMT0474       GLVFHVSYLGGDMPTFQINFSRPAGQVISQYYDFVRLGRDGYQAIHGASYANAQYVAQEL356
P9303_18041   GLVFHVSYLGGDMPTFQINFSRPAGQVISQYYDFVRLGRDGYQAIHGASYANAQYVAQEL356
sync_0455     ELVFHVTYLGGDMPTFQINFSRPAGQVIAQYHEFVRLGREGYRMLHMASHANAQYFAEKL332
Syn8016DRAFT  ELVFHVTYLGGDMPTFQINFSRPAGQVIAQYHEFVRLGREGYRMLHMASHANAQYFAEKL353
RS9916_40006  ELVFHVSYLGGDMPTFQINFSRPAGQVIAQYHEFVRLGREGYRLLHQASHSNAQYVAKAL353
CPCC7001_2574ELVFKVSYLGGDMPTFQINFSRPAGQVIAQYFTFVQLGREGYRRIHAVSHAVAQVVASAL338
EcGAD         ELVFNVDYLGGQIGTFAINFSRPAGQVIAQYYEFVRLGREGYTKVQNASYQVAAYLADEI357
               ***:* ****:: ** ***********:**. *::***:**  :: .*:  *  .*. :
                                         Glutamate binding residue 2
                                                      #
PMT0474       KKLGPFELINDGNPAGGIPTVVWTLRADQELGFNLYDLSDRLRLRGWQVPAYPFTGELAH416
P9303_18041   KKLGPFELIHDGNPARGIPTVVWTLRAGQELGFNLYDLSDRLRLRGWQVPAYPFTGELAH416
sync_0455     REMDLFRIIHDGTPDKGIPTVVWTLDDNPKYGFNLYDFADRLRMRGWQVPAYPFTGELES392
Syn8016DRAFT  REMDLFKIIHDGAPDQGIPTVVWTLDDNPDHGFNLYDFADRLRMRGWQVPAYPFTGELES413
RS9916_40006  GQMGPFQLIHDGAPEKGIPTVVWTLKEGVDPGFNLYDLADRLRMRGWQVPAYPFTGDLAH413
CPCC7001_2574QAMPLFEVLHDGNPHRGIPAVVWRLAPGQDPGFSLYDLADRLRVRGWQVPAYPFTGSLAA398
EcGAD         AKLGPYEFICTGRPDEGIPAVCFKLKDGEDPGYTLYDLSERLRLRGWQVPAFTLGGEATD417
                :  :..:  * *  ***:* : *  . . *:.***:::***:*******:.: *.

PMT0474       QAFQRILVKRDFSREMADLLLTDIRNAITHFESHPVKISLNANEAASTNHLGRSMVECRD476
P9303_18041   QAFQRILVKRDFSREMADLLLTDIRNAITHFESHPVKISLNATEAASTNHLGRSMVESLD476
sync_0455     TAFQRILVKRDFTRDMADLLLEDIRQAIQHFQKHPITSNLAATEGASYNHL---------443
Syn8016DRAFT  TAFQRILVKRDFTRDMADLLLQDIRQAIEHFQKHPITNNLLAAEAASYNHL---------464
RS9916_40006  HAFQRILVKRDFTREMADLLLDDIRTALAHFQKHPITSNLQASEAASYNHL---------464
CPCC7001_2574TPFQRILVKRGFTREMADLLLQDIRQAVEHLSRHPRAVPLSAAEAASYNHL---------449
EcGAD         IVVMRIMCRRGFEMDFAELLLEDYKASLKYLSDHPKLQGIAQQN--SFKHT---------466
               . **: :*.*  ::*:*** * : :: ::. **    :   :  * :*

PMT0474       AHG 479
P9303_18041   AHG 479
sync_0455     ---
Syn8016DRAFT  ---
RS9916_40006  ---
CPCC7001_2574---
EcGAD         ---
```

Figure 4.62 **Alignments of amino acid sequences of marine cyanobacterial glutamate decarboxylase comparing with that of *E. coli* (NP_416010).**

The identical residues in other sequences are indicated by a dash (*). Conserved residues in PLP-binding region and in glutamate-binding region are highlighted and underlined alphabets, respectively.

Next, nucleotide sequence alignment of marine cyanobacterial glutamate decarboxylase was performed as shown in Figure 4.63. Conserved nucleotide sequences were observed corresponding with the conserved amino acid residues in PLP-binding domain and substrate-binding region. Gene-specific primers were designed based on nucleotide sequence similarity among marine cyanobacterial GAD. Unfortunately, we did not successfully amplify of the target sequences. We did not get desired PCR product and nonspecific amplification occurred.

```
Syn8016DRAFT GTGGCACTGCATCAATCCCGTCATCATCTCCGTGACAGTGAGGAGCAGGCGTT------- 53
sync_0455    ------------------------------------------------------------
RS9916_40006 ATGGGGATTCATCGCTCCAGGCATCACCTGATCGACAGCGGCGAGCAGGCGCT------- 53
PMT0474      ATGGCCCTGCATCGTTCCAATCCCCGCTCCAACGATCTGGAAGAACATGCCATTGGGGAA 60
P9303_18041  ATGGCCCTGCATCGTTCTAATCCCCGCTCCAACGATCTGGAAGAACATGCCATTTGGGAA 60

Syn8016DRAFT --GGTTGATGCCATGCTCTCTCCTCTGCCGAAACATCACTTTCCTGGAGTAG-GGCGGGA110
sync_0455    ------------ATGCTCACCCCTCTGCCAAAGCATCACTTTCCTGGAGAAG-GGCGCGA 47
RS9916_40006 --CGTCGATGCGATGGTCGATCCCCTTCCGCGGGATCACTTCCCTGTCGATG-GCCGCGC110
PMT0474      ACCGTTGATGCATTGGTCTCACCATTACCAC-GCACGACTTTCCCGCAAGAGTACCGTCC119
P9303_18041  ACCGTTGATGCATTGGTCTCACCATTACCAC-GCGCGACTTTTCCGCAAGAGTGCCGTCC119
                          ** **   **  * **        ****  * *     *   **

Syn8016DRAFT AGGAAACTCCACAGTGCAACTTTTAAAAGAAGAGTTGCTCCTCGATGGGAATAGTAAGCA170
sync_0455    AGGGAATTCCACAGTGCAACTTTTGAGAGAAGAGCTACTTCTTGATGGCAATAGTAAGCA107
RS9916_40006 TGCGGACACCACCGTTCAACTGCTGAAGGAAGAGTTGTTGCTTGATGGCAACAGCAAGCA170
PMT0474      TGCATTAACAACATTTAATTTGCTCAAGGAGGAATTATTGCTTGACGGCAACAGCAAACA179
P9303_18041  TGCATTGACAACATTTAATTTGCTCAAGGAGGAGTTATTGCTTGACGGCAACAGCAAACA179
              *      * **  *  *  *  * *  ** **  *  * ** ** ** ** ** ** **

Syn8016DRAFT GAACTTAGCCACTTTTTGTCAGACTTATCAGGCGCAAAGC-GCGATGGAGTTGATGGCTC229
sync_0455    GAACTTAGCCACATTTTGTCAGACCTATCAAGCGCAAAGT-GCGATGGAGTTGATGACTC166
RS9916_40006 GAACCTGGCCACGTTTTGCCAGACCTATCAGG-GCTCTGCAGCGATGGAACTGATGGCCC229
PMT0474      AAATCTGGCCACCTTCTGTCAGACCTATGAAA-GCCAACAGGTGGCTGAGCTAATGGCCC238
P9303_18041  AAATCTGGCCACCTTCTGTCAGACCTATGAAA-GTCACCAGGTGGCTGATCTAATGGCCC238
              **  * ***** ** ** ***** *** *   *       * *   **  * *** * *

Syn8016DRAFT TGGGAGTGGATAAAAATCTCATCGATAAAGATGAATATCCGCAGACGGCTGAGCTTGAGA289
sync_0455    TTGGGGTGGATAAGAATCTGATCGATAAAGATGAATATCCCCAGACAGCTGAGCTTGAGG226
RS9916_40006 TCGGCGTGGATAAAAACCTGATCGACAAAGACGAATACCCCCAGACCGCTGAGGTGGAGC289
PMT0474      TCGCGGTTGACAAGAACCTGATCGACAAGGACGAATATCCCCAAACCGCAGAGATTGAAC298
P9303_18041  TCGCGGTTGACAAGAACCTGATCGACAAGGACGAATATCCCCAAACCGCAGAGATTGAAC298
             * *  ** ** ** ** ** ***** ** ** ***** ** ** ** ** *** * **

Syn8016DRAFT GTCGCTGTGTTTCGATGATGGCCGACTTATGGAATGCTCCTGGCGCTGCAGTTGGATGCT349
sync_0455    GCCGTTGCGTCTCGATGATGGCCGACTTGTGGAATGCTCCTGGCGCCGCAGTTGGATGCT286
RS9916_40006 GTCGTTGCGTGTCGATGATGGCCGATCTGTGGAATGCCCCGGGGGAGGCTATTGGGTGTT349
PMT0474      GCCGTTGTGTTTCGATGATGGCTGATTTATGGCATGCCCCCGGTGAAGCTGTGGGCTGCT358
P9303_18041  GCCGTTGTGTTTCGATGATGGCTGATTTATGGCACGCCCCCGGTGAAGCTGTGGGCTGCT358
             * ** ** ** *********** **  * *** * ** ** ** *  **  * ** ** *

Syn8016DRAFT CCACCATTGGGAGCAGCGAAGCGGCCATGCTCGGCGGGATGGCCGCGAAGTGGCGTTGGC409
sync_0455    CCACGATTGGGAGCAGTGAAGCAGCCATGCTTGGCGGGATGGCCGCTAAATGGCGTTGGC346
RS9916_40006 CCACCATCGGCAGCAGCGAAGCCTCAATGCTGGGGGGGATGGCCGCGAAATGGCGGTGGC409
PMT0474      CCACCATTGGTAGCAGTGAGGCCGCCATGCTGGGTGGCTTGGCTGCGAAATGGCGTTGGC418
P9303_18041  CCACCATCGGTAGCAGTGAGGCCGCCATGCTGGGTGGCTTGGCTGCGAAATGGCGTTGGC418
             **** ** ** ***** ** **  * ***** ** **  **** ** ** ***** ****

Syn8016DRAFT GAAAGCGTCGCGAGGCGGCTGGCTTGCCAACAGATAAGCCCAACATGGTGTGTGGCAGCG469
sync_0455    GCAAACGTCGCGAGGCTGCCGGGTTGCCAACAGATAAGCCCAATATGGTGTGTGGAAGTG406
RS9916_40006 GCAAGAAGCGACAGCAGGCAGGCCTGCCCACCGATCAACCCAATATGGTTTGCGGCAGCG469
PMT0474      GTGAACATCGCAAAGCGGCAGGTCAGTCGATCGATCGCCCCAACATGGTTTGCGGCAGTG478
P9303_18041  GTGAACATCGCAAAGCGGCAGGTCAGTCGATCGATCGCCCCAACATGGTTTGCGGCAGTG478
             *  *    **  *    ** **   * * *  ***   ***** ***** ** ** ** *
```

```
Syn8016DRAFT TGCAGATCTGCTGGAAGAAGTTTGCGCGCTATTGGGATATTGAAATGCGTGAATTAGAGA529
sync_0455    TTCAGATCTGCTGGAAGAAGTTTGCGCGTTATTGGGATATTGAAATGCGTGAATTAGAGA466
RS9916_40006 TGCAGATCTGTTGGAAGAAATTTGCCCGCTACTGGGATATCGAGATGCGGGAGCTGGAGA529
PMT0474      TACAAATCTGCTGGACGAAATTTGCCCGCTACTGGGACGTTGAGTTGCGGGAGGTGGAGA538
P9303_18041  TACAAATCTGCTGGACGAAATTTGCCCGCTACTGGGACGTTGAGTTGCGGGAGGTGGAGA538
             * ** ***** **** *** ***** ** ** *****  * **  **** **  * ****

Syn8016DRAFT TGCTTGCTGGTGAATTATGTATCAGTCCTGAGCGTGTTATCGAGGCTGTGGATGAGAACA589
sync_0455    TGCTTACTGGTGAATTGTGCGTCAGCCCTGAGCGAGTTCTTGAGGCTGTGGATGAGAACA526
RS9916_40006 TGCGTCCCGGAGATCTGTGCATCACCCCTGAGCGGGTGCTGGAGGCCGTGGATGAAAACA589
PMT0474      TGACCTCCGGCGAGCTCTGCATGTCTCCAGAACGAATGCTGGAGCAAGTGGATGAGAACA598
P9303_18041  TGACCTCCGGCGAGCTCTGCATGTCTCCAGAACGAATGCTGGAGCAAGTGGATGAGAACA598
             **    * ** **  * **  *    ** ** **  *  * ***   ******** ****

Syn8016DRAFT CGATTTTTGTTGTACCCACGCTTGGGGTGACGTATCACGGCCTTTATGAAGACATTGAGT649
sync_0455    CGATTTTCGTTGTACCCACTCTTGGAGTGACCTATCACGGTCTTTATGAGGATATTGAGT586
RS9916_40006 CCATCTTTGTGGTGCCCACGCTGGGGGTGACTTATCACGGCCTTTACGAGGATGTGGAGG649
PMT0474      CCATCGTTGTGGTACCTACCCTGGGCGTCACTTATCATGGCCTGTATGAAGACGTACAAG658
P9303_18041  CCATCGTTGTGGTGCCTACCCTGGGCGTCACTTATCACGGCCTGTATGAAGACGTACAAG658
             * **  * ** ** ** ** ** ** ** ** ***** ** ** ** ** **  *  *

Syn8016DRAFT CCATCAGCAAGGCTTTGGATGACCTTCAGGCTCGGACGGGCCTTGATGTGCCCATTCACG709
sync_0455    CTATTAGCAAGGCGTTGGATGATCTTCAGGCTCGTACTGGCCTTGATGTGCCGATTCATG646
RS9916_40006 CCATCAGCCGTGCCCTCGACGACTACCAGGCCCGCACCGGCATTGACATTCCGATTCACG709
PMT0474      CCGTCAGTCAGGCCCTCGATGAGCTGCAACAGCGAAAAGGACTCGACATTCCTATCCATG718
P9303_18041  CCATCAGTCAGGCCCTCGATGAGCTGCAACAGCGAAAAGGACTCGACATTCCTATCCATG718
             *  * **    **  * ** **    **    ** *  **  * **  * ** ** ** *

Syn8016DRAFT TGGATGCGGCCAGTGGTGGCTTTCTTGCTCCGTTCTGCGCACCGGATCTCCCCCTGTGGG769
sync_0455    TGGATGCGGCAAGTGGTGGCTTTTTGGCTCCGTTCTGCGCACCGGATCTCCCCCTTTGGG706
RS9916_40006 TCGATGGAGCGAGTGGTGGTTTTCTTGCTCCGTTCTGTGCCCCTGATCTGCCGCCCTGGG769
PMT0474      TGGATGCAGCCAGCGGTGGCTTTCTTGCTCCTTTCTGTGCCCCTGATCTAGCTCCCTGGG778
P9303_18041  TGGATGCAGCCAGCGGTGGCTTTCTTGCTCCTTTCTGTGCCCCTGATCTGGCTCCCTGGG778
             * ****  ** ** ***** *** * ***** ***** ** ** *****  * *  ****

Syn8016DRAFT ACTTTCGCTTGGAACGCGTGAAATCGATTAATGCTTCAGGTCATAAATTTGGTCTGGCAC829
sync_0455    ACTTTCGCTTGGAACGCGTGAAATCGATTAATGCTTCAGGTCATAAGTTTGGGTTGGCGC766
RS9916_40006 ATTTCAGGCTGGAGCGGGTCAAGTCGATTAATGCATCAGGCCACAAGTTCGGTCTTGCCC829
PMT0474      ATTTCCGCTTGCCGCGCGTGAAGTCAATCAACTCCTCTGGCCATAAGTTCGGCTTAGCTC838
P9303_18041  ATTTCCGTTTGCCGCGCGTGAAGTCAATCAACTCCTCTGGCCATAAGTTCGGCTTAGCTC838
             * **  *  **   ** ** ** ** ** **  * ** ** ** ** ** **  * ** *

Syn8016DRAFT CCCTGGGCGTGGGCTGGGTTCTCTGGCGT-AGTCAGGATGATCTGCCCGATGAGCTGGTC888
sync_0455    CCCTTGGTGTGGGCTGGGTTCTCTGGCGC-AGCCAGGAAGATCTGCCTGACGAGCTTGTC825
RS9916_40006 CCTTAGGTGTGGGTTGGGTGATGTGGCGT-AGTCCGGAGGATCTGCCCGATGAGCTGGTG888
PMT0474      CTCTGGGTGTGGGTTGGGTTCTTTGGCGTGAGTCCCG-TGATCTACCGGAAGGATTGGTT897
P9303_18041  CTCTGGGTGTGGGTTGGGTTCTTTGGCGTGAGTCCAG-TGATCTTCCGGAAGGATTGGTT897
             *  * ** ***** *****  * *****  ** *  *  ***** ** ** *   * **

Syn8016DRAFT TTTCACGTGACCTATCTGGGTGGAGACATGCCGACATTCCAGATTAATTTTTCAAGGCCG948
sync_0455    TTCCATGTGACCTATCTGGGTGGTGACATGCCGACATTCCAGATCAATTTTTCAAGACCT885
RS9916_40006 TTTCACGTCAGCTATCTGGGTGGCGACATGCCCACGTTTCAAATCAACTTCTCACGGCCT948
PMT0474      TTCCATGTGAGTTACCTAGGAGGCGATATGCCAACGTTTCAGATCAACTTCTCGCGGCCA957
P9303_18041  TTCCATGTGAGTTACCTAGGAGGCGATATGCCAACGTTTCAGATCAACTTCTCGCGGCCA957
             ** ** ** *  ** ** ** ** ** ***** ** ** ** ** ** ** **  * **
```

```
Syn8016DRAFT GCAGGTCAGGTGATCGCTCAATATCACGAATTTGTGCGCTTAGGTCGAGAGGGCTATCGC1008
sync_0455    GCTGGTCAGGTGATTGCCCAATACCACGAATTTGTGCGTTTGGGTCGAGAGGGTTATCGA 945
RS9916_40006 GCCGGGCAAGTGATTGCGCAGTACCACGAGTTTGTGCGTCTCGGCCGCGAGGGTTACCGG1008
PMT0474      GCGGGGCAGGTGATCTCCCAGTACTACGACTTTGTCCGCCTAGGTCGCGATGGTTATCAA1017
P9303_18041  GCGGGGCAGGTGATCTCCCAGTACTACGACTTTGTCCGCCTAGGTCGCGATGGTTATCAA1017
             ** ** ** *****  * ** **  **** ***** **  * ** ** ** ** ** *

Syn8016DRAFT ATGCTTCACATGGCCAGTCATGCCAATGCGCAGTACTTCGCCGAAAAATTAAGGGAGATG1068
sync_0455    ATGCTCCACATGGCCAGTCATGCCAATGCGCAGTATTTCGCGGAAAAATTACGGGAGATG1005
RS9916_40006 CTCCTGCATCAGGCCAGCCACAGCAATGCGCAATACGTCGCCAAGGCCCTCGGGCAGATG1068
PMT0474      GCCATCCATGGAGCGAGCTATGCCAATGCTCAATATGTTGCTCAAGAACTCAAAAAGCTA1077
P9303_18041  GCCATCCATGGAGCGAGCTATGCCAATGCTCAATATGTTGCTCAAGAACTCAAAAAGCTA1077
                 * **    ** **  *   ****** ** **  * **  *     *     ** *

Syn8016DRAFT GACCTTTTCAAAATCATCCATGACGGTGCTCCCGACCAGGGCATTCCCACCGTGGTTTGG1128
sync_0455    GACCTTTTCAGAATTATCCATGACGGCACCCCTGACAAAGGCATTCCCACTGTGGTTTGG1065
RS9916_40006 GGGCCTTTCCAGCTGATTCACGACGGCGCACCTGAGAAGGGCATACCCACGGTGGTGTGG1128
PMT0474      GGCCCATTTGAGTTGATAAACGATGGCAACCCAGCAGGTGGCATCCCCACGGTGGTATGG1137
P9303_18041  GGCCCATTTGAATTGATACACGATGGCAACCCAGCACGTGGCATCCCCACTGTGGTGTGG1137
             *  *  **     * **  * ** **    ** *     ***** ***** ***** ***

Syn8016DRAFT ACTCTTGATGACAATCCGGATCATGGCTTCAATCTCTATGACTTTGCCGATCGCTTGCGG1188
sync_0455    ACTCTGGATGACAATCCGAAGTATGGATTCAACTTGTATGACTTCGCTGATCGGTTGCGA1125
RS9916_40006 ACGCTCAAGGAGGGGGTGGACCCCGGGTTCAACCTCTATGACCTTGCGGATCGGCTGCGG1188
PMT0474      ACATTGCGAGCCGACCAAGAGCTTGGTTTTAACCTTTACGACCTCTCTGATCGACTGAGA1197
P9303_18041  ACATTGCGAGCCGGCCAAGAGCTTGGTTTCAACCTTTACGACCTCTCTGATCGACTGAGA1197
             **  *    *         *    ** ** **  * ** *** *  * *****  ** *

Syn8016DRAFT ATGCGTGGCTGGCAGGTGCCTGCCTATCCCTTTACGGGAGAACTGGA--ATCAACAGCCT1246
sync_0455    ATGCGGGGTTGGCAGGTGCCTGCCTATCCATTTACGGGTGAACTTGA--ATCAACCGCAT1183
RS9916_40006 ATGCGTGGTTGGCAGGTGCCGGCTTATCCCTTCACCGGCGATCTCGCCCATCA--TGCGT1246
PMT0474      TTACGTGGTTGGCAAGTGCCAGCTTATCCATTCACAGGTGAGCTTGCTCATCAA--GCCT1255
P9303_18041  TTACGTGGTTGGCAAGTGCCAGCTTATCCATTCACAGGTGAGCTTGCTCATCAA--GCCT1255
              * ** ** ***** ***** ** ***** ** ** ** ** ** *   ****   ** *

Syn8016DRAFT TCCAACGAATTTTGGTGAAGCGAGACTTCACTCGCGACATGGCGGACCTGCTTCTGCAAG1306
sync_0455    TCCAGAGGATCTTGGTGAAGCGAGATTTCACTCGCGACATGGCAGACCTTCTCCTGGAAG1243
RS9916_40006 TTCAACGCATCCTGGTGAAGCGCGATTTCACCCGCGAAATGGCCGATCTGCTGCTGGATG1306
PMT0474      TTCAGCGGATCTTGGTAAAACGCGATTTCTCACGTGAAATGGCTGATCTCCTACTTACCG1315
P9303_18041  TTCAGCGGATCTTGGTAAAACGCGATTTCTCACGTGAAATGGCTGATCTCCTACTTACCG1315
             * **  * **  **** ** ** ** *** * ** ** ***** ** ** ** **    *

Syn8016DRAFT ACATCAGGCAAGCCATTGAAC-ATTTTCAAAAGCACCCGATTACGAACAATCTGCTCGCC1365
sync_0455    ACATCAGGCAAGCCATTCAAC-ATTTCCAAAAACATCCGATTACAAGCAATCTGGCCGCC1302
RS9916_40006 ACATCCGG-ACGGCATTGGCCCATTTCCAGAAGCACCCGATCACCAGCAATCTGCAGGCA1365
PMT0474      ACATCCGCAACGCCAT-AACTCATTTCGAGAGTCATCCTGTCAAGATCAGTCTTAACGCT1374
P9303_18041  ACATCCGCAACGCCAT-AACTCATTTCGAGAGTCATCCTGTCAAGATCAGTCTTAACGCT1374
             ***** *  * * ***      ****  * *  ** **  * *  * ** ***    **

Syn8016DRAFT GCAGAGGCGGCGTCTTACAACCACCTC--------------TGA----------------1395
sync_0455    ACAGAGGGGGCGTCTTACAACCACCTC--------------TGA----------------1332
RS9916_40006 TCGGAAGCGGCGTCCTACAACCACCTC--------------TGA----------------1395
PMT0474      AATGAAGCAGCGTCTACTAATCATCTCGGCCGTTCAATGGTTGAATGCCGTGATGCGCAT1434
P9303_18041  ACTGAAGCAGCGTCTACTAATCATCTCGGCCGTTCAATGGTTGAATCCCTTGATGCGCAT1434
                ** *  *****    ** ** ***              ***
```

```
Syn8016DRAFT ------
sync_0455    ------
RS9916_40006 ------
PMT0474      GGATGA 1440
P9303_18041  GGATGA 1440
```

Figure 4.63 Nucleotide sequence alignment of marine cyanobacterial glutamate decarboxylase.

The identical residues in other sequences are indicated by a dash (*).

4.10 Partial characterization of GABA-synthesizing enzyme glutamate decarboxylase (GAD) in *A. halophytica*

4.10.1 Time course of glutamate decarboxylase in *A. halophytica*

A. halophytica cells were grown in the growth medium containing 0.5 M NaCl. Cells at mid log phase were harvested by centrifugation, washed twice, re-suspended with extraction buffer (25 mM Tris-HCl, pH7.6) and sonicated. The crude enzyme in the supernatant fraction was collected and kept at 4 °C for further analysis. The reaction mixture of GAD activity assay consisted of 50 mM Na-phosphate buffer, pH 5.8, 30 mM glutamate, 20 μM pyridoxal 5'-phosphate (PLP) and 0.5 mM Ca^{2+}. For primary screening, GAD activity *in vitro* was determined using spectrophotometric method by the method of Kitaoka and Nakano (1959) [55] with some modification. The activity of glutamate decarboxylase of *Aphanothece* cells was determined at interval time for 60 min as shown in Figure 4.64. The reaction mixture without glutamate was also prepared. The differences of GABA concentration between substrate-contained samples and non-substrate-contained samples were used as GAD activity to discriminate the internal GABA that was already present in the crude enzyme and synthesized GABA by glutamate application. The initial rate of GAD activity was observed within the first 5 min. The specific activity of GAD in *A. halophytica* supernatant was about 0.228 ± 0.011 $\mu mol.min^{-1}.mg^{-1}$ protein.

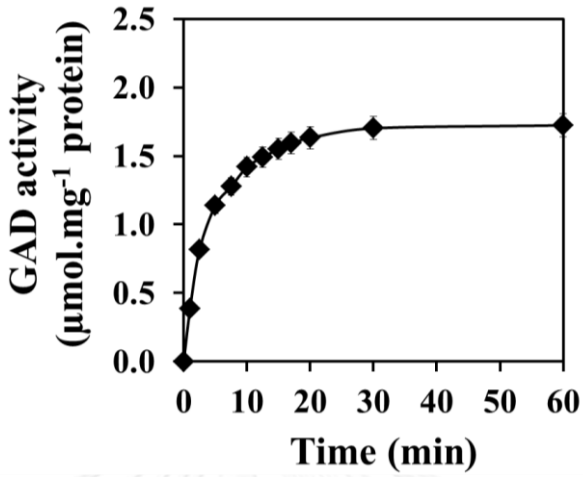

Figure 4.64 **Time course of *A. halophytica* glutamate decarboxylase activity.** GAD activity *in vitro* was determined using spectrophotometric method by the method of Kitaoka and Nakano (1959) [55] with some modification. The data are from three independent experiments with vertical bars representing standard errors of the means, n=3. Error bars are included in the graphs where some may be smaller than the symbols.

4.10.2 Optimization of enzyme activity assay conditions for glutamate decarboxylase activity of *A. halophytica*

4.10.2.1 Optimum extraction buffer and enzyme activity assay buffer

In this experiment, 25 mM Tris-HCl, pH 7.6, 25 mM Na-Phosphate Citrate buffer, pH 7.6 and 25 mM K-Phosphate Citrate buffer, pH 7.6 were used as extraction buffer. 50 mM Na-Phosphate Citrate buffer, pH 5.8 and 50 mM K-Phosphate Citrate buffer, pH 5.8 were used as activity assay buffer. The results showed that the suitable extraction buffer and enzyme activity assay buffer are 25 mM K-Phosphate Citrate buffer, pH 7.6 and 50 mM K-Phosphate Citrate buffer, pH 5.8, respectively as shown in Figure 4.65. Moreover, enzyme stability in 25 mM K-Phosphate Citrate buffer, pH 7.6 was higher than those in other buffers as shown in Table 4.15.

4.15.2.2 Optimum concentration of crude enzyme

The effect of crude enzyme concentration on *A. halophytica* GAD activity was determined. Concentrations of crude enzyme were varied from 0 to 500 µg protein. The value of the enzyme activity containing 50 µg protein of crude enzyme is referred as 100%. The highest GAD activity was obtained when used 100 µg protein of crude enzyme as shown in Figure 4.66. Thus, crude enzyme concentration at 100 µg protein was used for the further experiments.

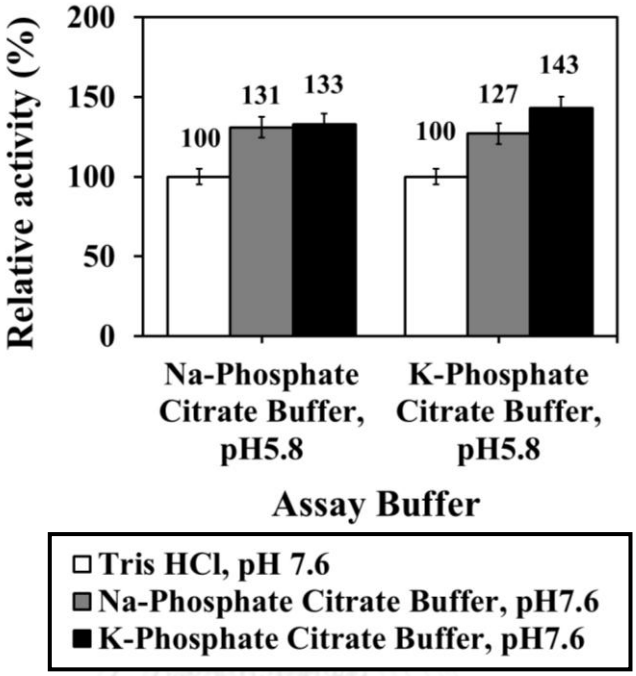

Figure 4.65 Effect of extraction buffer and enzyme activity assay buffer on *A. halophytica* GAD activity.

The value of the enzyme activity in 25 mM Tris-HCl, pH 7.6 in each enzyme activity assay buffer are shown as 100%. The data are from three independent experiments with vertical bars representing standard errors of the means, n=3.

Table 4.15 **Enzyme stability of *A. halophytica* GAD in different extraction buffer.**

Extraction Buffer	% Relative activity		
	Day 0	Day 9	Day 18
25 mM Tris-HCl, pH 7.6,	100 ± 3.23	78.38 ± 3.08	68.69 ± 2.97
25 mM Na-Phosphate Citrate buffer, pH 7.6	100 ± 4.05	86.71 ± 4.34	71.77 ± 3.59
25 mM K-Phosphate Citrate buffer, pH 7.6	100 ± 3.56	95.03 ± 3.24	90.48± 3.52

The percentage of relative activity at day 0 of each extraction buffer is shown as 100%.

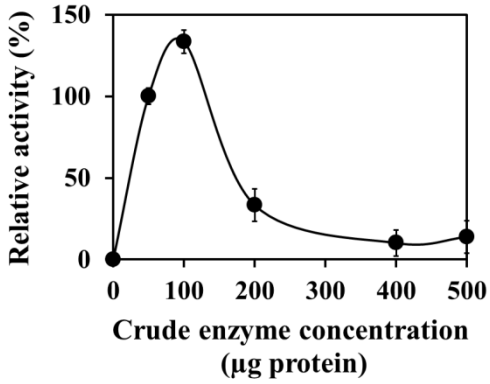

Figure 4.66 **Effect of crude enzyme concentration on *A. halophytica* GAD activity.**

The value of the enzyme activity at 50 µg protein of crude enzyme is shown as 100%. The data are from three independent experiments with vertical bars representing standard errors of the means, n=3. Error bars are included in the graphs where some may be smaller than the symbols.

4.10.2.3 Optimum concentration of glutamate and pyridoxal 5'-phosphate

The effect of concentration of glutamate and pyridoxal 5'-phosphate (PLP) on *A. halophytica* GAD activity was determined. Glutamate and PLP concentrations were varied at 0–50 mM and 0–40 μM, respectively. The highest GAD activity was observed at 30 mM glutamate and 20 μM PLP as shown in Figure 4.67A and Figure 4.67B. Thus, 50 mM glutamate and 20 μM PLP were used for the further experiments.

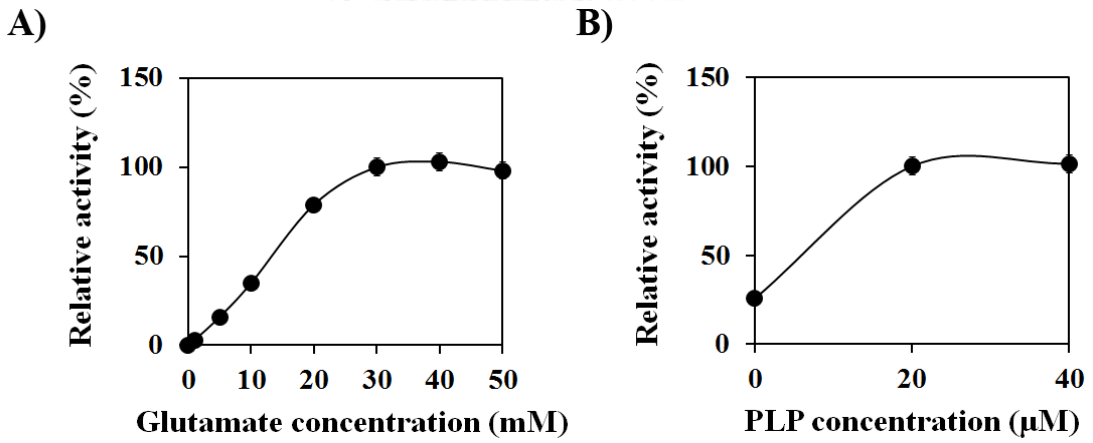

Figure 4.67 **Effect of concentration of glutamate (A) and pyridoxal 5'-phosphate (PLP; B) on *A. halophytica* GAD activity.**

The value of the enzyme activity at 30 mM glutamate (A) and 20 μM PLP (B) are shown as 100%. The data are from three independent experiments with vertical bars representing standard errors of the means, n=3. Error bars are included in the graphs where some may be smaller than the symbols.

4.10.2.4 Optimum $CaCl_2$ concentration

The effect of $CaCl_2$ concentration on *A. halophytica* GAD activity was determined. Concentrations of $CaCl_2$ were varied at 0 – 2 mM. The enzyme performed the highest GAD activity at 1 mM $CaCl_2$ as shown in Figure 4.68. Thus, $CaCl_2$ concentration at 1 mM was used for the further experiment.

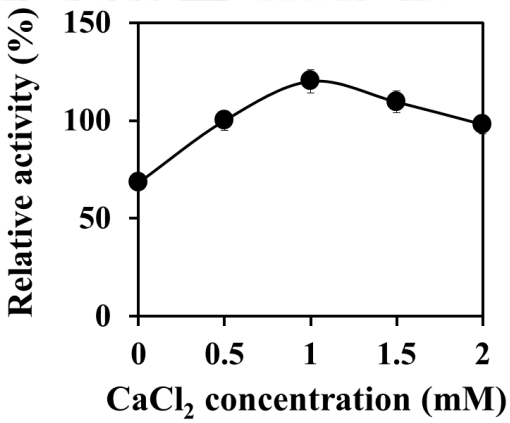

Figure 4.68 Effect of $CaCl_2$ concentration on *A. halophytica* GAD activity. The value of the enzyme activity at 0.5 mM $CaCl_2$ is shown as 100%. The data are from three independent experiments with vertical bars representing standard errors of the means, n=3. Error bars are included in the graphs where some may be smaller than the symbols.

4.10.2.5 Optimum pH and temperature

The optimum pH and temperature of enzymatic reaction were examined. The pH and temperature of enzymatic reaction were varied at pH 4.0–8.0 and at 20–60 °C, respectively. The optimum pH and temperature of enzymatic reaction are at pH 5.8 and at 30 °C, respectively as shown in Figure 4.69. The activity was lost significantly when pH and temperature were higher than pH 6.5 and 50 °C, respectively.

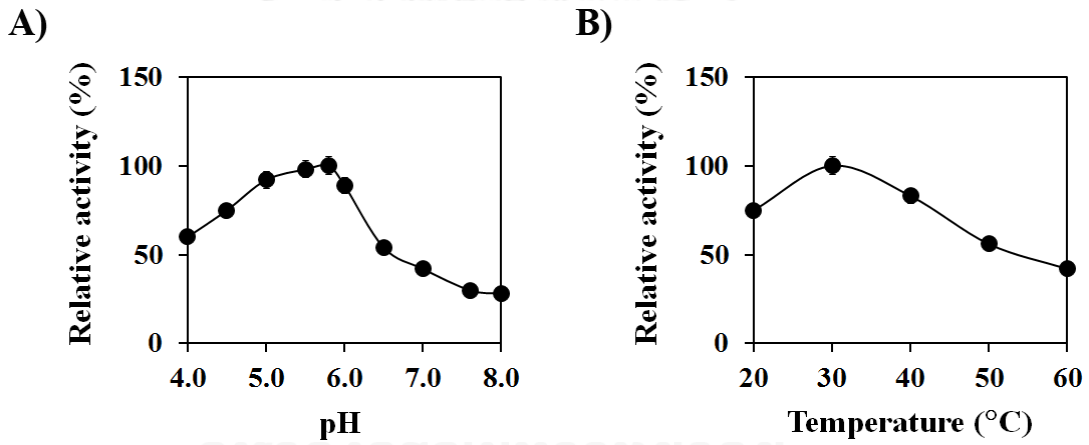

Figure 4.69 Effect of pH (A) and temperature (B) on *A. halophytica* GAD activity.

The value of the enzyme activity at pH 5.8 (A) and 30 °C (B) are shown as 100%. The data are from three independent experiments with vertical bars representing standard errors of the means, n=3. Error bars are included in the graphs where some may be smaller than the symbols.

4.10.2.6 GAD activity under the optimum enzymatic assay conditions

Mid-log phase *A. halophytica* cells were harvested and re-suspended with 25 mM K-Phosphate Citrate buffer, pH7.6 and sonicated. The crude enzyme was collected. The optimum condition of *A. halophytica* glutamate decarboxylase assay reaction was 100 µg protein of crude enzyme, 50 mM K-Phosphate Citrate buffer, pH 5.8, 30 mM glutamate, 20 µM pyridoxal 5'-phosphate (PLP) and 1 mM Ca^{+}. The optimum temperature for enzymatic reaction is at 30 °C. The GAD activity was examined under the optimum enzymatic assay condition. The activity of glutamate decarboxylase was determined at interval time for 60 min. The initial rate of GAD activity was observed within the first 5 min. The specific activity of GAD in *A. halophytica* supernatant was about 0.241 ± 0.012 $\mu mol.min^{-1}.mg^{-1}$ protein as shown in Figure 4.70.

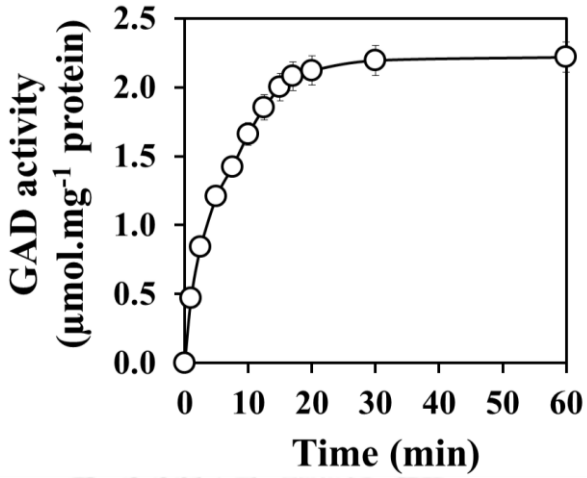

Figure 4.70 Time course of *A. halophytica* glutamate decarboxylase activity under the optimum enzymatic assay conditions.

GAD activity *in vitro* was determined using spectrophotometric method by the method of Kitaoka and Nakano (1959) [55] with some modification. The data are from three independent experiments with vertical bars representing standard errors of the means, n=3. Error bars are included in the graphs where some may be smaller than the symbols.

4.10.3 GAD activity assay using HPLC

To confirm the results of spectrophotometric method, GAD activity assay was performed and analyzed by HPLC**.** The HPLC chromatograms show the 338 nm UV signal that detects the *O*-phthalaldehyde (OPA) derivatized amino acids. The activity of GAD was assayed by measuring the quantity of GABA produced. The reaction mixture without glutamate was also prepared. Norvaline was used as internal standard. HPLC chromatograms of substrate-contained sample and non-substrate-contained sample were shown in Figure 4.71. The retention time of glutamate and GABA are about 2.130–2.183 and 10.599–10.679 min, respectively. Moreover, HPLC chromatogram of substrate-contained samples showed not only peak of GABA but also peaks of glycine, arginine, valine and leucine at 8.303, 9.581, 14.714 and 17.786, respectively (Figure 4.71B). Whereas, HPLC chromatogram of non-substrate-contained samples showed only peak of glutamate (Figure 4.71A). The results suggested that crude enzyme contains many enzymes that can catalyze glutamate to other compounds.

The differences of GABA concentration between substrate-contained samples and non-substrate-contained samples of each time points were used as GAD activity to discriminate the internal GABA that was already present in the crude enzyme and synthesized GABA by glutamate application. The activity of glutamate decarboxylase was determined at interval time for 60 min. The initial rate of GAD activity was observed within the first 2.5 min. The specific activity of GAD was 2.184 ± 0.077 and 5.155 ± 0.232 $nmol.min^{-1}.mg^{-1}$ protein at 0.5 M and 2 M NaCl, respectively as shown in Figure 4.72.

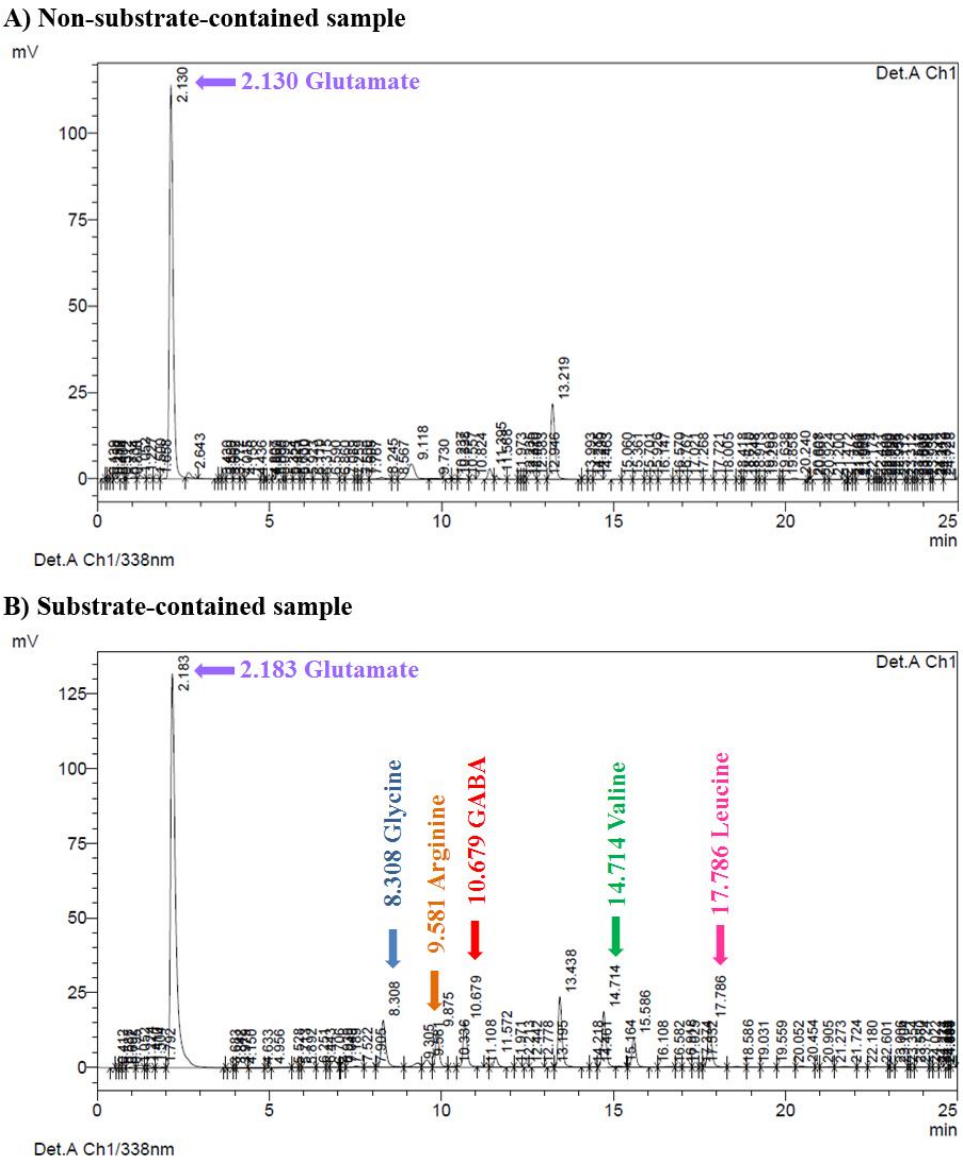

Figure 4.71 **HPLC chromatograms of non-substrate-contained sample (A) and substrate-contained sample (B) for GAD activity assay.**

The enzymatic reaction contains 100 µg protein of crude enzyme, 50 mM K-Phosphate Citrate buffer, pH 5.8, 30 mM glutamate, 20 µM pyridoxal 5'-phosphate (PLP) and 1 mM Ca^{+}. The enzymatic reactions were incubated at 30°C for 2.5 min.

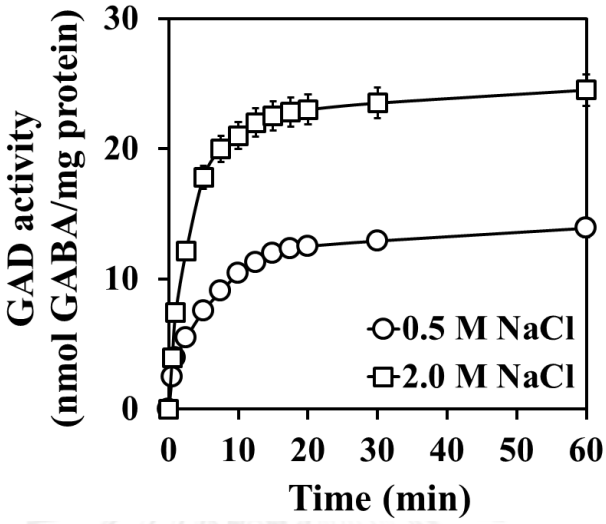

Figure 4.72 **Time course of *A. halophytica* glutamate decarboxylase activity under the optimum enzymatic assay conditions.**

GAD activity *in vitro* was determined using HPLC. The data are from three independent experiments with vertical bars representing standard errors of the means, n=3. Error bars are included in the graphs where some may be smaller than the symbols.

4.10.4 Effect of NaCl concentrations and pH values in adaptation medium on GAD activity in *A. halophytica*

In the present study, cells were pre-cultured under normal growth condition until mid-log phase before subjecting to different NaCl concentrations and to various pH values for 0-4 hours before harvesting cells, crude enzyme extraction and GAD activity assay. The results demonstrated that GAD activity of salt-stressed *Aphanothece* cells slightly increased comparing with normal condition. Whereas, cells without NaCl supplementation slightly decreased exhibited similar patterns comparing with normal condition (Figure 4.73A). Under acidic pH, GAD activity of *Aphanothece* cells was significantly increased comparing with normal condition. In contrast, GAD activity of *Aphanothece* cells under alkaline condition was significantly declined comparing with normal condition (Figure 4.73B).

GAD activity of cells that were adapted in 0.5 M NaCl (normal) or 2.0 M NaCl (salt stress) or with acidic pH (pH 4.0), or with both salt and acid-stress (2.0 M NaCl, pH 4.0) for 4 hrs was compared as shown in Figure 4.74. The enzyme activity of cells that were adapted in 0.5 M NaCl, pH 7.6 was used as control. The enzyme activity of cells that were adapted in 2.0 M NaCl, pH 7.6 and in 0.5 M NaCl, pH 4.0 was slightly increased about 1.12 and 1.28 folds, respectively. Interestingly, the enzyme activity of cells that were adapted in 2.0 M NaCl, pH 4.0 was significantly increased which was about 2.48 folds higher than control.

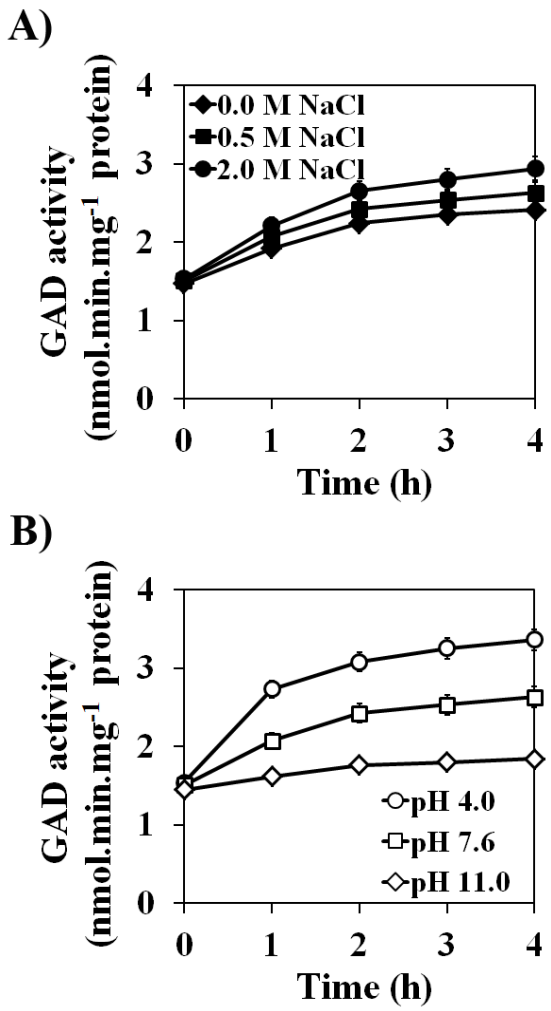

Figure 4.73 GAD activity in *A. halophytica* subjected to different salt concentration (A) and pH (B) for various times.

GAD activity in *A. halophytica* when cells were grown in the medium containing 0.5 M NaCl and adapted in medium containing different concentrations of NaCl for 4 hrs, (B) GAD activity in *A. halophytica* when cells were subjected to different pH conditions. The data are means with vertical bars representing standard errors of the means, n=3.

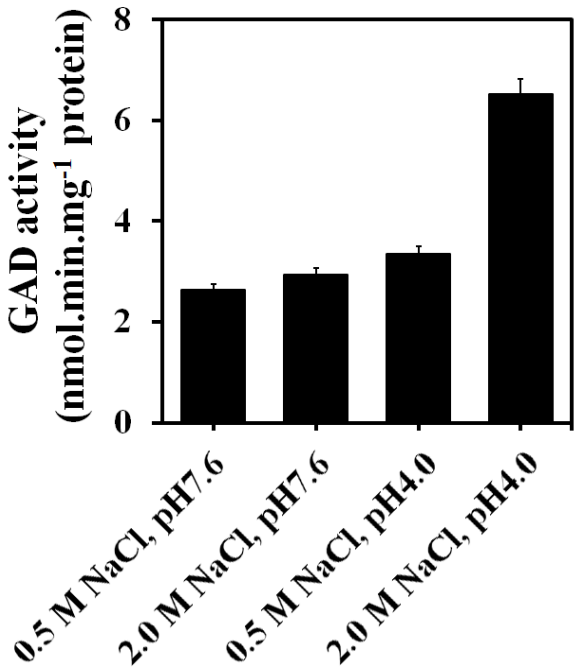

Figure 4.74 **GAD activity of *A. halophytica* under normal and stress conditions.**

Cells were grown in the medium containing 0.5 M NaCl and adapted in 0.5 M NaCl (normal) or 2 M NaCl (salt stress) or with acidic pH (pH 4.0), or combined 2 M NaCl and acidic for 4 hrs before harvesting cells and subjected to crude enzyme extraction and GAD activity assay. The data are means with vertical bars representing standard errors of the means, n=3.

4.11 GABA accumulation in *A. halophytica* and other cyanobacteria

In the present study, six cyanobacterial strains were tested for their ability to accumulate GABA under normal growth condition at mid-log phase cell. Table 4.16 shows that the efficiency of GABA accumulation depends on cyanobacterial strains. However, *A. halophytica* has the capacity to accumulate about 2-4 fold higher GABA than four tested cyanobacterial strains except for *Arthrospira platensis* under the same growth condition.

4.12 Induction of GABA accumulation in *A. halophytica*

4.12.1 GABA accumulation under salt stress in *A. halophytica*

Figure 4.75 shows the growth and GABA contents of *A. halophytica* under normal (0.5 M NaCl) and salt stress (2M NaCl) conditions. Salt stress led to the reduction of growth rate. In contrast, under salt stress condition cells accumulated higher GABA than that under normal condition with maximum content of approximately 2-fold increase being observed after 10 days of growth. It is apparent that the changes in GABA contents in both cells under normal and salt stress conditions occurred during the log phase of growth. The decline of GABA contents to the initial level was observed when cells entered the stationary growth phase.

Table 4.16 Comparison of the ability of GABA accumulation between *A. halophytica* with other cyanobacterial strains.

Cell Morphology	Cyanobacterial strain	Growth condition	GABA content ($nmol.g^{-1}$ DWC)
Unicellular	*Aphanothece halophytica*	Normal growth condition (0.5 M NaCl, pH 7.6)	2.056 ± 0.097
		Salt stress condition (2.0 M NaCl, pH 7.6)	4.12 ± 0.204
	Synechocystis sp. PCC[a] 6803	Normal growth condition	0.931 ± 0.058
	Synechococcus sp. PCC[a] 7942	Normal growth condition	1.367 ± 0.087
Filamentous	*Arthrospira platensis*	Normal growth condition	2.269 ± 0.107
Filamentous heterocystous	*Anabaena siamensis* TISTR[b] 8012	Normal growth condition	0.834 ± 0.029
	Anabaena sp. PCC[a] 7120	Normal growth condition	0.495 ± 0.009

[a] PCC = Pasteur Culture Collection (Paris, France).

[b] TISTR = Thailand Institute of Scientific and Technological Research, (Bangkok, Thailand).

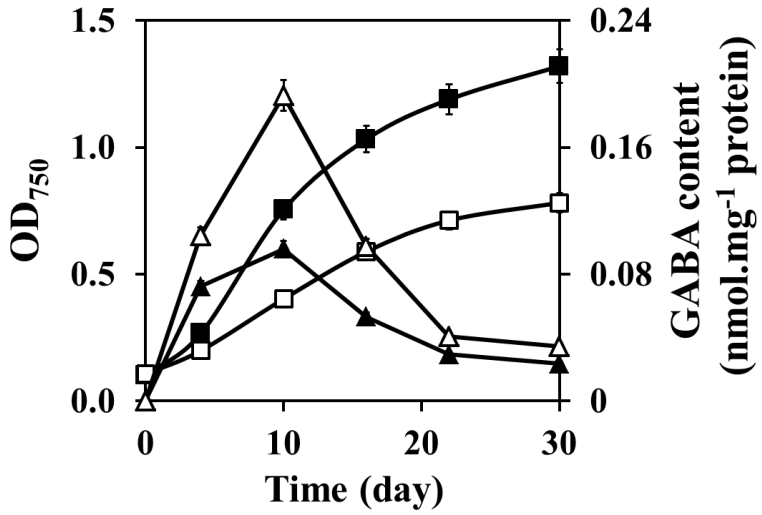

Figure 4.75 Growth and GABA contents of in *A. halophytica* under normal and salt-stress conditions.

Cells were grown for 30 days in the medium containing 0.5 M NaCl (normal) or 2.0 M NaCl (salt stress). At various time intervals, aliquots of the culture were determined for OD_{750} (■, normal; □, salt stress) and GABA content (▲,normal; △, salt stress). The data are means with vertical bars representing standard errors of the means, n=3.

4.12.2 Effect of sugars, cations, and anions on GABA accumulation in *A. halophytica*

To investigate the effect of ions and osmotic agents on GABA accumulation, cells were pre-cultured under growth medium containing 0.5 M NaCl until mid-log phase before subjecting to adaptation medium supplemented with 0.5 M of each reagent and incubation for 4 hrs before determination of GABA accumulation. As shown in Figure 4.76, sugar and alcohol sugar representing an osmotic agent slightly increased GABA accumulation in *A. halophytica.* Na^+ activated the GABA accumulation up to 1.4 fold, whereas Ca^{2+} and NO_3^- slightly activate the GABA accumulation up to 1.1 and 1.09 fold, respectively. In contrast to HCO_3^- and CO_3^{2-} obviously slightly decreased to 0.78 and 0.81 fold, respectively. Other ions had no effect on GABA accumulation under tested condition.

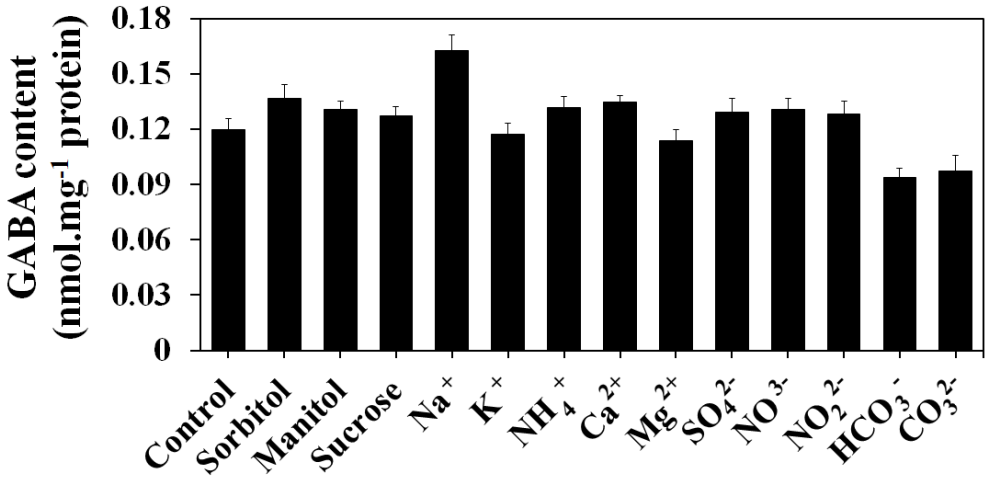

Figure 4.76 **Effect of sugars, cations, and anions on GABA accumulation in *A. halophytica*.**

Cells at mid-log phase were adapted in the assay medium supplemented with 0.5 M of each reagent and incubated for 4 h before determination of GABA accumulation. The data are from three independent experiments with vertical bars representing standard errors of the means, n=3.

4.12.3 Effect of NaCl concentration on GABA accumulation in *A. halophytica*

The effect of NaCl on GABA accumulation was extensively studied. Cells were pre-cultured under growth medium containing 0.5 M NaCl until mid-log phase before subjecting to adaptation medium with various NaCl concentrations from 0-3 M and incubation for 4 hrs. Figure 4.77 shows that GABA accumulation was significantly increased with increasing NaCl concentration up to 2 M resulted in the stimulation of GABA accumulation in *A. halophytica*. The optimal concentration of NaCl for glutamate uptake was 2.0 M with the maximum GABA accumulation at 0.190 ± 0.005 pmol. mg^{-1} protein about 1.6-fold higher than 0.5 M NaCl. When NaCl concentration was higher than 2M, GABA accumulation in *A. halophytica* was declined as shown in Figure 4.77.

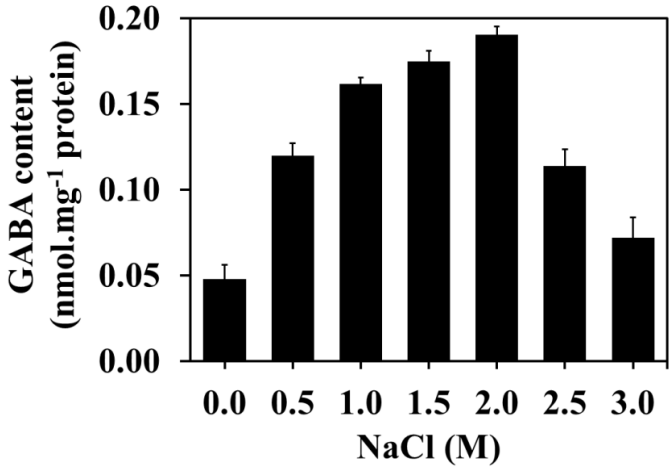

Figure 4.77 **Effect of NaCl concentration on GABA accumulation in *A. halophytica.***

Cells at mid-log phase were subjected to adaptation medium with various NaCl concentrations from 0-3 M and incubated for 4 h before determination of GABA accumulation. The data are from three independent experiments with vertical bars representing standard errors of the means, n=3.

4.12.4 Effect of external pH on GABA accumulation in *A. halophytica*

Changes in pH ranging from 3 to 11 were studied for the effect on GABA accumulation in *A. halophytica.* Figure 4.78 shows that acidic condition with the pH lowered to 4.0 stimulated higher accumulation of GABA than did neutral pH, the highest content of GABA was observed at pH 4.0 with an approximately 1.2–fold increment as compared to that of the normal growth condition at pH 7.6.

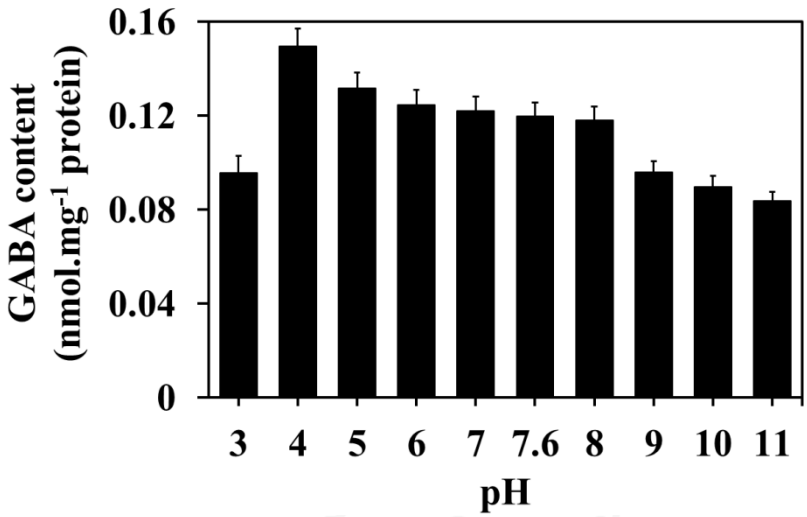

Figure 4.78 Effect of pH on GABA accumulation in *A. halophytica*.

Cells at mid-log phase were subjected to adaptation medium with various pH range of 3–11 and incubated for 4 h before determination of GABA accumulation. The data are from three independent experiments with vertical bars representing standard errors of the means, n=3.

4.12.5 Effect of temperature on GABA accumulation in *A. halophytica*

The effect of temperature on GABA accumulation was examined. Cells were pre-cultured under growth medium containing 0.5 M NaCl until mid-log phase before subjecting to adaptation medium and incubation at 25, 30, 35 and 40°C for 4 hrs. Figure 4.79 shows that the optimum temperature for GABA accumulation is at 30 and 35°C, whereas GABA accumulation was declined at 25 and 40°C.

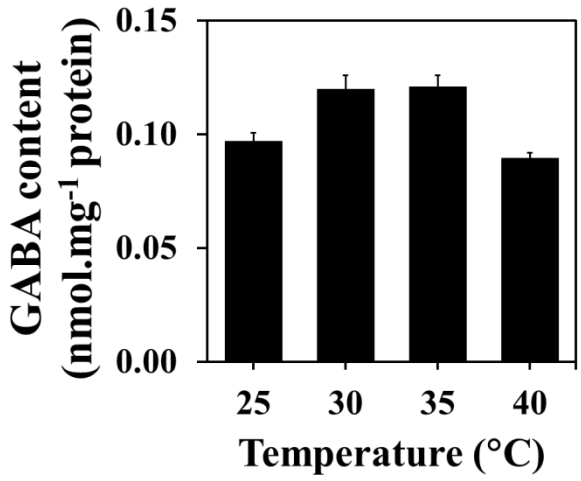

Figure 4.79 **Effect of temperature on GABA accumulation in *A. halophytica*.** Cells at mid-log phase were subjected to adaptation medium and incubated at various temperature from 25-40 °C for 4 h before determination of GABA accumulation. The data are from three independent experiments with vertical bars representing standard errors of the means, n=3.

4.12.6 Effect of pyridoxal-5-phosphate on GABA accumulation

Pyridoxal-5-phosphate (PLP) acts as coenzyme in lots of reactions including GABA-synthesizing enzyme glutamate decarboxylase (GAD). To investigate the effect of PLP on GABA accumulation, cells were pre-cultured under growth medium containing 0.5 M NaCl until mid-log phase before subjecting to adaptation medium supplemented with various PLP concentrations ranging from 0-20 μM and incubation for 4 hrs. Figure 4.80 shows that PLP supplementation could promote higher GABA accumulation. The highest GABA content was observed when supplemented with 10 μM PLP with the maximum GABA accumulation at 0.187 ± 0.009 $nmol.mg^{-1}$ protein. When PLP concentration was higher than 10 μM, GABA accumulation in *A. halophytica* was declined.

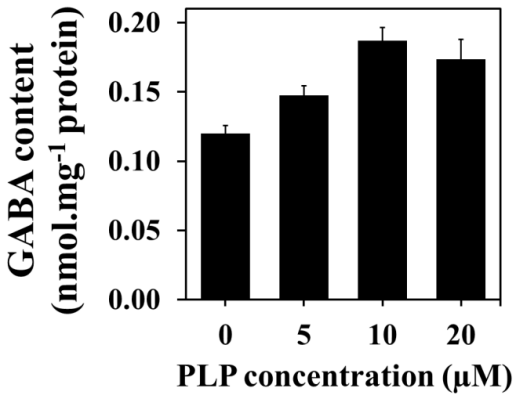

Figure 4.80 **Effect of pyridoxal-5-phosphate (PLP) on GABA accumulation in *A. halophytica*.**

Cells at mid-log phase were subjected to adaptation medium with various PLP concentrations from 0-20 µM and incubated for 4 h before determination of GABA accumulation. The data are from three independent experiments with vertical bars representing standard errors of the means, n=3.

4.12.7 Effect of salt and pH in adaptation medium on GABA accumulation

In the present study, cells at mid log phase were treated under different NaCl concentrations and pH values for various time points (0-4 hours) before determination of GABA by HPLC. The results demonstrated that *A. halophytica* slightly accumulated GABA under normal growth condition (containing 0.5 M NaCl, pH 7.6) up to 4 hrs (Figure 4.81A). Interestingly, cells under high salt stress (2.0 M NaCl) showed significantly enhanced GABA accumulation. In contrast, cells without NaCl supplementation showed no accumulation of GABA as evidenced by a decrease in GABA content within 1 hr of incubation. Under acidic pH stress, GABA accumulation was strongly induced within 1 hr (Figure 4.81B) suggesting that GABA accumulation was a short-term adaptive response to acidic stress.

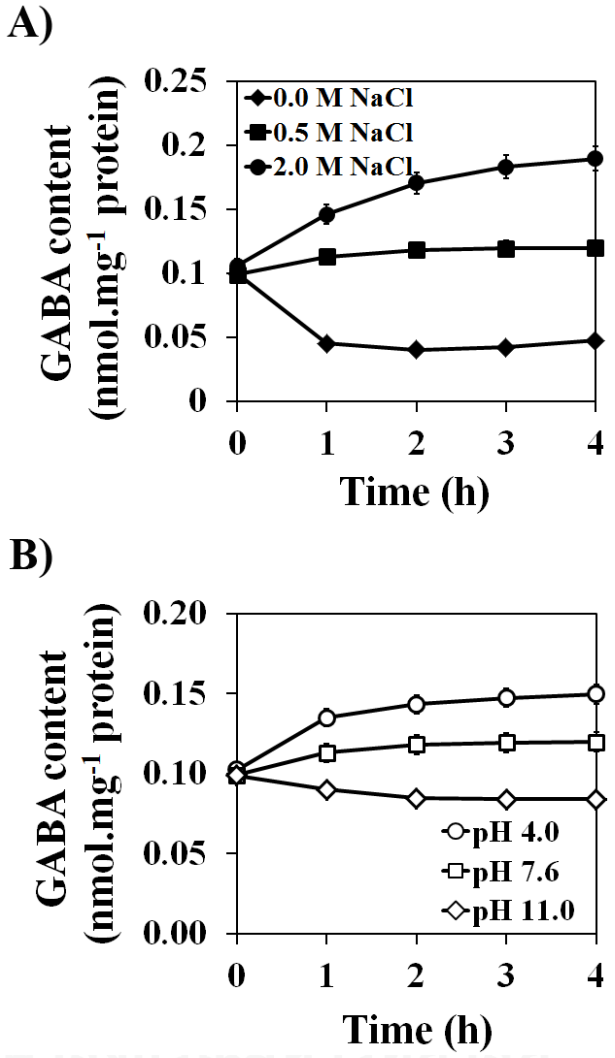

Figure 4.81 GABA accumulation in *A. halophytica* subjected to different salt concentration (A) and pH (B) for various times.

GABA accumulation when cells were grown in the medium containing 0.5 M NaCl and adapted in medium containing different concentrations of NaCl for 4 hrs, (B) GABA accumulation when cells were subjected to different pH conditions. The data are means with vertical bars representing standard errors of the means, n=3.

4.12.8 Effect of glutamate concentration on GABA accumulation of *A. halophytica*

To investigate the effect of glutamate concentration on GABA accumulation, cells were pre-cultured under growth medium containing 0.5 M NaCl until mid-log phase before subjecting to adaptation medium containing various concentrations of exogenous glutamate and incubation for 4 hrs. Figure 4.82A shows that GABA accumulation was significantly increased with increasing glutamate concentration up to 5 mM. When glutamate concentration was higher than 5 mM, GABA accumulation in *A. halophytica* was slightly declined. The maximum GABA accumulation was 0.373 ± 0.011 $nmol.mg^{-1}$ protein when cells stressed under the presence of 5 mM glutamate in medium containing 2 M NaCl and pH at 4.0. As expected, an increased exogenous glutamate under acid stress (pH 4.0) resulted in an increased GABA accumulation in both normal and salt-stressed *A. halophytica* with the highest GABA content observed with 5 mM glutamate in the medium. In contrast, supplementation of glutamate under neutral pH (pH 7.6) hardly affected GABA accumulation in both normal and salt-stressed cells.

The effect of exogenous glutamate on intracellular glutamate content of *Aphanothece halophytica* under different stresses was also determined. Figure 4.82B shows that exogenous glutamate caused no discernible differences in glutamate contents in cell adapted under normal growth condition, or under acid stress or under both salt and acid stresses. The increased glutamate content due

to the increase in exogenous glutamate was detected in cells under salt stress with maximum glutamate content 71.49 ± 3.56 nmol.mg^{-1} protein obtained with 5mM exogenous glutamate.

4.12.9 Effect of amino acid supplementation on GABA accumulation of *A. halophytica*

In the this study, cells were pre-cultured under growth medium containing 0.5 M NaCl until mid-log phase before subjecting to adaptation medium supplemented with 5 mM of each 20 amino acids and incubation for 4 hrs. The results in Figure 4.83 showed that addition of glutamate, glutamine aspartate and alanine slightly increased GABA accumulation under salt stress condition, whereas under acidic pH stress, GABA accumulation was strongly induced. Glutamate is the best amino acid to increase GABA accumulation at all tested condition. In contrast, other amino acids had no effect on GABA accumulation. The results showed that cells treated under high salt and acid stresses supplemented with increasing glutamate concentrations revealed a much higher content of GABA than those under other conditions. The maximum GABA accumulation was observed when cells stressed under the presence of 5M glutamate in medium containing 2 M NaCl and pH at 4.0, which was about 4 folds higher than those of the control.

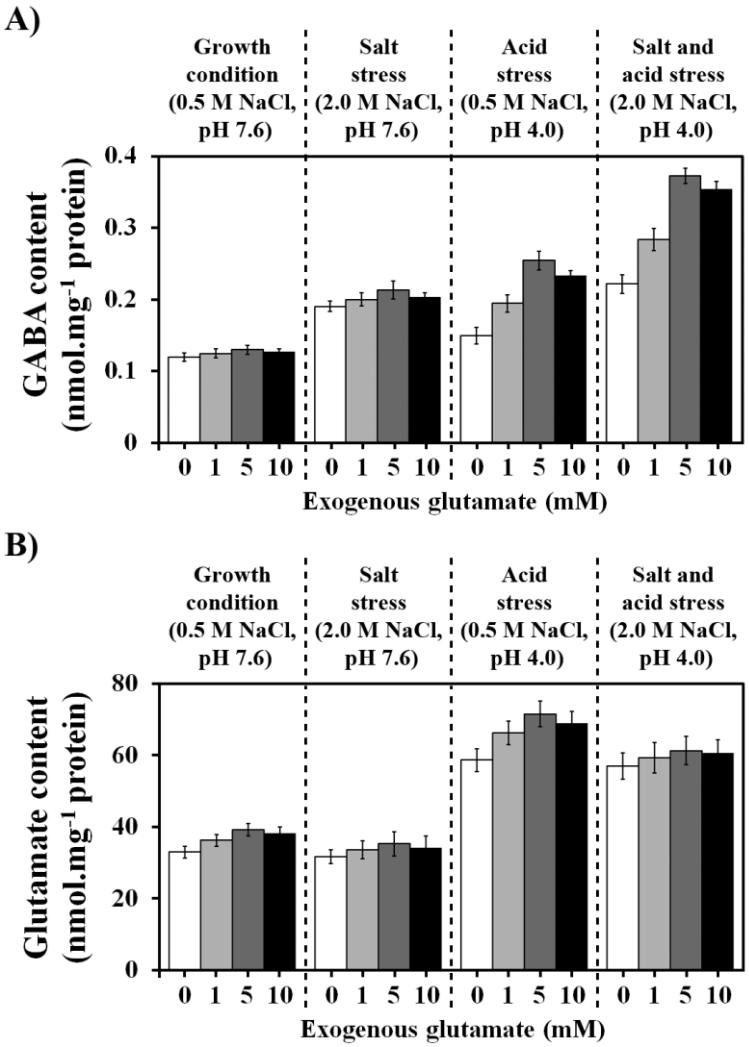

Figure 4.82 GABA (A) and glutamate (B) accumulation of *A. halophytica* under normal and stress conditions with various exogenous glutamate concentrations.

Cells were grown in the medium containing 0.5 M NaCl and adapted in 0.5 M NaCl (normal) or 2 M NaCl (salt stress) or with acidic pH (pH 4.0), or with both 2 M NaCl and acidic with the indicated concentration of exogenous glutamate for 4 hrs. The data are means with vertical bars representing standard errors of the means, n=3.

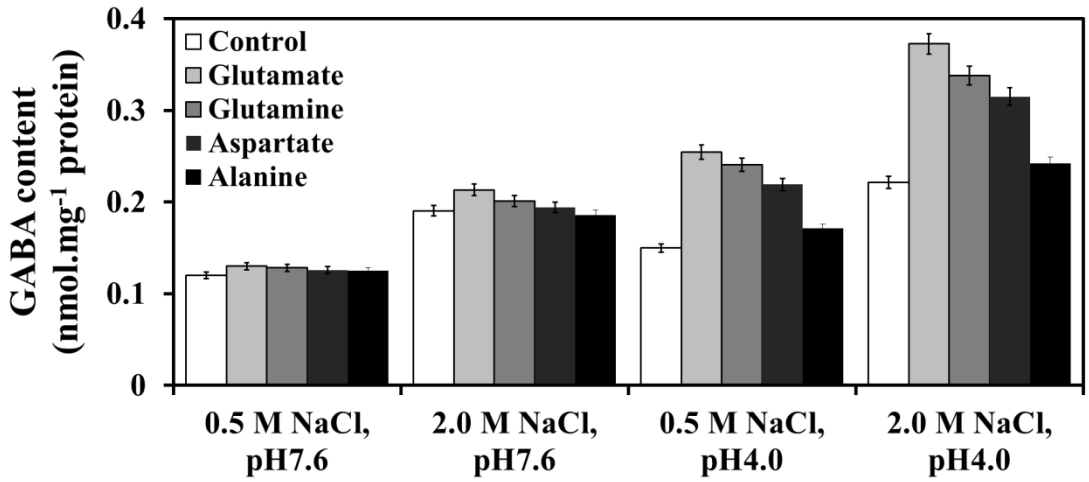

Figure 4.83 **GABA accumulation of *A. halophytica* under normal and stress conditions supplemented with 5 mM of each 20 amino acids.**

Cells were grown in the medium containing 0.5 M NaCl and adapted in 0.5 M NaCl (normal) or 2 M NaCl (salt stress) or with acidic pH (pH 4.0), or with both 2 M NaCl and acidic with 5 mM of each 20 amino acids for 4 hrs. The data are means with vertical bars representing standard errors of the means, n=3.

CHAPTER V
DISCUSSION

The results shown in this study clearly indicated that *Aphanothece halophytica* requires Na^+ for its growth and appears to be a halotolerant cyanobacterium. The growth of *A. halophytica* was significantly increased with increase in NaCl concentration up to 0.5 M as shown in Figure 4.1. The presence of 0.5 M NaCl resulted in the optimum growth and the growth subsequently decreased with increase in NaCl concentration similar to that previous reported by Takabe and colleague (1988) [108]. Under high NaCl concentration, NaCl affected cellular morphology resulting in a larger cell size as shown in Figure 4.2. Corresponding with the result of the salt-mediated alteration of cellular morphology of the fresh water cyanobacterium *Fremella diplosiphon* by Singh and colleagues (2013), they reported that cells of the salt stressed sample were bigger than that of control sample [99].

Growth rate of *A. halophytica* increased upon the increase of glutamate even until 50 mM (Figure 4.4A). The beneficial effects of glutamate on promoting the cell growth were more obvious when cells were grown at high salinity. The growth inhibitory effect of high salinity (2.0 M NaCl) was abolished when 50 mM glutamate was present in the medium (Figure 4.4B). These results indicated that exogenous glutamate enhanced growth of *A. halophytica* and had no toxicity to the *Aphanothece* cell in contrast with the results of *Synechococcus* sp. PCC 7942 and *Synechocystis* sp. PCC 6803. The effect of glutamate supplementation in culture medium on growth of cyanobacteria was reported such as *Anabaena variabilis* [20], *Anabaena cylindrical* PCC 7122 [86], *Anabaena* sp. PCC 7120 [36], *Nostoc* ANTH [98]

and *Nostoc muscorum* [82, 113]. The previous studies suggest that cyanobacterial can utilize glutamate as sole nitrogen source [74]. Glutamate enhances growth of *Anabaena cylindrical* PCC 7122 [86], whereas it is found to be growth inhibitory to *Anabaena variabilis* [20], *Nostoc* ANTH [98] and *Nostoc muscorum* [113]. Glutamate caused the reductions in nitrogenase activity [86] and inhibited heterocyst differentiation [98, 113]. Glutamate toxicity has general been attributed to imbalance of amino acid metabolism.

The uptake of glutamate into *A. halophytica* was characterized. We found that increasing the NaCl concentration apparently raised the glutamate uptake as shown in Figure 4.6. *A. halophytica* cells exhibited a high affinity (K_m 11.76 μM) for glutamate transport which was slightly affected by the increase in salinity (K_m 9.91 μM), whereas the V_{max} values for glutamate uptake under normal and salt stress condition were about 6.67 and 5.20 nmol.min^{-1}.mg^{-1} protein, respectively (Table 4.1). *Anabaena variabilis* have been reported to possess two transport systems for glutamate: high-affinity and low-affinity systems. The high-affinity systems for glutamate glutamate transport have K_m values of 100 μM and maximum rates of 14.4 nmol.min^{-1}.mg of Chl a^{-1}. The low-affinity systems have K_m value of 1.4 mM and maximum rate of 100 nmol.min^{-1}.mg of Chl a^{-1} [20]. On the other hand, whole cells of *Anabaena* sp. PCC 7120 exhibited K_m values of 0.5 mM and maximum rate of 30 nmol.min^{-1}.mg of Chl a^{-1} [35].

Ions and some osmotic agents were tested for the ability to act as a coupling ion for [U-^{14}C] glutamate *transport*. The results showed that sorbitol, mannitol, NH_4^+

and NO_3^- slightly increased the uptake of glutamate. Sucrose, other cations except Na^+ and anions were ineffective in driving [U-^{14}C] glutamate transport as shown in Figure 4.8. These results suggested that glutamate uptake in *A. halophytica* was stimulated by Na^+. Importantly, we found that the changes in NaCl concentration could affect glutamate uptake. The highest uptake of glutamate into *Aphanothece* cells occurred in broad range of 1-2 M NaCl (Figure 4.9). These results suggested that a moderate concentration of NaCl enhanced the glutamate transport. The optimum pH for glutamate transport is at pH 9.0 (Figure 4.10).

Drastic decrease of glutamate activity occurred when 100-fold "cold" glutamate was added in the assay medium under both normal and salt stress conditions. Moreover, aspartate, asparagine and glutamine could significantly inhibit the glutamate uptake of *A halophytica* (Figure 4.11). The addition of NEM and ionophores, namely gramicidin D, valinomycin, and amiloride, significantly diminished glutamate uptake suggesting that Na^+-gradient involves in glutamate transport into *Aphanothece* cells. DCCD, an H^+-ATPase inhibitor, also inhibited glutamate uptake activity. Moreover, glutamate uptake was slightly inhibited by uncoupling agents as well as metabolic inhibitors suggesting the coupling of glutamate uptake was energy dependent (Table 4.3). This suggests that there are at least two glutamate transport systems in *A. halophytica*, energy-dependent and Na^+-stimulated.

In cyanobacteria, amino acid transport systems have been studied in heterocyst-forming *Anabaena* sp. PCC 7120 [81] and a unicellular cyanobacterium *Synechocystis* sp. PCC 6803 [35, 58, 85]. In *Anabaena* sp. PCC 7120 [71, 72], three

amino acid transporters, neutral amino acid transporter system I (N-I), neutral amino acid transporter system II (N-II) and basic amino acid transporter (Bgt), have been reported [81], all of which are ABC type transporters. Glutamate uptake seems to be mediated by N-I and N-II systems. In *Anabaena* sp. PCC 7120, no glutamate specific transporter could be found [80, 81]. By contrast, in the case of *Synechocystis* sp. PCC 6803, four systems of amino acid transporters, neutral amino acid transporter (Nat), basic amino acid transporter (Bgt), monocomponent Na^+-dependent glutamate transporter (GltS) and C_4-dicarboxylate transport family (Gtr), have been reported [85]. Except GltS, three transport systems are ABC type transporters. Studies on the inactivation of these genes suggest that the uptake of glutamate in *Synechocystis* sp. PCC 6803 is mediated by GltS and Gtr although the involvement of still another transporter was suggested [85]. However, molecular properties of GltS have not been explored in any cyanobacteria.

Based on the shot gun sequencing of *A. halophytica*, it was shown that *A. halophytica* contains a unique Na^+-dependent glutamate transporter which exhibited low homology to the only known Na^+-dependent glutamate transporter from *Synechocystis* sp. PCC 6803 6803GltS-S (*slr1145*) and Na^+-dependent glutamate transporter from *E. coli* (EcGltS). The number of amino acid residues of ApGltS was larger than that of 6803GltS-S and EcGltS. In addition, ApGltS contains an extra transmembrane at C-terminal region. The phylogenetic tree of these proteins together with the proton coupled glutamate/aspartate transporters from *E. coli* (EcGltP), *Pyrococcus horikoshi* (PhGlt), and *Bacillus* (BsGltT) is shown in Figure 4.17.

ApGltS belongs to a different group from those of proton coupled glutamate/aspartate transporters, EcGltP, PhGlt, and BsGltT. Among cyanobacteria glutamate transporter proteins, ApGltS exhibited the high homology to some marine cyanobacterial GltS such as *Synechococcus* sp. PCC 7002 (SYNPCC7002), *Synechococcus* sp. WH7803 (SynWH7803), and *Prochlorococcus marinus* MIT9313 (PMT1553), *ThermoSynechococcus elongatus* BP-1 (ThSynBP-1) and *Synechocystis* sp. PCC 6803 (6803GltS-L, *slr0625*). Therefore, cyanobacterial GltS could be classified at least into two groups, one is the group of ApGltS which shows high homology to EcGltS (18% identity) and the other is the group of slr1145 which shows high homology to EcGltS (39% identity) as shown in Figure 4.17.

From the result of BLAST searches, we were able to identify the other Na^+-dependent glutamate transporter from *Synechocystis* sp. PCC 6803 6803GltS-L (*slr0625*). It should be noted that slr0625 was not mentioned previously. In 2001, Quintero and colleagues reported that *6803gltS-S* (*slr1145*) and *6803gtr* (*sll1102-4*) are involved in glutamate uptake in *Synechocystis* sp. PCC 6803. However, the double mutants of these genes reduced the uptake activity only to 40-55% of the wild-type values, suggesting the presence of additional glutamate uptake system. We suggested that 6803GltS-L (*slr0625*) would likely represent an additional glutamate uptake system with a key role for glutamate uptake in *Synechocystis* sp. PCC 6803.

Topological and site-directed mutagenesis studies on Na^+-dependent GltS have been carried out only for EcGltS [28, 107].Therefore, we compared the amino acid sequences of three typical GltS transporters, ApGltS, SYNPCC7002, and EcGltS as

shown in Figure 4.18. We have found that ApGltS and SYNPCC7002 exhibits low similarity to EcGltS but highly conserved especially in the putative pore-loop regions, V_b containing GGHGT motif and X_a containing GVTAT motif. However, ApGltS and SYNPCC7002 contain an extra transmembrane (the eleventh TMS) at C-terminal region (Figure 4.18 and Figure 4.19), suggesting the different localization of C-terminal tail among EcGltS, SYNPCC7002 and ApGltS, i.e. periplasmic space for the former and cytosolic space for the latter two. Hydropathy profiling of ApGltS shown in Figure 4.19 indicated that the transporter folds into two domains, five or six transmembrane segments and a pore-loop each [28, 107].

For attempts to express the ApGltS, *ApgltS* gene was amplified using pair of specific primers. Consequently, *ApgltS* gene was cloned and overexpressed in GltS-deficient *E. coli* mutant ME9107. The recombinant ApGltS which includes histidine tag at N-terminal could be expressed in *E. coli* system. The expression profile was analyzed by SDS-PAGE and immunoblotting using an anti-6xHis to confirm the molecular weight. Molecular mass of ApGltS was ≈ 52 kDa which is slightly higher than the calculated value of 50,976 Da (Figure 4.26). As shown in Figure 4.27, ApGltS could be expressed in *E. coli* ME9107 cells transformed with p*ApgltS* after induction by IPTG with optimal concentration at 1 mM, whereas no detectable band was observed in *E. coli* ME9107 transformed with pTrcHis2C.

Results in figure 4.29 suggested that the *E. coli* ME9107 expressing p*ApgltS* needs Na^+ to stimulate glutamate uptake. ApGltS might be a Na^+/glutamate symporter. This was based on indirect evidence showing the dependency of

glutamate uptake on the presence of Na^+ (Figure 4.29), and the increased uptake was observed upon increasing the concentration of NaCl in the assay medium (Figure 4.32). Kinetics studies revealed that ApGltS is a high affinity glutamate transporter with a K_m value of ≈ 5 μM (Table 4.7). The maximum rate was increased with increasing concentration of NaCl. The presence of 0.5 M NaCl in the assay medium increased V_{max} by about 3-fold. This ApGltS has a much higher affinity towards glutamate than other glutamate transporters from cyanobacteria such as SygltS (slr1145) from *Synechocystis* sp. PCC 6803 (K_m= 49 μM) [72]. Only GltS from *E. coli* B was shown to have similar affinity for glutamate, compared to ApGltS, with a K_m of 3.5 μM. Competition experiments revealed that glutamate, glutamine, aspartate and asparagine inhibited glutamate uptake (Figure 4.34), suggesting their similar structural component recognized by ApGltS. In 1989, Deguchi and colleagues reported that aspartate and asparagine showed no inhibition of glutamate uptake by *E. coli* GltS [25] whereas strong inhibition was observed for *ApGltS*. These results strongly suggest that the ApGltS transports not only glutamate but also aspartate, glutamine, and asparagine.

For the expression of ApGltS in a freshwater cyanobacterium *Synechococcus* sp. PCC 7942, pUC303-pGH-Amp was constructed and transformed into *Synechococcus* sp. PCC 7942**.** 1729 bp of the promoter region and coding region of *ApgltS* gene containing 6xHis-tag fragments was inserted into the *BamH*I sites in the middle of chloramphenicol resistance gene of pUC303-Amp. The glutamate uptake activity of *Synechococcus* sp. PCC 7942 expressing pUC303-pGH-Amp was

observed and compared with *Synechococcus* sp. PCC 7942 expressing pUC303-Amp. Interestingly, the glutamate uptake rate of *ApgltS*-expressing *Synechococcus* sp. PCC 7942 cells increased when NaCl concentration increased but that of control vector transformants did not significantly change in all NaCl concentrations as shown in Figure 4.54. Kinetics studies revealed that K_m values of *Synechococcus* sp. PCC 7942 expressing pUC303-Amp and *Synechococcus* sp. PCC 7942 expressing pUC303-pGH-Amp did not significantly change with K_m values of ≈ 7 μM, whereas the V_{max} values slightly increased upon the increase of NaCl concentrations (Table 4.11).

The presence of glutamate in the growth medium stimulated *A. halophytica* growth under high salinity conditions (Figure 4.4B). Under salt stress, *A. halophytica* had increased levels of the transcript of ApGltS-coding gene, *ApgltS,* (APPENDIX 29) and this would presumably lead to an increase in glutamate taken up by the cells under salt stress with exogenous glutamate. We proposed that the formation of $^{14}CO_2$ liberated from [U-^{14}C]-glutamate (Figure 4.56) is from the activity of 2 main enzymes a) glutamate decarboxylase: [U-^{14}C]-glutamate was directly catabolized to $^{14}CO_2$ and GABA and b) 2-oxoglutarate decarboxylase: First, [U-^{14}C]-glutamate was converted to 2-oxoglutarate, then 2-oxoglutarate was metabolized to $^{14}CO_2$ and succinic semialdehyde using 2-oxoglutarate decarboxylase. The effect of glutamate supplementation in culture medium on the content of cellular ions was shown in Figure 4.57. The increased exogenous glutamate in growth medium resulted in the increased intracellular ammonium ion comparing with the same condition but without glutamate supplementation. We suggested that exogenous glutamate was

taken up into *A. halophytica* cells and *A. halophytica* was able to use glutamate as metabolic fuel and as precursor of GABA. Moreover, extracellular glutamate may act as precursor for the synthesis of other main osmoprotectants such as glycine betaine, glutamate betaine, γ-aminobutyric acid (GABA), arginine and proline etc. As expected, cells under high salinity supplemented with increasing glutamate concentration showed a much higher content of glycine betaine than those under the same condition but without glutamate supplementation (Figure 4.58). Glutamate would likely be converted to glycine, a precursor for glycine betaine synthesis [118], via glyoxylate pathway by means of glutamate/glyoxylate aminotransferase [29].

In present study, we are also interested in enzymes in glutamate metabolic pathway in cyanobacteria. From the database searching, we found 10 groups of enzymes related in glutamate metabolic pathways as shown in Table 4.13. From Figure 4.56, *A. halophytica* could take up [U-^{14}C]-glutamate into the cell and the release of $^{14}CO_2$ from the cells was detected. We proposed that the formation of $^{14}CO_2$ liberated from [U-^{14}C]-glutamate may be from the activity of glutamate decarboxylase. γ-aminobutyric acid (GABA) is a valuable compound of the free amino acid pool mainly synthesized through the proton consuming GAD activity in the cytosol using glutamate as a substrate. Up to now, GABA metabolism in cyanobacteria remains elusive. Herein, we are interested in the GAD activity under various NaCl concentrations and pH values in *A. halophytica.* In preliminary step, GAD activity was monitored using spectrophotometric method. To confirm the results of spectrophotometric method, GAD activity assay was performed and analyzed by

HPLC. The differences of GABA concentration between samples with and without substrate of each time points were used as GAD activity to discriminate the internal GABA that was initially present in the crude enzyme. The result of HPLC chromatograms suggested that that crude enzyme contains many enzymes that can catalyze glutamate to many compounds such as glycine, arginine, valine, leucine and also GABA (Figure 4.71). This data suggested that spectrophotometric method measured the produced total amino acid content and this method was not specific for GABA determination.

GAD activity of mid-log phase *Aphanothece* cells grown in 0.5 M NaCl (normal) or 2 M NaCl (salt stress) was determined. The results suggested that GAD activity of salt-stressed *Aphanothece* cells was higher than that of normal condition about 2.36 folds (Figure 4.72). Next, the effect of different NaCl concentrations and pH values in adaptation medium on GAD activity in *A. halophytica* was observed. Mid-log phase *Aphanothece* cells grown in 0.5 M NaCl, pH 7.6 were transferred to new fresh medium containing 0.0, 0.5 and 2.0 M NaCl (Figure 4.73A) and to new fresh medium at pH 4.0, 7.6 and 11.0 (Figure 4.73B) for 0-4 hours before harvesting cells and subjected to crude enzyme extraction and GAD activity assay. The results demonstrated that GAD activity of salt-stressed *Aphanothece* cells slightly increased when compared to those under the absence and the presence of 0.5 M NaCl (Figure 4.73A). This suggested that under high salt stress GAD activity played little or no role in GABA accumulation. Under acidic pH, GAD activity of *Aphanothece* cells was significantly increased comparing with normal condition. On the other hand, GAD

activity of *Aphanothece* cells under alkaline condition was significantly declined (Figure 4.73B). GAD was likely a major enzyme used for induction of GABA accumulation under acid stress in *A. halophytica*. The accompanying increase of GAD activity which consumes intracellular H^+ under acid stress would raise the intracellular pH towards the favorable neutral pH, thus alleviating the toxic acidification inside the cells. Figure 4.97 showed that GAD activity of *Aphanothece* cells adapted in combined high salt and acidic condition (2.0 M NaCl, pH 4.0) was significantly increased about 3 folds comparing with normal condition (0.5 M NaCl, pH 7.6).

We also made a comparative analysis of GABA content of *A. halophytica* and other five cyanobacterial strains as shown in Table 4.16. *A. halophytica* has the capacity to accumulate about 2-4 fold higher GABA than four tested cyanobacterial strains except for *Arthrospira platensis* under the same growth condition. Moreover, mid-log phase *A. halophytica* cells grown under salt stress condition accumulated GABA with a 2-fold increase (Table 4.16, Figure 4.75). It is apparent that the changes in GABA contents in both cells under normal and salt stress conditions occurred during the log phase of growth. The decline of GABA contents to the initial level was observed when cells entered the stationary growth phase (Figure 4.75). This suggested the operation of active GABA shunt pathway of carbon metabolism in *A. halophytica* during its growth. It is also noted that despite the non-involvement of GABA as osmolyte to combat against salt stress in *A. halophytica*, an increase in GABA content indirectly plays a role in salt stress tolerance of this cyanobacterium.

Effect of sugars and ions on GABA accumulation was also determined. Cells were pre-cultured under growth condition until mid-log phase before subjecting to the medium containing different chemical agents for 4 h. Figure 4.76 shows that Na^+ significantly increased the accumulation of GABA. GABA accumulation was investigated under various external concentrations of NaCl and pH values. Figure 4.77 shows that GABA accumulation was increased about 1.6 folds when the concentration of NaCl was increased from 0.5 M to 2.0 M NaCl. This result is in agreement with previous reports in many plants showing the increased accumulation of GABA with the increase of NaCl concentration. For example, the cultivar seedling roots of soybean showed about an 11 to 17-fold increase of GABA when cells were subjected to 50-150 mM NaCl as compared with a control without supplementation of NaCl [121]. In tomato suspension, an increase of GABA accumulation was observed when cells were treated with 140 mM NaCl [7]. Figure 4.101 shows that acidic pH could promote higher accumulation of GABA than neutral pH. The highest content of GABA was observed at pH 4.0. Interestingly, GABA accumulation was declined under alkaline pH stress despite the fact that alkaline condition can support growth of *A. halophytica* with optimal growth occurring at pH 9.0. Our results of acid-induced GABA accumulation are in line with previous results in *Escherichia coli* where GAD activity was induced upon exposure to acid stress [64]. Moreover, many plant cultivars showed high GAD activity and increased level of GABA in response to cytosolic acidification [102, 103]. In cyanobacteria, there has been no report on the

effect of acid stress on GABA accumulation except for the effect of low pH on cell physiology and survival of *Synechocystis* sp. PCC 6308 [45].

The optimum temperature for GABA accumulation in *A. halophytica* is at 30-35°C (Figure 4.77). Figure 4.78 shows the effect of PLP supplementation in adaptation medium on GABA accumulation in *A. halophytica*. 10 μM PLP in the adaptation medium increased GABA accumulation about 1.5-fold compared to no PLP supplementation. PLP acts as coenzyme in several reactions including GABA-synthesizing enzyme glutamate decarboxylase (GAD).

Next, the effect of different NaCl concentrations and pH values in adaptation medium on GABA accumulation was investigated. The results demonstrated that *A. halophytica* slightly accumulated GABA under normal growth condition (containing 0.5 M NaCl, pH 7.6) up to 4 h (Figure 4.81A). Interestingly, cells under high salt stress (2.0 M NaCl) showed significantly enhanced GABA accumulation. In contrast, cells without NaCl supplementation showed no accumulation of GABA as evidenced by a decrease in GABA content within 1 hr of incubation (Figure 4.81A). Under acidic pH condition, GABA accumulation was strongly induced within 1 hr (Figure 4.81B) suggesting that GABA accumulation was a short-term adaptive response to acidic stress. The cyanobacterium *Synechocystis* sp. PCC 6308 stressed under acid pH medium had the ability to increase pH of the medium from 4 to 6 within 5 min, where pH 6 or above is a preferable pH for cell growth after pH stress [45]. The increased GABA accumulation in *A. halophytica* is a beneficial adaptive response to acid stress. The accompanying increase of GAD activity which consumes intracellular

H^+ under acid stress would raise the intracellular pH towards the favorable neutral pH, thus alleviating the toxic acidification inside the cells.

We showed that *A. halophytica* contained Na^+-dependent glutamate transporter (ApGltS) that functioned as glutamate transporter [8]. Thus, the presence of glutamate in medium may induce higher GABA accumulation in *A. halophytica*. As expected, an increased exogenous glutamate resulted in an increased GABA accumulation when cells were under either acid stress (0.5 M NaCl, pH 4.0) or both acid and salt-stress (2.0 M NaCl, pH 4.0) as shown in Figure 4.82A. Under the latter condition, *A. halophytica* accumulated the highest GABA content when 5 mM glutamate was present in the medium. Supplemented glutamate after being taken up by the cells is unlikely to undergo the usual conversion to 2-oxoglutarate, an intermediate of the TCA cycle, by the action of a reversible alanine aminotransferase. This is supported by the fact that cyanobacteria lack the 2-oxoglutarate dehydrogenase activity [105] and this necessitates the operation of GABA shunt pathway comprising GAD and GABA transaminase (GABA-T) as well as the newly discovered succinic semialdehyde dehydrogenase (SSDH) [125] reactions resulting in the formation of succinate which then joins the TCA cycle. The accumulated 2-oxoglutarate would rather enhance the formation of glutamate and this would further increase GABA content by the GAD activity presuming that both GABA-T and SSDH were less active under acidic pH 4.0. In contrast, supplementation of glutamate at a slightly alkaline pH of 7.6 hardly affected GABA accumulation in both normal and salt-stressed cells (Figure 4.82A). This suggested that under this condition the

GABA formed by GAD activity was further processed by GABA-T and SSDH to yield succinate which then entered the usual TCA cycle.

Previously we showed that the presence of high concentration of glutamate up to 50 mM in high salt medium stimulated the growth of *A. halophytica* and the presence of glutamate in the medium resulted in a significant increase of intracellular glycine betaine [8]. This suggested that exogenous glutamate under high salinity condition is used for supporting cell growth or for conversion to glycine, which is a precursor for glycine betaine synthesis. Interestingly, cells under both high salt and acid stress supplemented with increasing glutamate concentrations revealed a much higher content of GABA than those under other conditions. The maximum GABA accumulation was about 0.4 $nmol.mg^{-1}$ protein, a 3-fold increase, when cells were subjected to both salt and acid stresses in the presence of 5 mM glutamate compared to that under normal growth condition with no glutamate supplementation (Figure 4.82A). The effect of exogenous glutamate on intracellular glutamate content of *A. halophytica* under different stresses was also determined. Figure 4.82B shows that exogenous glutamate caused no discernible differences in glutamate contents in cells adapted under normal growth condition, or under salt stress or under both salt and acid stress. The increased intracellular glutamate content due to exogenous glutamate was seen in cells exposed to acid stress in the presence of 5 mM glutamate with maximum glutamate content ≈72 $nmol.mg^{-1}$ protein.

CHAPTER VI
CONCLUSIONS

The knowledge gained from this study can be summarized as following:

1. *Aphanothece halophytica* requires Na^+ for its growth.
2. The addition of glutamate, proline and glycine enhanced growth of *A. halophytica* under salt stress condition. The best amino acid is glutamate. The beneficial effect of glutamate on promoting the cell growth was more obvious when cells were grown at high salinity.
3. Exogenous glutamate enhanced growth of *A. halophytica* and had no toxicity to the *Aphanothece* cell at all tested glutamate concentration, whereas the increase of exogenous glutamate concentration resulted in higher retardation on growth of *Synechococcus* sp. PCC 7942 and *Synechocystis* sp. PCC 6803.
4. Exogenous glutamate was taken up into *Aphanothece* cells via the activity of glutamate transporter. The increasing NaCl concentration in assay medium significantly increased the glutamate uptake in *A. halophytica*
5. The effect of inhibitors on glutamate uptake activity in *A. halophytica* suggested that there are at least 2 glutamate transport systems in *A. halophytica*, Na^+-stimulated and energy-dependent.
6. Results of uptake experiment suggested that the main transport system for glutamate in *A. halophytica* is mediated by Na^+-dependent glutamate transporter.
7. Based on the shot gun sequencing of *A. halophytica*, the *ApgltS* gene encoded 476 amino acid residues of Na^+-dependent glutamate transporter

(ApGltS) contained 11 transmembrane segments. The deduced amino acid sequence of ApGltS exhibits low homology to GltS from *Synechocystis* sp. PCC 6803 and *E. coli* but highly conserved especially in the putative pore-loop regions, V_b containing GGHGT motif and X_a containing GVTAT motif.

8. The expression of ApGltS in *ApgltS*-expressing *E. coli* ME9107 and *Synechococcus* sp. PCC 7942 cells showed that the glutamate uptake rate of *ApgltS*-expressing cells increased when NaCl concentration increased.
9. Kinetics studies revealed that ApGltS is a high affinity glutamate transporter and the maximum velocity was significantly increased with increasing NaCl concentration.
10. *A. halophytica* contains Na^+/glutamate symporter (ApGltS) that functioned as glutamate transporter. ApGltS stimulates growth and confers salt stress tolerance on *A. halophytica* thriving in high salinity environments with sufficient available glutamate.
11. The exogenous glutamate which was taken up to the *A. halophytica* cells can be used as metabolic fuel and as precursor of other compounds such as glycine betaine, γ-aminobutyric acid (GABA), arginine, valine and leucine as shown in Figure 6.1.

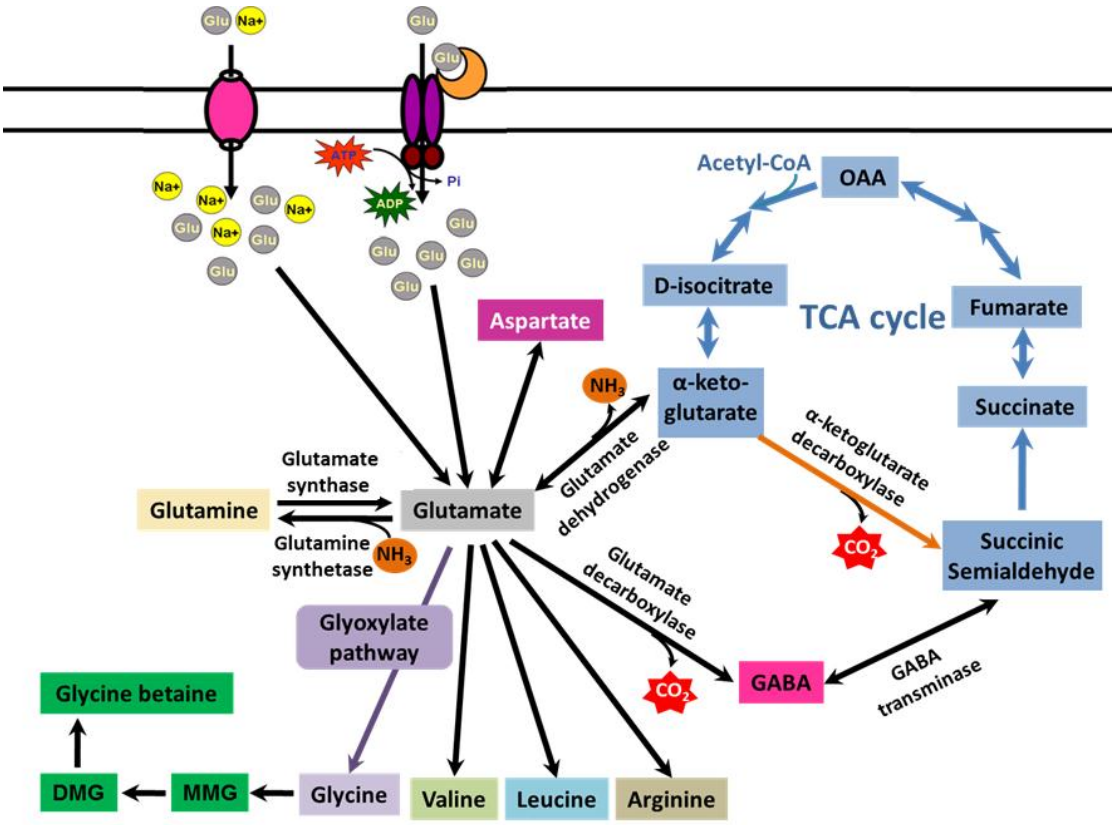

Figure 6.1 Glutamate transport system and proposed enzymatic pathways involved in the metabolism of glutamate in *A. halophytica.* (Modified from Bouché and Fromm 2004).

REFERENCES

1. Apte, S.K., Reddy, B.R., Thomas, J. (1987) Relationship between Sodium Influx and Salt Tolerance of Nitrogen-Fixing Cyanobacteria. Appl Environ Microbiol, **53**(8): pp. 1934-1939.
2. Arriza, J.L., Eliasof, S., Kavanaugh, M.P., Amara, S.G. (1997) Excitatory amino acid transporter 5, a retinal glutamate transporter coupled to a chloride conductance. Proceedings of the National Academy of Sciences, **94**(8): pp. 4155-4160.
3. Arriza, J.L., Kavanaugh, M.P., Fairman, W.A., Wu, Y.N., Murdoch, G.H., North, R.A., Amara, S.G. (1993) Cloning and expression of a human neutral amino acid transporter with structural similarity to the glutamate transporter gene family. Journal of Biological Chemistry, **268**(21): pp. 15329-15332.
4. Beudeker, R.F., Tabita, F.R. (1983) Control of photorespiratory glycolate metabolism in an oxygen-resistant mutant of Chlorella sorokiniana. J Bacteriol, **155**(2): pp. 650-656.
5. Boggess, S.F., Paleg, L.G., Aspinall, D. (1975) Delta-Pyrroline-5-carboxylic Acid Dehydrogenase in Barley, a Proline-accumulating Species. Plant Physiol, **56**(2): pp. 259-262.
6. Bohnert, H.J., Nelson, D.E., Jensen, R.G. (1995) Adaptations to Environmental Stresses. Plant Cell, **7**(7): pp. 1099-1111.
7. Bolarín, M.C., Santa-Cruz, A., Cayuela, E., Pérez-Alfocea, F. (1995) Short-term Solute Changes in Leaves and Roots of Cultivated and Wild Tomato Seedlings Under Salinity. J Plant Physiol, **147**(3–4): pp. 463-468.
8. Boonburapong, B., Laloknam, S., Yamada, N., Incharoensakdi, A., Takabe, T. (2012) Sodium-Dependent Uptake of Glutamate by Novel ApGltS Enhanced Growth under Salt Stress of Halotolerant Cyanobacterium *Aphanothece halophytica*. Biosci Biotechnol Biochem, **76**(9): pp. 1702-1707.
9. Booth, I.R., Higgins, C.F. (1990) Enteric bacteria and osmotic stress: Intracellular potassium glutamate as a secondary signal of osmotic stress? FEMS Microbiol Lett, **75**(2-3): pp. 239-246.
10. Bouche, N., Fromm, H. (2004) GABA in plants: just a metabolite? Trends Plant Sci, **9**(3): pp. 110-115.
11. Bown, A.W., Shelp, B.J. (1997) The Metabolism and Functions of [gamma]-Aminobutyric Acid. Plant Physiol, **115**(1): pp. 1-5.

12. Bradford, M.M. (1976) A rapid and sensitive method for the quantitation of microgram quantities of protein utilizing the principle of protein-dye binding. Anal Biochem, **72**: pp. 248-254.
13. Breitkreuz, K.E., Shelp, B.J., Fischer, W.N., Schwacke, R., Rentsch, D. (1999) Identification and characterization of GABA, proline and quaternary ammonium compound transporters from Arabidopsis thaliana. FEBS Letters, **450**(3): pp. 280-284.
14. Brock, T.D. (1976) Halophilic-blue-green algae. Arch Microbiol, **107**(1): pp. 109-111.
15. Brosnan, J.T. (2000) Glutamate, at the interface between amino acid and carbohydrate metabolism. J Nutr, **130**(4S Suppl): pp. 988S-990S.
16. Carmichael, W.W. (1992) Cyanobacteria secondary metabolites--the cyanotoxins. J Appl Bacteriol, **72**(6): pp. 445-459.
17. Casadaban, M.J., Chou, J., Cohen, S.N. (1980) In vitro gene fusions that join an enzymatically active beta-galactosidase segment to amino-terminal fragments of exogenous proteins: *Escherichia coli* plasmid vectors for the detection and cloning of translational initiation signals. J Bacteriol, **143**(2): pp. 971-980.
18. Caumette, P., Matheron, R., Raymond, N., Relexans, J.C. (1994) Microbial mats in the hypersaline ponds of Mediterranean salterns (Salins-de-Giraud, France). FEMS Microbiology Ecology, **13**(4): pp. 273-286.
19. Cayley, S., Lewis, B.A., Guttman, H.J., Record, M.T., Jr. (1991) Characterization of the cytoplasm of *Escherichia coli* K-12 as a function of external osmolarity. Implications for protein-DNA interactions in vivo. J Mol Biol, **222**(2): pp. 281-300.
20. Chapman, J.S., Meeks, J.C. (1983) Glutamine and glutamate transport by Anabaena variabilis. J Bacteriol, **156**(1): pp. 122-129.
21. Chiu, J., DeSalle, R., Lam, H.M., Meisel, L., Coruzzi, G. (1999) Molecular evolution of glutamate receptors: a primitive signaling mechanism that existed before plants and animals diverged. Mol Biol Evol, **16**(6): pp. 826-838.
22. Christensen, H.N., Greene, A.A., Kakuda, D.K., MacLeod, C.L. (1994) Special transport and neurological significance of two amino acids in a configuration conventionally designated as D. J Exp Biol, **196**: pp. 297-305.
23. Codd, G.A., Stewart, W.D. (1973) Pathways of glycollate metabolism in the blue-green alga Anabaena cylindrica. Arch Mikrobiol, **94**(1): pp. 11-28.

24. Cogne, G., Gros, J.B., Dussap, C.G. (2003) Identification of a metabolic network structure representative of Arthrospira (spirulina) platensis metabolism. Biotechnol Bioeng, **84**(6): pp. 667-676.
25. Deguchi, Y., Yamato, I., Anraku, Y. (1989) Molecular cloning of gltS and gltP, which encode glutamate carriers of *Escherichia coli* B. J Bacteriol, **171**(3): pp. 1314-1319.
26. Deguchi, Y., Yamato, I., Anraku, Y. (1990) Nucleotide sequence of gltS, the Na+/glutamate symport carrier gene of *Escherichia coli* B. J Biol Chem, **265**(35): pp. 21704-21708.
27. Dimroth, P. (1987) Sodium ion transport decarboxylases and other aspects of sodium ion cycling in bacteria. Microbiol Rev, **51**(3): pp. 320-340.
28. Dobrowolski, A., Sobczak-Elbourne, I., Lolkema, J.S. (2007) Membrane topology prediction by hydropathy profile alignment: membrane topology of the Na(+)-glutamate transporter GltS. Biochemistry, **46**(9): pp. 2326-2332.
29. Eisenhut, M., Ruth, W., Haimovich, M., Bauwe, H., Kaplan, A., Hagemann, M. (2008) The photorespiratory glycolate metabolism is essential for cyanobacteria and might have been conveyed endosymbiontically to plants. Proceedings of the National Academy of Sciences, **105**(44): pp. 17199-17204.
30. Eliasof, S., Arriza, J.L., Leighton, B.H., Kavanaugh, M.P., Amara, S.G. (1998) Excitatory amino acid transporters of the salamander retina: identification, localization, and function. J Neurosci, **18**(2): pp. 698-712.
31. Engelke, T., Jording, D., Kapp, D., Pühler, A. (1989) Identification and sequence analysis of the Rhizobium meliloti dctA gene encoding the C4-dicarboxylate carrier. J Bacteriol, **171**(10): pp. 5551-5560.
32. Fernandes, T.A., Iyer, V., Apte, S.K. (1993) Differential responses of nitrogen-fixing cyanobacteria to salinity and osmotic stresses. Appl Environ Microbiol, **59**(3): pp. 899-904.
33. Fish, S.A., Codd, G.A. (1994) Bioactive compound production by thermophilic and thermotolerant cyanobacteria (blue-green algae). World J Microbiol Biotechnol, **10**(3): pp. 338-341.
34. Flores, E., Herrero, A. (1994) Assimilatory Nitrogen Metabolism and Its Regulation. In: The Molecular Biology of Cyanobacteria, D. Bryant, Editor., Springer Netherlands. pp. 487-517.
35. Flores, E., Muro-Pastor, A. (1990) Mutational and kinetic analysis of basic amino acid transport in the cyanobacterium *Synechocystis* sp. PCC 6803. Arch Microbiol, **154**(6): pp. 521-527.

36. Flores, E., Muro-Pastor, M.I. (1988) Uptake of glutamine and glutamate by the dinitrogen-fixing cyanobacterium Anabaena sp. PCC7120. FEMS Microbiol Lett, **56**(2): pp. 127-130.
37. Forde, B.G. (2013) Glutamate signalling in roots. Journal of Experimental Botany.
38. Forde, B.G., Lea, P.J. (2007) Glutamate in plants: metabolism, regulation, and signalling. Journal of Experimental Botany, **58**(9): pp. 2339-2358.
39. Frank, L., Hopkins, I. (1969) Sodium-stimulated transport of glutamate in *Escherichia coli.* J Bacteriol, **100**(1): pp. 329-336.
40. Fulda, S., Huckauf, J., Schoor, A., Hagemann, M. (1999) Analysis of Stress Responses in the Cyanobacterial Strains *Synechococcus* sp. PCC 7942, *Synechocystis* sp. PCC 6803, and *Synechococcus* sp. PCC 7418: Osmolyte Accumulation and Stress Protein Synthesis. Journal of Plant Physiology, **154**(2): pp. 240-249.
41. Goude, R., Renaud, S., Bonnassie, S., Bernard, T., Blanco, C. (2004) Glutamine, glutamate, and alpha-glucosylglycerate are the major osmotic solutes accumulated by Erwinia chrysanthemi strain 3937. Appl Environ Microbiol, **70**(11): pp. 6535-6541.
42. Halpern, Y.S., Barash, H., Dover, S., Druck, K. (1973) Sodium and potassium requirements for active transport of glutamate by *Escherichia coli* K-12. J Bacteriol, **114**(1): pp. 53-58.
43. Halpern, Y.S., Barash, H., Druck, K. (1973) Glutamate transport in *Escherichia coli* K-12: nonidentity of carriers mediating entry and exit. J Bacteriol, **113**(1): pp. 51-57.
44. Herrero, A., Flores, E. (1990) Transport of basic amino acids by the dinitrogen-fixing cyanobacterium Anabaena PCC 7120. J Biol Chem, **265**(7): pp. 3931-3935.
45. Huang, J.J., Kolodny, N.H., Redfearn, J.T., Allen, M.M. (2002) The acid stress response of the cyanobacterium *Synechocystis*sp. strain PCC 6308. Arch Microbiol, **177**(6): pp. 486-493.
46. Incharoensakdi, A., Wutipraditkul, N. (1999) Accumulation of glycinebetaine and its synthesis from radioactive precursors under salt-stress in the cyanobacterium *Aphanothece halophytica.* Journal of Applied Phycology, **11**(6): pp. 515-523.
47. James, R.A., Blake, C., Byrt, C.S., Munns, R. (2011) Major genes for Na+ exclusion, Nax1 and Nax2 (wheat HKT1;4 and HKT1;5), decrease Na+

accumulation in bread wheat leaves under saline and waterlogged conditions. J Exp Bot, **62**(8): pp. 2939-2947.

48. Jay, D.G., David, R.V. (2006) Potassium glutamate as a transcriptional inhibitor during bacterial osmoregulation. EMBO J, **25**(7): pp. 1515-1521.
49. Jiang, B., Fu, Y., Zhang, T. (2010) Gamma-Aminobutyric Acid. In: Bioactive Proteins and Peptides as Functional Foods and Nutraceuticals. Wiley-Blackwell. pp. 121-133.
50. Joset, F., Jeanjean, R., Hagemann, M. (1996) Dynamics of the response of cyanobacteria to salt stress: Deciphering the molecular events. Physiologia Plantarum, **96**(4): pp. 738-744.
51. Kaneko, T., Sato, S., Kotani, H., Tanaka, A., Asamizu, E., Nakamura, Y., Miyajima, N., Hirosawa, M., Sugiura, M., Sasamoto, S., Kimura, T., Hosouchi, T., Matsuno, A., Muraki, A., Nakazaki, N., Naruo, K., Okumura, S., Shimpo, S., Takeuchi, C., Wada, T., Watanabe, A., Yamada, M., Yasuda, M., Tabata, S. (1996) Sequence analysis of the genome of the unicellular cyanobacterium *Synechocystis* sp. strain PCC6803. II. Sequence determination of the entire genome and assignment of potential protein-coding regions. DNA Res, **3**(3): pp. 109-136.
52. Kanner, B.I., Sharon, I. (1978) Active transport of L-glutamate by membrane vesicles isolated from rat brain. Biochemistry, **17**(19): pp. 3949-3953.
53. Kao, O.H., Berns, D.S., Town, W.R. (1973) The characterization of C-phycocyanin from an extremely halo-tolerant blue-green alga, Coccochloris elabens. Biochem J, **131**(1): pp. 39-50.
54. Kempf, B., Bremer, E. (1998) Uptake and synthesis of compatible solutes as microbial stress responses to high-osmolality environments. Arch Microbiol, **170**(5): pp. 319-330.
55. Kitaoka, S., Nakano, Y. (1969) Colorimetric determination of omega-amino acids. J Biochem, **66**(1): pp. 87-94.
56. Knoop, H., Gründel, M., Zilliges, Y., Lehmann, R., Hoffmann, S., Lockau, W., Steuer, R. (2013) Flux Balance Analysis of Cyanobacterial Metabolism: The Metabolic Network of *Synechocystis* sp. PCC 6803. PLoS Comput Biol, **9**(6): pp. e1003081.
57. Knoop, H., Zilliges, Y., Lockau, W., Steuer, R. (2010) The metabolic network of *Synechocystis* sp. PCC 6803: systemic properties of autotrophic growth. Plant Physiol, **154**(1): pp. 410-422.

58. Labarre, J., Thuriaux, P., Chauvat, F. (1987) Genetic analysis of amino acid transport in the facultatively heterotrophic cyanobacterium *Synechocystis* sp. strain 6803. J Bacteriol, **169**(10): pp. 4668-4673.

59. Laloknam, S., Tanaka, K., Buaboocha, T., Waditee, R., Incharoensakdi, A., Hibino, T., Tanaka, Y., Takabe, T. (2006) Halotolerant cyanobacterium *Aphanothece halophytica* contains a betaine transporter active at alkaline pH and high salinity. Appl Environ Microbiol, **72**(9): pp. 6018-6026.

60. Larsson, M., Larsson, C.M., Ullrich, W.R. (1982) Regulation by amino acids of photorespiratory ammonia and glycolate release from ankistrodesmus in the presence of methionine sulfoximine. Plant Physiol, **70**(6): pp. 1637-1640.

61. Lea, P.J., Miflin, B.J. (2003) Glutamate synthase and the synthesis of glutamate in plants. Plant Physiology and Biochemistry, **41**(6–7): pp. 555-564.

62. Lee, S.J., Gralla, J.D. (2004) Osmo-Regulation of Bacterial Transcription via Poised RNA Polymerase. Molecular Cell, **14**(2): pp. 153-162.

63. Liao, K., Lane, M.D. (1995) Expression of a Novel Insulin-Activated Amino Acid Transporter Gene During Differentiation of 3T3-L1 Preadipocytes into Adipocytes. Biochemical and Biophysical Research Communications, **208**(3): pp. 1008-1015.

64. Ma, Z., Richard, H., Tucker, D.L., Conway, T., Foster, J.W. (2002) Collaborative regulation of *Escherichia coli* glutamate-dependent acid resistance by two AraC-like regulators, GadX and GadW (YhiW). J Bacteriol, **184**(24): pp. 7001-7012.

65. Mansour, M.M.F. (1998) Protection of plasma membrane of onion epidermal cells by glycinebetaine and proline against NaCl stress. Plant Physiology and Biochemistry, **36**(10): pp. 767-772.

66. McCue, K.F., Hanson, A.D. (1990) Drought and salt tolerance: towards understanding and application. Trends in Biotechnology, **8**(0): pp. 358-362.

67. Meldrum, B.S. (2000) Glutamate as a neurotransmitter in the brain: review of physiology and pathology. J Nutr, **130**(4S Suppl): pp. 1007S-1015S.

68. Mendzhul, M.I., Lysenko, T.G., Shainskaia, O.A., Busakhina, I.V. (2000) [Activity of tricarboxylic acid cycle enzymes in cyanobacteria Spirulina platensis]. Mikrobiol Z, **62**(1): pp. 3-10.

69. Miller, R., Hofmann, A., Hartmann, R., Halbig, A., Schano, K.-H. (1992) Measuring dynamic surface and interfacial tensions. Advanced Materials, **4**(5): pp. 370-374.

70. Miner, K.M., Frank, L. (1974) Sodium-stimulated glutamate transport in osmotically shocked cells and membrane vesicles of *Escherichia coli.* J Bacteriol, **117**(3): pp. 1093-1098.
71. Montesinos, M.L., Herrero, A., Flores, E. (1995) Amino acid transport systems required for diazotrophic growth in the cyanobacterium Anabaena sp. strain PCC 7120. J Bacteriol, **177**(11): pp. 3150-3157.
72. Montesinos, M.L., Herrero, A., Flores, E. (1997) Amino acid transport in taxonomically diverse cyanobacteria and identification of two genes encoding elements of a neutral amino acid permease putatively involved in recapture of leaked hydrophobic amino acids. J Bacteriol, **179**(3): pp. 853-862.
73. Narayan, V.S., Nair, P.M. (1990) Metabolism, enzymology and possible roles of 4-aminobutyrate in higher plants. Phytochemistry, **29**(2): pp. 367-375.
74. Neilson, A.H., Larsson, T. (1980) The utilization of organic nitrogen for growth of algae: physiological aspects. Physiologia Plantarum, **48**(4): pp. 542-553.
75. Noiraud, N., Maurousset, L., Lemoine, R. (2001) Transport of polyols in higher plants. Plant Physiology and Biochemistry, **39**(9): pp. 717-728.
76. Nunnery, J.K., Mevers, E., Gerwick, W.H. (2010) Biologically active secondary metabolites from marine cyanobacteria. Curr Opin Biotech, **21**(6): pp. 787-793.
77. Papageorgiou, G., Murata, N. (1995) The unusually strong stabilizing effects of glycine betaine on the structure and function of the oxygen-evolving Photosystem II complex. Photosynthesis Research, **44**(3): pp. 243-252.
78. PEARCE, J., LEACH, C.K., CARR, N.G. (1969) The Incomplete Tricarboxylic Acid Cycle in the Blue-green Alga Anabaena Variabilis. Journal of General Microbiology, **55**(3): pp. 371-378.
79. Peddie, C.J., Cook, G.M., Morgan, H.W. (1999) Sodium-Dependent Glutamate Uptake by an Alkaliphilic, Thermophilic Bacillus Strain, TA2.A1. J Bacteriol, **181**(10): pp. 3172-3177.
80. Pernil, R., Herrero, A., Flores, E. (2010) A TRAP Transporter for Pyruvate and Other Monocarboxylate 2-Oxoacids in the Cyanobacterium Anabaena sp. Strain PCC 7120. J Bacteriol, **192**(22): pp. 6089-6092.
81. Pernil, R., Picossi, S., Mariscal, V., Herrero, A., Flores, E. (2008) ABC-type amino acid uptake transporters Bgt and N-II of Anabaena sp. strain PCC 7120 share an ATPase subunit and are expressed in vegetative cells and heterocysts. Mol Microbiol, **67**(5): pp. 1067-1080.

82. Prakasham, R., Singh, A.K., Singh, H.N., Rai, A.N. (1991) Inorganic nitrogen regulation of glutamate uptake in the cyanobacterium Nostoc muscorum. Physiologia Plantarum, **82**(2): pp. 257-260.

83. Prieto-Santos, M.I., Martín-Checa, J., Balaña-Fouce, R., Garrido-Pertierra, A. (1986) A pathway for putrescine catabolism in *Escherichia coli.* Biochimica et Biophysica Acta (BBA) - General Subjects, **880**(2–3): pp. 242-244.

84. Prince, W.S., Villarejo, M.R. (1990) Osmotic control of proU transcription is mediated through direct action of potassium glutamate on the transcription complex. J Biol Chem, **265**(29): pp. 17673-17679.

85. Quintero, M.J., Montesinos, M.L., Herrero, A., Flores, E. (2001) Identification of genes encoding amino acid permeases by inactivation of selected ORFs from the *Synechocystis* genomic sequence. Genome Res, **11**(12): pp. 2034-2040.

86. Rawson, D.M. (1985) The Effects of Exogenous Amino Acids on Growth and Nitrogenase Activity in the Cyanobacterium Anabaena cylindrica PCC 7122. Journal of General Microbiology, **131**(10): pp. 2549-2554.

87. Reed, R., Stewart, W. (1988) The responses of cyanobacteria to salt stress.

88. Riccardi, G., de Rossi, E., Milano, A. (1989) Amino acid biosynthesis and its regulation in cyanobacteria. Plant Science, **64**(2): pp. 135-151.

89. Robinson, S., Jones, G. (1986) Accumulation of Glycinebetaine in Chloroplasts Provides Osmotic Adjustment During Salt Stress. Functional Plant Biology, **13**(5): pp. 659-668.

90. Samsonova, N.N., Smirnov, S.V., Altman, I.B., Ptitsyn, L.R. (2003) Molecular cloning and characterization of *Escherichia coli* K12 ygjG gene. BMC Microbiol, **3**(1): pp. 2.

91. Santoro, M.M., Liu, Y., Khan, S.M.A., Hou, L.X., Bolen, D.W. (1992) Increased thermal stability of proteins in the presence of naturally occurring osmolytes. Biochemistry, **31**(23): pp. 5278-5283.

92. Schellenberg, G.D., Furlong, C.E. (1977) Resolution of the multiplicity of the glutamate and aspartate transport systems of *Escherichia coli.* Journal of Biological Chemistry, **252**(24): pp. 9055-9064.

93. Scott-Taggart, C.P., Van Cauwenberghe, O.R., McLean, M.D., Shelp, B.J. (1999) Regulation of Γ-aminobutyric acid synthesis in situ by glutamate availability. Physiologia Plantarum, **106**(4): pp. 363-369.

94. Shafqat, S., Tamarappoo, B.K., Kilberg, M.S., Puranam, R.S., McNamara, J.O., Guadaño-Ferraz, A., Fremeau, R.T. (1993) Cloning and expression of a novel Na(+)-dependent neutral amino acid transporter structurally related to

mammalian Na+/glutamate cotransporters. Journal of Biological Chemistry, **268**(21): pp. 15351-15355.

95. Shelp, B.J., Bown, A.W., McLean, M.D. (1999) Metabolism and functions of gamma-aminobutyric acid. Trends Plant Sci, **4**(11): pp. 446-452.
96. Shelp, B.J., Bozzo, G.G., Trobacher, C.P., Zarei, A., Deyman, K.L., Brikis, C.J. (2012) Hypothesis/review: contribution of putrescine to 4-aminobutyrate (GABA) production in response to abiotic stress. Plant Sci, **193-194**: pp. 130-135.
97. Shen, B., Jensen, R.G., Bohnert, H.J. (1997) Mannitol Protects against Oxidation by Hydroxyl Radicals. Plant Physiol, **115**(2): pp. 527-532.
98. Singh, S. (1993) Regulation of glutamate metabolism in the cyanobiont Nostoc ANTH by nitrogen sources. Journal of Basic Microbiology, **33**(1): pp. 41-45.
99. Singh, S.P., Montgomery, B.L. (2013) Salinity impacts photosynthetic pigmentation and cellular morphology changes by distinct mechanisms in Fremyella diplosiphon. Biochemical and Biophysical Research Communications, **433**(1): pp. 84-89.
100. Slotboom, D.J., Konings, W.N., Lolkema, J.S. (1999) Structural Features of the Glutamate Transporter Family. Microbiology and Molecular Biology Reviews, **63**(2): pp. 293-307.
101. Smirnoff, N., Cumbes, Q.J. (1989) Hydroxyl radical scavenging activity of compatible solutes. Phytochemistry, **28**(4): pp. 1057-1060.
102. Snedden, W.A., Arazi, T., Fromm, H., Shelp, B.J. (1995) Calcium/Calmodulin Activation of Soybean Glutamate Decarboxylase. Plant Physiol, **108**(2): pp. 543-549.
103. Snedden, W.A., Koutsia, N., Baum, G., Fromm, H. (1996) Activation of a recombinant petunia glutamate decarboxylase by calcium/calmodulin or by a monoclonal antibody which recognizes the calmodulin binding domain. J Biol Chem, **271**(8): pp. 4148-4153.
104. Soontharapirakkul, K., Promden, W., Yamada, N., Kageyama, H., Incharoensakdi, A., Iwamoto-Kihara, A., Takabe, T. (2011) Halotolerant cyanobacterium *Aphanothece halophytica* contains an Na+-dependent F1F0-ATP synthase with a potential role in salt-stress tolerance. J Biol Chem, **286**(12): pp. 10169-10176.
105. Steinhauser, D., Fernie, A.R., Araujo, W.L. (2012) Unusual cyanobacterial TCA cycles: not broken just different. Trends Plant Sci, **17**(9): pp. 503-509.

106. Suzuki, A., Knaff, D. (2005) Glutamate synthase: structural, mechanistic and regulatory properties, and role in the amino acid metabolism. Photosynthesis Research, **83**(2): pp. 191-217.

107. Szvetnik, A., Gal, J., Kalman, M. (2007) Membrane topology of the GltS Na+/glutamate permease of *Escherichia coli.* FEMS Microbiol Lett, **275**(1): pp. 71-79.

108. Takabe, T., Incharoensakdi, A., Arakawa, K., Yokota, S. (1988) CO(2) Fixation Rate and RuBisCO Content Increase in the Halotolerant Cyanobacterium, *Aphanothece halophytica*, Grown in High Salinities. Plant Physiol, **88**(4): pp. 1120-1124.

109. Thompson, J.D., Gibson, T.J., Plewniak, F., Jeanmougin, F., Higgins, D.G. (1997) The CLUSTAL_X windows interface: flexible strategies for multiple sequence alignment aided by quality analysis tools. Nucleic Acids Res, **25**(24): pp. 4876-4882.

110. Tolner, B., Poolman, B., Konings, W.N. (1992) Characterization and functional expression in *Escherichia coli* of the sodium/proton/glutamate symport proteins of Bacillus stearothermophilus and Bacillus caldotenax. Mol Microbiol, **6**(19): pp. 2845-2856.

111. Tolner, B., Poolman, B., Wallace, B., Konings, W.N. (1992) Revised nucleotide sequence of the gltP gene, which encodes the proton-glutamate-aspartate transport protein of *Escherichia coli* K-12. J Bacteriol, **174**(7): pp. 2391-2393.

112. Tolner, B., Ubbink-Kok, T., Poolman, B., Konings, W.N. (1995) Cation-selectivity of the L-glutamate transporters of *Escherichia coli*, Bacillus stearothermophilus and Bacillus caldotenax: dependence on the environment in which the proteins are expressed. Mol Microbiol, **18**(1): pp. 123-133.

113. Vaishampayan, A. (1982) AMINO ACID NUTRITION IN THE BLUE-GREEN ALGA NOSTOC MUSCORUM. New Phytologist, **90**(3): pp. 545-549.

114. Waditee, R., Bhuiyan, M.N., Rai, V., Aoki, K., Tanaka, Y., Hibino, T., Suzuki, S., Takano, J., Jagendorf, A.T., Takabe, T., Takabe, T. (2005) Genes for direct methylation of glycine provide high levels of glycinebetaine and abiotic-stress tolerance in *Synechococcus* and Arabidopsis. Proc Natl Acad Sci U S A, **102**(5): pp. 1318-1323.

115. Waditee, R., Hibino, T., Nakamura, T., Incharoensakdi, A., Takabe, T. (2002) Overexpression of a Na+/H+ antiporter confers salt tolerance on a freshwater

cyanobacterium, making it capable of growth in sea water. Proc Natl Acad Sci U S A, **99**(6): pp. 4109-4114.

116. Waditee, R., Hibino, T., Tanaka, Y., Nakamura, T., Incharoensakdi, A., Hayakawa, S., Suzuki, S., Futsuhara, Y., Kawamitsu, Y., Takabe, T., Takabe, T. (2002) Functional characterization of betaine/proline transporters in betaine-accumulating mangrove. J Biol Chem, **277**(21): pp. 18373-18382.

117. Waditee, R., Hibino, T., Tanaka, Y., Nakamura, T., Incharoensakdi, A., Takabe, T. (2001) Halotolerant cyanobacterium *Aphanothece halophytica* contains an Na(+)/H(+) antiporter, homologous to eukaryotic ones, with novel ion specificity affected by C-terminal tail. J Biol Chem, **276**(40): pp. 36931-36938.

118. Waditee, R., Tanaka, Y., Aoki, K., Hibino, T., Jikuya, H., Takano, J., Takabe, T., Takabe, T. (2003) Isolation and functional characterization of N-methyltransferases that catalyze betaine synthesis from glycine in a halotolerant photosynthetic organism *Aphanothece halophytica.* J Biol Chem, **278**(7): pp. 4932-4942.

119. Wallsgrove, R.M., Keys, A.J., Lea, P.J., Miflin, B.J. (1983) Photosynthesis, photorespiration and nitrogen metabolism. Plant, Cell & Environment, **6**(4): pp. 301-309.

120. Wiangnon, K., Raksajit, W., Incharoensakdi, A. (2007) Presence of a Na+-stimulated P-type ATPase in the plasma membrane of the alkaliphilic halotolerant cyanobacterium *Aphanothece halophytica.* FEMS Microbiol Lett, **270**(1): pp. 139-145.

121. Xing, S.G., Jun, Y.B., Hau, Z.W., Liang, L.Y. (2007) Higher accumulation of gamma-aminobutyric acid induced by salt stress through stimulating the activity of diamine oxidases in Glycine max (L.) Merr. roots. Plant Physiol Biochem, **45**(8): pp. 560-566.

122. Yaronskaya, E., Vershilovskaya, I., Poers, Y., Alawady, A., Averina, N., Grimm, B. (2006) Cytokinin effects on tetrapyrrole biosynthesis and photosynthetic activity in barley seedlings. Planta, **224**(3): pp. 700-709.

123. Yernool, D., Boudker, O., Jin, Y., Gouaux, E. (2004) Structure of a glutamate transporter homologue from Pyrococcus horikoshii. Nature, **431**(7010): pp. 811-818.

124. Yopp, J.H., Albright, G., Miller, D.M. (1979) Effects of Antibiotics and Ultraviolet Radiation on the Halophilic Blue-Green Alga, *Aphanothece halophytica*. In: Botanica Marina. pp. 267.

125. Zhang, S., Bryant, D.A. (2011) The Tricarboxylic Acid Cycle in Cyanobacteria. Science, **334**(6062): pp. 1551-1553.

126. Zhu, J.K. (2001) Plant salt tolerance. Trends Plant Sci, **6**(2): pp. 66-71.

APPENDICES

APPENDIX 1

pBluescript II SK (+)

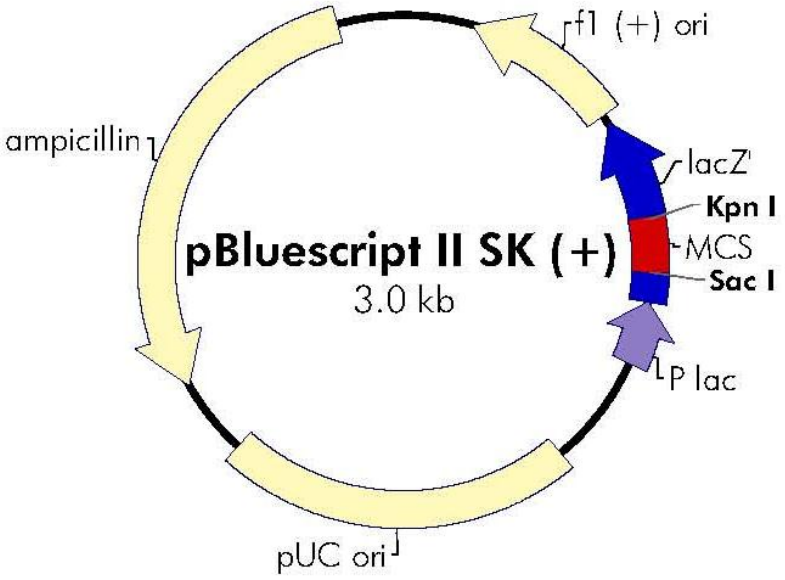

pBluescript II SK (+/–) Multiple Cloning Site Region (sequence shown 598–826)

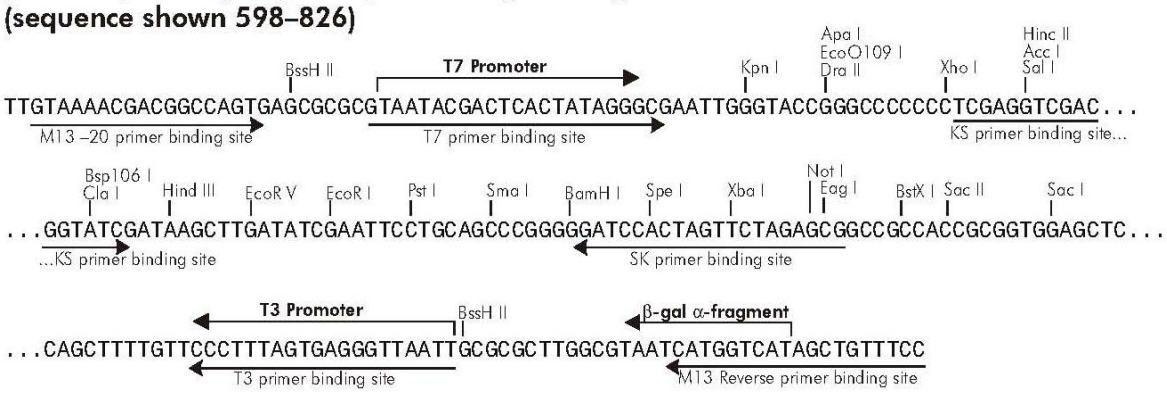

APPENDIX 2

pTrcHis2C

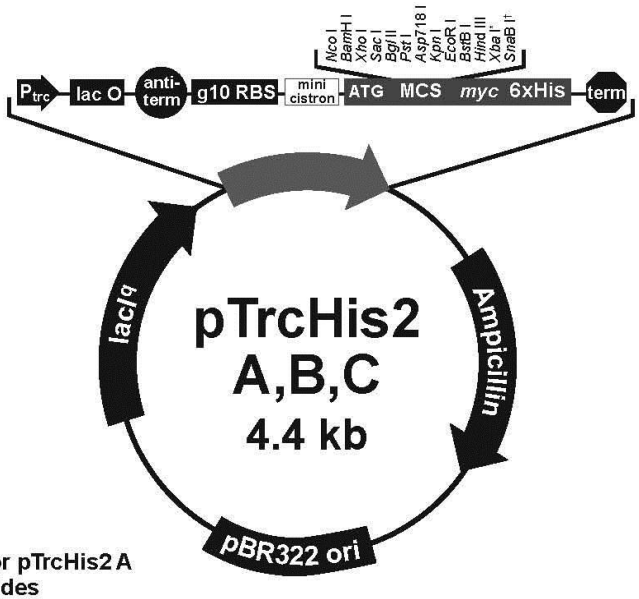

Comments for pTrcHis2 A
4406 nucleotides

trc promotor region: bases 190-382
-35 region: bases 193-198
-10 region: bases 216-221
lac operator (*lac*O): bases 228-248
*rrn*B antitermination signal: bases 264-333
gene 10 region: bases 346-354
Ribosome binding site: bases 369-373
pTrcHis forward priming site: bases 370-390
Minicistron ORF: bases 383-409
Reinitiation RBS: bases 398-403
Expression ATG: bases 413-415
Multiple cloning site: bases 411-464
myc epitope: bases 471-503
Polyhistidine tag: bases 516-533
*myc*His reverse priming site: bases 508-527
*rrn*B T1 and T2 transcriptional terminators: bases 639-796
Ampicillin resistance ORF: bases 1076-1936
pBR322 origin: bases 2081-2754
Lac Repressor (*lac*I^q) ORF: bases 3285-4367

* *Xba* I is only found in pTrcHis2 B

† *Sna*B I is only found in pTrcHis2 C

```
                    pTrcHis forward priming site
                    RBS                          Mini cistron                    RBS                  Nco
361  AAAATTAAAG AGGTATATAT TA ATG TAT CGA TTA AAT AAG GAG GAA TAA ACC
                                 Met Tyr Arg Leu Asn Lys Glu Glu ***

     BamH I        Xho I Sac I Bgl II     Pst I Asp718 I Kpn I     EcoR I  BstB I Hind III  SnaB I
413  ATG GATCCGAGCT CGAGATCTGC AGCTGGTACC ATATGGGAAT TCGAAGCTTA CGTA
     Met

                                   myc epitope tag                          Sal I
461  GAA CAA AAA CTC ATC TCA GAA GAG GAT CTG AAT AGC GCC GTC GAC CAT
     Glu Gln Lys Leu Ile Ser Glu Glu Asp Leu Asn Ser Ala Val Asp His

     ProBond™ binding domain
510  CAT CAT CAT CAT CAT TGA GTTTA
     His His His His His ***
```

APPENDIX 3

pCR®2.1

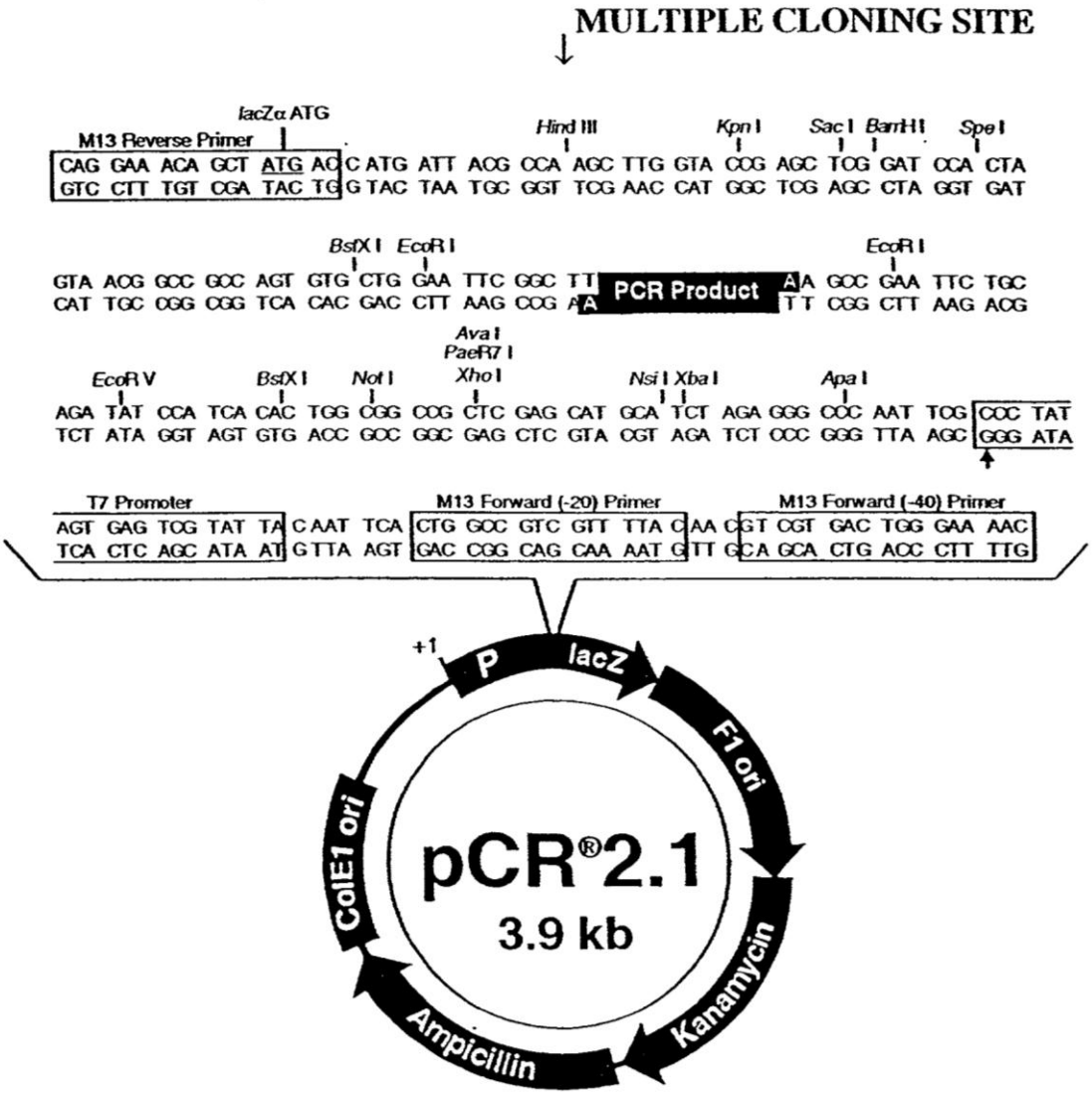

APPENDIX 4

pQF50

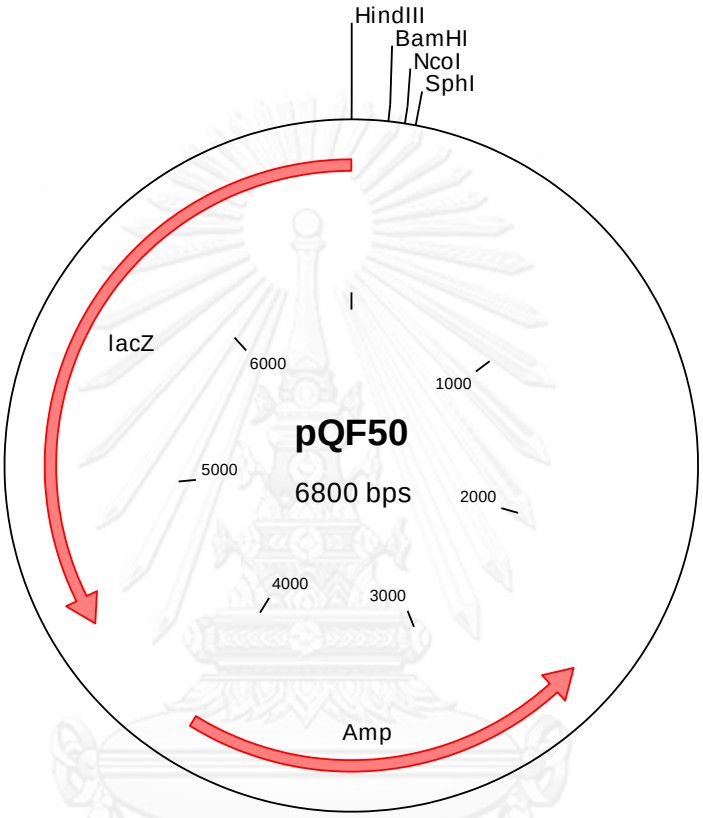

APPENDIX 5

pUC303

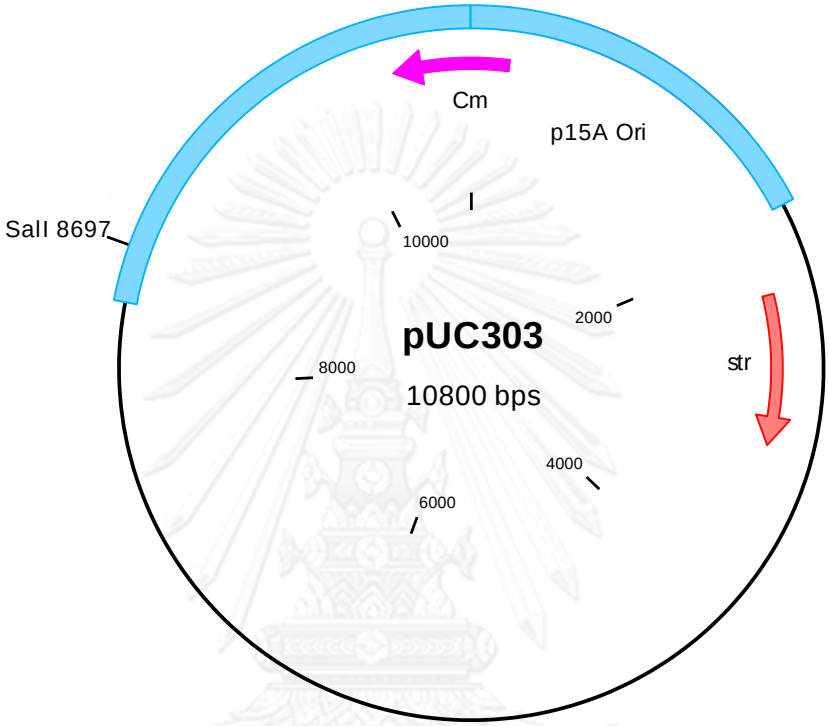

APPENDIX 6

BG_{11} and BG_{11} + Turk Island Salt Solution

Reagents:

<u>Stock solution (100 ml each)</u>

Solution I: K_2HPO_4	3.135 g
Solution II: $MgSO_4.7H_2O$	7.5 g
Solution III: $CaCl_2.2H_2O$	3.6 g
Solution IV: Na_2CO_3	2.0 g
Solution V:	
EDTA	0.1 g
Citric acid	0.1 g
Ferric ammonium citrate	0.6 g

<u>Stock solution (500 ml)</u>

Solution VI:	
H_3BO_3	1.43 g
$ZnSO_4.7H_2O$	110 mg
$Na_2MoO_4.2H_2O$	195 mg
$MnCl_2.4H_2O$	0.905 g
$CuSO_4.5H_2O$	39.5 mg
$Co(NO_3)_2.6H_2O$	24.5 mg

All stock solutions were sterilized by filtered through 0.45 μm nitrocellulose membrane and stored at 4 °C.

BG_{11} **medium (1,000 ml)**

	Solid medium	Liquid medium
Bacto-agar	15 g	-
$NaNO_3$	1.5 g	1.5 g
Solution I	1 ml	1 ml
Solution II	1 ml	1 ml
Solution III	1 ml	1 ml
Solution IV	1 ml	1 ml
Solution V	1 ml	1 ml
Solution VI	1 ml	1 ml
H_2O added up to	1000 ml	1000 ml

Remark: The culture medium was mixed, adjusted pH to 7.6 by adding 2 M NaOH, then added distrilled water to the final volume 1000 ml. The medium was sterilized by autoclaving at 15 lb/in^2 for 15 mins.

BG_{11} **medium + Turk Island Salt Solution (1,000 ml)**

	Solid medium	Liquid medium
Bacto-agar	15 g	-
$NaNO_3$	1.5 g	1.5 g
KCl	0.67 g	0.67 g
$MgSO_4.7H_2O$	6.92 g	6.92 g
$MgCl_2.6H_2O$	5.5 g	5.5 g
$CaCl_2.2H_2O$	1.47 g	1.47 g
Solution I	1 ml	1 ml
Solution II	1 ml	1 ml
Solution III	1 ml	1 ml
Solution IV	1 ml	1 ml
Solution V	1 ml	1 ml
Solution VI	1 ml	1 ml
NaCl (0.5M)	29.22 g	29.22 g
H_2O added up to	1000 ml	1000 ml

Remark: The culture medium was mixed, adjusted pH to 7.6 by adding 2 M NaOH, then added distrilled water to the final volume 1000 ml. The medium was sterilized by autoclaving at 15 lb/in^2 for 15 mins.

APPENDIX 7

Luria-Bertani medium

Luria-Bertani medium (LB medium) (Maniatis et al., 1982) (1000 ml)

	Liquid medium	Solid medium
Bacto tryptone	10 g	10 g
Yeast extract	5 g	5 g
NaCl	5 g	5 g
Agar	-	15 g

All compositions were dissolved together with 800 ml of distilled water. Adjust volume of solution to 1litre with deionized water. The medium was sterilized by autoclaving at 15 lb/in^2 for 15 mins. If needed, selective antibiotic drug was then supplemented.

APPENDIX 8

Minimal medium A (MMA)

Reagents:

5x Stock MMA solution (1000 ml)

K_2HPO_4	10.5 g
KH_2PO_4	4.5 g
$(NH_4)_2SO_4$	1.0 g
$HOC(COONa)(CH_2COONa)_2.\ 2H_2O$	0.5 g
$MgSO_4.7H_2O$	0.1 g

All compositions were dissolved together with 800 ml of distilled water. The mixture was adjusted pH to 7.6 with 6 M NaOH and adjust volume of solution to 1litre with deionized water. The medium was sterilized by autoclaving at 15 lb/in^2 for 15 mins.

5 M NaCl (100 ml)

NaCl	29.2 g

The mixture was dissolved with 50 ml of distilled water and adjust volume of solution to 100 ml with deionized water. The chemical was sterilized by autoclaving at 15 lb/in^2 for 15 mins.

20% glucose (100ml)

Glucose	20.0 g

The mixture was dissolved with 50 ml of distilled water and adjust volume of solution to 100 ml with deionized water. The chemical was sterilized by filtered through 0.45 μm nitrocellulose membrane.

APPENDIX 9

Antibiotics, IPTG and X-gal

Reagents:

100 mg/ml ampicillin (1ml)

Ampicillin	100 mg

Dissolved with 1 ml sterilized distilled water and sterilized by filtered through 0.45 µm nitrocellulose membrane and stored at -20 °C.

100 mg/ml streptomycin (1ml)

Streptomycin	100 mg

Dissolved with 1 ml sterilized distilled water and sterilized by filtered through 0.45 µm nitrocellulose membrane and stored at -20 °C.

50 mg/ml chloramphenicol (1ml)

Chloramphenicol	50 mg

Dissolved with 1 ml Ethanol and sterilized by filtered through 0.45 µm nitrocellulose membrane and stored at -20 °C.

1 M IPTG (1ml)

Isopropyl-1-thio-β-D-galactopyranoside	238 mg

Dissolved with 0.9 ml sterilized distilled water. The mixture was adjusted volume of solution to 1 ml with sterilized distilled water and sterilized by filtered through 0.45 µm nitrocellulose membrane and stored at -20 °C.

20 mg/ml X-gal (1ml)

5-bromo-4-chloro-3-indolyl-beta-D-galactopyranoside 20 mg

Dissolved with 1 ml DMSO (dimethyl sulfoxide) and sterilized by filtered through 0.45 µm nitrocellulose membrane. Wrapped tube in foil and stored at -20 °C.

APPENDIX 10

Scintillation fluid

Scintillation fluid (1,000 ml)

2, 5-diphenyloxazole (PPO)	5.5 g
1, 4-bis (5-phenyloxazole-2-yl) benzene (POPOP)	0.1 g

The mixture was dissolved with 1,000 ml of a solution composed of 667 ml Toluene and 333 ml of Triton X-100. The solution should be stored in a brown bottle in a cool dark place.

APPENDIX 11

Determination of protein by Bradford's method

Assay

Prepare 10 µl of sample protein solution into in microtube, and then add 1 ml of Bradford working buffer and vortex. The reaction mixture was incubated at 30°C for 10 mins. Finally, the absorbance was measured at 595 nm. The protein content was calculated by comparison to the standard curve of BSA.

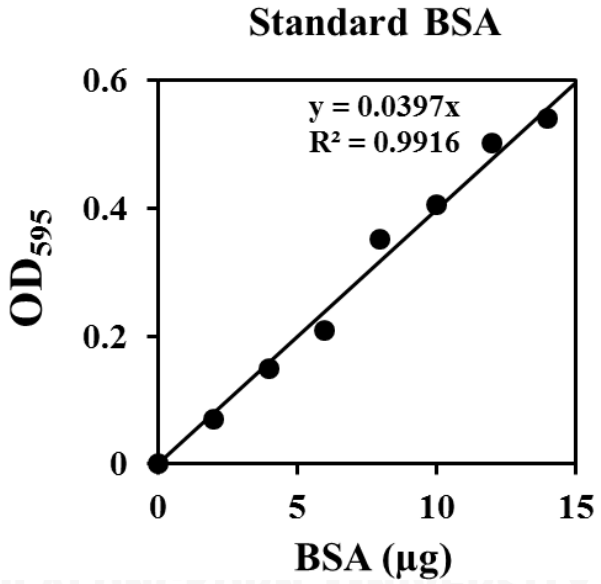

APPENDIX 12

Agarose gel electrophoresis for DNA

Reagents:

TBE buffer 20X

Tris base	242.2 g (1 M)
H_3BO_3	132.6 g (1 M)
$Na_2EDTA \cdot 2H_2O$	29.6 g (40 mM)

All compositions were dissolved together with 1,600 ml of distilled water. and adjusted pH to 8.3 with H_3BO_3. Bring volume to 2000 ml with deionized water. The chemical was sterilized by filtered through 0.45 µm nitrocellulose membrane and autoclaving at 15 Ib/in^2 for 15 mins and stored at room temperature

DNA gel loading buffer (10X sample buffer)

0.5 M EDTA/NaOH pH 7.5	2.0 ml (0.1 M)
Glycerol	5.0 ml (50% v/v)
H_2O	2.5 ml
20% (w/v) SDS	0.5 ml (1% w/v)
Xylene cyanol	5-10 mg
Bromophenol Blue	5-10 mg

All compositions were mixed together and divided into 1-ml aliquots and stored at 4°C.

1 mg/ml Ethidium bromide

Ethidium bromide	0.1 g

Dissolved with 100 ml of distilled water and mix well. The chemical was stored at 4°C in a darkened bottle.

Method for agarose gel preparation

In a flask that is about three times the volume of gel solution to be made, add the desired amount of 1X TBE. Add desired amount of agarose, swirl and bring to a boil in the microwave. Gently swirl the flask to help dissolve the agarose and boil again. Repeat until agarose is dissolved. Cool the flask in the 65°C bath for about 5-10 min. Pour the solution into a levered gel forming mold with the well-forming comb in place, remove any air bubbles from the surface with a Pasteur pipet. Allow the gel to cool and set for about 30 min before using.

Note: Gels can be saved by placing them in a Zip-loc bag with some wet paper and storing the tightly sealed bag in the fridge. After storing gels, rehydrate them by allowing to stand submerged in the gel box for about 10-15 mins prior to loading the samples

Method for running DNA on agarose gel:

To measure the size and the amount of DNA in the sample, gels are run submerged in reservoir buffer (1X TBE) in an electrophoretic chamber. Samples are prepared by adding 0.1 volume of sample buffer 10X, heating for 10 min at 65°C, and applying into the gel slots. The appropriate amount of λ/HindIII or 1 kb GeneRuler™ (Fermentas, USA) was also load to the gel to serve as a DNA marker.

Generally, the gel was run at 100 volts until bromphenol blue migrated to the other egde. Gels must be stained after running by soaking for about 10 min in water (250 mL) containing about 100 µl of 1 $mg.ml^{-1}$ Ethidium Bromide (EtBr). Destain for about 10 min in water, then view on UV light box in dark room. Permanent records of gels are made by photography. Alternately, gels can be stained while they run by adding 10 µl of 1 $mg.ml^{-1}$ EtBr per 100 ml of reservior buffer prior to running the gel. In this case, no destaining is necessary. The concentration and molecular weight of DNAs sample were estimated by comparing with the intensity and relative mobility of λ/HindIII or 1 kb GeneRuler™ (Fermentas, USA).

APPENDIX 13

Restriction enzyme digestion

Restriction endonuclease was used to cut DNA based on its specific binding property and cleaving double-stranded DNA at a specific sequence. The condition of digestion was performed as recommended by the enzyme manufacturer. Typically, a reaction contains about 0.5-1 µg of DNA. In a final volume of 10 µl containing 1x enzyme reaction buffer and 2-5 units of restriction enzyme. The reaction was gently mixed and incubated at appropriate temperature of each restriction enzyme for optimum time. If the enzyme require different reaction temperatures, start with the enzyme that requires a lower temperature, then add the second enzyme and incubate at the higher temperature.

APPENDIX 14

DNA marker preparation

λ/*Hind*III DNA marker

λ DNA (0.4 mg/ml)	30 µl (12 µg)
10X buffer (for *Hind*III)	9 µl
H_2O	50 µl
*Hind*III	1 µl

All compositions were mixed together and incubated at 37°C for 3 hrs. Add 10 µl of 10X DNA loading buffer to the reaction (final concentration is 120 ng.µl^{-1}).

λ/ *Eco*RI and *Hind*III DNA marker

λ DNA (0.4 mg/ml)	30 µl (12 µg)
10X buffer	9 µl
H_2O	49 µl
*Hind*III	1 µl
*Eco*RI	1 µl

All compositions were mixed together and incubated at 37°C for 3 hrs. Add 10 µl of 10X DNA loading buffer to the reaction (final concentration is 120 ng.µl^{-1}).

APPENDIX 15

Modified blunt-ending

For filling recessed 3' termini	For removing protruding 3' termini
1 µL solution containing 1 mM dNTPs and 1U Klenow per 1 µg of DNA, incubate for 15 mins at room temperature. After incubation, heat inactivate at 75 °C for 10 min	2 µL solution containing 1 mM dNTPs and1-2U T4 DNA polymerase per 1 µg of DNA, incubate for 15 mins at 12 °C. After incubation, heat inactivate at 75 °C for 10 min

APPENDIX 16

DNA ligation

To calculate the appropriate amount of PCR product (insert) used in ligation reaction, the following equation was used:

$$\frac{\text{ng of vector} \times \text{kb size of insert}}{\text{kb size of vector}}$$

The 10 µl ligation reaction was composed of 5 µl of 2× T4 DNA ligase buffer, 3 weiss units of T4 DNA ligase, and the appropriate amount of the PCR product. The reaction was incubated at 4 °C overnight.

APPENDIX 17

E. coli transformation by heat shock method

1. Preparation of competent cells

Reagents:

100 mM $CaCl_2$ (1000 ml)

$CaCl_2 \cdot 2H_2O$	14.7 g

The mixture was dissolved with 800 ml of distilled water and adjust volume of solution to 1000 ml with deionized water. The chemical was sterilized by autoclaving at 15 lb/in^2 for 15 mins and stored at -20 °C.

15% (v/v) Glycerol (100 ml)

Glycerol	15 ml

Dissolved with 85 ml of distilled water and sterilized by filtered through 0.45 µm nitrocellulose membrane.

Method:

200 µl overnight culture of *E. coli* DH5α was inoculated into 100 ml sterile LB medium, and then grown at 37 °C, 250 rpm until OD_{620} reached 0.3-0.4. The culture was incubated on ice for 30 mins. The cells were collected by centrifugation at 5,000 xg, 4 °C for 10 mins. The pellet was resuspended with 100 ml of cold 0.1 M $MgCl_2$ and centrifuged at 5,000 *xg*, 4 °C for 10 mins. A supernatant was discarded then the pellet was resuspended with 100 ml of cold 0.1 M $CaCl_2$ and incubated on ice for 30-60 mins. After incubation, the cell suspension was centrifuge at 5,000 *xg*, 4 °C, for 10

mins. A supernatant was discarded then the pellet was resuspended with 3 ml of cold 0.1 M $CaCl_2$ containing 15% glycerol. The cell suspension was aliquot 100 µl per tube on ice prior to immediate drop into liquid nitrogen. The competent cells were stored at -80 °C until use.

2. Heat shock transformation

The plasmid (1-10 ng) was mixed with cold cell suspension in microtube and place on ice for 45 min. The mixture was incubated at 42 °C for 90 sec and placed on ice for 5 mins. The cell suspension was transferred into a new sterile tube containing 1 ml of LB broth. The transformed cells were incubated at 37 °C, 200 rpm for 1 hr and spreaded onto the LB agar plate containing appropriate antibiotic. For color production from lacZ-bearing plasmids, the plates are prepared earlier by spreading with IPTG and X-gal. The plate was incubated at 37 °C overnight.

APPENDIX 18

Preparation of *E. coli* plasmid by alkaline lysis method

Reagents:

Lysis buffer (Solution I)

Tris base	1.51 g (50 mM)
$Na_2EDTA \cdot 2H_2O$	0.93 g (10 mM)

All compositions were dissolved together with 200 ml of distilled water. and adjusted pH to 8.0 with HCl. Bring volume to 250 ml with deionized water. The chemical was sterilized by autoclaving at 15 lb/in^2 for 15 mins. After autoclave, 25 mg of RNase was added and stored at 4°C.

Alkaline-SDS solution (Solution II)

1 M NaOH	50 ml (200 mM)

Dissolved with 150 ml of distilled water, mix well, then add 12.5 ml of and 20% (w/v) SDS and adjust volume of solution to 250 ml with deionized water. The chemical was sterilized by autoclaving at 15 lb/in^2 for 15 mins and stored at room temperature.

High salt buffer (Solution III)

Potassium acetate	73.6 g (3 M)

Dissolved with 150 ml of distilled water. The mixture was adjusted pH to5.5 with glacial acetic acid and bring volume to 250 ml with sterile H_2O. The chemical was sterilized by autoclaving at 15 lb/in^2 for 15 mins and stored at room temperature.

TE buffer

Tris base	0.3 g (10 mM)
$Na_2EDTA \cdot 2H_2O$	0.09 g (1 mM)

All compositions were dissolved together with 200 ml of distilled water and adjusted pH to 8.0 with HCl. Bring volume to 250 ml with deionized water. The chemical was sterilized by autoclaving at 15 lb/in^2 for 15 mins and stored at room temperature.

Method:

A single colony of *E. coli* haboring recombinant plasmid was grown in 1.5 ml of LB solution containing appropriate antibiotic at 37 °C for overnight with shaking. The cells were harvested by centrifugation at 4,000 g for 10 min at 4 °C and suspended in 100 µl of solution I by vigorous vortexing. After 5 mins incubation at room temperature, the cells were lysed by the addition of 200 µl of freshly prepare solution II, mixed by gently inversion and incubated on ice for 5 min. The cell lysate was neutralized by gently mixing with 150 µl of solution III followed by 5 mins incubation on ice. The mixture was centrifuged at 12,000 rpm for 5 min at 4 °C. The

clear lysate was collected, extracted once with phenol:chloroform:isoamylalcohol (25: 4:1). Subsequently, the plasmid was precipitated by adding 2 volumes of ice-cold absolute ethanol, mixed by inversion several times before incubated at -20 °C for 10 mins and then centrifuged for 10 min at 12,000 rpm at 4 °C. The plasmid was washed with 70% ethanol and recollected by centrifugation for 3 min. Finally, the air-dried pellet was dissolved in 20 µl of TE buffer and stored at -20 °C.

APPENDIX 19

SDS polyacrylamide gel electrophoresis

Reagents:

30% (w/v) Acrylamide and 0.8% (w/v) N,N'-methylene-bis-acrylamide (100 ml)

Acrylamide	29.2 g
N,N'-methylene-bis-acrylamide	0.8 g

The volume of mixture was adjusted to 100 ml with distilled water and then the mixture was stirred until completely dissolved.

1.5 M Tris-HCl pH 8.8 (100 ml)

Tris (hydroxymethyl) aminomethane	18.17 g

The mixture was adjusted pH to 8.8 with 1 N HCl and adjusted volume to 100 ml with distilled water.

2 M Tris-HCl pH 8.8 (100 ml)

Tris (hydroxymethyl) aminomethane	24.2 g

The mixture was adjusted pH to 8.8 with 1 N HCl and adjusted volume to 100 ml with distilled water.

0.5 M Tris-HCl pH 6.8 (100 ml)

Tris (hydroxymethyl) aminomethane	6.06 g

The mixture was adjusted pH to 6.8 with 1 N HCl and adjusted volume to 100 ml with distilled water.

1 M Tris-HCl pH 6.8 (100 ml)

Tris (hydroxymethyl) aminomethane	12.1 g

The mixture was adjusted pH to 6.8 with 1 N HCl and adjusted volume to 100 ml with distilled water.

10% (w/v) Ammonium persulfate (1 ml)

Ammonium persulfate	0.1 g

The volume of mixture was adjusted to 1 ml with distilled water.

10% (w/v) SDS (100 ml)

SDS	10 g

The volume of mixture was adjusted to 100 ml with distilled water.

Solution B (SDS-PAGE)

2 M Tris-HCl pH 8.8	75 ml
10% SDS	4 ml
Distilled water	21 ml

Solution C (SDS-PAGE)

1 M Tris-HCl pH 6.8	50 ml
10% SDS	4 ml
Distilled water	46 ml

0.5% (w/v) Bromophenol blue (10 ml)

Bromophenol blue	0.05 g

The volume of mixture was adjusted to 10 ml with distilled water.

Sample buffer

1 M Tris-HCl pH 6.8	0.6 ml
Glycerol	0.8 ml
10% SDS	2 ml
β-mercaptoethanol	0.5 ml
0.5% bromophenol blue	0.5 ml
distilled water	5.8 ml

The ratio of sample and sample buffer is 4:1. The mixture was heated for 5 mins in boiling water before loading to the gel.

Electrophoresis buffer (1000 ml)

Tris (hydroxymethyl) aminomethane	3 g
Glycine	14.4 g
SDS	1 g

The volume of mixture was adjusted to 1000 ml with distilled water (pH should be approximately 8.3). Do not adjust pH with acid or base.

Staining solution (1000 ml)

Coomassie Blue R-250	10 g
Methanol	450 ml
Glacial acetic acid	100 ml

Destaining solution (1000 ml)

Methanol	100 ml
Glacial acetic acid	100 ml

SDS-PAGE preparation:

12% separating gel

30% acrylamide solution	4.17 ml
Solution B	2.5 ml
Distilled water	3.33 ml
Mix gently, then add:	
10% ammonium persulfate	50 µl
TEMED	5 µl

Pipet the solution into the gel sandwiches to a level about 2 ml below the bottom of the teeth of the gel comb. Overlay the gels with H_2O. A sharp water-gel interface will appear under the H_2O layer when the gel has polymerized.

5% stacking gel

30% acrylamide solution	1.67 ml
Solution C	2.5 ml
Distilled water	5.8 ml
Mix gently, then add:	
10% ammonium persulfate	50 µl
TEMED	5 µl

Fill the tops of the gel sandwiches with the stacking gel mixture. Insert the well-forming combs into the gels. Taking care not to introduce bubbles under the "teeth". Allow the gels to set for at least 1 hr. They may be stored at 4°C in a plastic bag containing wet pieces of paper before using.

APPENDIX 20

Buffer for Western blotting

Blotting transfer buffer

Final concentration per litre

39 mM glycine

48 mM Tris-base

0.037% SDS

20% methanol

PBS buffer (Phosphate Buffered Saline)

Final concentration per litre

10 mM sodium phosphate pH 7.4

150 mM NaCl

Blocking solution

5% (w/v) skim milk and 0.01% Tween 20 in PBS buffer

APPENDIX 21

Detection reagent for Western blotting

Reagents:

18 ml of 150 mM Barbital pH 9.6

2 ml of 0.1% NTB (Nitro Blue Tetrazolium)

80 µl of 1 M $MgCl_2$

200 µl of 0.5% BCIP (5-bromo-4-chloro-3-indolyl phosphate)

Method:

Detection reagent for Western blotting should be freshly prepared and used within 30 mins. When the bands are of the desired intensity, wash the nitrocellulose membrane with deionized water 2-3 times and take photograph.

APPENDIX 22

Uptake activity of GltS-deficient *E. coli* mutant ME9107

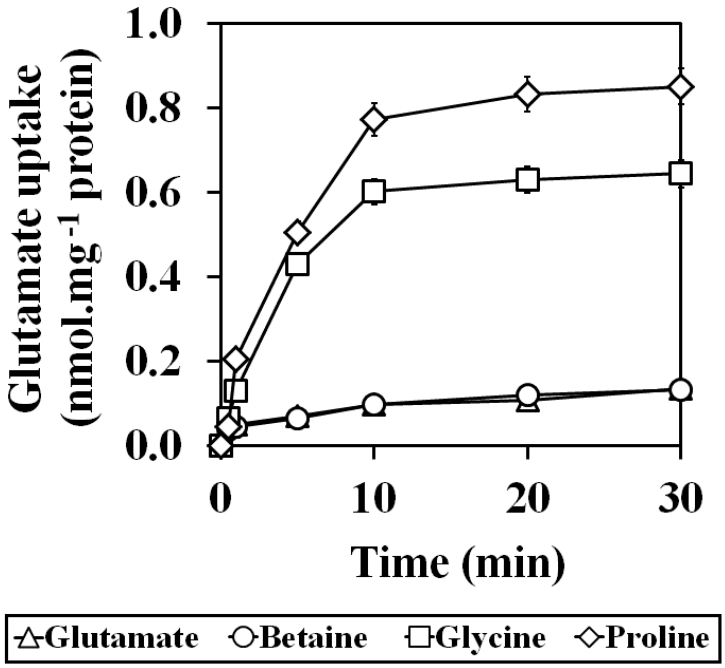

APPENDIX 23

The result of transcription start site prediction using

The Berkeley Drosophila Genome Project (BDGP)

Promoter predictions for 1 prokaryotic sequence with score cutoff 0.80
(transcription start shown in larger font):
Promoter predictions for promoter*ApgltS* :

Start	**End**	**Score**	**Promoter Sequence**
24	69	0.99	ATTTTTAGGTGATTAAAAGCATTATATAATATACTATAAATCACTTTTAC
88	133	0.95	GTTTTTTCTCTATCTTAGGTCAGATTCAATACATTATTGAACCTTTGCAT
117	162	0.92	TACATTATTGAACCTTTGCATCCCTGAAATGTAATAATTGCTACTACTTG
161	206	0.99	TACTTGCTGACAGGAAAGCTCCCACACTGTAACCTGTCTCTACTGCACTC

APPENDIX 24

The result of promoter sequence prediction using GENETYX7

[GENETYX : Search for Promoter Sequence]
Date : 2013.11.02
Filename : promoter*ApgltS*
Sequence Size : 273
Sequence Position: 1 - 273

Minimum Score : 50.00

SCORE	-35[TTGACA]	SPACE	-10[TATAAT]
60.95	TAGATT (21 - 26)	21	TATAAT (48 - 53)
55.62	TTTTTA (25 - 30)	17	TATAAT (48 - 53)
55.03	TTTAGG (27 - 32)	15	TATAAT (48 - 53)
55.62	TTTAGG (27 - 32)	17	TAATAT (50 - 55)
53.25	TTTAGG (27 - 32)	20	TATACT (53 - 58)
54.44	GTGATT (32 - 37)	15	TATACT (53 - 58)
54.44	GTGATT (32 - 37)	17	TACTAT (55 - 60)
57.40	TTGAAC (124 - 129)	16	TGTAAT (146 - 151)
60.36	TTGAAC (124 - 129)	19	AATAAT (149 - 154)
54.44	CTGACA (167 - 172)	17	TAACCT (190 - 195)

Total : 10

APPENDIX 25

The result of promoter analysis using Prokaryotic Promoter Prediction

```
hmmpfam - search one or more sequences against HMM database
HMMER 2.3.2 (Oct 2003)
Copyright (C) 1992-2003 HHMI/Washington University School of Medicine
Freely distributed under the GNU General Public License (GPL)
- - - - - - - - - - - - - - - - - - - - - - - - - - - - - - - - - - - - -
HMM file:                 all.hmm
Sequence file:            input_sequence.fasta
- - - - - - - - - - - - - - - - - - - - - - - - - - - - - - - - - - - -

Query sequence: proApgltS-S
Accession:      [none]
Description:    [none]

Scores for sequence family classification (score includes all domains):
Model           Description                          Score   E-value  N
--------        -----------                          -----   ------- ---
sigmaA_19bp                                           1.5      0.17   1
sigmaA_15bp                                           1.8      0.17   1
sigmaA_17bp                                           0.6      0.18   1
sigmaA_16bp                                           0.2      0.22   1
flpab                                                 0.3      0.25   1
sigmaA_18bp                                           0.1      0.26   1
sigmabif                                             -0.8      0.56   1
siga consensus                                       -0.6      0.65   1

Parsed for domains:
Model           Domain  seq-f seq-t    hmm-f hmm-t      score  E-value
--------        ------- ----- -----    ----- -----      -----  -------
sigmaA_17bp       1/1      25    53 ..     1    25 []     0.6     0.18
sigmaA_19bp       1/1      25    55 ..     1    29 []     1.5     0.17
sigmabif          1/1      25    53 ..     1    30 []    -0.8     0.56
sigmaA_16bp       1/1      26    53 ..     1    26 []     0.2     0.22
sigmaA_18bp       1/1      29    58 ..     1    27 []     0.1     0.26
sigmaA_15bp       1/1      32    58 ..     1    24 []     1.8     0.17
siga consensus    1/1      43    54 ..     1    10 []    -0.6     0.65
flpab             1/1     255   268 ..     1    13 []     0.3     0.25
```

```
Alignments of top-scoring domains:
sigmaA_17bp: domain 1 of 1, from 25 to 53: score 0.6, E = 0.18
                   *->TTgacaaatt.ta.aaaaa.tg.TAtAAT<-*
                      TT   a  t +t++aaa  +t +TAtAAT
  proApgltS-    25    TTTTTAGGTGaTTaAAAGCaTTaTATAAT    53
sigmaA_19bp: domain 1 of 1, from 25 to 55: score 1.5, E = 0.17
                   *->Ttgacaaaaaaa.aaaaaaat.tgaTAtaaT<-*
                      Tt+  a  + a++aaaa  at+ +aTA+ aT
  proApgltS-    25    TTTTTAGGTGATtAAAAGCATtATATAATAT    55
sigmabif: domain 1 of 1, from 25 to 53: score -0.8, E = 0.56
                   *->ttgacaaaataaaaaaaaaagtgatataat<-*
                      tt   a  + a++ aaaa  +t atataat
  proApgltS-    25    TTTTTAGGTGATT-AAAAGCATTATATAAT    53
sigmaA_16bp: domain 1 of 1, from 26 to 53: score 0.2, E = 0.22
                   *->ttgaaaaatta.aa.aatatgaTAtaaT<-*
                      tt++a  +  ++aa+a  at aTAtaaT
  proApgltS-    26    TTTTAGGTGATtAAaAGCATTATATAAT    53
sigmaA_18bp: domain 1 of 1, from 29 to 58: score 0.1, E = 0.26
                   *->ttgacaaattt.t.aaaaaaatg.TAtaAT<-*
                      t g   a+t++++  a++a+at +TAta T
  proApgltS-    29    TAGGTGATTAAaAgCATTATATAaTATACT    58
sigmaA_15bp: domain 1 of 1, from 32 to 58: score 1.8, E = 0.17
                   *->ttgaaaaa.taa.aaat.tgaTataAT<-*
                       tga  aa++  ++ at+t+aTata T
  proApgltS-    32    GTGATTAAaAGCaTTATaTAATATACT    58
siga consensus: domain 1 of 1, from 43 to 54: score -0.6, E = 0.65
                   *->t.tg.tAtaata<-*
                       +t +tAtaata
  proApgltS-    43    CaTTaTATAATA    54
flpab: domain 1 of 1, from 255 to 268: score 0.3, E = 0.25
                   *->tgattttaatca.a<-*
                       gatt ta+tca+a
  proApgltS-   255    GGATTATAGTCAaA    268
```

flpab flp-regulon, flp-regulator binding domain

APPENDIX 26

β-galactosidase activity assay

Reagents:

Z-buffer stock solution

Na_2HPO_4	4.27 g
NaH_2PO_4 H_2O	2.75 g
KCl	0.375 g
$MgSO_4$ $7H_2O$	0.125 g

The mixture was adjusted pH to 7.0 and adjusted volume to500 ml with distilled water. Do not autoclave. The chemical was stored at 4°C..

For complete Z-buffer -- Prior to daily use mix:

50 ml Z-buffer

0.14 ml ß-mercaptoethanol

4 mg.ml^{-1} ONPG (Sufficient for 100 assays -- make fresh daily)

o-nitrophenyl-ß-D-galactoside (o-nitrophenyl-ß-D-galactopyranoside) 80 mg

Dissolved with 20 ml of distilled water and mix well.

1 M Na_2CO_3 (Sufficient for 100 assays)

Na_2CO_3	5.3 g

Dissolved with 50 ml of distilled water and mix well. The chemical was stored at 4°C.

APPENDIX 27

Plasmid transformation into *Synechococcus* sp. PCC 7942

1. Preparation of competent cells

The cells grown in 100 ml of **BG_{11}** medium at 7th day were collected by centrifugation at 5,000 g, 4 °C for 10 mins. The pellet was resuspended with 10 ml of new **BG_{11}** medium and the cell suspension was aliquot 1 ml/tube for immediately transformation.

2. Transformation

The plasmid was mixed with 1 ml of the cell suspension in microtube and incubated on a rotary shaker at 30 °C, 160 rpm under continuous illumination by cool white fluorescence tubes of 25 µmol photon m^{-2} s^{-1} for overnight. The transformed cells were spreaded onto the BG_{11} agar plate containing appropriate antibiotic. The plate was incubated at 30 °C until the green colonies appear and then subcultured into BG_{11} liquid medium containing the same antibiotic as in the plate.

APPENDIX 28

Synechococcus sp. PCC 7942 plasmid extration

Reagents:

Solution I (100 ml)

5.0 ml 1.0 M Glucose

2.5 ml 1.0 M Tris-HCl, pH 8.0

2.0 ml 0.5 M EDTA, pH 8.0

After autoclave 20 µg ml^{-1} of RNase was added and stored at 4°C.

Solution II (25 ml)

0.5 ml 10 M NaOH

1.25 ml 20% SDS

Solution III (500 ml)

147 g potassium acetate

57.5 ml glacial acetate

Autoclave and store at 4°C.

Method:

A 5-ml cell culture was harvested by centrifugation at 8,000 g for 10 min at 4 °C and suspended in 100 µl of solution I by vigorous vortexing. The cell suspension was incubated with lysozyme (5 mg ml^{-1}) for 30 min at 37 °C. After that the cells were lysed by the addition of 200 µl of freshly prepare solution II, mixed by gently

inversion and incubated on ice for 5 min. The cell lysate was neutralized by gently mixing with 150 µl of solution III followed by 5 mins incubation on ice. The mixture was centrifuged at 12,000 rpm for 5 min at 4 °C. The clear lysate was collected, extracted once with phenol:chloroform:isoamylalcohol (25:24:1). Subsequently, the plasmid was precipitated by adding 2 volumes of ice-cold absolute ethanol, mixed by inversion several times before incubated at -20 °C for 10 mins and then centrifuged for 10 min at 12,000 rpm at 4 °C. The plasmid was washed with 70% ethanol and recollected by centrifugation for 3 min. Finally, the air-dried pellet was dissolved in 20 µl of TE buffer (10 mM Tris-HCl and 1mM EDTA pH 8.0) and stored at -20 °C.

APPENDIX 29

Expression of *ApgltS* gene under salt stress

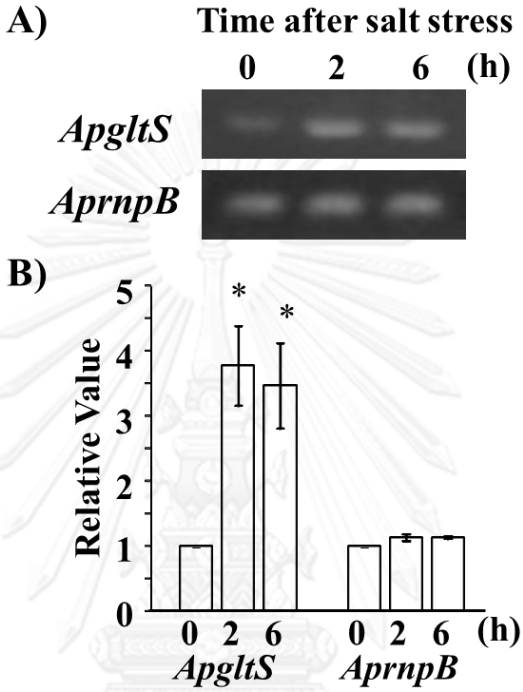

Transcription level of *ApgltS* gene in *A. halophytica* under salt stress. *A. halophytica* cells were collected after 0, 2 and 6 h growth in the medium containing 2.5 M NaCl. RT-PCR analysis was performed. PCR products were checked by agarose gel electrophoresis as shown in A). Relative values of the amount of mRNA for *ApgltS* and *AprnpB* are shown in B). Ribonuclease P (*AprnpB*) gene was used as control. The values at time 0 of each gene were set to 1.0. Asterisk indicates significant difference ($P < 0.05$) from the values at time 0.

VITA

Miss Bongkoj Boonburapong was born on December 24, 1979 in Bangkok, Thailand. She graduated with the a Bachelor of Science in Microbiology, Faculty of Science, King Mongkut's University of Technology Thonburi in 2000 and Master of Science in Biochemistry, Faculty of Science, Chulalongkorn University in 2006. She has further studied for the Doctor of Philosophy (Ph.D.) degree in Program of Biochemistry, Faculty of Science, Chulalongkorn University since 2008. During her study, the output of research work can be summarized as follows:

1. Boonburapong B, Laloknam S, Yamada N, Incharoensakdi A, Takabe T (2012) Sodium-dependent uptake of glutamate by novel ApGltS enhanced growth under salt stress of halotolerant cyanobacterium Aphanothece halophytica. Biosci Biotechnol Biochem 76:1702-1707

2. Boonburapong B, Laloknam S, Incharoensakdi A (2014) Accumulation of gamma-aminobutyric acid in halotolerant cyanobacterium Aphanothece halophytica under salt and acid stress. (submitted)

Grant:

2008-2012: The Office of the Higher Education Commission, Thailand through a grant in the program "Strategic Scholarships for Frontier Research Network for the Ph.D. Program, Thai Doctoral degree". Bangkok, Thailand. Grant No. 178/2551

2009-2014: The 90th Anniversary of Chulalongkorn University Fund (Ratchadaphiseksomphote Endowment Fund for a Ph.D. Scholarship, Bangkok, Thailand.